Virulence factors of Attaching and Effacing pathogens

By

Natalia Giannakopoulou

Department of Microbiology & Immunology

McGill University, Montreal, Quebec, Canada

December 2018

A thesis submitted to McGill University in partial fulfillment of the requirements of the degree of Doctor of Philosophy.

TABLE OF CONTENTS

ABSTRACT	4
RÉSUMÉ	6
ACKNOWLEDGMENTS	8
CONTRIBUTION TO ORIGINAL KNOWLEDGE	9
CONTRIBUTION OF AUTHORS	11
PREFACE TO CHAPTER 1	13
CHAPTER 1: GENERAL INTRODUCTION	14
1. Attaching & Effacing pathogens	
1.1 Enteropathogenic Escherichia coli	
1.2 Enterohemorrhagic <i>Escherichia coli</i>	
1.3 Citrobacter rodentium	
2. Host defense against A/E pathogens	21
3. A/E pathogen virulence and fitness factors	
3.1 Type 3 secretion system	
3.1.1.1 Tir	
3.1.1.2 Map	29
3.1.2 Non-LEE encoded effectors	
3.1.2.1 NleA	
3.2 Adherence factors	
3.3 Shiga toxin	
3.4 Two Component Systems	34
PREFACE TO CHAPTER 2	40
CHAPTER 2: Systematic analysis of two-component systems in G	
positive and negative roles in virulence	41
ABSTRACT	41
INTRODUCTION	42
MATERIALS AND METHODS	45
RESULTS	52
DISCUSSION	70
ACKNOWLEDGEMENTS	74
SUPPLEMENTARY INFORMATION	75
PREFACE TO CHAPTER 3	88
CHAPTER 3 The Virulence Effect of CpxRA in Citrobacter rodenti	ium Is Independent of the
Auxiliary Proteins NlpE and CpxP	89
ABSTRACT	
INTRODUCTION	91
MATERIALS AND METHODS	94
RESULTS	100
DISCUSSION	111
ACKNOWLEDGMENTS	118
SLIPPI EMENTAL INFORMATION	119

APPENDIX 1	158
PREFACE TO CHAPTER 4	160
CHAPTER 4: The Virulence Factor NIeA is O-glycosylated Upon Host Cell Translocation.	161
ABSTRACT	161
INTRODUCTION	162
MATERIALS AND METHODS	163
RESULTS	170
DISCUSSION	184
CHAPTER 5: DISCUSSION	187
General Overview/Summary	187
Two-component systems during infection with <i>C. rodentium</i>	188
ArcAB	189
RcsBC	190
RstAB	191
UhpAB	192
ZraRS	
BarA/UvrY	193
QseBC	194
CpxRA	194
NleA undergoes an apparent mobility shift upon translocation into the host cell	
Conclusion	
REFERENCES Error! Bookmark not o	defined

ABSTRACT

Citrobacter rodentium is a murine pathogen used to model the intestinal infections caused by Enteropathogenic and Enterohaemorrhagic Escherichia coli (EPEC and EHEC), two diarrheal pathogens responsible for morbidity and mortality in developing and developed countries, respectively. These bacteria are members of a group of pathogens that form characteristic attaching and effacing lesions on enterocytes during infection. During an infection, these bacteria must sense and adapt to the host gut environment. In order to adapt to changing environmental cues and modulate expression of specific genes, bacteria use two-component signal transduction systems (TCS). We hypothesized that intestinal bacteria might employ TCSs to adapt to the host gut environment. We performed a global in vivo screen of the expression and virulence effects of all 26 TCSs of C. rodentium, and deletion of several TCSs led to avirulent ($\Delta cpxRA$), or moderately attenuated ($\triangle arcA$, $\triangle rcsB$, $\triangle zraRS$, $\triangle rstAB$, $\triangle uhpAB$) strains. Fecal CFU loads during infection of susceptible mice, as well as immunofluorescence staining of infected intestinal tissue sections revealed that the $\triangle cpxRA$ strain is defective in colonization and cell adherence. In E. coli, the Cpx TCS is reportedly activated in response to signals from the outer-membrane lipoprotein NlpE. We therefore investigated the role of NlpE in virulence, by deleting NlpE and another reported sensing component of CpxRA, CpxP. We found that neither the $\triangle nlpE$, $\triangle cpxP$ nor the $\triangle nlpE\triangle cpxP$ strains were significantly attenuated, suggesting that an NlpE- and CpxP-independent pathway is important for intestinal infection. To further elucidate the mechanisms behind the contrasting virulence phenotypes, we performed microarrays and showed that gene expression patterns of the $\triangle nlpE$ and $\triangle cpxP$ strains were distinct from that of $\triangle cpxRA$. We detected 162 genes downregulated in the $\Delta cpxRA$ mutant, relative to wild-type, which were not similarly regulated in the auxiliary protein mutants. We hypothesize that this group of genes, including genes involved in maltose

metabolism, and T6SS secretion may contribute to the loss of virulence of $\Delta cpxRA$. Real-time qPCR analysis revealed that the $\Delta rcsB$ mutant has decreased expression of genes required for colanic acid biosynthesis suggesting a defect in capsule production, and the $\Delta arcA$ mutant has decreased expression of components of the Type 3 secretion system (T3SS). Notably, the T3SS is essential to A/E pathogens in order to translocate effectors proteins into host cells. These proteins modulate host cell pathways to favour bacterial replication and survival. During the course of our work, we detected an apparent size shift of one T3SS effector, NleA, following its translocation into host cells. This led us to hypothesize that it might be modified by the host. Bioinformatic and functional analyses are consistent with the modification of NleA by host-mediated O-glycosylation, a modification that has not previously been described for a bacterially-translocated protein. Together, these findings increase our understanding of host/pathogen interactions during EPEC, EHEC, and *C. rodentium* infections.

RÉSUMÉ

Citrobacter rodentium est un pathogène de la souris et un modèle pour étudier l'infection intestinale par les *Escherichia coli* entéropathogènes (EPEC) et entérohémorragiques (EHEC) chez l'humain. EPEC et EHEC causent des diarrhées contribuant respectivement à la morbidité et la mortalité dans les pays en développement et les pays développés. C. Rodentium, EPEC et EHEC appartiennent à une famille de pathogènes qui induisent des lésions d'attachement et d'effacement (A/E) caractéristiques sur les entérocytes pendant l'infection. Lors des infections, ces bactéries doivent détecter et s'adapter à l'environnement intestinal de l'hôte. Afin de s'adapter aux changements de signaux environnementaux et de moduler l'expression de gènes cibles, les bactéries utilisent des systèmes régulateurs à deux composants (TSC). Nous émettons l'hypothèse que les bactéries intestinales utilisent des TSC pour s'adapter à l'intestin de l'hôte. Nous avons effectué un dépistage global in vivo afin de déterminer l'expression de l'ensemble des 26 TCS chez C. rodentium, ainsi que leur effet sur la virulence. Nous avons trouvé que la délétion de certains TSC a complètement ($\Delta cpxRA$) ou modérément ($\Delta arcA$, $\Delta rcsB$, $\Delta zraRS$, $\Delta rstAB$, $\Delta uhpAB$) atténués la virulence. Suite à l'infection de souris susceptibles par C. rodentium, la charge fécale (énumérée par les CFU) et la coloration par immunofluorescence de tissus intestinaux infectés ont révélé que la souche $\Delta cpxRA$ a un défaut de colonisation et d'adhérence cellulaire. Chez E. coli, le TSC Cpx est activé par des signaux provenant de la lipoprotéine NlpE, liée à la membrane externe. Afin d'étudier son rôle dans la virulence, nous avons supprimé nlpE, ainsi qu'une deuxième protéine de signalisation de CpxRA, CpxP. Nous avons constaté que la virulence de $\Delta nlpE$, $\Delta cpxP$ et $\Delta n l p E \Delta c p x P$ n'étaient pas significativement atténuées. Cela suggère qu'une voie de signalisation indépendante de NlpE et CpxP contrôle la virulence de C. rodentium. Pour mieux définir les mécanismes à l'origine des phénotypes de virulence observés, nous avons effectué des

analyses par puces à ADN et nous avons démontré que les profils d'expression génique des souches $\Delta nlpE$ et $\Delta cpxP$ étaient distincts du profil de la souche $\Delta cpxRA$. Comparé au type sauvage, 162 gènes étaient sous-exprimés dans le mutant $\Delta cpxRA$. Ces gènes n'étaient pas régulés de manière similaire chez les mutants des protéines auxiliaires. Nous émettons l'hypothèse que ce groupe de gènes, y compris les gènes impliqués dans le métabolisme du maltose, et la sécrétion des protein par un T6SS contribuent à la perte de virulence chez la souche C. rodentium $\Delta cpxRA$. Une analyse par qPCR a révélé que le mutant $\Delta rcsB$ sous-exprime des gènes nécessaires à la biosynthèse de l'acide colanique, suggérant un défaut de production de la capsule. De plus, le mutant $\Delta arcA$ sousexprime les gènes reliés au système de sécrétion de type 3 (T3SS). T3SS est essentiel aux pathogènes A/E pour la translocation des protéines effectrices dans les cellules hôtes. Ces protéines modulent les voies de signalisation chez les cellules hôtes pour favoriser la réplication et la survie des bactéries. Suite à sa translation dans la cellule hôte, nous avons détecté un changement de taille d'une protéine effectrice T3SS, NleA, une observation intéressante de ce travail. Cela nous a conduits à émettre l'hypothèse que NleA pourrait être modifié par l'hôte. Les analyses bioinformatiques et fonctionnelles concordent avec la modification de NleA par la glycosylation induite par l'hôte. La modification d'une protéine d'origine bactérienne n'a jamais été décrite auparavant. Ensemble, ces résultats ont des conséquences importantes pour notre compréhension des interactions hôte/pathogène au cours des infections intestinales reliées à EPEC, EHEC et C. rodentium.

ACKNOWLEDGMENTS

First, I would like to thank my supervisors, Dr. Samantha Gruenheid and the late Dr. Hervé Le Moual for the opportunity to work on the projects presented in this thesis. Their continued support, advice, and guidance have helped me grow as a scientist and as a person throughout these years. Sam and Hervé you both have exemplified what it means to be an outstanding supervisor and scientist, and you have instilled in me qualities that will follow me for the rest of my career. Thank you. I dedicate this thesis to the memory of Dr. Hervé Le Moual.

I would like to thank Dr. Sébastien Faucher for his mentorship during such difficult circumstances, as well as his expertise in the elusive world of microarrays. I am truly grateful for the countless hours you spent troubleshooting with me. Dr. Nilmini Mendis – thank you for the help with the microarrays and the countless sanity checks you have provided over the past year.

To past and present members of the Gruenheid, Le Moual labs, and MRCCT – thank you for your friendship, support, countless laughs and coffee runs. Especially, Tyler Cannon – thanks for the countless times you've let me fire you, and for being a sounding board when I've needed one. Anshul Sinha – thanks for teaching me the ins and outs of the NBA, and for being my partner in crime in navigating the difficult circumstances in the past year.

I would like to thank Lei Zhu and Dr. Nilmini Mendis for translating my abstract. Also, thank you to Dr. Irah King for being a member of my Advisory Committee and for his thousands of questions.

Marilena, thank you for being you - for always being around for a hug or a squeal, depending on what the occasion required. Ryan, thanks for nerding out with me. Dalya, thank you for being an endless supply of laughs and midnight chats, and for giving me a reality check whenever I needed one.

To my family, thank you for always being there, even from a distance. To my parents, thank you for giving me the tools and values to pursue what I want in life. Μαμά, μπαμπά, Μυρτώ, γιαγιά, Άγγελε, Πάνο, Μαίρη, Παύλο, σας αγαπώ και ας σας παιδεύω. Αυτό που τώρα ξεκινάει, πολύ μου πάει. Αίεν Υψικρατείν.

CONTRIBUTION TO ORIGINAL KNOWLEDGE

- 1. This was the first global analysis of *in vivo* expression and role in virulence of all TCSs in *C. rodentium*.
- 2. This work showed that the deletion of certain TCSs in *C. rodentium* alters the outcome of infection of susceptible mice.
- 3. Of the 26 TCSs in *C. rodentium*, CpxRA has the most striking effect on virulence, with 100% survival of susceptible mice infected with $\Delta cpxRA$ *C. rodentium*.
- 4. The virulence effect of the $\triangle cpxRA$ strain of *C. rodentium* is independent of auxiliary proteins NlpE and CpxP.
- 5. Mice infected with the $\Delta rcsB$ strain of *C. rodentium* show a modest survival phenotype, with delayed mortality and 20% survival. This phenotype correlates with a defect in colanic acid biosynthesis gene transcription, which would be predicted to alter the capsule of the bacteria.
- 6. Loss of the ArcAB led to a slight virulence defect in *C. rodentium*, likely due to a defect in the regulation of its Type 3 Secretion System (T3SS), impacting its ability to translocate virulence factors into the host cell.
- 7. The RstAB, UhpAB, and ZraRS mutants of C. rodentium show slight attenuation in vivo.
- 8. The BarA-UvrY mutant of *C. rodentium* is slightly more virulent that wild-type *C. rodentium*.
- 9. The first microarray analysis of the CpxRA regulon of *C. rodentium* which identified many candidate genes and pathways that may contribute to the virulence phenotype of CpxRA, including maltose metabolism, adherence, and T6SS.
- 10. NleA, a T3SS effector important for virulence, is post-translationally modified upon translocation into the host cell. The apparent mobility shift of NleA is not due to

phosphorylation, ubiquitination, or N-glycosylation, and the data is consistent with NleA being O-glycosylated upon translocation into the host cell.

CONTRIBUTION OF AUTHORS

The work presented in this thesis was published, or is in preparation for publication, as follows:

Chapter 1. General Introduction

The literature review was written by NG and edited by SG.

Chapter 2.

Thomassin, JL.*, Leclerc, JM.*, Giannakopoulou, N.*, Zhu, L., Salmon, K., Portt, A., Daigle, F., Le Moual, H., Gruenheid, S. Systematic Analysis of Two-Component Systems in *Citrobacter rodentium* Reveals Positive and Negative Roles in Virulence. *Infect Immun*, 85(2). doi:10.1128/iai.00654-16. (2017).

*Equal contributions

NG performed the mouse experiments with technical assistance from LZ, the phenotyping of infected mice, the immunofluorescence, the *in vitro* adherence assays, and the T3SS qPCR experiments. JLT, JLM, KS, and AP generated the mutants and performed the biochemical characterizations. SG and HLM designed the experiments and supervised the work. All authors contributed to writing the manuscript.

Chapter 3.

Giannakopoulou, N., Mendis, N., Zhu, L., Gruenheid, S., Faucher, SP., Le Moual, H. The Virulence Effect of CpxRA in *Citrobacter rodentium* Is Independent of the Auxiliary Proteins NlpE and CpxP. *Front Cell Infect Microbiol*, *8*, 320. doi:10.3389/fcimb.2018.00320. (2018).

NG participated in the design of the experiments, generated the mutants, and performed the experiments. NM helped with the microarrays and the microarray analysis. LZ helped with the mouse infections. HLM, SG, and SF designed the experiments and supervised the work. All authors participated in data analysis. The manuscript was written by NG and edited by NM, HLM, SG, and SF.

Chapter 4.

Giannakopoulou, N., Burns, L., Gruenheid, S., **The Virulence Factor NleA is O-glycosylated Upon Host Cell Translocation.** *Manuscript in preparation*.

NG participated in the design of the experiments, performed all the experiments and analyzed all the data. LB performed the *in vivo* SDS-PAGE, under NG's supervision. SG designed the experiments, and supervised the work. The manuscript was written by NG and edited by SG.

Chapter 5. Discussion and Overall Conclusions

The discussion was written by NG and edited by SG.

PREFACE TO CHAPTER 1

This thesis explores virulence factors of attaching and effacing pathogens, Enteropathogenic *Escherichia coli*, Enterohemorrhagic *Escherichia coli*, and the murine model *Citrobacter rodentium*. This literature review provides the necessary background, and is comprised of three parts. The first section, "Attaching and Effacing pathogens", provides information on these pathogens and their characteristic colonization of the host. The second section, "Host defense against A/E pathogens", provides information on the host-pathogen interaction, specifically in *C. rodentium*. Finally, the third section, "A/E pathogen virulence and fitness factors", delineates mechanisms of virulence of these pathogens, and provides information on the Type 3 secretion system and its effectors, as well as two-component signal transduction systems.

CHAPTER 1: GENERAL INTRODUCTION

1. Attaching & Effacing pathogens

The attaching and effacing (A/E) pathogens are a small group of related Gram-negative diarrheal pathogens that share a unique characteristic mechanism of colonization of intestinal epithelial cells: the formation of A/E lesions. This group includes enteropathogenic Escherichia coli (EPEC), enterohemorrhagic E. coli (EHEC), the related mouse pathogen Citrobacter rodentium, as well as Escherichia albertii, rabbit-enteropathogenic E. coli (REPEC), porcineenteropathogenic E. coli (PEPEC), and dog-enteropathogenic E. coli (DEPEC) [1, 2]. A/E lesions are formed when these bacteria attach to intestinal epithelial cells, efface the microvillar architecture, and form actin-rich pedestals beneath the adherent bacteria (Figure 1) [3]. The ability to form A/E lesions is encoded within a highly conserved pathogenicity island, known as the Locus of Enterocyte Effacement (LEE), which is shared by EPEC, EHEC, and C. rodentium. The LEE is a pathogenicity island of approximately 35kb (with some slight differences between pathogens), and 41 open reading frames (ORFs), flanked by insertion sequences, and encodes a Type 3 Secretion System (T3SS), as well as multiple effector proteins translocated into host cells by the T3SS [4-8]. One T3SS-translocated effector protein important for this process is the translocated intimin receptor (Tir). Tir is translocated into the host cell where it is embedded into the host membrane [5, 9]. The extracellular domain of Tir then binds the bacterial outer membrane adhesin intimin, resulting in the intimate attachment of the bacterial cell to the host epithelial cell [5, 9]. The intracellular domains of Tir bind proteins within the host cell leading to the recruitment of Neural Wiskott-Aldrich syndrome protein (N-WASP) and the actin-related protein 2/3 (Arp2/3)

complex to the site of attachment. As a result, actin nucleation occurs and characteristic actin pedestals are formed [10]. Despite the numerous similarities between these A/E pathogens, there exist some important differences, which will be highlighted below.

1.1 Enteropathogenic Escherichia coli

Enteropathogenic *Escherichia coli* (EPEC) is a Gram-negative food-borne human pathogen which colonizes the small intestine and is responsible for diarrheal disease, mainly in the developing world. EPEC was discovered in the 1940s, and at the time was prevalent in both the developed and developing world. It has since largely disappeared from the developed world, and is predominantly found in outbreaks of infantile diarrhea in the developing world [11]. For children under the age of 5, these outbreaks can be fatal, especially in Sub-Saharan Africa and South Asia [1]. While the exact infectious dose has not been determined, a study with human volunteers used an infectious dose of 10¹⁰ CFU in order to cause infection [12].

EPEC can be subdivided into typical and atypical strains, depending on whether the strain harbors the *E. coli* adherence factor plasmid (pEAF) [13]. The pEAF plasmid encodes the bundle forming pilus, which allows EPEC to form microcolonies on the surface of intestinal epithelial cells (Figure 1A) [14, 15]. Atypical EPEC (aEPEC) is a highly heterogeneous group, more closely related to EHEC, in genetic characteristics and reservoirs. These strains often derive from typical strains which have lost plasmids encoding virulence genes, and are often present in asymptomatic children [16]. Notably, aEPEC strains are often untypable by the classical method of serotyping their O and H antigens, for LPS and flagella respectively. Because EPEC is generally a human-specific pathogen, direct assessment of virulence of EPEC is rare. One study which infected human

volunteers with typical EPEC O127:H6 showed a wide range of responses to infection [12]. The exact mechanism by which EPEC elicits diarrhea is unknown; however, changes in ion secretion, loss of absorptive surface, inflammation, and increased intestinal permeability may be contributing factors [1, 17].

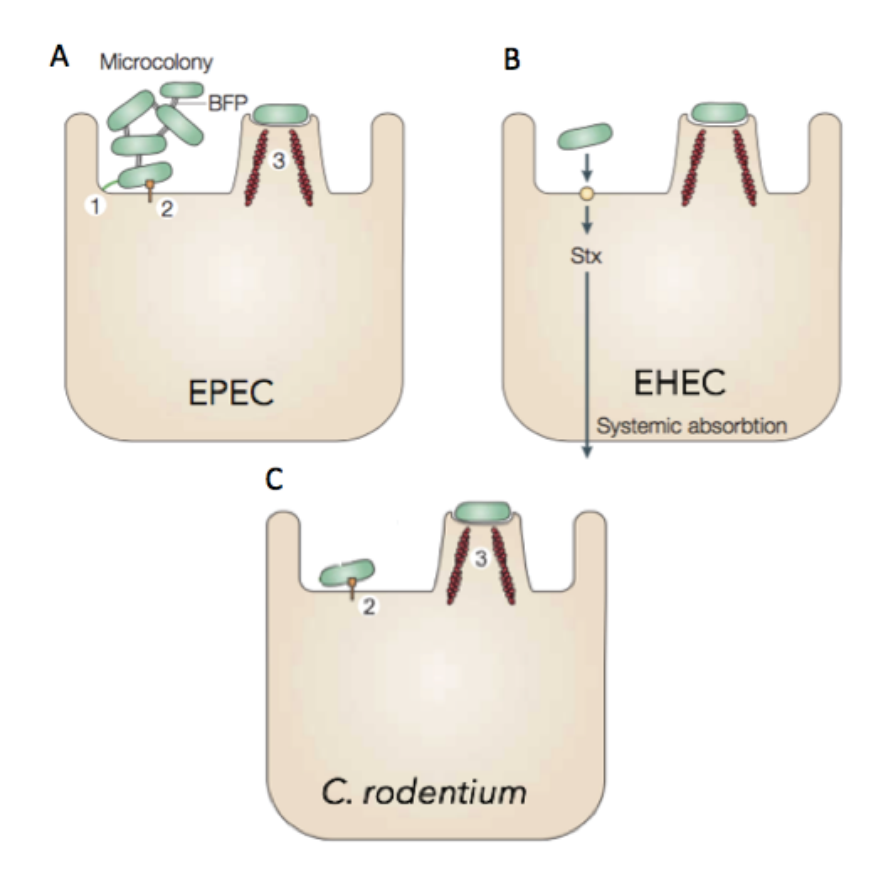


Figure 1: Schematic representation of EPEC, EHEC and C. rodentium.

A) EPEC adhere to the enterocyte, effacing the microvillar architecture and forming A/E lesions, characterized by 1) initial adhesion and formation of a microcolony (in EPEC, mediated by the Bundle Forming pilus (BFP), 2) T3SS, and 3) formation of actin rich pedestals. B) EHEC attaches similarly, however it does not form microcolonies. The Shiga toxin (Stx) is absorbed through the bloodstream. C) *C. rodentium* forms similar A/E lesions. Figure modified from [17].

1.2 Enterohemorrhagic Escherichia coli

Enterohemorrhagic *E. coli*, or EHEC, is also a diarrheal pathogen forming characteristic A/E lesions (Figure 1B). It was first discovered in 1982, as the causative agent of bloody diarrhea in outbreaks in Michigan and Oregon, USA [18, 19]. EHEC can be transmitted through food and water. An important reservoir for EHEC is the natural flora of cattle, where EHEC does not cause disease due to the absence of Shiga toxin (Stx) receptors in the bovine GI tract and blood vessels [20-24]. As such, ingestion of undercooked ground beef is a common risk factor for outbreaks of EHEC [11, 21, 25, 26]. Other vehicles of EHEC transmission include raw vegetables, such as lettuce, as well as unpasteurized apple juice [27, 28]. An outbreak in Japan, in the 1990s, with over 9000 cases, was caused by contaminated uncooked radish sprouts [29]. Recently, outbreaks in the USA, in Michigan and Virginia were traced to contaminated alfalfa sprouts [30]. Finally, water sources, such as recreational and municipal water sources, have also been implicated in outbreaks [31, 32]. The high infectivity of EHEC is also due to the rather low infectious dose required – less than 100 CFU [17].

In contrast to EPEC which colonizes the small intestine, EHEC colonizes the colon. Recently, a study reported that EHEC uses biotin to determine its tropism in the intestine [33]. Humans cannot synthesize biotin, and thus obtain it from external sources, such as nutrition. The majority of biotin is absorbed in the small intestine, thereby creating a gradient of biotin, with the highest concentrations in the small intestine, and lowest in the colon [34, 35]. EHEC senses the low biotin levels of the colon and signals through the global regulator Fur in order to increase expression of the LEE and promote colonization of the colon [33]. EHEC causes hemorrhagic colitis, and in 1983, EHEC was linked to hemolytic uremic syndrome (HUS) – a potentially fatal

condition [36]. HUS is characterized by thrombocytopenia, acute kidney failure, and hemolytic anemia [37]. This condition develops in 14% of children under the age of 10 years old, once infected with EHEC O157:H7 [38]. In a recent epidemiological study of 350 EHEC outbreaks in the USA, approximately 4% of cases progressed to HUS, with a 0.5% mortality rate [39]. The reason behind the increased severity of disease is the presence of the Shiga toxin (Stx) in EHEC (Figure 1B) [40]. This phage-encoded toxin, also known as verocytotoxin, can be found in two isoforms, Stx1 and Stx2 [41]. Stx1 is almost identical to the Shiga toxin of Shigella dysenteriae, and can lead to HUS [42, 43]. In contrast, Stx2 is only 55% similar to Stx1 in amino acid composition, and cannot be neutralized by the same antibodies [17, 44]. Stx2 is associated with more severe disease in humans [42]. Stx is an AB₅ toxin, with one central enzymatically-active A subunit, surrounded by 5 B subunits. The exact mechanism through which Stx gets absorbed into the bloodstream is unknown, but likely to involve transcytosis. The Stx toxin B subunit binds to globotriaosylceramides (Gb3s), receptors expressed on Paneth cells, renal epithelial cells, and endothelial cells [40, 45-47]. The toxin is secreted by EHEC, absorbed into the blood stream, and then travels to the site of Gb3 receptors. Binding of the B subunit of the toxin to the Gb3 receptors induces membrane invaginations to promote endocytosis. Once endocytosed, the toxin trafficks to the Golgi apparatus where the A subunit, an RNA glycosidase, inhibits protein synthesis by removing an adenine from 28S rRNA. As a result, apoptosis is induced [1, 48]. Notably, the Stx is also released by lambdoid phage-mediated lysis of the bacterial cell due to the S.O.S. response arising from DNA damage [49]. As such, the use of antibiotics, which can induce the S.O.S. response, is highly discouraged for treatment of EHEC infections.

1.3 Citrobacter rodentium

Citrobacter rodentium is another member of the A/E pathogen family, and was first isolated in the 1960s, as the etiologic agent of transmissible murine colonic hyperplasia in mouse colonies at Argonne National Laboratory in the United States, and the National Institute of Health in Japan [50, 51]. There exist two strains of C. rodentium, namely DBS100 and ICC168, both isolated from an outbreak at Yale University in 1971 [52-54]. C. rodentium is a widely used murine model to study EPEC and EHEC, due to their pathological similarities and the conservation of the LEE (Figure 1C) [52, 55]. C. rodentium shares 67% of its genes with EPEC and EHEC [56]. Following infection of mice with 10⁸-10⁹ CFU, the bacteria can be found in the cecum, the first part of the large intestine, within hours, and the distal colon by day 2-3 post infection [57]. The majority of the bacterial inoculum is killed in the stomach, and the exact dose to begin colonization of the intestine is not known. The outcome of infection greatly depends on the mouse strain. In resistant strains, such as C57BL/6, NIH Swiss, and Balb/c, C. rodentium causes self-limiting colitis and clearance by day 21-28 post infection [58]. In contrast, susceptible strains, such as C3H/HeJ, suffer from 100% mortality by day 10-12 post infection, and severe disease characterized by significant colonic hyperplasia and diarrhea [58]. It has been reported that fluid therapy of mice, by intensive rehydration, can rescue mortality [59]. Further, genetic studies showed a major locus, Cri1, on chromosome 15 is responsible for susceptibility of C3H/HeJ and other susceptible mice, such as C3H/HeOuJ and FVB [60]. Specifically, increased levels of Rspo2, a Wnt pathway agonist, are detected in susceptible mice, leading to increased proliferation and decreased differentiation of intestinal epithelial cells [61, 62]. Rspo2 induction leads to the activation of the canonical Wnt pathway, leading to an undifferentiated epithelium, thereby leading to animals succumbing to infection through loss of intestinal function [61, 62].

2. Host defense against A/E pathogens

As EHEC and EPEC are human-specific pathogens, most of what we know regarding the host response to A/E pathogens comes from *C. rodentium* infection in mice. The first line of defense in the gut, during *C. rodentium* infection, is the extensive mucus layer [63]. The colon has two mucus layers: the outer layer, of variable thickness, which is loosely attached; and the inner layer, approximately 50µm thickness, which is more firmly attached to the enterocytes [64, 65]. The inner mucus layer is devoid of bacteria, whereas the outer mucus layer is heavily colonized by commensals and acts as a nutrient source [65]. Both mucus layers are primarily composed of MUC2, a highly glycosylated mucin responsible for the structural integrity of the mucus layer, which is secreted by goblet cells [65, 66]. The exact mechanism of how *C. rodentium* bypasses the inner mucus layer is not known; however, a recent study has shown by RNA sequencing, that infected susceptible mice, exhibit a downregulation of *muc2*, when compared to infected resistant mice [67]. Downregulation of *muc2* could impair the mucus layer, enabling easier access to the intestinal epithelium; however, this remains to be characterized.

After surpassing the mucus layer, the bacteria are recognized by Pattern Recognition Receptors (PRRs) such as TLRs on the surface of epithelial and myeloid cells, and nucleotide-binding oligomerization domain-containing (NOD) proteins within epithelial cells (Figure 2) [68-71]. The main TLRs involved are TLR2 and TLR4, recognizing lipoproteins and LPS, respectively (Figure 2) [68, 69]. TLRs then activate the myeloid differentiation primary response 88 (MyD88) protein and TIR-domain-containing adapter-inducing interferon-β (TRIF) signaling, with the subsequent activation of nuclear factor-κB (NF-κB) (Figure 2). NF-κB signaling leads to the downstream recruitment of innate immune cells, such as macrophages, neutrophils, and dendritic

cells, and the production of pro-inflammatory cytokines IL-6, IL-12, IL-23 and TNF α [71-73]. Through NOD signaling, there is a recruitment of ILC3 cells to the cecum, which produce IL-17 and IL-22, contributing to clearance of *C. rodentium*. *C. rodentium* infection also triggers the NACHT, LRR and PYD domains-containing protein 3 (NLRP3) inflammasome, which leads to the activation of caspase 1 and 11, and secretion of IL-1 β and IL-18 [71, 74]. Mice deficient in caspase 1 and mice deficient in TLR2 suffer increased bacterial burden, weight loss, and pathology [68, 75].

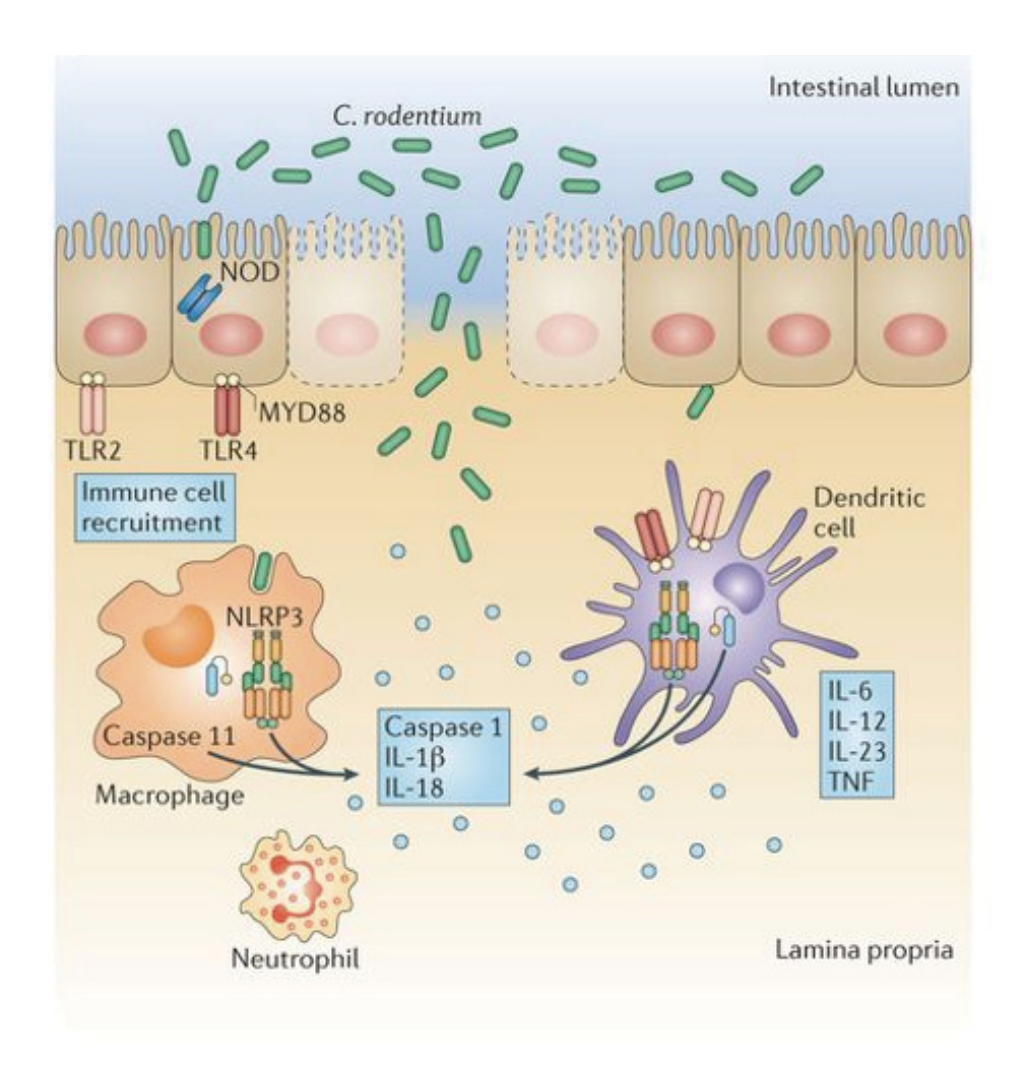


Figure 2: The innate immune response to C. rodentium infection

C. rodentium is recognized by TLR2 and TLR4 on epithelial and myeloid cells, leading to the activation of MyD88 and NFκB signaling and the secretion of pro-inflammatory cytokines IL-6, IL-12, IL-23, and TNF. The NLRP3 inflammasome is also activated, leading to the secretion of IL-1β and IL-18. Figure reproduced from [71].

Aside from the innate immune response, combatting *C. rodentium* infection also requires the adaptive immune response. CD4⁺ T cells and B cells are indispensable for the protective response to *C. rodentium*, and mice lacking either of these cells types are hypersusceptible to infection, leading to systemic dissemination [76, 77]. T_H17 cells, a CD4 subtype, are important in *C. rodentium* infection, as they secrete IL-17A, a pro-inflammatory cytokine which leads to the recruitment of neutrophils [78, 79]. In addition, T_H22 cells are important due to the secretion of IL-22, which upregulates antimicrobial peptides by epithelial cells, contributing to the clearance of *C. rodentium* [80].

The gut microbiota also plays an important role during *C. rodentium* infection. Recent studies used fecal microbiota transplants (FMT) in an attempt to uncover the role of gut commensals in colonization and disease progression. In two studies, the transfer of the microbiota from resistant mice to genetically susceptible mice lead to transfer of resistance, with delayed colonization and mortality of the susceptible mice [81, 82]. Specifically, in one study, the transfer of resistance was linked to increased IL-22 production in the susceptible mice [81]. In terms of bacterial communities, the susceptible mice which received FMT showed an increase in Bacteroidetes, and a decrease of Firmicutes [81]. Another study showed that increased levels of T_H17 cells, and in turn secretion of IL-17 and IL-22 was linked to increased segmented filamentous bacteria (SFB) in the gut microbiota of the mice [83]. This increase in IL-17 and IL-22 lead to increased host resistance to *C. rodentium* [83]. Another study infected germ-free mice, and noted that the germ-free mice were heavily colonized, and were unable to clear the infection, even by day 42 post infection [84]. These mice survived infection, and showed similar neutrophil, macrophage, and T cell responses as the ones of specific pathogen-free (SPF) mice [84].

3. A/E pathogen virulence and fitness factors

In order to cause disease, A/E pathogens have a multitude of virulence factors. Some virulence factors are secreted, such as the effectors of the T3SS. Other virulence factors, two-component systems (TCS), enable the bacterial cell to sense the host environment, adapt, and adjust gene expression. A/E pathogens also encode adhesins, enabling them to adhere to host cells, either by being directly involved in A/E lesion formation, such as intimin, or the bundle-forming pilus of EPEC, which enables it to aggregate into microcolonies [11]. Finally, EHEC specifically encodes the Shiga toxin, which has been described above.

3.1 Type 3 secretion system

Type 3 Secretion Systems (T3SS) are highly specialized secretion machines found in many Gram-negative pathogens, such as EPEC, EHEC, *Yersinia* species, *Salmonella enterica*, *Shigella* species, *Pseudomonas aeruginosa*, *Burkholderia pseudomallei*, *Vibrio* species, and *Chlamydia* species [85]. The T3SS is a multimeric system composed of approximately 20 genes, forming a continuous channel from the bacterial cytoplasm to the host cytoplasm, in order to secrete effectors to carry out a multitude of functions (Figure 3) [86, 87]. In A/E pathogens, the T3SS and multiple effectors are encoded within the LEE, and T3SS construction is a highly ordered hierarchical process [88]. The process begins with the assembly of the needle and inner rod proteins, the secretion of the translocators, and finally the secretion of the effectors (Figure 3). The translocators include EspA, the major component of the needle structure forming the continuous channel between the bacterial membrane and the host cytoplasm [89, 90]. EspB and EspD form the portion of the T3SS that is inserted into the host cell membrane [91]. EscN is structurally similar to the F_0/F_1 ATPase [92], and is responsible for providing the energy required for the T3SS, and a $\Delta escN$

strain of EHEC is deficient in T3SS [93]. In EPEC, EHEC and *C. rodentium*, the switch between translocators and effectors is governed by SepL and SepD [6, 94, 95]. In the absence of these proteins, secretion of translocators is abolished, but secretion of effectors is enhanced [94].

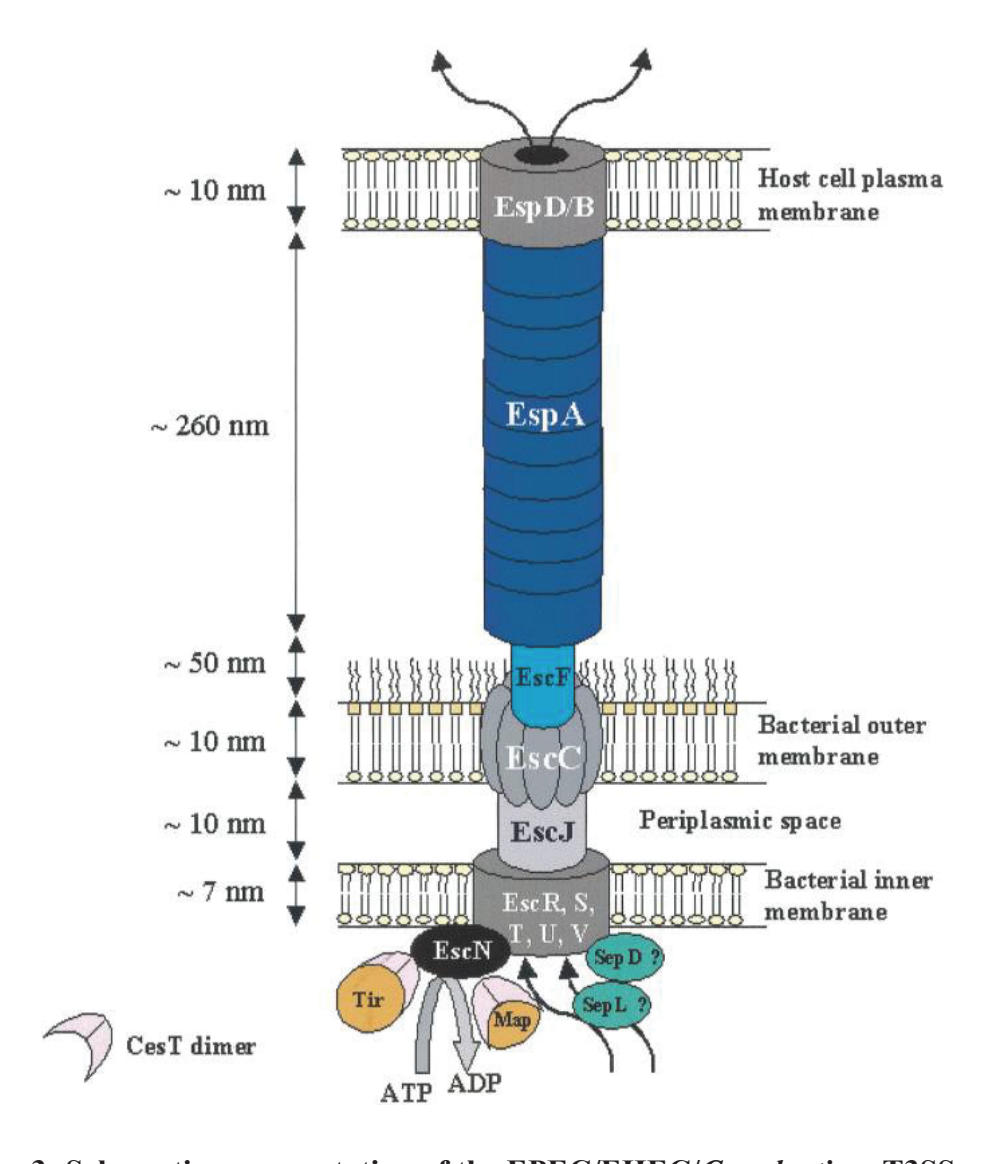


Figure 3: Schematic representation of the EPEC/EHEC/C. rodentium T3SS

The inner ring of the T3SS is composed of Esc-family proteins, followed by the lipoprotein EscJ in the periplasmic space, and EscF in the outer membrane. The translocon is composed of EspA, and the translocation pore in the host cell membrane is composed of EspB and EspD. The energy required for the function of the T3SS is provided by the ATPase EscN. Figure reproduced from [86].

3.1.1 LEE-encoded effectors

The LEE encodes 41 genes in 5 operons. Of these genes, there are 7 LEE-encoded effectors [6, 96]. The remaining genes are regulators, such as *ler*, *grlA*, *and grlR*, translocators, such as *espA* and *espB*, and structural units, such as *escN* and *ecsC* [6]. The virulence effects of all LEE-encoded genes in *C. rodentium* has previously been assessed, and for many of these effectors, host cell binding partners have been identified through a variety of methods and in a variety of cell types [6]. The *in vivo* relevance of these interactions remains mostly uncharacterized. The most characterized LEE-encoded effectors are Tir, Map, and EspF, and they will be discussed in more detail below. Table 1 below denotes all LEE-encoded effectors, their effect on virulence in mice, and potential host-binding partners.

Table 1: LEE-encoded effectors

LEE-encoded Effector	Effect on virulence in mice when deleted	Potential Host-binding partners
Tir	Full attenuation [6]	IQGAP1, Nck, 14-3-3tau, α-actinin, talin, cortactin, vinculin, cytokeratin 18 [96]
Map	Slight attenuation [6]	EBP50, NHERF1 [96]
EspB*	Full attenuation [6]	antitrypsin, α-catenin, myosin [96]
EspF	Attenuated in early bacterial colonization [6]	ABCF2, actin, profilin, arp2/3, cytokeratin18, sortin nexin 9, N-WASP [96]
EspH	Slight attenuation [6]	Unknown [96]
EspZ	Severely attenuated colonization [6]	Unknown [96]
EspG	Attenuated in early bacterial colonization [6]	Tubulin [96]

A table depicting the characterized LEE-encoded effectors, their effect on virulence of mice, and potential or characterized host-binding factors. Table modified from [96].

3.1.1.1 Tir

Tir is one of the most well studied LEE-encoded T3SS effectors, and one of the first to be translocated to the host cell. Upon formation of the T3SS, Tir is translocated and embedded into

^{*}although EspB is classified as a translocator, an effector function in host cells has been proposed.

the host cell membrane. [97]. Tir is composed of an N-terminal cytoplasmic domain and a Cterminal cytoplasmic domain, divided by an extracellular intimin binding domain [96]. Interaction with intimin in the bacterial membrane triggers actin nucleation and pedestal formation. EPEC Tir is tyrosine phosphorylated on tyrosine 474 of its cytoplasmic domain, leading to recruitment and binding of the SH2-domain-containing adaptor protein Nck [97]. This then leads to the recruitment of Neural Wiskott-Aldrich syndrome protein (N-WASP) and the actin-related protein 2/3 (Arp2/3) complex to the site of attachment. As a result, actin nucleation occurs and characteristic actin pedestals are formed [10]. In vitro, it has been demonstrated that EPEC Tir requires phosphorylation at residues 474, serine 434 and serine 463 in order to form pedestals [98, 99]. However, ex vivo experiments with EPEC, where human intestinal explants were infected in vitro, revealed that this phosphorylation is not necessary for A/E lesion formation, suggesting that pedestals and A/E lesions are distinct [100]. Further, in C. rodentium, mutation of these residues (leading to a mutant that cannot be phosphorylated) did not affect disease progression, whereas deletion of Tir lead to complete attenuation [6, 101, 102]. Notably, EHEC Tir is not tyrosine phosphorylated and pedestal formation occurs in an Nck-independent manner [103]. Instead, along with Tir, EHEC translocates EspF_U/TccP into the host cell, a bacterial effector which acts to activate N-WASP in the place of Nck [104-106]. Unlike Nck, however, there is no direct binding of EspF_U/TccP to Tir [107]. This is instead mediated by IRSp53, a host protein that regulates membrane and actin dynamics [108].

3.1.1.2 Map

Map (mitochondrial-associated protein) is a T3SS secreted effector which targets the mitochondria to disrupt its membrane potential [109, 110]. Map has been linked to multiple other

cell functions, as it is reported to induce Cdc-42-dependent filopodia formation in a mitochondria-independent manner, by mimicking the active form of Rho family small G proteins [110-112]. Further, Map promotes the uptake of EPEC by non-phagocytic cells [113]. Finally, Map has been shown to be important for tight junction disruption *in vitro* for EPEC and *C. rodentium* [114-116]. The loss of Map leads to an attenuated strain of *C. rodentium*, harboring colonization defects [117].

3.1.1.3 EspF

EspF targets to the mitochondria [118-121]. EspF has been reported to have a multitude of binding partners and functions within the host cell. In EPEC, EspF is required to induce the mitochondrial death pathway through the release of cytochrome C [118]. Further, EspF interacts with host cell protein Abcf2 within mitochondria to induce apoptosis [122]. EspF is also necessary for the disruption of tight junctions, in conjuction with other effectors, such as Map, EspG, NleA, and Tir [114, 123-125]. However, the exact mechanism by which EspF is involved in the disruption of tight junctions remains unknown [126]. Another mechanism of disease with diarrheal pathogens is water reabsorption, which is usually achieved through aquaporins. EspF targets sodium hydrogen exchanger 3 (NHE3) activity, aquaporin 2 and 3 localization, and inactivation of the sodium-D-glucose cotransporter (SGLT-1) [127-129]. Aquaporins are significantly displaced in mice infected with *C. rodentium*, and this is proposed to contribute to diarrheal symptoms [128]. Finally, EspF binds sortin nexin 9 (SNX9), and has been shown *in vitro* to enhance invasion and membrane tubulation of epithelial cells [130].

3.1.2 Non-LEE encoded effectors

In the early 2000s, several studies lead to the identification of effectors of the LEE-encoded T3SS that were not encoded within the LEE itself, but within other pathogenicity islands in the genome [6, 131, 132]. In 2003, the cycle inhibiting factor, or Cif, was discovered. Cif is encoded on a lambdoid phage, and is involved in cytoskeleton rearrangement and also G_2 cell cycle arrest; however, it is unique to only certain lineages of A/E pathogens [131, 133]. In 2004, the non-LEE effector A, or NleA, was discovered, and it will be discussed further below [132]. Finally, also in 2004, a systematic analysis of all 41 open reading frames of the LEE, and in some cases the abrogation of T3SS, lead to the discovery of six other non-LEE encoded effectors [6]. Table 2 below denotes all non-LEE-encoded effectors, their effect on virulence in mice, and potential host-binding partners.

Table 2: Non-LEE-encoded effectors

Non-LEE-encoded Effector	Effect on virulence in mice	Potential Host-binding partners
NleA	Full attenuation [6]	Sec24, PDZK11, SNX27, NLRP3, MAIS3, TCOF
NleH1	Moderate defect [134]	Ribosomal protein S3 [135]
EspJ	Higher levels of colonization than wild-type [136]	WD repeat-containing protein 23 (WDR23), Src, centromere protein H, intraflagellar transport protein 20 homologue, MORF4 family-associated protein 1-like 1, synembryn-A [96, 137, 138]
NleB2	Reduced colonization, reduced colonic hyperplasia [139]	GAPDH [140]
NleC	Fully virulent [139]	P300, p50, p65 [96, 141-143]
NleD	Fully virulent [139]	Unknown
NleG	Unknown	UBE2D2 [144]
NleH2	Moderate defect [134]	Ribosomal protein S3 [145]
NleF	Slight decrease in competitive index experiments with wild-type [146]	Caspase-4, caspase-8, caspase-9 [147]
NleE2	Fully virulent [139]	Unknown
EspG2/Orf3	Decreased colonization [148]	Tubulin

NleB1	Reduced colonization, reduced	MAP7, GAPDH, TRADD, FADD,
	colonic hyperplasia [139]	RIPK1, developmentally regulated GTP-
		binding protein 2, leucine-rich repeat-
		containing protein 18, DNA-directed
		RNA polymerases I, II, and III subunit
		RPABC1 [96, 137, 149-151]
NleE1	Fully virulent [139]	Unknown
EspL2	Decreased colonization [152]	MAP7, annexin-2 [96, 153]

A table depicting the characterized non-LEE-encoded effectors, their effect on virulence in mice, and potential or characterized host-binding factors. Table modified from [96].

Note: Cif is not listed in Table 2 as it is not present in all A/E pathogens

3.1.2.1 NleA

The first characterized translocated effector not encoded within the LEE was the non-LEEencoded effector A, or NleA [132]. NleA is absent from non-pathogenic strains of E. coli, but conserved among EPEC, EHEC, and C. rodentium. In EHEC, nleA is more prevalent in strains associated with outbreaks rather than non-outbreak associated strains (100% versus 33%; P < 0.0001) [154]. While the mechanisms underlying the impact of NleA on virulence are not well defined, it is known that NleA is absolutely required for virulence, associates tightly with host membranes, and it localizes to the Golgi apparatus [132]. NIeA binds to Sec24 paralogues of the COPII complex [155]. COPII vesicles mediate protein transport from the endoplasmic reticulum to the Golgi apparatus [156]. It has been previously shown, that in vitro, NleA inhibits COPII vesicle cargo packaging and/or vesicle budding [155]. A mutant of NleA showing diminished interaction with Sec24 is unable to affect COPII trafficking and confer virulence in vivo [157]. NleA is also important for tight junction disruption, which correlates with its ability to inhibit COPII-mediated secretion [158]. Finally, for the activation of the NLRP3 inflammasome, NLRP3 must be deubiquitinated [159]. One study reported that NleA binds ubiquitinated NLRP3 in macrophages, thereby preventing its deubiquitination and consequent inflammasome activation [159]. Through this mechanism, NleA dampens the levels of IL-1\beta secretion [159].

3.2 Adherence factors

Adherence factors of A/E pathogens promote adherence through a multitude of mechanisms. Our knowledge of adherence factors for these pathogens is limited, however there have been some recent reports implicating various proteins to adherence phenotypes. For example, the outer membrane adhesin intimin, is the receptor of the effector Tir, described above. Through the interaction of Tir and intimin, intimate bacterial attachment is promoted, leading to colonization. Loss of intimin in *C. rodentium* leads to loss of virulence, similar the phenotype in a Δ*tir* mutant [6]. In EPEC, the presence of the EPEC adherence factor plasmid (pEAF), enables the bacteria to assemble the bundle forming pilus (BFP), and form microcolonies on epithelial cells [11]. In a human study, pEAF was deemed necessary for the full virulence of EPEC [160]. Finally, *C. rodentium* harbours two classical type IV pilus operons, *kfc* and *cfc*, which have been implicated in adherence [161, 162]. A *C. rodentium* strain with a loss of *cfc* or *kfc* is unable to adhere in vivo [161, 162].

3.3 Shiga toxin

The Shiga toxin (Stx) is a well characterized virulence factor of EHEC, and discussed in greater detail above. EPEC and *C. rodentium* do not naturally encode a Shiga toxin. The injection of Stx into mice results in renal damage and inflammation [163, 164]. However, as mentioned previously, mice are naturally resistant to EHEC. Recently, in order to develop a murine model to be able to study both Stx and A/E lesions, the Stx phage was inserted into *C. rodentium* [165]. When the resulting strain, *C. rodentium* (λstx_{2dact}), is orally administered to mice, the bacteria will form A/E lesions, but also cause renal and intestinal damage, as expected by the Stx [165]. As such, this new model enables the study of Stx pathogenesis *in vivo*.

3.4 Two Component Systems

Bacteria must be able to sense their environment and adapt gene expression based on specific stimuli. One of the ways in which bacteria achieve this is with two-component signal transduction systems (TCS). TCSs are basic stimulus-response systems, composed of an inner membrane-bound histidine kinase and a corresponding response regulator in the cytoplasm of the cell (Figure 4) [166]. The N-terminus of the histidine kinase will detect a stimulus, and the histidine kinase will undergo auto-phosphorylation at a conserved histidine residue in the cytoplasmic domain (Figure 4) [166, 167]. The output domain of the histidine kinase interacts with the input domain of the response regulator and consequently phosphorylates an aspartate residue on the response regulator [166]. Upon phosphorylation, conformational changes occur in the response regulator in order to differentially regulate gene expression through DNA binding [168]. Typically, histidine kinases have a dual function, being able to both phosphorylate and dephosphorylate the response regulator [169]. Prototypical TCSs involve a histidine kinase with a specific cognate response regulator; however, in certain cases, crosstalk may occur between systems, while the exact occurrence and relevance of this *in vivo* remains unknown [169, 170]. Further, while most TCSs follow the simple model depicted in Figure 4, certain TCSs have more refined models. For example, the phosphorelay Rcs TCS is composed of the membrane bound sensor kinase RcsC, where upon stimulus will get autophosphorylated and transfer the phosphate to a membrane bound phosphotransmitter protein, RcsD [171, 172]. RcsD will then be responsible for transferring the phosphate to the cytoplasmic response regulator RcsB [172, 173]. Consequently, RcsB will either homodimerize or heterodimerize with the cytoplasmic protein RcsA, to carry out its transcriptional response. It is important to note that the regulons of the RcsB homodimers and the RcsB-RcsA heterodimers overlap but are distinct [171].

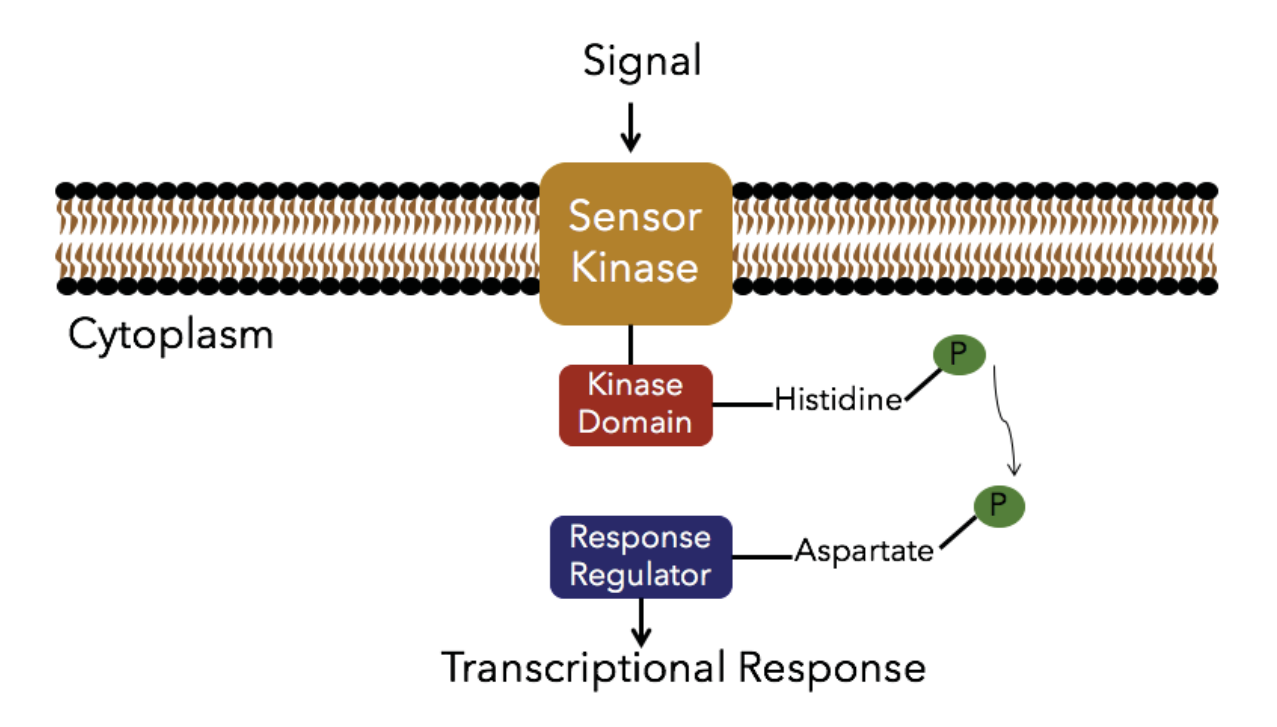


Figure 4: Schematic representation of Two Component Signal Transduction Systems (TCS) TCSs are composed of a membrane bound sensor kinase and a cytoplasmic response regulator. Upon stimulus, the sensor kinase is autophosphorylated at a conserved histidine residue, followed by the transfer of the phosphate to an aspartate residue in the cytoplasmic response regulator. The response regulator goes on to carry out a transcriptional response, often by DNA-binding.

Regulation of virulence by TCSs has been studied extensively in many bacteria; however, TCS modulation of virulence in A/E pathogens remained relatively uncharacterized at the time the work in this thesis was undertaken. Recently, the QseBC and QseFE TCSs which sense epinephrine and norepinephrine in the gut have been implicated in modulation of *C. rodentium* virulence. Epinephrine is synthesized by the adrenal medulla, whereas norepinephrine is synthesized locally in the gut, by the enteric nervous system [174, 175]. Epinephrine is transported to the gut through the bloodstream [174]. At steady state, the host converts these neurotransmitters to their inactive states; however, the gut microbiome has the ability to revert them to their original active states by removal of an added glucuronic acid residue [176]. It has been reported that EHEC uses QseBC and QseEF to sense epinephrine and norepinephrine [177]. Loss of these TCSs leads to an inability to sense epinephrine and norepinephrine, and attenuation of EHEC in an infant rabbit model of disease [176]. Recently, loss of signaling by these TCSs has been reported to lead to moderately attenuated virulence in the *C. rodentium* mouse model of infection, using a low dose of infection (10⁵ CFU) [176].

The CpxRA TCS is one of the key envelope stress responses in Gram negative bacteria [178-180]. There exist a multitude of signals that can activate the CpxRA TCS, including overproduction and mislocalization of the membrane lipoprotein NlpE [181-183], overproduction of type IV pilus components [184, 185], alkaline pH [184, 186], drugs targeting peptidoglycan synthesis, such as mecillinam, cephalexin and A22 [182], curli overproduction [187], ethanol, dibucaine, indole [188], attachment to abiotic surfaces [189], high osmolarity [187] and changes in membrane lipid composition [190]. In the presence of envelope stress, the histidine kinase CpxA will autophosphorylate at the conserved histidine, and consequently transfer the phosphoryl group

to the response regulator CpxR. In the absence of a stimulus, CpxA will exhibit phosphatase activity and retain CpxR in an inactive state [191]. The CpxRA TCS is also under the control of a periplasmic negative regulator, CpxP. One study reported that overexpression of CpxP lead to a three- to five-fold reduction of signaling by CpxRA [192, 193]. The inhibitory capacity of CpxP is proposed to be mediated by an α -helix in the N-terminal domain of the protein, and CpxP is also subject to DegP proteolysis within the cell [194].

In EPEC, *in vitro* experiments have uncovered that the activation of CpxRA has been implicated in the downregulation of several LEE operons [195]. Another study reported that induction of the Cpx TCS in EPEC lead to a decrease in motility, as well as a marked decrease of EscJ and EscC ring components of the T3SS [196]. It was also found that EPEC CpxRA is a repressor of *nuo* and *cyo* – two large macromolecular complexes of the inner membrane which facilitate aerobic respiration [197, 198]. Notably, however, the authors in that study also detected decreased levels of aerobic respiration in the absence of CpxRA signaling, suggesting that CpxRA is necessary for the proper assembly and folding of these macromolecular complexes [197].

Previous work in our lab characterized the CpxRA TCS in the context of C. rodentium virulence [199]. We detected activation of Cpx in vivo, upon infection of C57BL/6J mice with wild-type C. rodentium by measuring expression levels of cpxR, cpxA, and cpxP by qRT-PCR. Using lacZ fusions with the spy promoter, one of the most activated promoters by CpxRA, we detected that alkaline pH of 8.5 is an activator of CpxRA in C. rodentium, an activator previously reported in E. coli [184, 199]. In vivo, the effect of deletion of cpxRA on colonization and virulence in C57BL/6J mice infected with wild-type, $\Delta cpxRA$, and $\Delta cpxRA$::cpxRA C. rodentium was

assessed. At days 4 and 9p.i., the $\Delta cpxRA$ -infected animals showed decreased C. rodentium colonization as measured by fecal bacterial shedding [199]. The mice infected with the $\Delta cpxRA$ strain also displayed a significant decrease in colonization at day 12p.i. in the colon, as well as lower spleen index, relative to wild-type infected mice, which measures splenomegaly – a measure of inflammation [199]. The complementation of cpxRA in the $\Delta cpxRA::cpxRA$ strain restored bacterial colonization and shedding to wild-type levels. Histological analysis and pathology scoring of colon sections revealed lower pathology in the mice infected with the $\Delta cpxRA$ strain, with lowered shedding of cells in the intestinal lumen and goblet cells loss. A hallmark of C. rodentium infection is loss of normal tissue architecture and epithelial hyperplasia, which can be measured by increased crypt heights. The mice infected with the $\Delta cpxRA$ strain had crypt heights approximately half the size of wild-type and $\Delta cpxRA::cpxRA$ animals [199]. To determine whether the decreased colonization was due to a defective T3SS or an altered growth rate, secreted protein assays were done, and showed that secretion of all three strains was comparable [199]. Further, there was no growth defect in LB, and only a slightly longer lag phase in DMEM, confirming that the *in vivo* phenotypes were not due to altered T3SS or growth defects [199].

The loss of CpxRA signaling rendered *C. rodentium* severely attenuated, with 100% survival of susceptible C3H/HeJ mice [199]. Wild-type-infected animals succumbed to infection by day 10p.i., whereas the mice infected with $\Delta cpxRA$ survived to experimental endpoint at day 30. By day 30, the mice had gained weight, showed no signs of illness, and were expected to survive indefinitely. Complementation of the cpxRA TCS ($\Delta cpxRA::cpxRA$) restored survival phenotypes to those of wild-type [199]. At day 3, 6, and 9 post infection, the $\Delta cpxRA$ animals showed a 1-2 log difference in bacterial shedding, and cleared the infection by day 28 post infection [199]. Finally, in order to determine the expression kinetics of cpxRA activation, qPCR

was performed on day 4 and 9 post infection colon samples. There was a significantly higher expression level of *cpxR*, *cpxA*, and *cpxP* at day 4 post infection in susceptible mice, suggesting that CpxRA is temporally regulated [199].

The CpxRA TCS has been implicated in virulence of other infection models. Specifically, in Legionella pneumophila, CpxRA controls the expression of many virulence factors, and alters the ability to replicate in protozoa [200, 201]. In Shigella sonnei, CpxRA has the ability to control virulence by post-transcriptionally processing the T3SS regulator InvE, and pH-dependent regulation of virF, the regulator of invasion factors ipaBCD and virG [202, 203]. In Salmonella enterica serovar Typhimurium, the deletion of CpxR had no effect on virulence, however the deletion of cpxA and the constitutive activation of cpxRA decreased the ability of the bacterium to grow in mice [204]. In Vibrio cholerae, CpxRA allows adaptation to conditions of low iron, that would be found in the host environment [205]. Further in V. cholerae El Tor strain C6706 expression of CpxRA leads to a decrease in virulence factors, such as the toxin-coregulated pilus and cholera toxin, in vitro [206]. In the greater wax moth larva model of Galleria mellonella, the deletion of cpxR, which inactivates the Cpx response, lead to moderate attenuation of EPEC [207]. Constitutive activation of cpxRA with the cpxA24 mutation lead to complete loss of virulence in the G. mellonella model [207]. Finally, in Haemophilus ducreyi, the deletion of cpxRA does not impact virulence of the insect pathogen, however once again, the constitutive activation of cpxRA leads to a decrease in the expression of the lspB-lspA2 operon, responsible for the bacterium's ability to resist phagocytosis [208, 209]. In EHEC, loss of cpxA leads to high levels of cpxR, which negatively regulates the LEE and the associated T3SS, by repressing ler and lon, two positive regulators of the LEE [210]. Further, loss of cpxA leads to decreased adherence in vitro.

PREFACE TO CHAPTER 2

Two component signal transduction systems (TCSs) are stimulus-response systems responsible for sensing environmental cues and adjusting gene expression. TCSs have been previously reported in many bacteria to modulate a multitude of pathways. In Chapter 2 of this thesis we explored the effect of all 26 TCSs of the murine model C. rodentium in the context of virulence. We found that the individual deletion of seven TCSs (CpxRA, RcsBC, ArcAB, ZraRS, UhpAB, RstAB, BarA-UvrY) positively or negatively affected virulence of C. rodentium in susceptible C3H/HeJ mice. More specifically, we detected six hypovirulent mutants (CpxRA, RcsBC, ArcAB, ZraRS, UhpAB, RstAB), and one slightly hypervirulent mutant (BarA-UvrY). We then characterized the hypovirulent mutants further, by monitoring bacterial shedding and pathology. For the three mutants with the most striking attenuation (CpxRA, ArcAB, RcsBC) we explored the phenotypes further, and went on to show that the Δ arcA strain may be attenuated due to a defect in type 3 secretion regulation, the Δ rcsB strain may be attenuated due to capsule modification, whereas the most strikingly attenuated strain, Δ cpxRA, is not due to either of these reasons.

CHAPTER 2:

Systematic analysis of two-component systems in Citrobacter rodentium reveals positive and negative roles in virulence

ABSTRACT

Citrobacter rodentium is a murine pathogen used to model intestinal infections caused by the human diarrheal pathogens enterohaemorrhagic and enteropathogenic Escherichia coli. During infection bacteria use two-component systems (TCSs) to detect changing environmental cues within the host, allowing for rapid adaptation by altering the expression of specific genes. In this study, 26 TCSs were identified in C. rodentium and qPCR analysis showed that they are all expressed during murine infection. These TCSs were individually deleted and the *in vitro* and *in* vivo effects were analyzed to determine the functional consequences. In vitro analyses only revealed minor differences and, surprisingly, type III secretion (T3S) was only affected in the $\Delta arcA$ strain. Murine infections identified 7 mutants with either attenuated or increased virulence. In agreement with the *in vitro* T3S assay, the $\Delta arcA$ strain was attenuated and defective in colonization and cell adherence. The $\Delta rcsB$ strain was among the most highly attenuated strains. The decrease in virulence of this strain may be associated with changes to the cell surface, as congo red binding was altered and qPCR revealed that expression of the wcaA gene, which has been implicated in colanic acid production in other bacteria, was drastically downregulated. The $\Delta uvrY$ strain exhibited increased virulence compared to the wild-type, which was associated with a significant increase in bacterial burden within the mesenteric lymph nodes. The systematic analysis of virulence-associated TCSs and investigation of their functions during infection may open new avenues for drug development.

INTRODUCTION

Citrobacter rodentium is a murine-restricted pathogen that is the causative agent of transmissible colonic hyperplasia [211]. Together with enteropathogenic and enterohemorrhagic Escherichia coli (EPEC and EHEC), C. rodentium belongs to the attaching and effacing (A/E) family of intestinal pathogens [58]. These bacteria share numerous virulence factors, including those responsible for the formation of typical A/E lesions characterized by intimate attachment to intestinal epithelial cells, localized effacement of microvilli, and the formation of actin-rich pedestals beneath sites of bacterial adherence. EPEC causes diarrhea that kills several hundred thousand children each year in the developing world [14]. EHEC is commonly associated with outbreaks of foodborne diarrheal illness in the developed world [11]. The similarities between EPEC, EHEC, and C. rodentium infections have resulted in C. rodentium being widely used and recognized as a surrogate model to study intestinal infections caused by the human-restricted pathogens EPEC and EHEC [58, 212, 213].

Following oral inoculation of mice with *C. rodentium*, bacteria initially colonize a patch within the caecum. A few days later, *C. rodentium* can be found in the distal colon. This tissue tropism and infection pattern is similar to what is observed during human EHEC infections, where bacteria initially colonize Peyer's patches in the ileum before colonizing the colon [57]. Once present in the colon, *C. rodentium* colonizes to high levels (> 10⁹ colony forming units (CFUs)/g of tissue) between 7 and 14 days post-infection in most mouse strains [214]. In some mouse strains, such as C57BL/6, NIH Swiss and BALB/c, *C. rodentium* causes self-limited infection and the mice clear the infection by 21-28 days post-infection [214]. In contrast, other murine strains, such as C3H/HeJ, C3H/HeOuJ, and FVB experience significantly more hyperplasia and suffer high levels

of mortality between 6 and 10 days post-infection [59, 214]. Both the non-lethal and lethal murine models are used to provide insight into the infection process and pathogenesis of A/E pathogens.

Two-component systems (TCSs) are used by bacteria to detect changes in their environment and promote an adaptive response to survive [215, 216]. The typical TCS consists of a membrane bound histidine kinase (HK) sensor and a cytoplasmic response regulator (RR) that usually acts as a transcriptional regulator. TCS genes can be encoded as pairs with the RR and HK genes part of a single transcriptional unit, or the RR and HK genes can be unlinked within the chromosome. In addition, orphan RR genes that lack a cognate HK have been identified. The HK senses specific ligands or environmental cues, which result in the auto-phosphorylation of a conserved histidine residue of the HK cytoplasmic domain. The phosphoryl group is subsequently transferred to a specific aspartate residue in the RR. This affects its DNA-binding properties and results in changes in the transcription of specific genes. Activation of a TCS has been shown to affect the expression of few to hundreds of genes, impacting either specific or multiple processes [198, 217, 218]. Many TCSs affect bacterial metabolism, in addition to functions that may be associated with environmental persistence [219]. Other TCSs have been directly implicated in bacterial virulence. For example, TCSs such as Salmonella enterica PhoPQ and Bordetella pertussis BygAS are known master regulators of virulence [220, 221].

The number of TCSs varies between bacterial species; members of the *Enterobacteriaceae* family typically possess 20-30 TCSs [222]. In *E. coli*, most studies have focused on the analysis of TCS gene and regulon expression under different *in vitro* conditions [223-226]. In contrast, most *in vivo* studies do not examine TCS expression patterns and instead use a genetic approach

to identify TCSs that affect virulence. For example, in uropathogenic *E. coli* the BarA/UvrY, CpxRA, KguSR, and OmpR/EnvZ TCSs affect *in vivo* virulence, although their *in vivo* expression patterns remain unknown [227-231]. In EPEC and EHEC, several TCSs including CpxRA, FusKR, PhoBR, QseBC, and QseFE have been implicated in the regulation of virulence genes, *in vitro* and more recently *in vivo* for QseBC and QseFE [195, 232-236]. In this study, using *C. rodentium* infection of mice, we assessed the relative expression of each *C. rodentium* RR gene during *in vitro* growth and *in vivo* infection of C3H/HeJ and C57BL/6J mice. In addition, we deleted each TCS in *C. rodentium* and analyzed the effect both *in vitro* and *in vivo* in an effort to determine the functional consequences of these gene deletions. This work is the first systematic study that combines RR gene expression analysis and TCS gene-deletions during *in vivo* infection of a native host using an A/E pathogen and provides valuable data for future characterization of *C. rodentium* TCSs.

MATERIALS AND METHODS

Bacterial strains, plasmids and growth conditions

All strains and plasmids used in this study are listed in Table S1 in the supplemental material. Bacteria were routinely cultured at 37°C with aeration (200 rpm) in Luria-Bertani broth (LB; 1% [w/v] tryptone, 0.5% [w/v] yeast extract, 1% [w/v] NaCl) or in N-minimal medium adjusted to pH 7.5 and supplemented with 0.2% glucose and 1 mM MgCl₂. For minimal growth conditions bacteria were cultured in M9 medium supplemented with 0.2% glucose, 2 mM MgSO₄ and 0.1 mM CaCl₂. When appropriate, LB was supplemented with chloramphenicol (Cm; 30 μg/ml), or DL-diaminopimelic acid (DAP; 50 μg/ml).

RNA extraction and cDNA synthesis

Total RNA was extracted from *in vitro*- and *in vivo*-harvested samples using TRIzol reagents according to the manufacturer's instructions. Contaminating DNA was removed using the TURBO DNase I from the TURBO DNA-*free* kit (Ambion). The absence of contaminating DNA was confirmed by qPCR using *rpoD* primers (Table S2). The concentration and purity of extracted RNA were analyzed by measuring the absorbances at 260 and 280 nm using a NanoDropTM ND-2000 spectrophotometer (Thermo Scientific). First strand cDNA synthesis was performed on 100 ng total RNA collected from *C. rodentium* cells grown *in vitro* or on 1 μg total RNA isolated from the mouse colon samples using Superscript III (Life Technologies) as specified by the manufacturer. As a negative control, a reaction mixture without Superscript III (NRT) was included for each sample.

Primer design for in vivo qPCR

C. rodentium-specific primers were designed using Primer-BLAST software [237]. For each gene, primers and size of the expected amplicons are listed in Table S2. Primers were screened for the unintended amplification of *Mus musculus*, *Escherichia coli*, and other *Citrobacter* species. cDNA isolated from uninfected C3H/HeJ and C57BL/6J mice or a pure culture of *C. rodentium* was used to test the specificity of the primer pairs.

qRT-PCR

qPCR reactions were performed in a Rotor-Gene 3000 thermal cycler (Corbett Research) using the Maxima SYBR Green qPCR kit (Thermo Scientific), according to the manufacturers' instructions. All reactions were performed in triplicate. The NRT samples were used as negative controls to assure that the samples were free of genomic DNA. Relative expression levels of genes were calculated by normalizing the threshold cycle (C_T) of the assayed genes to the C_T of the endogenous control PCD gene. The comparative C_T method ($2^{-\Delta ACT}$ or $2^{-\Delta CT}$) was used to calculate relative quantification of gene expression as described in [238]. The primary sigma factor PCD (σ^{70}) was chosen as an internal control because expression of PCD in E. PCD in E and E independent of the growth phase [239]. Results are expressed as the means E D of three experiments performed in triplicate for each gene transcript. A threshold cycle value of 40, which is the limit of detection of our assay, was assigned to samples that did not emit fluorescence during a qPCR cycle and is denoted by a dashed line in our results.

In vivo C. rodentium infections

All animal experiments were performed under conditions specified by the Canadian Council on Animal Care and were approved by the McGill University Animal Care Committee. C57BL/6J and C3H/HeJ mice were purchased from the Jackson Laboratory (Bar Harbor, ME, USA) and maintained in a specific pathogen-free facility at McGill University. Four-week old mice were orally gavaged with C. rodentium strains. For oral inoculations, bacteria were grown for 17.5 h in 3 ml of LB with aeration. Mice were infected by oral gavage of 0.1 ml of overnight culture containing $2-3 \times 10^8$ CFUs of C. rodentium. The infectious dose was verified by plating of serial dilutions of the inoculum on MacConkey agar (Difco). For RNA analysis, three mice were infected for each time point. C3H/HeJ mice were sacrificed on day 4 and day 9 post-infection and C57BL/6J mice were sacrificed on day 9 post-infection. The terminal centimeter of distal colon was collected from infected mice, homogenized in 1 ml of TRIzol using a polytron homogenizer (Kinematica) and stored at -80°C. For survival analysis, the mice were monitored daily and were euthanized if they met any of the following clinical end points: 20% body weight loss, hunching and shaking, inactivity, body condition score <2. To determine colonization-levels of mice, mice were euthanized on day 6 or 9 post-infection and bacterial loads were enumerated in the entire colon after weighing and homogenization in 1 ml of sterile phosphate-buffered saline (PBS) using a polytron homogenizer. Homogenates were serially diluted in sterile PBS and 0.1 ml aliquots of each serial dilution were plated on MacConkey agar. Plates containing between 30 and 300 colonies were counted. When bacterial loads were low, leading to the undiluted sample plate having <30 colonies, the number of colonies on this plate was counted. For histological analysis, the last 0.5 cm of the colon of infected mice was fixed in 10% neutral-buffered formalin, processed, cut into 3 µm sections and stained with haematoxylin and eosin. An expert veterinary pathologist performed histological analysis in the histology facility at the Life Sciences Complex in McGill University.

Construction of deletion strains

The bacterial strains and plasmids used in this study are listed in Table S3. DH5 α and DH5αλpir were routinely used for genetic manipulations. DNA purification, cloning, and transformation were performed according to standard procedures [240]. The C. rodentium deletion strains were generated by sacB gene-based allelic exchange [241]. Genomic DNA from C. rodentium was used as a template to PCR-amplify the upstream (primer pairs 1 and 2; Table S3) and downstream (primer pairs 3 and 4; Table S3) sequences of a TCS operon or RR gene. The upstream and downstream regions of the uvrY gene were then used directly in an overlap PCR. For all other constructs, the resultant PCR products corresponding to the upstream and downstream regions of the TCS or RR genes were treated with XhoI, NheI or KpnI, as appropriate (Table S3), purified, and ligated together. An aliquot of the ligation mixtures was used as a template to PCRamplify the entire product using primer pairs 1 and 4 (Table S3). The resultant PCR products were treated with the appropriate restriction enzymes, found within the sequences of primer pairs 1 and 4 (Table S3), then ligated into pRE112 that had been treated with the same restriction enzymes generating the suicide vectors used for homologous recombination. The sequences of these plasmids were verified by sequencing (Genome Québec). The suicide vectors were conjugated into wild-type C. rodentium using E. coli χ7213 as the donor strain. Integration of the plasmid into the chromosome was selected for by plating bacteria on LB agar supplemented with Cm. Cmresistant transformants of C. rodentium were then plated on peptone agar containing 5% sucrose to isolate colonies that were sucrose resistant. The resultant colonies were also tested for Cm sensitivity. Gene deletions were verified by PCR using primer pairs 1 and 4 (Table S3).

Adherence assays

In vitro adherence assays of *Citrobacter rodentium* were performed as previously described [242]. Briefly, HeLa cells were seeded at a concentration of 5.0x10⁴ cells/coverslip, and incubated for 24 h before infection. Cells were incubated for 30 min in 1ml of DMEM (Life Technologies), supplemented with 2% fetal bovine serum. Cells were infected with an overnight culture of *C. rodentium* DBS100 or Δ*arcA* at a MOI of 1:100, for 8 h at 37°C with 5% CO₂. Coverslips were washed 3 times with PBS to remove non-adherent bacteria, and fixed in 2.5% paraformaldehyde for 15 min. Monolayers were then washed 3 X 5 min with PBS, and permeabilized with PBS supplemented with 0.1% Triton X-100. Coverslips were blocked in PBS containing 0.1% Triton X-100 and 2% BSA, overnight at 4°C. Cells were then incubated with anti-Citrobacter LPS rabbit polyclonal antibody for 1 h, followed by three washes with PBS containing 0.1% Triton X-100 and incubation with anti-rabbit Alexa 488 and DAPI for 30 min. Coverslips were subsequently mounted in Prolong Gold and imaged on a Zeiss Axiovert 200M microscope with a Zeiss Axiocam Monochrome camera. Ten fields of view were imaged per sample, and the number of *C. rodentium* per cell was calculated. The adherence of the wild-type strain was set at 100%.

Fluorescent microscopy

C3H/HeJ mice were infected with *C. rodentium* as described above. Mice were sacrificed on day 6 post-infection ($\Delta uvrY$) and day 9 post-infection ($\Delta rcsB$, $\Delta arcA$). The third most distal centimeter of colon was fixed in 10% neutral-buffered formalin, paraffin-embedded and cut into 4

μm sections. The paraffin-embedded samples were deparaffinized in xylene twice for 5 min, followed by a rehydration in a gradient of ethanol and water: 100% ethanol twice for 5 min, 95% ethanol for 5 min, 70% ethanol for 5 min and dH₂O for 5 min. Antigen recovery was completed by boiling the slides in a solution of citric acid and sodium citrate for 10 min. The slides were washed with PBS containing 0.2% Tween 20 and blocked in PBS containing 0.2% Tween 20, 3% BSA and 10% FBS for 1 hour at 37°C, and incubated with anti-Citrobacter LPS rabbit polyclonal antibody in PBS containing 0.2% Tween 20 and 3% BSA at 4°C for 3 h. Slides were then incubated in anti-rabbit Alexa 488 (Life Technologies) in PBS containing 0.2% Tween 20 and 3% BSA for 1 h at 37°C, followed by 5 min in DAPI (Sigma) in PBS containing 0.2% Tween 20 and 3% BSA. Slides were then mounted in Prolong Gold (Life Technologies), and on a Zeiss Axiovert 200M microscope with a Zeiss Axiocam Monochrome camera.

Secretion Assays

Bacterial secretion assays were performed as described elsewhere [243]. Briefly, overnight cultures of bacteria were subcultured 1:50 into 6-well tissue culture plates containing Dulbecco's modified eagle medium (DMEM; Gibco) and incubated for 6 h at 37°C with 5% CO₂. After incubation, whole cells were separated from the culture medium by centrifugation. The supernatants were transferred to clean tubes and the bacterial pellets, now referred to as whole cell lysates, were resuspended in electrophoresis sample buffer (ESB; 0.0625 M Tris-HCl [pH 6.8], 1% [w/v] SDS, 10% glycerol, 2% [v/v] 2-mercaptoethanol, 0.001% [w/v] bromphenol blue), boiled and stored at -20°C. Contaminating cells in the supernatant were removed by centrifugation $(13,000 \times g, 2 \text{ min})$. The proteins in the supernatant, now referred to as secreted proteins, were precipitated with 10% (v/v) 6 M trichloroacetic acid. Precipitated secreted proteins were collected

by centrifugation (13,000 \times g, 30 min at 4°C), washed with ice-cold acetone, air-dried, and resuspended in ESB. Protein samples were boiled and aliquots were separated on 10% SDS-PAGE gels and visualized by coomassie blue staining. or transferred onto PVDF membranes for western blot analyses using anti-DnaK (Stressgen) or anti-EspB (Clone 2A11) antibodies.

Congo red binding

Congo red binding assays were used to monitor putative changes in the structures present on the surface of *C. rodentium* colonies. Briefly, bacteria were inoculated onto LB or YESCA (1% [w/v] casamino acids, 0.1% [w/v] yeast extract, 2% [w/v] agar) media supplemented with Congo red (0.002% [w/v]) and incubated for 16 h at 37°C aerobically or anaerobically [244]. The next day, colonies that were red were determined to have bound congo red and those that remained white did not.

RESULTS

Global analyses of TCS gene expression in vitro and in vivo

The TCSs encoded by *C. rodentium* are listed in Table S4. To assess expression of the 26 putative RR genes *in vitro*, qPCR was performed using cDNA prepared from *C. rodentium* cells grown to mid-log phase in both LB and DMEM. Relative expression levels were normalized to the expression of the control gene *rpoD* and data were analyzed using the 2^{-ΔCT} method [238]. Similar results were obtained when 16S was used as the control gene (data not shown). As shown in Figure 1A, the expression level of the 26 RR genes was heterogeneous and spread over 4 logs. Notably, whereas all RR genes were significantly expressed in DMEM, the expression of five RR genes (*creB*, *fusR*, *pmrA*, *qseF*, and *yedW*) was below the detection limit in the LB-grown samples, indicating that they are not significantly expressed under this growth condition (Fig. 1A). In addition, several genes were differentially expressed in the two *in vitro* growth conditions: expression of *baeR*, *ompR*, and *ypdB* was increased by at least 2-fold and expression of *dpiA*, *phoP*, *rcsB*, *uvrY*, and *zraR* was decreased by at least 2-fold in DMEM compared to LB (Fig. 1A). Overall, these data show that several RR genes are differentially expressed during growth in LB and DMEM and that all 26 RR genes are expressed during growth in DMEM.

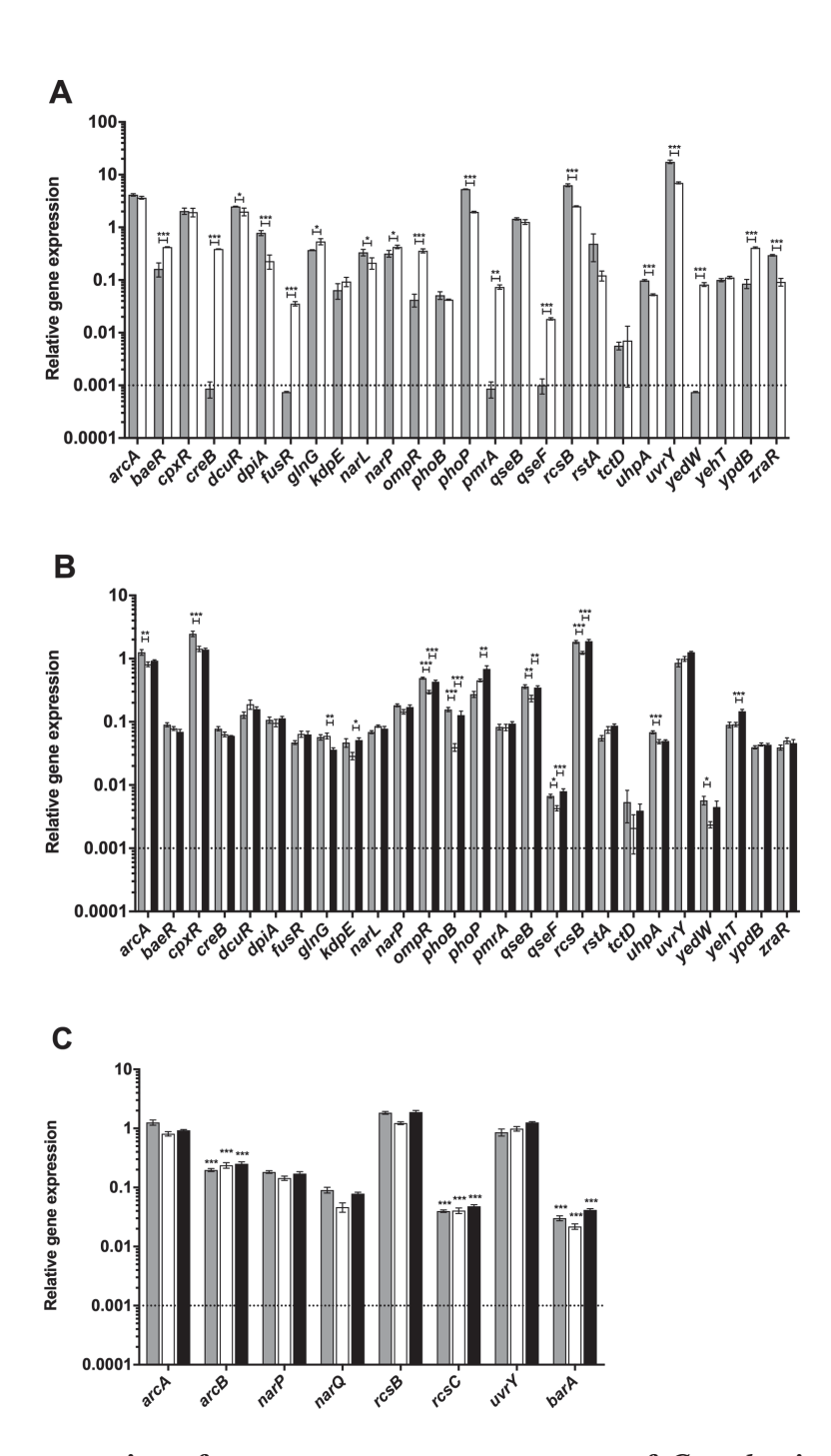


FIG 1. Relative expression of two-component system genes of *C. rodentium in vivo* and *in vitro*. Real-time RT-PCR was performed to detect expression levels of each RR gene relative to the primary sigma factor, *rpoD*. Dotted lines indicate the limit of detection of the assay. (A) Total RNA was prepared from *C. rodentium* cultures grown in DMEM (gray bars) and LB broth (open bars). (B) Total RNA was prepared from the terminal centimeter of the colon of infected C3H/HeJ

mice on day 4 (gray bars) and day 9 (open bars) postinfection and C57BL/6J mice on day 9 (black bars) postinfection. An analysis of variance (ANOVA) followed by Tukey's post hoc analysis was used to determine statistical significance for both in vitro and in vivo growth (***, P < 0.001; **, P < 0.01; *, P < 0.05). (C) Expression levels of the RR genes arcA, narP, rcsB, and uvrY and their unlinked cognate HK sensor genes, arcB, narQ, rcsC, and barA, were measured by real-time RT PCR using total RNA samples described for panel B. An unpaired t test was used to determine statistical significance between each HK sensor gene and its cognate RR from the same in vivo condition (***, P < 0.001).

To assess the expression of the 26 C. rodentium RR genes during intestinal infection, qPCR was performed using cDNA prepared from total RNA isolated from the distal colons of infected mice at day 4 and 9 post-infection. We assessed RR expression in both innately susceptible C3H/HeJ and more resistant C57BL/6J mice, since we hypothesized that the intestinal environment would differ significantly between these two models. Robust and reproducible C. rodentium gene expression signals were obtained from C3H/HeJ mice at days 4 and 9 postinfection, whereas in C57BL/6J mice, reproducible C. rodentium gene expression data was only obtained from the day 9 post-infection samples. This is likely due to the comparatively lower loads of C. rodentium in C57BL/6J mouse colons during early infection [60]. To ensure that the expression measured was the result of the specific amplification of transcripts from C. rodentium, control qPCR experiments were performed on cDNA prepared from total RNA isolated from uninfected C3H/HeJ and C57BL/6J mice using all TCS primer pairs, except cpxR and rpoD that we previously validated using the same criteria [243]. As expected, all primer pairs were unable to amplify a product from uninfected murine samples, indicating that the signals detected are C. rodentium-specific and not the result of unwanted amplification of microbiota or murine genes (data not shown).

Notably, all 26 RR genes were significantly expressed during infection of both mouse strains and at both time points examined in C3H/HeJ mice (Fig. 1B). Overall, there was a large range in the expression levels of the different RR genes in infected mice with a 100 to 1,000-fold difference between the most and the least expressed genes. In all infection conditions, the most highly expressed RR genes were *arcA*, *cpxR*, *rcsB*, and *uvrY*, which were all expressed at levels similar to *rpoD* (Fig. 1B). Importantly, several RR genes were differentially expressed between

the C3H/HeJ and C57BL/6J murine strains at day 9 post-infection (*ompR*, *phoB*, *qseF*, *rcsB*, *yehT*, *glnG*, *phoP*, *qseB*, *kdpE*). Additionally, several RR genes were differentially expressed at the two time points of infection in C3H/HeJ mice (*cpxR*, *ompR*, *phoB*, *rcsB*, *uhpA*, *arcA*, *qseB*, *qseF* and *yedW*). These data indicate that there are differences in RR gene expression between the lethal and non-lethal murine infection models and at different time points of infection.

Although most TCS genes are organized in operons, the *arcA/arcB*, *narP/narQ*, *rcsB/rcsC*, and *uvrY/barA* TCSs are part of different transcriptional units in the *C. rodentium* genome. As shown in Fig. 1C, as assessed by qPCR, all unlinked HK genes were significantly expressed *in vivo*. Most HK sensor genes were expressed at lower levels than their respective RR genes, which is not unprecedented, since lower HK than RR transcript levels were also observed *in vivo* for the linked *cpxRA* TCS [243].

Assessment of the roles of C. rodentium TCSs in bacterial virulence

To systematically assess the roles of the *C. rodentium* TCSs in bacterial virulence during intestinal infection, we used sacB-gene based allelic exchange to generate bacterial strains bearing individual in-frame deletions for each of the 26 TCSs in *C. rodentium*. For those TCSs where the HK and RR are expressed as an operon, both the HK and RR were deleted. In the case of unpaired TCSs, only the RR was deleted. The primers used to generate the deletion strains are provided in Table S3. Prior to testing our strains in a murine infection, we subjected our mutants to a panel of *in vitro* tests to analyze carbohydrate assimilation, growth rate, oxygen requirements and stress tolerance. The $\Delta dpiAB$ and $\Delta phoPQ$ strains were unable to use citrate as a secondary carbon source, the $\Delta arcA$ strain was no longer able to catalyze the decarboxylation of ornithine into

putrescine and the $\triangle arcA$ and $\triangle cpxRA$ strains were slightly more susceptible to alkaline pH (data not shown). Other than the differences listed above, the deletion strains behaved similarly to the wild-type and were then used to assess the contribution of each TCS to *C. rodentium* virulence in C3H/HeJ mice.

Of the 26 TCS-knockout strains tested, 19 were not significantly different from wild-type $C.\ rodentium$ in terms of mean survival time following infection (Fig. S1). Consistent with our previous data [243], the $\Delta cpxRA$ deletion mutant was highly attenuated for virulence, with 100% survival of mice infected with this strain (Fig. 2). Five additional TCS deletion strains ($\Delta arcA$, $\Delta rcsB$, $\Delta rstAB$, $\Delta uhpAB$, $\Delta zraRS$) were also significantly attenuated for virulence; mice infected with these strains displayed delayed mortality, with some mice surviving infection in the case of $\Delta rcsB$ (Fig. 2). Surprisingly, deletion of uvrY resulted in a $C.\ rodentium$ strain with increased virulence. Mice infected with this strain had a significantly shorter mean survival time than mice infected with wild-type $C.\ rodentium$ (Fig. 2).

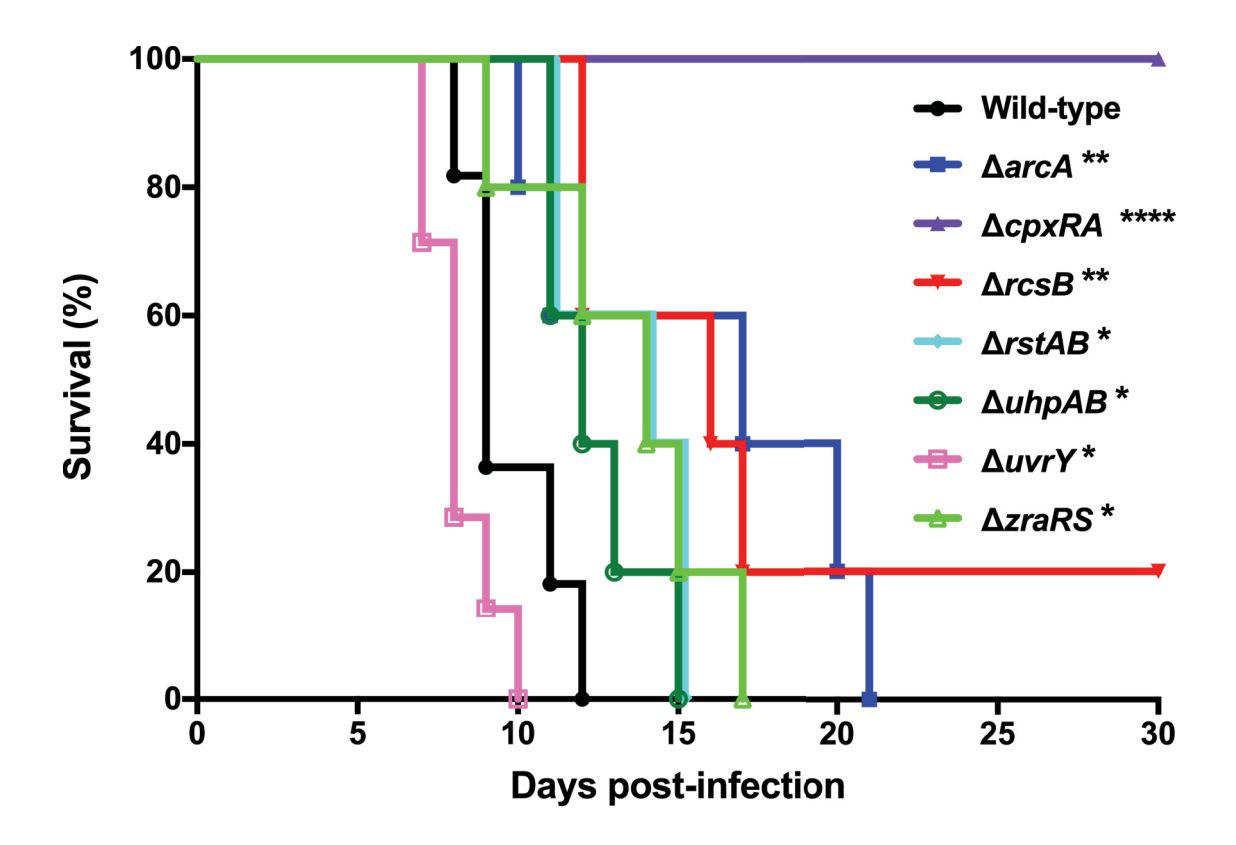


FIG 2. Survival of female C3H/HeJ mice after infection with *C. rodentium*. Animals were orally gavaged with 2×10^8 to 3×10^8 CFU of *C. rodentium* wild type or a TCS deletion strain. Animals were monitored for 30 days postinfection as described in Materials and Methods. The data are pooled from two independent experiments with 5 to 7 mice per group. The log rank (Mantel-Cox) method was used to determine statistical significance (****, P < 0.0001; **, P < 0.01; *, P < 0.05).

To further investigate the attenuation of the $\triangle arcA$, $\triangle rcsB$, $\triangle rstAB$, $\triangle uhpAB$, and $\triangle zraRS$ strains we monitored the shedding of *C. rodentium* in the feces, indicative of total bacterial burden, at days 3, 6, and 9 post-infection as well as overall histopathology at day 9 post-infection (Fig. 3). The already described wild-type and $\Delta cpxRA$ strains were included in these analyses as controls [243]. As expected, wild-type C. rodentium loads increased swiftly and steadily during the course of infection, reaching a peak of between 10⁹ and 10¹⁰ CFUs /g of feces by day 9 post-infection. In contrast, and in agreement with our previous data, the $\Delta cpxRA$ strain displayed delayed colonization with lower levels of colonization at all time points, and greater variability in bacterial burden than the wild-type strain [243]. Of the other TCS deletion strains analyzed, only the $\Delta arcA$ mutant displayed significantly lower colonization levels than the wild-type strain (Fig. 3A-C). The other attenuated strains colonized mice to similar levels as wild-type C. rodentium at all time points, suggesting that the attenuation of these strains is unrelated to decreased or delayed bacterial colonization. Additionally, the only TCS deletion strain with significantly different pathology scores from the wild-type strain on day 9 post-infection was $\Delta cpxRA$, as we previously described [243] (Fig. 3D).

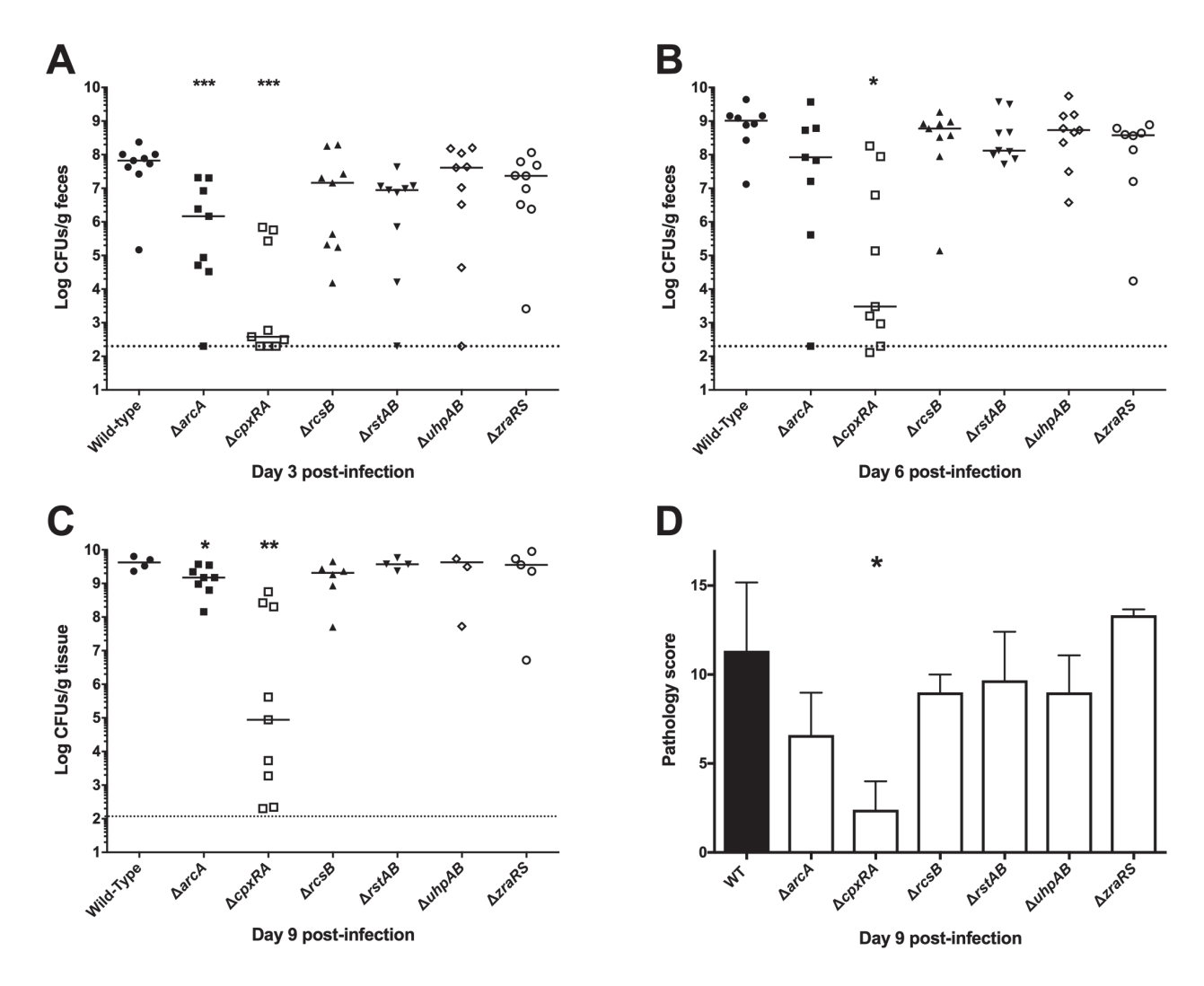


FIG 3. Bacterial burden and pathology scoring in female C3H/HeJ mice infected with hypovirulent mutants of C. rodentium. Susceptible mice were orally gavaged with 2×10^8 to 3×10^8 CFU of C. rodentium wild type or a TCS deletion strain, and fecal burden of C. rodentium was assessed at days 3 (A), 6 (B), and 9 (C) postinfection by plating on MacConkey agar and counting CFU. At day 9, due to significant illness manifestation, in the absence of fecal matter, colon was homogenized and plated. By day 9 postinfection, several of the mice infected with the wild type and the less attenuated TCS deletion strains had succumbed to infection, leading to fewer samples analyzed at this time point in those groups. Dotted lines indicate the limit of detection of the assay. The data are pooled from two experiments with 4 to 5 mice per group per

experiment. A Mann-Whitney test was used to determine statistical significance (***, P < 0.001; **, P < 0.01; *, P < 0.05). (D) The last 0.5 cm of the colon of infected mice was stained by hematoxylin and eosin, and histological scoring was performed in a blinded fashion by a board-certified veterinary pathologist, as described in reference [239]. An unpaired t test was used to determine statistical significance between each TCS deletion strain and the wild-type strain (*, P < 0.05).

Virulence-associated phenotype of C. rodentium $\triangle arcA$

Figure 2 demonstrates that the three TCSs with the greatest influence on C. rodentium virulence are ArcAB, CpxRA, and RcsBC. We previously characterized the $\Delta cpxRA$ mutant [243]. We next sought to perform a more detailed analysis of the consequences of arcA deletion on C. rodentium virulence. To further investigate the colonization defect of this strain (Fig. 3)., we examined the localization of the bacteria in vivo, in colonic cross sections taken from mice at day 9 post-infection (Fig. 4A). At this time point, wild-type C. rodentium localized mainly to the colonic mucosal surface, in some cases extending more deeply into the crypts and with a minor proportion found within the lumen (Fig. 4A; top panels). In agreement with the bacterial load data (Fig. 3), staining of tissue sections revealed lower amounts of *C. rodentium* present in sections of mice infected with the $\triangle arcA$ strain compared to mice infected with the wild-type strain (Fig. 4A). However, the C. rodentium that was present in the $\triangle arcA$ -infected colon sections localized to the mucosal surface, similar to what was seen for the wild-type bacteria (Fig. 4A; bottom panels). We also tested the $\triangle arcA$ strain in an *in vitro* HeLa cell adherence assay and found it to be significantly deficient for in vitro cell adherence (Fig. 4B). C. rodentium adherence in vitro and colonization in vivo are both strongly enhanced by the secretion of effectors through the bacteria's type III secretion system (T3SS). Therefore, we tested the $\triangle arcA$ strain for T3SS function using an *in vitro* secretion assay. As shown in Figures 4C and S2, T3S was severely affected in the $\Delta arcA$ strain, but functional in all other TCS deletion strains. Furthermore, qPCR analysis demonstrated significant decreases in the expression of the T3SS translocator genes espA and espB in the arcA mutant (Fig. 4D and E). Thus, we propose that C. rodentium $\Delta arcA$ is attenuated for virulence because of a defect in the regulation of the T3SS, leading to a significant impairment in its ability to colonize the host.

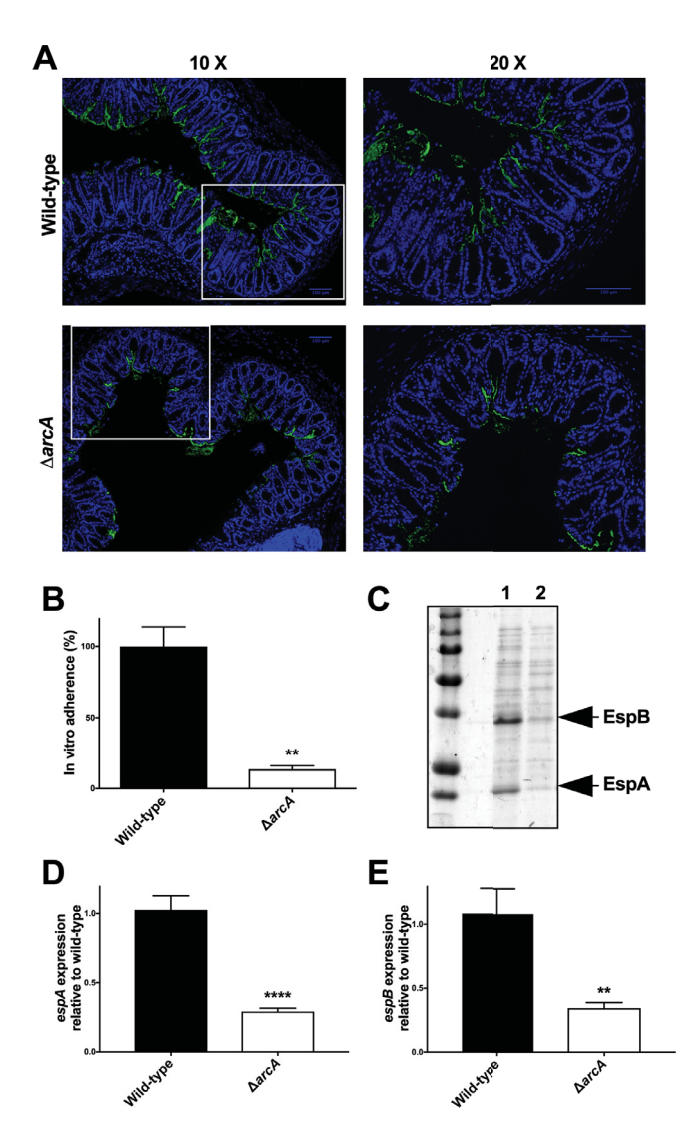


FIG 4. Attenuation of *C. rodentium* $\Delta arcA$ strain. (A) Localization of *C. rodentium* wild-type and $\Delta arcA$ strains in distal colon samples of day 9 infected susceptible mice. Sections were stained with DAPI (blue) and anti-*Citrobacter* LPS (green). Panels on the right show a zoomed-in view of the boxed areas in the panels on the left. Scale bars, 100 µm. (B) In vitro adherence assay. HeLa cells were infected with *C. rodentium* wild-type and $\Delta arcA$ strains for 8 h. After extensive washing, the samples were fixed and stained with DAPI and anti-*Citrobacter* LPS. The total number of bacteria per HeLa cell was counted, and adherence was expressed as a percentage of wild-type adherence levels. An unpaired t test was used to determine statistical significance (**, P < 0.01). (C) Total secreted proteins of the *C. rodentium* wild-type (lane 1) and $\Delta arcA$ (lane 2) strain were

prepared, separated on a 10% SDS-PAGE gel, and stained with Coomassie blue. The positions of two of the major T3SS-secreted proteins, EspA and EspB, are indicated with arrows to the right of the gel. (D and E) Expression levels of the espA (D) and espB (E) genes by C. rodentium wild-type and $\Delta arcA$ strains were measured by real-time RT-PCR. Data were normalized to rpoD expression levels. Statistical significance was assessed by performing an unpaired t test (****, P < 0.0001; **, P < 0.01).

Virulence-associated phenotype of C. rodentium $\triangle rcsB$

We next further investigated the attenuation of C. rodentium $\Delta rcsB$ that had a significant virulence defect, but unlike $\Delta arcA$, did not display a significant difference in intestinal colonization levels. As above, we examined the localization of the bacteria, in comparison with wild-type C. rodentium, within infected colon cross sections (Fig. 5A). As described above, wild-type C. rodentium localized to the colonic mucosal surface, with some bacteria extending more deeply into the crypts and a minor proportion of cells within the lumen (Fig. 5A; top panels). In contrast, a higher proportion of C. rodentium $\Delta rcsB$ localized to the intestinal lumen, with a lower proportion than wild-type at the mucosal surface and/or penetrating into the crypts (Fig 5A; bottom panels). In contrast to the $\Delta arcA$ mutant, C. rodentium $\Delta rcsB$ was not deficient in T3SS function (Fig. S2).

A recent report indicated that EHEC $\Delta rcsB$ displays diminished binding of the dye Congo Red, suggesting alterations in its surface structures [245]. We found that the *C. rodentium* $\Delta rcsB$ strain had increased Congo Red binding under all growth conditions tested (Table S5). While the Congo red binding data are different from the result reported for EHEC, both results suggest alterations to surface structures in these strains. In other bacteria, rcsB is known to be required for the regulation of the wca operon, in which wcaA is the first gene of the operon coding for a glycosyl transferase implicated in the production of the capsular component colanic acid [246]. To test if the wca operon was affected by deletion of rcsB in C. rodentium, we examined expression of wcaA in the wild-type and $\Delta rcsB$ strains using qPCR. We found the $\Delta rcsB$ strain to be strikingly deficient in wcaA expression (Fig. 5B). Although this requires further investigation, we hypothesize that the virulence defect in C. rodentium $\Delta rcsB$ may be related to alterations in surface structures, potentially including colanic acid.

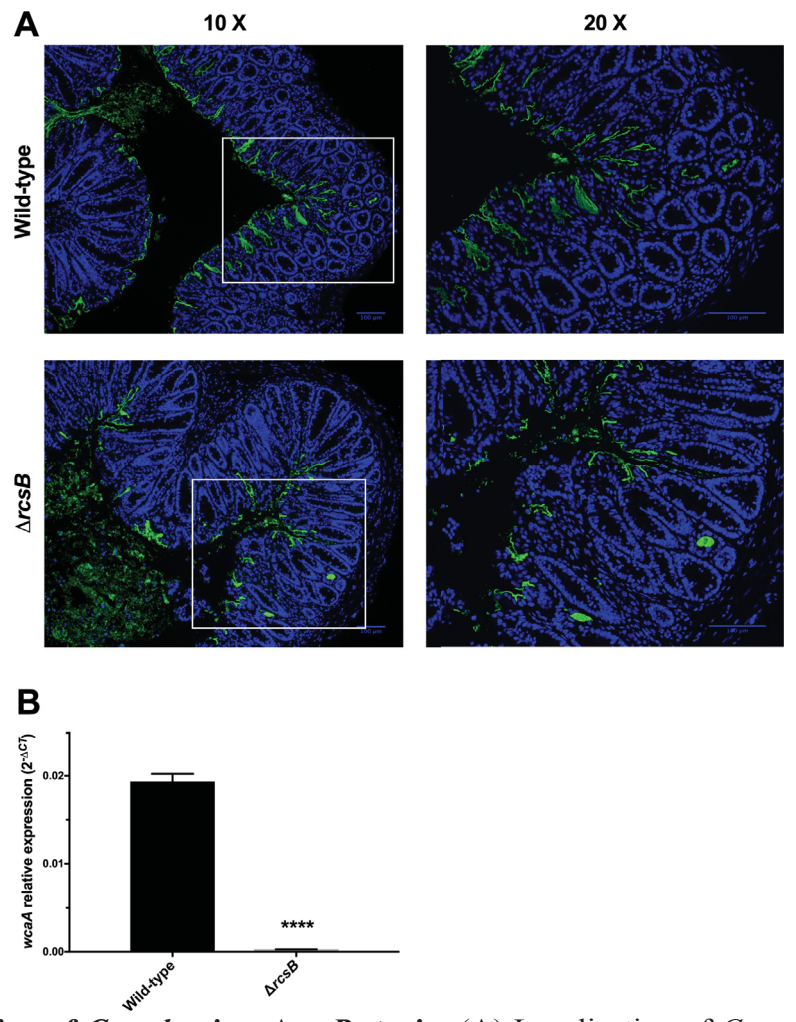


FIG 5. Attenuation of *C. rodentium* $\Delta rcsB$ strain. (A) Localization of *C. rodentium* wild-type and $\Delta rcsB$ strains in distal colon samples of day 9 infected susceptible mice. Sections were stained with DAPI (blue) and anti-*Citrobacter* LPS (green). Panels on the right show a zoomed-in view of the boxed areas in the panels on the left. Scale bars, 100 µm. (B) Total RNA was extracted from wild-type- and $\Delta rcsB$ strain-infected mouse colons, and real-time RT PCR was performed to detect levels of the wcaA gene relative to the primary sigma factor, rpoD. An unpaired t test was used to determine statistical significance (****, P < 0.0001).

Investigation of increased virulence of C. rodentium $\Delta uvrY$

In addition to the investigations performed above for the most attenuated TCS deletion strains, we also wanted to perform a more detailed characterization of the increased virulence of C. rodentium $\Delta uvrY$. We analyzed the colonization of the $\Delta uvrY$ strain at days 3 and 6 postinfection and found that fecal loads were not significantly different in mice infected with $\Delta uvrY$ compared to wild-type C. rodentium (Fig. 6A). Thus, the increased virulence of the $\Delta uvrY$ strain is not due to increased bacterial replication and/or survival in the host intestinal tract. However, we did note a significant increase in the amount of C. rodentium present in the mesenteric lymph nodes of mice infected with the $\Delta uvrY$ strain (Fig. 6B), indicating an enhanced ability of the $\Delta uvrY$ strain to translocate from the intestine to this site or an enhanced ability to resist bacterial killing once translocated. We examined the localization of the bacteria, in comparison with wild-type C. rodentium, within infected colon cross sections (Fig. 6C). Because of the increased mortality at early time points in $\Delta uvrY$ -infected mice, we assessed this at day 6 post-infection. At this time point, wild-type C. rodentium localized mainly to the colonic mucosal surface, with less bacteria extending into the crypts than was observed at day 9 post-infection (Fig. 6C; compare with Fig. 4A and 5A). The localization of C. rodentium $\Delta uvrY$ was indistinguishable from that of wild-type bacteria (Fig. 6C). In addition, the $\Delta uvrY$ strain was indistinguishable from wild-type C. rodentium in the T3SS assay (Fig. S2), indicating that the enhanced virulence of C. rodentium $\Delta uvrY$ is unlikely to be attributed to enhanced intestinal colonization, cell adherence, or T3S.

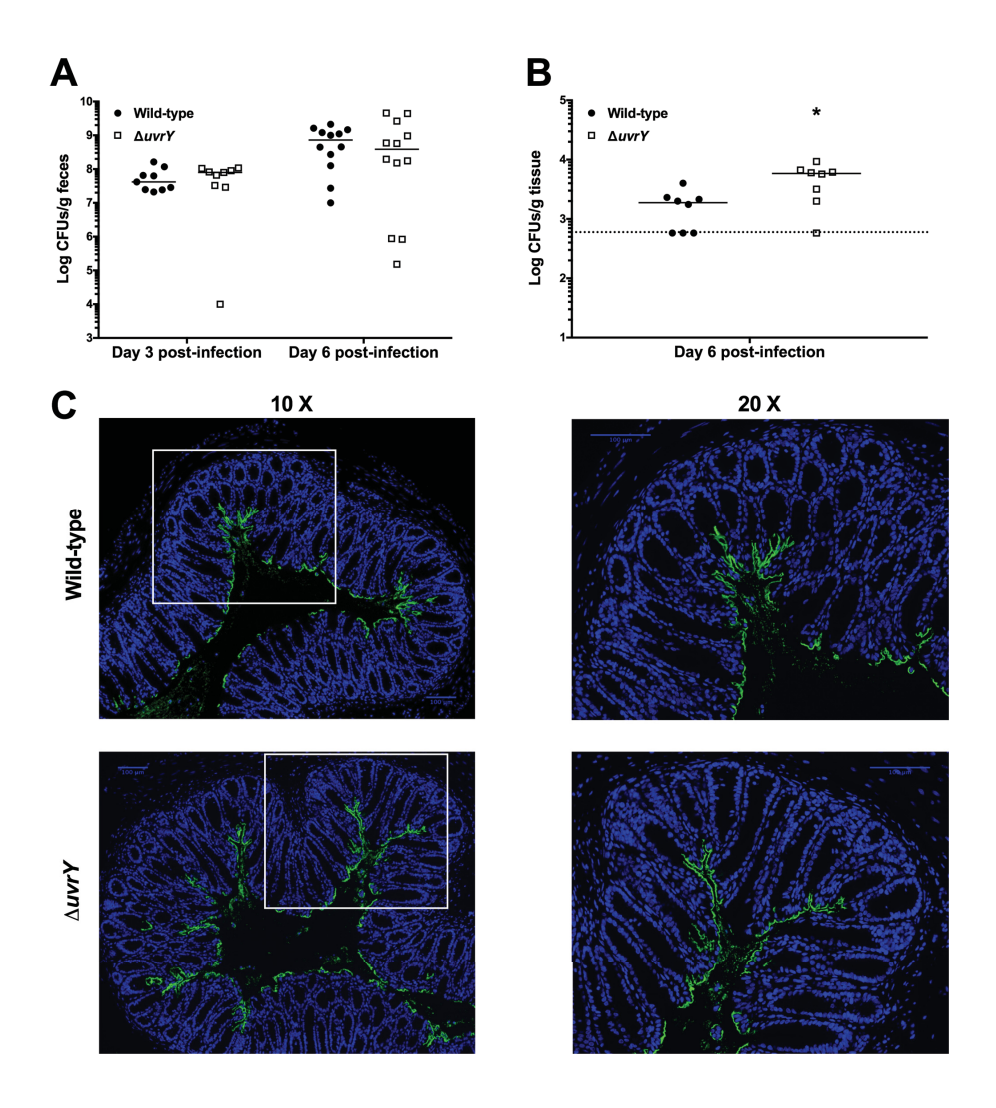


FIG 6. Increased virulence of *C. rodentium* $\Delta uvrY$ strain. Susceptible mice were orally gavaged with 2×10^8 to 3×10^8 CFU of the *C. rodentium* wild-type or $\Delta uvrY$ strain. (A) Fecal bacterial burden was assessed at days 3 and 6 postinfection. The data are pooled from two experiments (day 3) and 3 experiments (day 6) with 4 to 5 mice per group per experiment. (B) Mesenteric lymph node bacterial burden was assessed at day 6 postinfection by plating on MacConkey agar and enumerating CFU. The data are pooled from two experiments with 4 mice per group per experiment. A Mann-Whitney test was used to determine statistical significance (*, P < 0.05). (C) Localization of *C. rodentium* wild type and $\Delta uvrY$ strains in distal colon samples of day 6 infected susceptible mice. Sections were stained with DAPI (blue) and anti-*Citrobacter* LPS (green). Panels

on the right show a zoomed-in view of the boxed areas in the panels on the left. Scale bars, $100\,$ $\mu m.$

DISCUSSION

TCSs that typically consist of a membrane-bound HK sensor and a cytoplasmic RR are key players in bacterial adaptation to environmental changes [216]. During infection, enteric pathogens need to adapt to various environments encountered along the intestinal tract and, thus, rely on TCSs for successful colonization [247]. Here we combined a systematic in vivo study analyzing TCS gene expression with infection experiments that identify the TCSs that are necessary for C. rodentium colonization and/or virulence. This murine pathogen is used as a surrogate model to study the human-restricted pathogens EHEC and EPEC [213]. In a previous study, we showed that the C. rodentium $\Delta cpxRA$ strain was avirulent, since all mice infected with this strain survived the infection [243]. Our current results show that in addition to CpxRA, there are 5 additional TCSknockout strains with attenuated virulence (Fig. 2). In addition, we found that the $\Delta uvrY$ strain has enhanced virulence compared to wild-type. At the infectious dose used in this study, deletion of the other TCSs did not affect the survival of infected mice. Recently, Moreira et al., uncovered a role in C. rodentium virulence for the QseBC and QseFE TCSs that respond to the catecholamines epinephrine and norepinephrine in the gut [236]. However, the effect on mouse survival was only observed using a much lower infectious dose than the one used in the current study. We anticipate that using lower infectious doses may reveal additional TCSs with subtle effects on virulence. Out of the TCSs that most impact C. rodentium colonization or virulence, it is striking that two of them (i.e. CpxRA and RcsBC) are involved in envelope stress responses, indicating, perhaps unsurprisingly, that the C. rodentium envelope is subjected to extensive stress in the murine intestinal tract. It is also interesting to note that the TCSs revealed to have the most striking roles in virulence in our studies, were also the ones found to be most highly expressed in vivo, during intestinal infection (Fig. 1B).

So far, few studies performed a systematic screening of all TCSs of enteric bacteria to identify the ones involved in either colonization and/or virulence [248, 249]. PhoPQ and EnvZ/OmpR were the only two TCSs found to be critical for Yersinia pestis resistance to host innate immunity in a mouse model of plague [249, 250]. None of these two TCSs were identified in our study. While the reasons for this dissimilarity are not known, we speculate that it may be due to differences in the host-associated lifestyles of these two pathogens. In contrast, our data identifying CpxRA, ArcAB and RcsBC as TCSs that are important for C. rodentium colonization and/or virulence are in perfect agreement with the study by Lasaro et al., that found that mutation of the same TCSs produced strong colonization defects for the MP1 E. coli murine commensal strain [248]. In the current study, we also identified effects of the ZraRS, RstAB, and UhpAB TCSs on C. rodentium infection, although these TCSs appear to have a more modest role in colonization and/or virulence than CpxRA, ArcAB and RcsBC. ZraRS has been previously linked to zinc and lead-sensing, and has recently also been linked to the cell-envelope stress response to zinc [251], making it the third TCS that is likely involved in the cell-envelope stress response during in vivo infection. RstAB has been shown to be essential for infection of chickens by avian pathogenic E. coli [252]. Finally, UhpAB is involved in glucose-6-phosphate transport in E. coli. Future studies are required to investigate if this TCS detects the different levels of glucose-6phosphate present in the jejunum, duodenum and colon during infection [253].

Deletion of the *C. rodentium arcA* RR gene results in both a colonization defect and attenuated virulence (Fig. 4). The ArcAB TCS is known to control the transition from aerobic growth to microaerobic or anaerobic growth in response to the redox status of the ubiquinone electron carriers [254]. Therefore, a functional ArcAB TCS appears to be required for bacterial

adaptation to the anaerobic environment of the mouse large intestine. ArcA is also a global RR controlling transcription of a plethora of genes, including virulence genes. Remarkably, our data revealed that $\Delta arcA$ is the only strain with a defect in T3S (Fig. 4 and S2). Therefore, it is plausible that the virulence defect of $\Delta arcA$ is due to a reduced ability of this strain to translocate effector proteins, including the Tir protein, in intestinal epithelial cells.

Deletion of the rcsB RR gene results in attenuation of virulence exemplified by a delay in mouse death and the survival of some mice infected with this mutant (Fig. 2). As for the CpxRA TCS, the RcsBC TCS is also associated with envelope stress. The RcsC receptor responds to outer membrane and peptidoglycan-related stresses [254]. The RcsB-induced genes affect the cell envelope properties, including the presence of the colanic acid capsule and curli [171]. In agreement, we found that wcaA gene coding for a glycosyl transferase involved in colanic acid synthesis is poorly expressed in this mutant. In addition, enhanced binding of Congo red to the cell surface of this strain suggests that the cell surface of this mutant is perturbed. Therefore, it is plausible that the $\Delta rcsB$ mutant is either more susceptible to the host innate defences or more easily recognized by the host immune system.

Deletion of the *C. rodentium uvrY* RR gene results in a more rapid death of infected mice and increased bacterial load in the mesenteric lymph nodes (Fig. 6). The BarA/UvrY TCS controls the transcription of the small RNA genes *csrB* and *csrC* that interact with the RNA-binding protein CsrA and, in turn, prevent its interaction with its mRNA targets [255, 256]. By antagonizing CsrA, BarA/UvrY regulates carbon metabolism, biofilm formation, motility and virulence in Proteobacteria [257]. The fact that inactivation of a TCS results in increased virulence is not

unprecedented, inactivation of the CovRS (CsrRS) TCS in the Gram-positive pathogen *Streptococcus pyogenes* results in the up-regulation of various virulence factors, including the hyaluronic acid capsule, streptolysin S, streptokinase and the cysteine protease SpeB [258]. In light of this study, we hypothesize that *C. rodentium* UvrY also acts as an indirect negative regulator of virulence genes.

TCSs are the main signal transduction systems in bacteria and are absent from mammalian cells. As such, they are promising targets for the development of novel antimicrobial drugs [259, 260]. The TCSs we have identified in this study impact intestinal colonization and/or virulence of *C. rodentium*, a mouse pathogen that serves as a model for human pathogens such as EHEC and other Shiga toxin-producing *E. coli*. Since the use of classical antibiotics to treat these infections is controversial, due to the risk of increased Shiga toxin production and release, antivirulence approaches such as targeting TCSs may provide novel treatment options. Studies on the TCSs identified here, including genetic complementation of the mutants, further elucidation of the mechanisms underlying the virulence effects, and investigation as to their conservation of function in related human pathogens will be important future directions to pursue.

ACKNOWLEDGEMENTS

We thank Mr. Eugene Kang for the gift of cDNA and Dr. Yannick D. Tremblay for helpful discussion.

FUNDING INFORMATION

This work was supported by grants from the Fonds de Recherche du Québec - Nature et Technologies (FRQNT 2013-PR-165926) to H.L.M., S.G. and F.D. and from the Canadian Institutes of Health Research (CIHR, MOP-15551) to H.L.M. and S.G.. S.G. is supported by a Senior Chercheur-Boursier award from the Fonds de Recherche du Québec – Santé (FRQS). J.-L.T. was supported by a Hugh Burke fellowship from the McGill Faculty of Medicine.

SUPPLEMENTARY INFORMATION

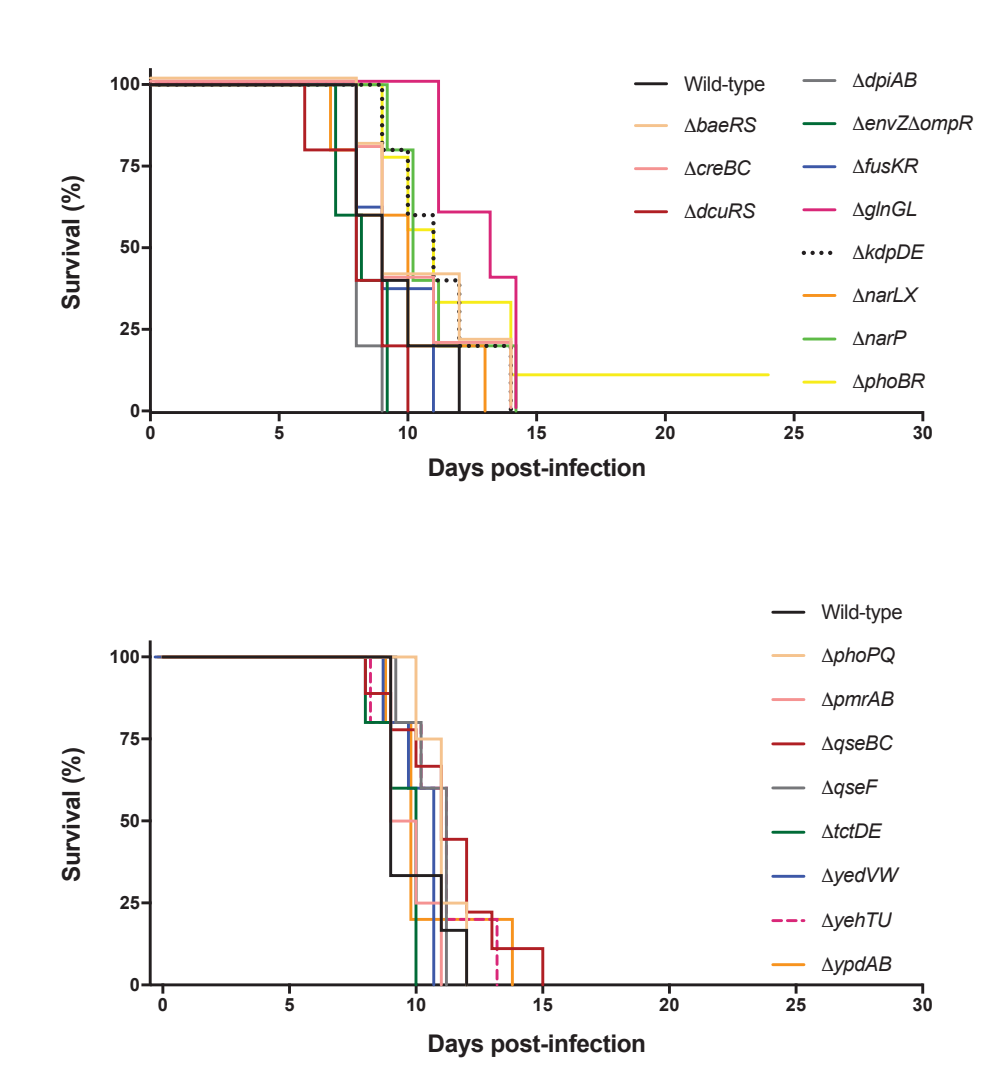


Fig S1. Survival of female C3H/HeJ mice after infection with *C. rodentium*. Animals were orally gavaged 2-3x10⁸ CFUs of *C. rodentium* wild-type or a TCS deletion strain. Animals were monitored for 30 days post-infection as described in the materials and methods (n=5-7). The log rank (Mantel-Cox) method was used to test for statistical significance, none were significantly different from wild-type.

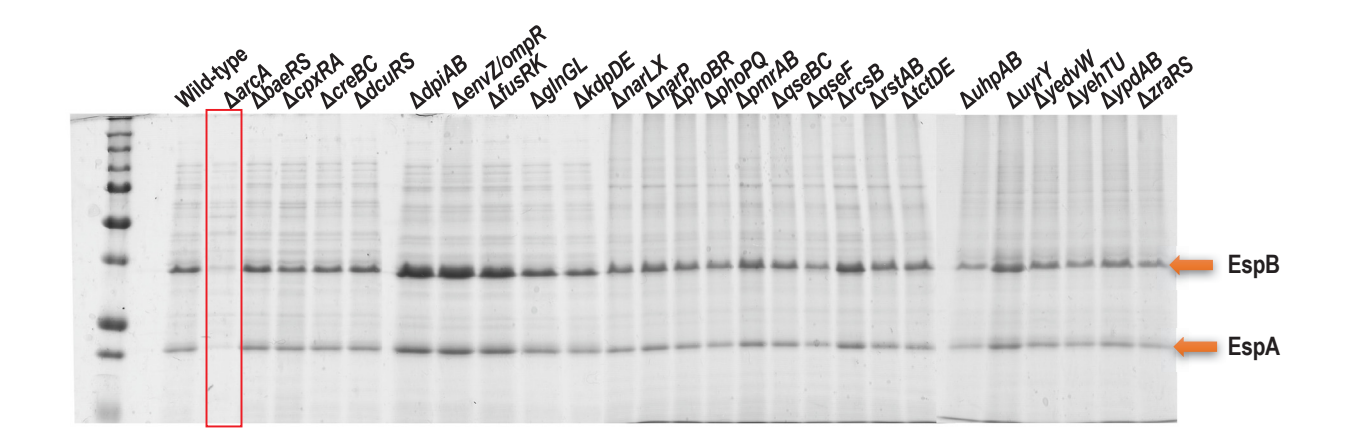


Fig S2. T3S is functional in all TCS deletion strains with the exception of $\Delta arcA$. Total secreted proteins of the *C. rodentium* wildtype and TCS deletion strains were prepared, as described in Materials and Methods, and separated on 10% SDS-PAGE gels subsequently stained with Coomassie blue.

TABLE S1 Strains and plasmids used in this study

Strain or plasmid	Description	Reference or
		source
Citrobacter rodentium		
Wild-type	C. rodentium DBS100	[55]
$\Delta arcA$	DBS100 ΔarcA	This study
$\Delta baeRS$	DBS100 ΔbaeRS	This study
$\Delta cpxRA$	DBS100 Δ <i>cpxRA</i>	[199]
$\Delta creBC$	DBS100 $\Delta creBC$	This study
$\Delta dcuRS$	DBS100 $\Delta dcuRS$	This study
$\Delta dpiAB$	DBS100 $\Delta dpiAB$	This study
$\Delta fusRK$	DBS100 ΔfusKR	This study
$\Delta g ln G L$	DBS100 $\Delta g lnGL$	This study
$\Delta k dp ED$	DBS100 $\Delta kdpED$	This study
$\Delta narLX$	DBS100 ΔnarLX	This study
$\Delta narP$	DBS100 ΔnarP	This study
$\Delta ompR\Delta envZ$	DBS100 $\triangle ompR\Delta envZ$	This study
$\Delta phoBR$	DBS100 ΔphoBR	This study
$\Delta phoPQ$	DBS100 ΔphoPQ	[261]
$\Delta pmrAB$	DBS100 ΔpmrAB	[262]
$\Delta qseBC$	DBS100 $\Delta qseBC$	This study
$\Delta qseF$	DBS100 $\Delta qseF$	This study
$\Delta rcsB$	DBS100 $\Delta rcsB$	This study
$\Delta rstAB$	DBS100 Δ <i>rstAB</i>	This study
$\Delta tctDE$	DBS100 $\Delta tctDE$	This study
$\Delta uhpAB$	DBS100 Δ <i>uhpAB</i>	This study
$\Delta uvrY$	DBS100 ΔuvrY	This study

$\Delta yedWV$	DBS100 ΔyedWV	This study
$\Delta yehTU$	DBS100 $\Delta yehTU$	This study
$\Delta y p dBA$	DBS100 $\Delta ypdBA$	This study
$\Delta zraRS$	DBS100 $\Delta zraRS$	This study
Escherichia coli		
$DH5\alpha$	HuA2 $\Delta(lac)U169$ phoA glnV44 ϕ 80lacZ Δ M15 endA recA	Invitrogen
	$hsdR17 (r_M^- m_K^+) thi-1 gyrA96 relA1$	
DH5αλpir	$K\text{-}12\ F^-\ \varphi 80 \textit{lacZ} \Delta M15\ \textit{endA}\ \textit{recA}\ \textit{hsdR17}\ (r_M^-\ m_K^+)\ \textit{supE44}$	
	thi-1 gyrA96 relA1 Δ(lacZYA-argF)U169 λpir	
χ7213	thr-1 leuB6 fhuA21 lacY1 glnV44 recA1 asdA4 thi-1 RP4-2-	[263]
	Te::Mu [-pir] Kan ^r	
Plasmids		
pRE112	Sucrose-sensitive (sacB1) suicide vector; Cm ^r	[264]
$p\Delta arcA$	$\Delta arcA$ deletion construct in pRE112	This study
$p\Delta baeRS$	$\Delta baeRS$ deletion construct in pRE112	This study
$p\Delta creBC$	$\Delta creBC$ deletion construct in pRE112	This study
$p\Delta dcuRS$	$\Delta dcuRS$ deletion construct in pRE112	This study
$p\Delta dpiAB$	$\Delta dpiAB$ deletion construct in pRE112	This study
$p\Delta fusRK$	$\Delta fusRK$ deletion construct in pRE112	This study
$p\Delta glnGL$	$\Delta g lnGL$ deletion construct in pRE112	This study
$p\Delta kdpED$	$\Delta k dp ED$ deletion construct in pRE112	This study
$p\Delta narLX$	$\Delta narLX$ deletion construct in pRE112	This study
$p\Delta narP$	$\Delta narP$ deletion construct in pRE112	This study
$p\Delta phoBR$	$\Delta phoBR$ deletion construct in pRE112	This study
$p\Delta qseBC$	$\Delta qseBC$ deletion construct in pRE112	This study
p $\Delta qseF$	$\Delta qseF$ deletion construct in pRE112	This study
$p\Delta rcsB$	$\Delta rcsB$ deletion construct in pRE112	This study
pΔ <i>rstAB</i>	$\Delta rstAB$ deletion construct in pRE112	This study

p∆ <i>tctDE</i>	$\Delta tctDE$ deletion construct in pRE112	This study
$p\Delta uhpAB$	$\Delta uhpAB$ deletion construct in pRE112	This study
$p\Delta uvrY$	$\Delta uvrY$ deletion construct in pRE112	This study
$p\Delta yedWV$	$\Delta yedWV$ deletion construct in pRE112	This study
$p\Delta yehTU$	$\Delta yehTU$ deletion construct in pRE112	This study
p∆ <i>ypdBA</i>	$\Delta y p dBA$ deletion construct in pRE112	This study
p $\Delta zraRS$	$\Delta zraRS$ deletion construct in pRE112	This study

TABLE S2 Primers used for qPCR

Gene	Forward primer $(5' \rightarrow 3')$	Reverse primer $(5' \rightarrow 3')$	Product size (bp)
16S	TGTCTACTTGGAGGTTGTGCCCTT	TGCAGTCTTCCGTGGATGTCAAGA	193
arcA	GCCCGGATGGCGAGCAATAC	CAGCTCGCGACCGGTCATTT	125
arcB	CTATCTGAGCGTGCTGGAGTCAAA	CCAGCTGTTGCAGATGACGAA	119
baeR	CTTGACCTGACTCCCGCCGA	CGATCGGTCACCACCCGGTA	122
barA	CCTGATGGATATTCAGATGCC	CGCCAGATAGTCATTCATACC	163
cpxR	GGAACAGGCGCTGGAGCTTC	ACGGGGGTCTGGTGTCTG	120
creB	CGCTGTCGCTTACGCGCTAT	CGGCCCAGACGCTTTCCATC	102
dcuR	TGGCGAATGCGGTGAATATC	ACGTCCCGTTACGCCATAAT	107
dpiA	CAGCGCGAGTCAGCGACAAA	TTCACCGCGTTCAGCGTCAG	108
fusR	GCTTACTCCGCGAGAGCGTG	GGCGCGATACACATGGACCG	112
glnG	TGATTACCTGCCAAAACCGT	TCGGACCGTTGATCTGGATA	113
kdpE	GTCCGGCAGACCGAGATCGA	AGGCCATTCGCCGCTTTCTG	140
narL	GCCAGGCATGAACGGACTGG	CGCCGTCACGACGTCTTCTT	109
narP	CGAACCGTCTCGACCCCGAT	TAATTTGCGCCGTCACGCCA	108
narQ	GTTGCAGATCATCCGTGAAG	CGAATATACACCGTGTGGTTG	111
ompR	GAAACCGTTTAACCCGCGTGAACT	AACTTACCAAAGGCAATCACCGCC	117
phoB	CTCGACATGGGACCGACCGA	TGCACATCGACCGTGCGATC	137
phoP	AGCTGTAACATCAAGGCGTC	GTCGATCAACGATGAGGTGA	111
pmrA	GGATCAGCACCGGCAGGGTA	GCAATGTCTGGAGAGCGGCC	122
qseB	ACTGGTTCACCGACGGTCGT	AATGTCGCGCCCGTCCATTC	104
qseF	GCGACGCAAAAGGGGGTCTT	ACGATAGACTCGCGCCAGCT	128
rcsB	GAAATCGCCAAGAAGCTGAAC	CAGGGTCACAGAAGAGAGATAG	123
rcsC	TGGGGAGAGGCCACGCTATG	TCCGCTGACGACCTGTTGGT	143
rpoD	ATCAAAGCGAAAGGTCGTAGCCAC	CCATCATCACGCGCATACTGTTCA	130
rstA	AGGCGCACCGAACGATTGAC	GCGCGTTTGCGTCTGCATTT	137
tctD	GGAAGATAACCGTGAGCTGG	AACTCTCGCTATGCAACAGG	116
uhpA	CCATCATGCTTTCGGTACAC	CTACAGCGTTTGGAGAGGA	88
uvrY	CGCGAGTTGCAGATTATGCTGAT	TTACACAGGCCATGGCGAATTG	176
yedW	TTTGCCTTACTGCCCGCGAC	TTCTCAACTGCGCGCGTACC	126
yehT	GCCAGGAGCGCAGTAAGCAG	GCGACGTCGTCCATCTGCAA	115
ypdB	ACAGCACAACCGCGTCGATG	GCTTCCACCGCGTGCTCTTT	144

zraR	TTCCCCTGCTGGCTGAGCAT	GGCATTTTCCAGCTCGCGGA	137
wcaA	TTCGGGCGATAAAATCGGTG	GAATTGACCGCGTTATGGGT	151
espA	ATCTTACGGCTGAGTTAAGCG	CGGCTATTATCCACCGTCG	97
espB	TCTCATCTGTCCTGGGGATT	ACTTCAGAGGCGGTATTGAC	124

TABLE S3 Primers used to generate gene deletion strains

Deletion strain	Primer	Sequence (5'→3')	Restriction site
$\Delta arcA$	arcA_1	CTAGGAGCTCGACATCCTGAAGCGCATCGA	SacI
	arcA_2	CTAGCTCGAGGATAAGAATGTGCGGGGTCT	XhoI
	arcA_3	CTAGCTCGAGTAAGCGGTTTACCACCGTCA	XhoI
	arcA_4	CTAGTCTAGAGATGACAGGCAGGTACAGCA	XbaI
$\Delta baeRS$	baeRS_1	CTAGGAGCTCCAGTAAAGGCATGGGCTTGT	SacI
	baeRS_2	CTAGGCTAGCAAAATCGCCAGAAACAGCTTG	NheI
	baeRS_3	CTAGGCTAGCCGCCTGCAGAATGGCTTAAC	NheI
	baeRS_4	CTAGTCTAGACCGGGGTCAGACATAATCAG	XbaI
$\Delta creBC$	creBC_1	CTAGGAGCTCCTCTGCAGGTGCCACTTGGA	SacI
	creBC_2	CTAGGCTAGCCATCTGCTGCATATTTCTTCCC	NheI
	creBC_3	CTAGGCTAGCCTTCACCGTCACTTCACATAA	NheI
	creBC_4	CTAGTCTAGACAGCAGATACTGCATCGGAT	XbaI
$\Delta dcuRS$	dcuRS_1	CTAGGAGCTCGTCACTACCTATCTGAGCACC	SacI
	dcuRS_2	CTAGGCTAGCCATGGTGGTCCCGGATTGAC	NheI
	dcuRS_3	CTAGGCTAGCTGTCAGTAGACGCCAACGGC	NheI
	dcuRS_4	CTAGTCTAGAGATCTTTACCGCGGAACCAG	XbaI
$\Delta dpiAB$	dpiAB_1	CTAGGAGCTCACCATAATGTCGGGAACCGT	SacI
	dpiAB_2	CTAGGCTAGCCGGAAATGCTAACTGGCGAAA	NheI
	dpiAB_3	CTAGGCTAGCGCATTTATCGCGGGTGATACA	NheI
	dpiAB_4	CTAGTCTAGATCCAGACCGCTGCAATACAT	XbaI
$\Delta fusRK$	fusKR_1	CTAGGAGCTCGGCGGCTGCAGGTTGATAAT	SacI
	fusKR_2	CTAGGCTAGCGTCCTCTTCGAGACTGAGTA	NheI
	fusKR_3	CTAGGCTAGCCCCACAAATTTGCAACAAACCC	NheI
	fusKR_4	CTAGTCTAGAAAGGCCAATCAGCATTTGCG	XbaI
$\Delta glnGL$	glnGL_1	CTAGGAGCTCCTCCTACAAGCGTCTGGTCC	SacI
	glnGL_2	CTAGGCTAGCCATCTGCAGTCTCCTGACAG	NheI
	glnGL_3	CTAGGCTAGCGGAATGGAGTAAGCGTTCAC	NheI
	glnGL_4	CTAGTCTAGAGAGGTCCAGCGTCTGGTTAA	XbaI

$\Delta kdpED$	kdpDE_1	CTAGGAGCTCGGCGCCGTTTATCGGGATT	SacI
	kdpDE_2	CTAGGCTAGCGTTTCCACCACGCCAACCA	NheI
	kdpDE_3	CTAGGCTAGCCCACAGGATGGCGCAATAAT	NheI
	kdpDE_4	CTAGTCTAGAGACGATGAAGTACCGTTCAG	XbaI
$\Delta narLX$	narLX_1	CTAGGAGCTCGAAGCTGATGTTCGCCATAC	SacI
	narLX_2	CTAGGCTAGCACCTTCTTCCTTCAGGTTGC	NheI
	narLX_3	CTAGGCTAGCATCAGGAACGTATCTTCT	NheI
	narLX_4	CTAGTCTAGAAACAGGCGAAACAGTTTGCTT	XbaI
$\Delta narP$	narP_1	CTAGGAGCTCCAAGTTCCTGTGGGCAACTT	SacI
	narP_2	CTAGGCTAGCAGGCATAGTTATCTCCTGAGA	NheI
	narP_3	CTAGGCTAGCCAGTGACGAAAACCACGTTG	NheI
	narP_4	CTAGTCTAGAGCATCATTCGATATCGCCAC	XbaI
$\Delta phoBR$	phoBR_1	CTAGGAGCTCAGCGTCCCGATGTAAATGTC	SacI
	phoBR_2	CTAGGCTAGCCAGAATACGTCTCGCCATGA	NheI
	phoBR_3	CTAGGCTAGCCTGACAGGCGATTGTAATGC	NheI
	phoBR_4	CTAGTCTAGATGCACGTAAGCGTGGAGGAT	XbaI
$\Delta qseBC$	qseBC_1	GCTCTAGACGCGCCGTCTTCTTTGGTCCAGA	XbaI
	qseBC_2	GCGATATCGGTGAACCAGTCGACGCAAAAGC	EcoRV
	qseBC_3	GCGATATCGGCAATCTGCCGGAGGAGGATT	EcoRV
	qseBC_4	GCGAGCTCCGCGTAGCCGTGGCAGCCTTCTT	SacI
$\Delta qseF$	qseF_1	CGGGGTACCCTGAGTATCGCCCGGGATTG	KpnI
	qseF_2	CTAGGCTAGCGCTTATCATGGCGATACCTC	NheI
	qseF_3	CTAGGCTAGCGAGTAGCTCCGCAACATACC	NheI
	qseF_4	CTAGTCTAGAGCACAGAGTGAAGGTCTGCG	XbaI
$\Delta rcsB$	rcsB_1	CTAGGAGCTCGCGAAGTCGACAACCTGCAT	SacI
	rcsB_2	CTAGGCTAGCGTTCATGTATAAGGCTACCTTGC	NheI
	rcsB_3	CTAGGCTAGCGAGTAATCGCTTTTCGCCGT	NheI
	rcsB_4	CTAGTCTAGAGCTGATCAGCATGATGGACG	XbaI
$\Delta rstAB$	rstAB_1	CTAGGAGCTCTTTACCGATTACGTGGTGGAG	SacI
	rstAB_2	CTAGGCTAGCACTTCCGGATCGTCTTCAACA	NheI
	rstAB_3	CTAGGCTAGCGATCGGTTTCTCAGGCGATG	NheI

	rstAB_4	CTAGTCTAGACTATCTCAGCGAAGAGGAGT	XbaI
$\Delta tctDE$	tctDE_1	CGGGGTACCGCGGTCTGCTGGAGCTTTT	KpnI
	tctDE_2	CTAGGCTAGCGCCAGCTCACGGTTATCTTC	NheI
	tctDE_3	CTAGGCTAGCGACGCAGTAACCTTCCTTTTG	NheI
	tctDE_4	CTAGTCTAGAGTGATGGCGAGATCAGAATAG	XbaI
$\Delta uhpAB$	uhpAB_1	CTAGGAGCTCGCCTGATGATGAACATTCAG	SacI
	uhpAB_2	CTAGGCTAGCGGTGATCATGATTTTGTCCTGAC	NheI
	uhpAB_3	CTAGGCTAGCGCCTAAGGAGCGGCATGTTT	NheI
	uhpAB_4	CTAGTCTAGACCTCTTTGTGCGAGCATTCC	XbaI
$\Delta uvrY$	uvrY_1	GCTCTAGACCGCGGAGTATACCATAAGC	XbaI
	uvrY_2	CTCCGCATTCACCAGTTCGTGGTCATCAA	_ <i>a</i>
	uvrY_3	AACTGGTGAATGCGGAGACGTTAACAAGC	- ^a
	uvrY_4	GCGAGCTCCGTTCGGGAAAGGACCAAAAT	SacI
$\Delta yedWV$	yedVW_1	CTAGGAGCTCCCACGAACTGGATCGCCAAT	SacI
	yedVW_2	CTAGGCTAGCGTTGTCTTCAATCAGTAAAATCTTC	NheI
	yedVW_3	CTAGGCTAGCTGAGTGCGGGTTGCGGTCGC	NheI
	yedVW_4	CTAGTCTAGACGCTGACCGGATACATCTTATTC	XbaI
$\Delta yehTU$	yehTU_1	CTAGGAGCTCCGGGTGGTGTCATGGATATT	SacI
	yehTU_2	CGGGGTACCGAAACACGCACATTTGCTGAA	KpnI
	yehTU_3	CGGGGTACCCGTCGCTATCTGAAAAGTTTG	KpnI
	yehTU_4	CTAGTCTAGATGGAGGCTTTCCTCAACGC	XbaI
$\Delta ypdBA$	ypdAB_1	CTAGGAGCTCGCTTGGGTTAGGCACCAGTA	SacI
	ypdAB_2	CTAGGCTAGCCCGCCAGCAGCATAGTAAATA	NheI
	ypdAB_3	CTAGGCTAGCGAAGGAGTTCAGGCAGTTAAT	NheI
	ypdAB_4	CTAGTCTAGATGATCCCGGACAGCAAGTAT	XbaI
$\Delta zraRS$	zraRS_1	CTAGGAGCTCGTCAATGGACGTGAGCGTGG	SacI
	zraRS_2	CTAGGCTAGCCATACTCTCCTTCGCCTTTC	NheI
	zraRS_3	CTAGGCTAGCCGTTAGTTTTGCTCGCGTTC	NheI
	zraRS_4	CTAGTCTAGAGGTCGCCGAAAGTCGAAACC	XbaI

^a This construct was generated by overlap PCR.

TABLE S4 Two-component signaling systems of C. rodentium and E. coli^a

TABLE S4 Two-component signaling systems of <i>C. rodentium</i> and <i>E. coli</i> *.					
Two-component	Putative Function	<i>C</i> .	E. coli	EHEC	EPEC
System	1 didn't 1 diletion	rodentium	K12	LIILC	LI LC
ArcA/ArcB	Anaerobic respiration	+	+	+	+
AtoC/AtoS	Acetoacetate metabolism	-	+	-	+
BaeR/BaeS	Multidrug efflux	+	+	+	+
CpxR/CpxA	Envelope stress response	+	+	+	+
CreB/CreC	Phosphate regulation	+	+	+	+
CusR/CusS	Metal efflux	-	+	+	+
DcuR/DcuS	Response to dicarboxylate	+	+	+	+
DpiA/DpiB	Citrate fermentation	+	+	+	+
EvgA/EvgS		-	+	+	+
FusR/FusK	Fucose sensing	+	-	+	_
GlnG/GlnL	Nitrogen assimilation	+	+	+	+
KdpE/KdpD	Potassium transport	+	+	+	+
NarL/NarX	Nitrogen metabolism	+	+	+	+
NarP/NarQ	Nitrogen metabolism	+	+	+	+
OmpR/EnvZ	Osmotic regulation	+	+	+	+
PhoB/PhoR	Phosphate regulation	+	+	+	+
PhoP/PhoQ	Virulence	+	+	+	+
PmrA/PmrB	LPS modifications	+	+	+	+
QseB/QseC	Quorum sensing	+	+	+	+
QseF/QseE	Amino sugar metabolism	+	+	+	+
RcsB/RcsC/RcsD	Capsule synthesis	+	+	+	+
RstA/RstB	Resistance mechanisms	+	+	+	+
TctD/TctE	Tricarboxylate transport	+	-	_	_
TorR/TorS	7	-	+	+	+
UhpA/UhpB	Hexose phosphate uptake	+	+	+	+
UvrY/BarA	Carbon metabolism	+	+	+	+
YedW/YedV	Copper homeostasis	+	+	+	+
YehT/YehU	Unknown	+	+	+	+
YpdB/YpdA	Unknown	+	+	+	+
ZraR/ZraS	Response to Zn	+	+	+	+
3 m : 1 ::0 :1 mcc	1 11 0 1	NT 1 CF 1			- ~

^a To identify the TCSs encoded by *C. rodentium*, a BLAST search was performed against the *C. rodentium* genome using the DNA sequence of the *C. rodentium phoP* response regulator. This search identified 26 RR genes and their cognate HK sensors. Orphan RRs (*hnr*) and genes encoding

chemotaxis proteins (*cheY* and *cheB*) were omitted. This list is in agreement with databases available online (Prokaryotic 2-Component Systems, P2CS, http://www.p2cs.org and Microbial Signal Transduction database, http://mistdb.com). With few exceptions, the *C. rodentium* genome shares the same TCSs as the prototypical A/E pathogens EHEC EDL933 and EPEC E2248/69.

TABLE S5 Congo red binding to selected *C. rodentium* strains.

Strains	Aerobic		Anaerobic		
	LB	YESCA	LB	YESCA	
Wild-type	+	+	+	+	
$\Delta arcA$	+	+	+	+	
$\Delta rcsB$	++	++	++	++	
$\Delta uvrY$	+	+	+/-	+	

PREFACE TO CHAPTER 3

In Chapter 2 we showed that the manipulation of multiple TCSs can alter the virulence of C. rodentium. The most striking attenuation phenotype was in the $\Delta cpxRA$ strain, where upon loss of CpxRA 100% of susceptible mice survived this otherwise lethal infection. In Chapter 3 we explored the auxiliary proteins NlpE and CpxP, and their roles in virulence. NlpE is a reported outer membrane lipoprotein activator of CpxRA, whereas CpxP is the reported periplasmic negative regulator of the TCS. We found that deletion of these auxiliary proteins did not recapitulate direct inactivation of the CpxRA TCS by deletion of cpxRA. In order to further evaluate this phenotype, we performed microarrays on the $\Delta cpxRA$, $\Delta nlpE$, and $\Delta cpxP$ strains. We analyzed the microarray data with the hypothesis that loss of virulence may correlate with loss of gene expression, similarly to the virulence phenotype of the highly attenuated $\Delta cpxRA$ strain, compared to the fully virulent auxiliary protein mutants. We detected many genes in a multitude of pathways which could be contributing to the attenuation of the $\Delta cpxRA$ strain, including maltose metabolism and adherence.

CHAPTER 3 The Virulence Effect of CpxRA in *Citrobacter rodentium* Is Independent of the Auxiliary Proteins NlpE and CpxP

ABSTRACT

Citrobacter rodentium is a murine pathogen used to model the intestinal infection caused by Enteropathogenic and Enterohemorrhagic Escherichia coli (EPEC and EHEC), two diarrheal pathogens responsible for morbidity and mortality in developing and developed countries, respectively. During infection, these bacteria must sense and adapt to the gut environment of the host. In order to adapt to changing environmental cues and modulate expression of specific genes, bacteria can use two-component signal transduction systems (TCS). We have shown that the deletion of the Cpx TCS in C. rodentium leads to a marked attenuation in virulence in C3H/HeJ mice. In E. coli, the Cpx TCS is reportedly activated in response to signals from the outermembrane lipoprotein NlpE. We therefore investigated the role of NlpE in C. rodentium virulence. We also assessed the role of the reported negative regulator of CpxRA, CpxP. We found that as opposed to the $\triangle cpxRA$ strain, neither the $\triangle nlpE$, $\triangle cpxP$ nor the $\triangle nlpE/\triangle cpxP$ strains were significantly attenuated, and had similar in vivo localization to wild-type C. rodentium. The in vitro adherence of the Cpx auxiliary protein mutants, $\Delta nlpE$, $\Delta cpxP$, $\Delta nlpE\Delta cpxP$, was comparable to wild-type C. rodentium, whereas the $\Delta cpxRA$ strain showed significantly decreased adherence. To further elucidate the mechanisms behind the contrasting virulence phenotypes, we performed microarrays in order to define the regulon of the Cpx TCS. We detected 393 genes differentially regulated in the $\Delta cpxRA$ strain. The gene expression profile of the $\Delta nlpE$ strain is strikingly different than the profile of $\Delta cpxRA$ with regards to the genes activated by CpxRA. Further, there is no clear inverse correlation in the expression pattern of the $\Delta cpxP$ strain in comparison to $\Delta cpxRA$. Taken together, these data suggest that in these conditions, CpxRA activates gene expression in a largely NlpE- and CpxP-independent manner. Compared to wildtype, 161 genes were downregulated in the $\Delta cpxRA$ strain while being upregulated or unchanged in the Cpx auxiliary protein deletion strains. This group of genes, which we hypothesize may contribute to the loss of virulence of $\Delta cpxRA$, includes T6SS components, ompF, the regulator for colanic acid synthesis, and several genes involved in maltose metabolism.

INTRODUCTION

Enteropathogenic and Enterohemorrhagic *Escherichia coli* (EPEC and EHEC) are Gramnegative food-borne diarrheal pathogens, transmitted through the fecal-oral route [58]. They are responsible for high morbidity and mortality in both the developed and developing world. In the case of EHEC, disease can progress to hemorrhagic colitis and hemolytic uremic syndrome due to the production of the Shiga toxin, which is lacking in EPEC [58]. The related murine pathogen, *Citrobacter rodentium*, is a natural mouse pathogen, first isolated in Japan and the United States of America as the etiologic agent of transmissible murine colonic hyperplasia in mouse colonies [50, 52]. *C. rodentium* is a widely used model to study EPEC and EHEC due to their pathological similarity and difficulty in infecting mice with the human pathogens [52, 55]. EHEC, EPEC, and *C. rodentium* are members of a group of pathogens known for their ability to form attaching and effacing lesions (A/E lesions) during infection [58]. Specifically, the bacteria attach to intestinal epithelial cells, efface the microvillar architecture, and form actin-rich pedestals beneath the adherent bacteria [3, 58].

To survive during a host infection, bacteria must be able to sense the surrounding environment and adapt their gene expression accordingly. One of the ways in which bacteria sense the environment is through the use of two-component signal transduction systems (TCS). TCSs are typically composed of a membrane-bound sensor kinase and a cytoplasmic response regulator. Following activation by a stimulus, the sensor kinase will become auto-phosphorylated on a histidine residue in the cytoplasmic domain [166]. The phosphate is then transferred to a conserved aspartate residue on a cytoplasmic response regulator, which will carry out a specific

transcriptional response, either upregulating or downregulating target genes, generally by binding directly to the cognate DNA sequences of the target gene [166, 191].

Previous work by our group and others has uncovered several TCSs involved in the regulation of virulence properties of *C. rodentium*. Specifically, the inactivation of RstAB, UhpAB, ZraRS, RcsBC, and ArcAB TCSs leads to delayed mortality in susceptible C3H/HeJ mice [265]. The CpxRA TCS deletion strain has the most striking effect, leading to 100% survival of susceptible mice [199]. The QseBC and QseEF TCSs, which respond to epinephrine and norepinephrine, are also important in virulence of *C. rodentium* [176].

The CpxRA TCS is one of the key envelope stress responses in Gram-negative bacteria. It is activated by a multitude of signals, including misfolded proteins [266], alkaline pH [186], changes in membrane lipid composition [190], high osmolarity [187, 188, 267], and attachment to abiotic surfaces [189]. The CpxRA TCS is composed of the inner membrane-bound histidine kinase CpxA, and the cytoplasmic response regulator CpxR. Upon external stimulus, the CpxA becomes auto-phosphorylated, and transfers the phosphate group to CpxR.

In addition to our work in *C. rodentium*, the Cpx TCS has been implicated in virulence modulation in other bacteria. In *Haemophilus ducreyi*, deletion of CpxA leads to the bacterium's inability to infect humans by decreasing its serum resistance [208]. In *Legionella pneumophila*, CpxRA contributes to the bacterium's ability to replicate in protozoa and controls the expression of a multitude of virulence factors [200, 201]. In *Salmonella enterica* serovar Typhimurium, impaired CpxRA function leads to the inability of the bacteria to replicate in mice, as well as to

decreased adherence and invasion of eukaryotic cells [204]. Further, CpxRA is a positive regulator of the virulence factor *virF* of *Shigella sonnei* [203]. In EHEC, high levels of CpxR are known to act negatively on critical components of EHEC virulence: the Locus of Enterocyte Effacement (LEE) and its associated Type 3 Secretion System (T3SS) [210]. CpxR represses *ler* and *lon*, two known positive regulators of the LEE, and negatively affects EspABD, the translocators of the T3SS [210]. However, our previous work in *C. rodentium* did not uncover a striking defect in T3SS activity in the absence of CpxRA [265]. In EPEC, CpxRA has been implicated in the regulation of the Bundle Forming Pilus (BFP), an important adherence factor that is not present in *C. rodentium* [268].

In *E. coli*, the Cpx system is regulated by a periplasmic auxiliary protein, CpxP, overexpression of which dampens the Cpx response through a negative feedback loop, as *cpxP* is one of the most highly regulated genes in the Cpx TCS [193]. In contrast, the loss of *cpxP* results in modest upregulation of the Cpx pathway, without making the system blind to inducing cues [193]. Upstream of CpxA, the outer membrane-anchored lipoprotein NlpE acts as an activator of the response [181]. NlpE-dependent activation of Cpx occurs to suppress toxicity of misfolded proteins, as well as in response to adherence to abiotic surfaces [181, 189, 269]. There exist some NlpE-independent cues for Cpx activation, such as alkaline pH [184, 186] and drugs targeting peptidoglycan synthesis [182]. However, there also exist numerous cues in which the role of NlpE is entirely uncharacterized [172]. The involvement of NlpE and CpxP in *C. rodentium* virulence remains unclear.

In order to gain further insight into the cause of the virulence defect associated with the loss of CpxRA in *C. rodentium*, we characterized the role of the putative upstream activator of the Cpx pathway, NlpE, as well as the role of the most prominent auxiliary protein, CpxP. NlpE has been previously implicated in the activation of Cpx in multiple contexts in *E. coli* and EHEC. However, NlpE activation of Cpx *in vivo* remains uncharacterized. We generated chromosomal deletions of *nlpE*, *cpxP*, and a double mutant of both genes in *C. rodentium*, and investigated the role of each gene during infection of susceptible C3H/HeJ mice. We found that the effect of CpxRA on *C. rodentium* virulence is NlpE- and CpxP-independent. We further characterized the regulon of CpxRA, NlpE, and CpxP using microarrays, in order to uncover differentially regulated genes, and to provide further insight into the differential effects of these proteins. We found a large number of Cpx target genes that are regulated independently of NlpE and CpxP.

MATERIALS AND METHODS

Bacterial strains, plasmids, and growth conditions

All strains and plasmids used in this study are listed in Table S1. Bacterial strains were routinely cultured at 220 rpm at 37°C in Luria Bertani (LB) broth (1% [wt/vol] tryptone, 0.5% [wt/vol] yeast extract, 1% [wt/vol] NaCl). Subculturing, when needed, was done in Dulbecco's Modified Eagle media (DMEM; Wisent). When appropriate, LB was supplemented with chloramphenicol (Cm; 30 μg/ml) or diaminopimelic acid (DAP; 50 μg/ml). This study was carried out in accordance with the McGill biosafety guidelines and regulations, under biosafety permit number B-07706.

Construction of deletion strains – sacB gene-based allelic exchange

The C. rodentium deletion strains were generated by sacB gene-based allelic exchange, as described previously [270]. All primers used in this study are listed in Table S2. Briefly, genomic DNA of *C. rodentium* was used as a template to amplify the upstream and downstream sequences of a target gene (primers 1 and 2, and 3 and 4, respectively). Each segment was digested using XbaI, XhoI, or KpnI, as appropriate (New England Biolabs). Following digestion, the segments were purified and ligated using T4 DNA ligase (Thermo Scientific). Next, the ligated product was PCR-amplified with iProof High-Fidelity DNA Polymerase (Biorad), using primers 1 and 4. The amplified segment was further digested using the appropriate enzymes, and was then ligated into pRE112 plasmid which had been digested with XbaI and KpnI (New England Biolabs). The resulting suicide vector plasmid was transformed into CaCl₂ chemically-competent E. coli χ7213 [271]. The E. coli χ 7213 strain was used as a donor strain in order to conjugate the suicide vectors into wild-type C. rodentium, as previously described [270]. Briefly, 25 µl of an overnight culture of transformed E. coli χ7213 and 25 μl of an overnight culture of C. rodentium were combined on the surface of an LB-DAP plate, for 1 h at 37°C. The conjugation product was plated on LB agar plates supplemented with Cm (30 µg/ml). Colonies that were Cm-resistant were then plated on peptone agar containing 5% sucrose and incubated at 16-18°C for several days in order to isolate colonies that were sucrose resistant. The sucrose-resistant colonies were also screened for Cm sensitivity. Gene deletion was verified by PCR and sequencing of gDNA (Genome Quebec) using primers 1 and 4.

In vivo Citrobacter rodentium infections

This study was carried out in accordance with the recommendations of the Canadian Council on Animal Care. The protocol was approved by the McGill University Animal Care Committee. Female C3H/HeJ mice were purchased from Jackson Laboratories and maintained in a specific-pathogen-free facility at McGill University. Wild-type or mutant C. rodentium DBS100 strains were grown overnight in 3 ml LB broth, 220 rpm, at 37°C. Female four- to five-week-old mice were orally gavaged with 100 µl of overnight culture, containing 2-3 x 10⁸ CFU. The infectious dose was verified by plating of serial dilutions of the inoculum on MacConkey agar (Difco). For survival experiments, the mice were monitored daily for 30 days, and were euthanized if any of the following clinical endpoints were met: 20% body weight loss, hunching and shaking, inactivity, and body condition score of <2 [272]. For fluorescent microscopy, the mice were euthanized on day 9 post infection. To detect C. rodentium colonization at days 3, 6, 9 post infection, fecal pellets or the terminal centimeter of the colon were homogenized in 1 ml PBS, and serially diluted and plated on MacConkey agar (Difco). C. rodentium was identified by its distinctive colony morphology. Plates with colonies between 30 and 300 were enumerated. In the case of low bacterial loads, with undiluted plate counts below 30, this plate was enumerated.

Adherence assays

In vitro adherence assays of *C. rodentium* were performed as previously described [242]. Briefly, HeLa cells were cultured in DMEM with 10% heat-inactivated fetal bovine serum (FBS), and seeded at 5.0 x 10⁴ per well on glass coverslips in a 24-well plate. Overnight bacterial cultures were grown in 3 ml LB, 220 rpm, at 37°C. Prior to infection, HeLa cells were incubated for 30 min in 1 ml of DMEM (Wisent), supplemented with 2% heat inactivated FBS (Seradigm). Cells

were infected at a starting MOI of 1:100 for 8 h at 37°C, 5% CO₂. Coverslips were washed 3 times in PBS with calcium and magnesium (Wisent) to remove non-adherent bacteria, and then fixed in 2.5% paraformaldehyde (Thermo) for 15 min. Following fixation, samples were permeabilized in 0.1% Triton X-100 (BioShop) in PBS, and blocked overnight in 2% bovine serum albumin (Sigma) with 0.1% Triton X-100 in PBS. Samples were then stained with a rabbit anti-*Citrobacter* LPS antibody (Mast Group), followed by Alexa 488-conjugated anti-rabbit secondary antibody (Invitrogen) and 4',6-diamidino-2-phenylindole (DAPI; Sigma). Coverslips were mounted in Prolong Gold (Invitrogen) and imaged on a Zeiss Axiovert 200M microscope with a Zeiss Axiocam monochrome camera. Ten random fields of view were assessed per sample, and the total number of bacteria and cells were enumerated using Fiji software [273].

Fluorescence microscopy

C3H/HeJ mice were infected with strains of *C. rodentium* as described above. Mice were euthanized on day 9 post infection, and the third most distal centimeter of the colon was fixed in 10% neutral buffered formalin. The tissue was paraffin-embedded and cut into 4 µm sections. The slides were deparafinized in xylene twice for 5 min, followed by rehydration in a gradient of 100% ethanol twice for 5 min, 95% ethanol for 5 min, 70% ethanol for 5 min, and dH₂O for 5 min. The samples were then boiled in 1.8mM citric acid and 8.2mM sodium citrate in dH₂O for 10 min, for antigen retrieval. The slides were left to cool down at RT for 10 min in the buffer, and were subsequently washed with PBS containing 0.2% Tween 20. Further, the samples were blocked in PBS containing 0.2% Tween 20, 10% FBS, and 3% BSA for 1 h at 37°C. The samples were stained with anti-*Citrobacter* LPS rabbit polyclonal antibody in PBS containing 0.2% Tween 20 and 3% BSA at 4°C for 3 h. Following the primary antibody, the samples were incubated with anti-rabbit

Alexa 488 secondary antibody and DAPI in PBS containing 0.2% Tween 20 and 3% BSA at 37°C for 1 h. Finally, the samples were mounted in Prolong Gold, and imaged on a Zeiss Axiovert 200M microscope with a Zeiss Axiocam monochrome camera. Images were assembled using Fiji [273].

RNA extraction

Bacteria were cultured overnight in LB broth, 220 rpm, at 37°C. Strains were subcultured 1:50 in 50 ml DMEM, at 220 rpm and 37°C, until an OD600 of 0.5-0.6. Cells were pelleted at 4°C. Pellets were resuspended in 1 ml of TRIzol reagent (Life Technologies) and stored at -20°C until further extraction. Samples were thawed at RT, and 200 µl of chloroform was added, followed by 15 s of vigorous shaking. The samples were then incubated at RT for 2-3 min. Contents were transferred to Phase-lock Heavy Gel tubes (Quantabio) and centrifuged at 12000 x g for 15 min at RT. Following centrifugation, the aqueous layer (about 600 µl) was transferred to a fresh microcentrifuge tube, followed by the addition of 600 µl of isopropanol and 1 µl glycogen (Ambion). The contents were mixed by gently inverting the tube, and were incubated at RT for 10 min. The samples were centrifuged at maximum speed at 4°C for 10 min, and while working on ice, the supernatant was removed. The pellet was washed with 1 ml ice-cold ethanol, and centrifuged at maximum speed for 10 min at 4°C in a microcentrifuge. The supernatant was removed, the pellets were air-dried, and resuspended in 40 µl of RNase-free dH₂O. Further, RNA samples were treated with Turbo DNase (Ambion) for 30 min. Samples were evaluated by NanoDrop to ensure quality and quantity, and by PCR, using 16S rDNA primers, to ensure no DNA contamination.

Microarrays

cDNA and Labelling

RNA was extracted and purified as described above. Labelling was done as described previously [274]. Briefly, 15 µg of RNA was reverse transcribed to cDNA with the addition of random hexamers, Superscript II reverse transcriptase (Life Sciences) and a mix of dATP, dTTP, dCTP, dGTP (NEB) and aminoallyl dUTP (Sigma). The cDNA was then labelled using Alexa Fluor 647, whereas genomic DNA (extracted from wild-type *C. rodentium*) was labelled using Alexa Fluor 546 (Invitrogen), as described previously [274].

Microarray hybridization

The microarray slides were custom-made using photolithography by MYcroarray, with 3 probes of 45 nucleotides each, per gene, against the *C. rodentium* DBS100 genome [53]. The labelled cDNA and gDNA were hybridized onto the microarray slide as described previously [274]. The microarrays were scanned using an InnoScan microarray scanner (Innopsys), and the data was analyzed using Mapix software. The samples were normalized to wild-type, and the genes with a log₂ ratio of mutant/wild-type >1 or <-1, and p<0.05 were considered differentially expressed and significant. The microarray data are available from Gene Expression Omnibus, https://www.ncbi.nlm.nih.gov/geo/, accession number GSE114699.

RESULTS

Susceptible mice do not survive infection with *Citrobacter rodentium* mutants of the Cpx TCS auxiliary proteins NlpE and CpxP.

To assess the virulence contribution of the Cpx TCS auxiliary proteins (Figure 1A), we used sacB gene-based allelic exchange to generate knock out strains of C. rodentium, each lacking either NlpE ($\Delta nlpE$), CpxP ($\Delta cpxP$), or a double mutant ($\Delta nlpE\Delta cpxP$), We confirmed that both NlpE and CpxP are homologous to those found in E. coli K-12 MG1655, at 79% and 88% sequence identity, respectively. We infected susceptible C3H/HeJ mice with each strain, and virulence was assessed (Figure 1B, 2). As our group has previously reported, the $\Delta cpxRA$ deletion rendered the strain avirulent, with 100% survival of susceptible mice (Figure 1B) [199]. As expected, the complemented $\Delta cpxRA$: cpxRA strain restored virulence, with mortality comparable to wild-type (Figure 1B). The mice infected with the Cpx auxiliary protein mutant strains ($\Delta nlpE$, $\Delta cpxP$, $\Delta nlpE\Delta cpxP$) succumbed to infection with similar kinetics as the cohort infected with wild-type C. rodentium (Figure 1B).

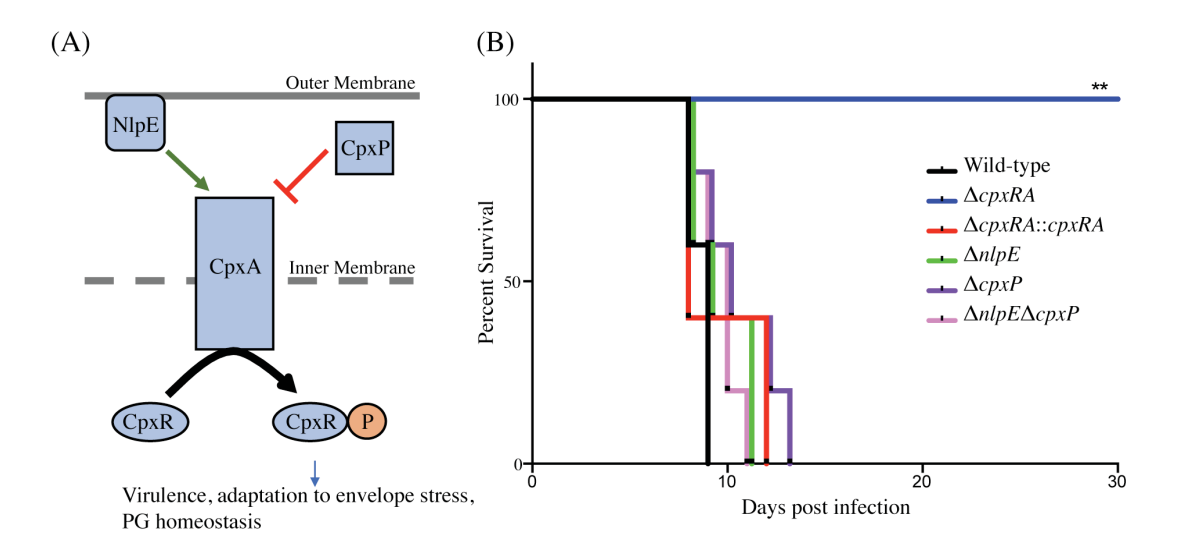


Figure 1: Survival of susceptible mice after infection with Cpx TCS mutant strains of Citrobacter rodentium.

(A) TCSs are used by bacteria in order to sense environmental stress. The membrane bound histidine kinase (CpxA) is activated by an external signal and propagates a cascade of phosphorylation leading to a transcriptional response by the cytoplasmic response regulator (CpxR). The Cpx TCS has a reported upstream outer membrane sensor, NlpE, and a periplasmic inhibitor, CpxP. (B) Female C3H/HeJ mice were infected by oral gavage with 2-3x10 8 colony forming units of wild-type C. rodentium, or a TCS mutant strain. Survival was monitored for 30 days post infection. The log-rank (Mantel-Cox) method was used to determine statistical significance. (**, P < 0.01), (n=5)

To further characterize this virulent phenotype, we assessed fecal C. rodentium loads at day 3 and 6 post infection, as well as colonic tissue C. rodentium loads at day 9 post infection. The wild-type C. rodentium loads increased as expected throughout infection, peaking at day 9 (Figure 2). As our group previously reported, the $\Delta cpxRA$ C. rodentium loads were significantly lower throughout the course of infection, an important internal control for our study (Figure 2) [199]. Similarly as expected, the $\Delta cpxRA$::cpxRA strain had C. rodentium loads comparable to wild-type levels at all time points (Figure 2) [199]. The Cpx TCS auxiliary protein mutants, however, showed no significant difference in bacterial burden and the mice were colonized to levels similar to wild-type, at all time points (Figure 2). Taken together, these data indicate that the deletion of the reported sensors of the Cpx TCS (NlpE, CpxP) does not recapitulate the deletion of the TCS itself.

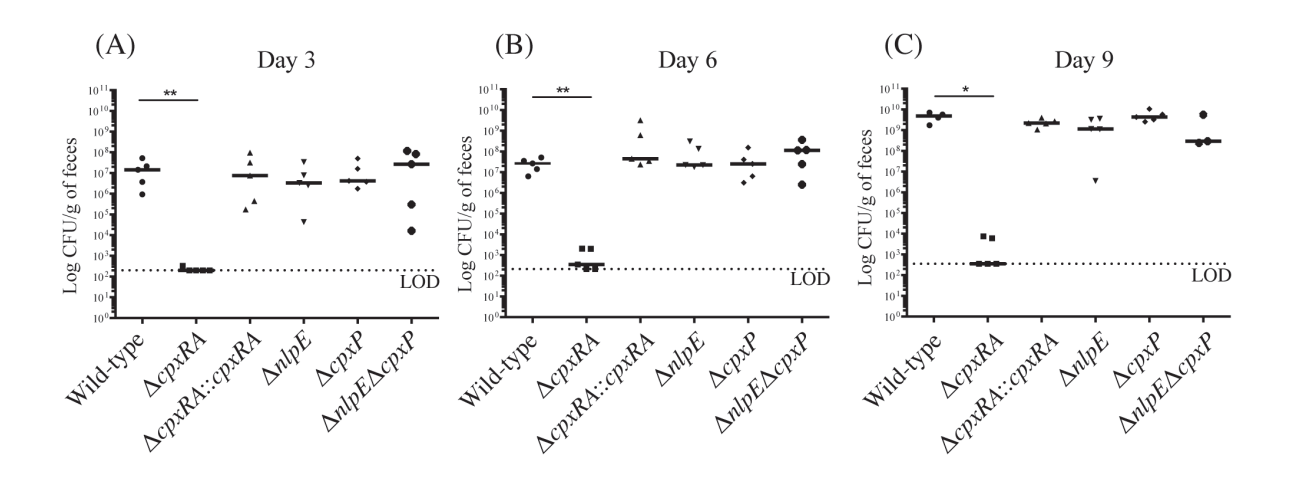


Figure 2: Bacterial burden in female C3H/HeJ mice after infection with Cpx TCS mutant strains of *Citrobacter rodentium*.

Female C3H/HeJ mice were infected as described previously, and fecal bacterial burden was assessed at day 3 (A), 6 (B), and 9 (C) post infection by plating on MacConkey agar and counting Colony Forming Units (CFU). At day 9 post infection, due to significant illness manifestation, in the absence of fecal matter, colon was homogenized and plated on MacConkey agar. A Mann-Whitney test was used to determine significance between each mutant strain and wild-type (**, P < 0.01; *, P < 0.05). (LOD = Limit of detection; day 3, day 6: n=5; day 9: n=3-5; black bar denotes the median)

Bacterial localization in the colon of susceptible mice infected with Cpx TCS auxiliary protein mutants is comparable to that of wild-type *C. rodentium*.

We aimed to further characterize the implication of these sensors in C. rodentium virulence by localizing the bacteria in intestinal tissue of infected mice. Susceptible C3H/HeJ mice were infected as previously, and euthanized on day 9 post infection. Colonic tissue sections were stained with DAPI, as well as anti - C. rodentium LPS antibody, in order to detect both the intestinal architecture and C. rodentium (Figure 3). Wild-type C. rodentium exhibited widespread localization on the colonic mucosal surface, with some localizing in the lumen of the intestine and some deeper within the crypts (Figure 3). Conversely, there was no detectable $\Delta cpxRA$ C. rodentium in the tissue sections, consistent with decreased bacterial loads (Figure 3). In contrast, the cpxRA complemented strain restored C. rodentium colonization and distribution to wild-type levels (Figure 3). Notably, the $\Delta nlpE$, $\Delta cpxP$, and $\Delta nlpE\Delta cpxP$ strains all exhibited widespread colonization and localization across the mucosal surface, similar to wild-type (Figure 3).

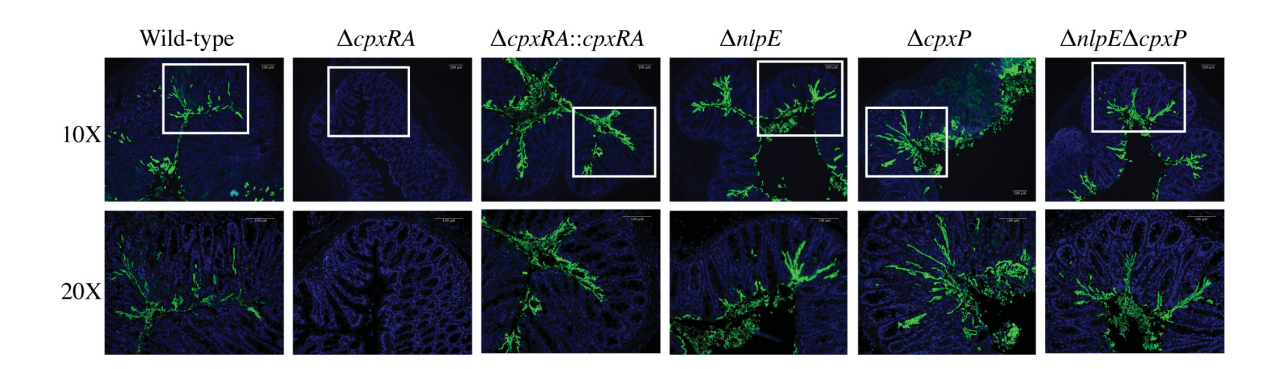


Figure 3: *In vivo* localization of wild-type and Cpx TCS mutant strains of *Citrobacter rodentium* in the intestine of C3H/HeJ mice.

Localization of *C. rodentium* wild-type and Cpx TCS mutant strains in distal colon samples of day 9 infected C3H/HeJ mice. Sections stained with DAPI (blue) and anti-*Citrobacter* LPS (green). White boxes on 10X images denote the area of the 20X higher magnification image. Scale bars at 100μm. Representative images shown from n=3-4 biological replicates. Scale bars 100μm.

In vitro bacterial adherence of Cpx TCS and auxiliary protein mutants.

Next, we wanted to further characterize the implication of these sensors in *C. rodentium* virulence by characterizing their ability to adhere to HeLa cells *in vitro*. HeLa cells were infected with wild-type or mutant *C. rodentium*, and then stained with DAPI and anti - *C. rodentium* LPS antibody, in order to enumerate total bacteria and cells. Consistent with the bacterial burden and *in vivo* localization data, the $\Delta cpxRA$ mutant displayed a significantly decreased ability, by 60%, to adhere to HeLa cells *in vitro* (Figure 4). The $\Delta cpxRA$::cpxRA strain restored bacterial adherence to wild-type levels (Figure 4). Notably, the Cpx TCS auxiliary protein mutants $\Delta nlpE$, $\Delta cpxP$, and $\Delta nlpE\Delta cpxP$ displayed adherence similar to wild-type, further supporting the fact that these mutants are fully virulent. As such, the *in vitro* adherence phenotypes presented in these assays further support the *in vivo* colonization phenotypes.

Relative Adherence in vitro

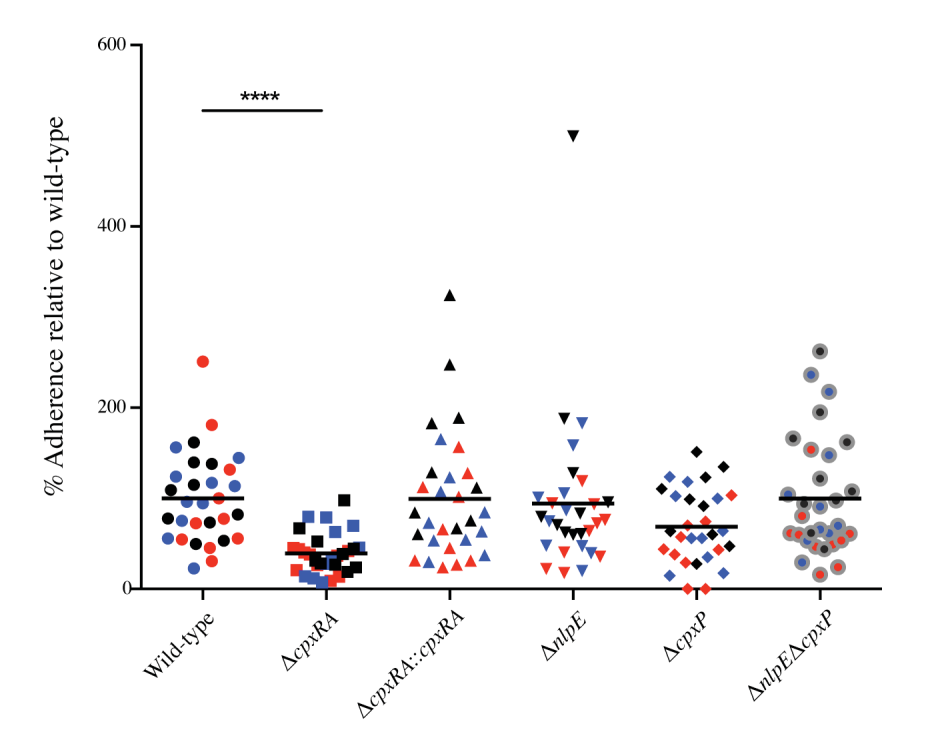


Figure 4: *In vitro* adherence of wild-type and Cpx TCS mutant strains of *Citrobacter rodentium* on HeLa cells.

HeLa cells were infected with *C. rodentium* wild-type or a Cpx TCS mutant strain for 8 hrs. The samples were fixed and stained with DAPI and anti-*Citrobacter* LPS. Samples were imaged on a Zeiss Axiovert 200M microscope. Total number of bacteria per HeLa cell were counted. The 3 biological replicates for each strain are colour-coded. Each replicate consists of 10 fields of view. A non-parametric one-way ANOVA was used to determine statistical significance (****, P < 0.0001). Bars denote the mean.

General profile of gene expression between $\Delta cpxRA$ and auxiliary protein mutants supports the respective virulence phenotypes.

To further examine the disparity in phenotypes between our strains we sought to compare the regulon of the Cpx TCS and its auxiliary proteins. Our hypothesis is that genes repressed only in $\triangle cpxRA$ but not in $\triangle nlpE$ and in $\triangle cpxP$ could be responsible for the virulence defect of $\triangle cpxRA$. To this end, we performed microarray experiments on the wild-type, $\Delta cpxRA$, $\Delta nlpE$, and $\Delta cpxP$ strains of C. rodentium to determine the bacterial genes regulated by each TCS/sensor in vitro. We have previously confirmed that the expression profiles of the TCS during growth in DMEM closely resembles that seen in vivo, and hence used this condition to grow the strains [265]. To gain insight into the virulence-associated CpxRA regulome, we focused our analysis on the genes differentially regulated (p<0.05, \log_2 ratio of mutant/wild-type >1 or <-1) in the $\Delta cpxRA$ strain compared to wild-type (Figure 5, Table S3). There are 393 genes differentially regulated in the $\Delta cpxRA$ strain relative to wild-type, of which 228 are upregulated and 165 genes are downregulated (Figure 5A-B). Further, there are 357 differentially regulated genes in the \(\Delta nlpE \) regulon, of which 345 are upregulated and 12 are downregulated (Figure 5A-B). In the $\Delta cpxP$ regulon, there are 793 differentially regulated genes, of which 767 are upregulated and 26 are downregulated (Figure 5A-B). There exists some overlap in the genes differentially regulated in each of the single mutant strains, as seen in Figures 5A and 5B.

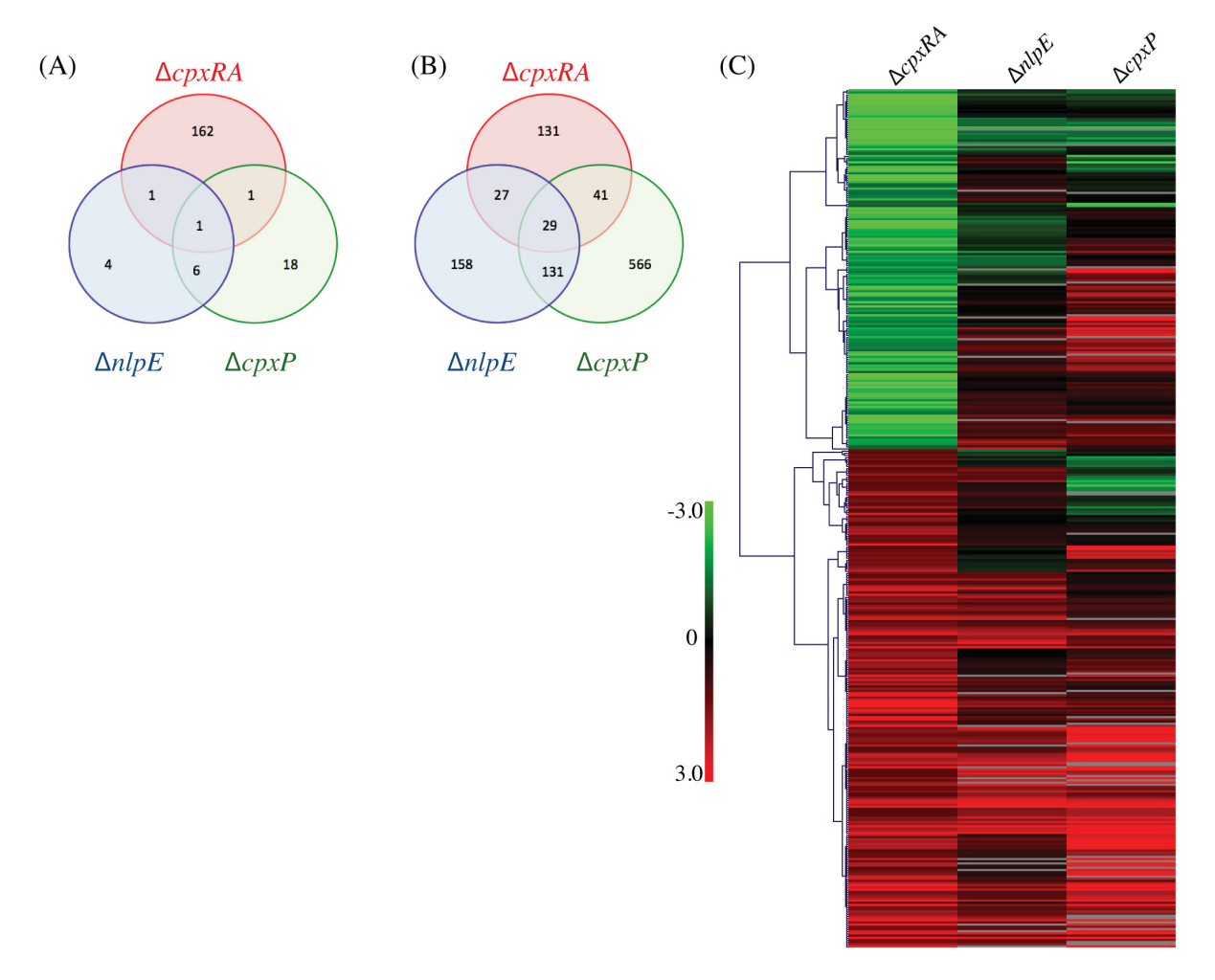


Figure 5: General gene expression profile of all mutant strains relative to wild-type.

Strains were grown in DMEM and RNA was extracted from three biological replicates. The expression profiles of mutant strains were compared to that of the wild-type C. rodentium. (A) Venn diagram of the downregulated genes in each deletion strain. (B) Venn diagram of the upregulated genes in each deletion strain. (C) Genes differentially expressed in Δ cpxRA were clustered with Hierarchical clustering, using Pearson Uncentered correlation. Upregulated genes are shown in red, and downregulated genes are in green. Genes displayed are differentially expressed in the Δ cpxRA C. rodentium strain. An unpaired t-test was used to determine statistical significance (p \leq 0.05).

We hypothesized that genes downregulated in the $\Delta cpxRA$ strain but either unchanged or upregulated in all other strains could be responsible for the virulence defect. To this end, we detected 161 genes significantly downregulated in the $\Delta cpxRA$ strain that were upregulated or unchanged in the Cpx auxiliary protein deletion strains. This list includes known virulence factors, outer membrane proteins, metabolism proteins, plasmids, and putative prophage genes (Table 1, Table S3).

Genes differentially expressed in $\Delta cpxRA$ were analyzed with Hierarchical clustering, using the Pearson Uncentered correlation (Figure 5C). For some genes, the values for $\Delta cpxP$, and $\Delta nlpE$ are not statistically significant. See Supplementary Table S3 for details. As seen in Figure 5C, the expression profile of the $\Delta nlpE$ strain correlates well with patterns seen in the $\Delta cpxRA$ strain for genes repressed by CpxRA (upregulated in the mutant). However, in the subset of genes activated by CpxRA, the correlation between the $\Delta nlpE$ and $\Delta cpxRA$ strains is not evident, indicating that in these conditions, induction of expression of genes by CpxRA is acting in a largely NlpE-independent manner. If NlpE was required for activation of the Cpx TCS, all genes downregulated in the $\triangle cpxRA$ strain would also be downregulated in the $\triangle nlpE$ strain, but instead we found that the majority of these genes were upregulated or unchanged (Figure 5). Further, since CpxP is proposed to be a negative regulator of the Cpx TCS, we hypothesized that gene expression in $\Delta cpxRA$ would be inversely correlated with the gene expression in the $\Delta cpxP$ strain. To the contrary, we detect a correlation similar to that of the $\Delta nlpE$ strain, where the repressed genes correlate with expression patterns in the $\Delta cpxP$ strain, and only some of the activated genes are inversely correlated, suggesting that CpxP is not acting as a global negative regulator of the Cpx response in these conditions (Figure 5).

DISCUSSION

In the dynamic setting of infection, bacteria must be able to sense environmental cues and adapt gene expression accordingly. Through the use of two-component systems (TCSs), bacteria utilize an inner membrane-bound sensor kinase to sense a signal, which is subsequently transferred to a cytoplasmic response regulator through phosphate transfer [166]. The cytoplasmic response regulator binds to cognate DNA sequences in specific target genes in order to alter their expression [166]. Several TCSs have been implicated in virulence of A/E pathogens, both by our group and others [176, 199, 265]. In this study, we specifically evaluate the CpxRA TCS virulence defect in the context of upstream signalling through the NlpE lipoprotein. We also aim to determine the effect of the negative regulator protein CpxP on virulence. The $\Delta nlpE$ and $\Delta cpxP$ strains exhibited no defect in virulence, as the mice succumbed to infection with similar kinetics to those infected with wild-type *C. rodentium*. Further, *in vivo* localization experiments and *in vitro* adherence experiments showed no difference between the auxiliary protein mutants and wild-type. As such, we suggest that the virulence defect previously shown in the absence of CpxRA is independent of both NlpE and CpxP.

With the use of microarrays, we determined the regulon of the $\Delta cpxRA$, $\Delta nlpE$, and $\Delta cpxP$ deletion strains. Based on their proposed functions, we hypothesized that genes differentially expressed in the $\Delta cpxRA$ strain should be directly correlated with those in the $\Delta nlpE$ strain, and inversely correlated with those in the $\Delta cpxP$ strain. In contrast to our hypothesis, we found that a significant number of genes in the $\Delta cpxRA$ deletion strain are regulated independently of both auxiliary proteins. As such, the genes regulated by CpxRA independently of NlpE and CpxP are good candidates to explain the lack of virulence of the $\Delta cpxRA$ strain. We hypothesize that the

virulence-associated effect of CpxRA is due to the differential regulation of a combination of genes, rather than a single gene. Certain candidate genes, however, are more likely to be playing a role than others.

The Type 3 Secretion System (T3SS) is absolutely essential to the virulence of A/E pathogens. As such, screening for a downregulation of effectors and translocators of this system is an attractive target for virulence defects. We detected an uncharacterized putative T3SS effector, annotated as espO, to be downregulated in the $\Delta cpxRA$ strain, but unchanged in all other strains, relative to wild-type C. rodentium (Table 1, Table S3).

Another candidate that arose in our study is the Type VI Secretion System (T6SS), present in Gram-negative bacteria. The T6SS is a membrane-spanning molecular structure which is assembled in the cytoplasm before being propelled towards a target bacterial or eukaryotic cell [275]. The T6SS transfers effectors to the target cell in order to cause cell damage. It can inject toxins into eukaryotic cells that interfere with the cytoskeleton, and also translocate antibacterial effectors targeting bacterial cells directly [275-277]. The genome of *C. rodentium* harbors two T6SS clusters, CTS1 and CTS2 [56, 278]. CTS1 has a frameshift mutation in the *cts11* gene which results in a premature stop codon [278]. However, due to a sequence of consecutive adenosines prior to this stop codon, slippage can occur, leading to a functional CTS1 T6SS [279]. Two genes in the CTS1 cluster, cts1G, cts1F are downregulated in the $\Delta cpxRA$ regulon (Table 1). The cts1F gene is a Forkhead-associated protein, and cts1G is associated with the VgrG family [56]. VgrG is exposed at the surface and acts as a cell-puncturing device, before likely being secreted into the host cell, where is has been reported to crosslink actin *in vitro* [276]. As such, a downregulation

in this system could limit the ability of *C. rodentium* to compete with commensal bacteria for access to the intestinal epithelium, which is crucial for its ability to colonize the host or interact with eukaryotic cells. This effect would possibly make *C. rodentium* unfit for its colonization and survival within the gut.

Maltose is essential for the colonization of the gut by EHEC O157:H7 [280]. We detect the downregulation of multiple genes involved in maltose metabolism in the $\Delta cpxRA$ strain, whereas they are unchanged in the auxiliary protein mutants. These genes include the maltoporin lamB, the substrate-binding protein malE, the permease protein malG, the maltodextrin phosphorylase malP, the periplasmic protein malM, the ATP-binding protein malK, and the permease protein mslF (Table 1, S3). These genes are involved in maltose and maltodextrin transport and metabolism in commensal and pathogenic $E.\ coli\ [280]$. Further, maltose metabolism genes are upregulated in $E.\ coli\$ in the presence of mucus, suggesting a role in the gut environment [281]. As such, the downregulation of these genes could render the $\Delta cpxRA$ strain unable to use maltose as a nutrient source, which may be important in the intestine.

We detected a significant downregulation of the gene ygdI, in the $\Delta cpxRA$ strain, while remaining unchanged in the $\Delta nlpE$ strain and upregulated in the $\Delta cpxP$ strain. In silico analysis using CD-search, TMHMM and SignalP revealed that YgdI is a putative small lipoprotein with a DUF903 domain, a Sec-dependent signal sequence, and a putative transmembrane helix which is likely cleaved during export [282-284]. Taken together, this in silico analysis suggests that the YgdI lipoprotein may be localized to the periplasm. Further, YgdI is highly and positively regulated by RpoS, a sigma factor that responds to a multitude of stressors [285, 286]. Since a

significant role of the Cpx TCS is to respond to misfolded proteins [266], it is conceivable that YgdI could be involved in mitigating membrane or periplasmic stress resulting in misfolded proteins. This will require further experimentation.

Further, two biofilm-related genes were downregulated in $\Delta cpxRA$. bdm, a biofilm-dependent modulation gene, was repressed 10-fold relative to the wild-type (Table 1, Table S3). bdm expression is known to be reduced within biofilms; however, overexpression reportedly increased biofilm production [287, 288]. bdm expression occurs in response to osmotic shock and is reported to be under the control of the Rcs TCS, thereby suggesting a link between the Rcs and Cpx TCSs [289]. bssR, a biofilm regulator, was downregulated approximately 6-fold in $\Delta cpxRA$. The bssR transcript is induced in the stationary phase and has been shown to impact biofilm formation through a complex pathway involving indole regulation, and the uptake and export of autoinducer 2 [290, 291]. While the link between biofilm formation and virulence is ill-defined in C. rodentium, overlap between these two systems is documented in other bacterial species and is mediated by quorum sensing systems [292].

Fable 1 - Selected gene	s signiii		vnregulate		<u>ка.</u>	T	
Function	Gene	T-Test WT vs ΔcpxRA	Δ <i>cpxRA</i> - WT	T-Test WT vs ΔnlpE	ΔnlpE- WT	T-Test WT vs ΔcpxP	Δ <i>cpxP</i> -WT
biofilm regulator	bssR	0.0041	-2.54	0.2405	0.68	0.0217	1.96
carbamoyl-phosphate				1			1
synthase small chain	carA	0.0209	-1.26	0.4502	0.61	0.2437	-0.40
cobalamin biosynthesis							
protein CbiG	cbiG	0.0211	-1.23	0.1584	0.41	0.0070	1.02
colanic acid capsullar							
biosynthesis activation							
protein A	rcsA	0.0292	-3.45	0.3549	0.24	0.2449	-0.05
GntR-family							
transcriptional regulator		0.0054	-2.34	0.4119	1.15	0.0185	1.13
LysR-family							
transcriptional regulator	ttdR	0.0145	-1.67	0.2140	0.77	0.3299	-1.17
maltodextrin							
phosphorylase	malP	0.0086	-4.75	0.0854	-1.52	0.3346	-1.27
maltoporin (maltose-	1 D	0.0164	5.01	0.1660	2.20	0.1640	2.55
inducible porin)	lamB	0.0164	-5.91	0.1668	-2.38	0.1648	-2.55
maltose operon	1111	0.0042	4.20	0.0647	1 17	0.2269	1.20
periplasmic protein	malM	0.0042	-4.39	0.0647	-1.17	0.2268	-1.30
maltose transport system, permease protein	mslF	0.0089	-5.80	0.2379	-1.34	0.4134	0.06
maltose transport system,	mstr	0.0089	-3.80	0.2379	-1.34	0.4134	0.00
permease protein	malG	0.0068	-5.48	0.2072	-1.30	0.1935	-1.97
maltose transport system,	maro	0.0000	3.10	0.2072	1.50	0.1755	1.77
substrate-binding protein	malE	0.0126	-5.88	0.2793	-1.76	0.1719	-1.99
maltose/maltodextrin							
transport system,ATP-							
binding protein	malK	0.0116	-4.27	0.2263	-1.80	0.2833	1.74
mannose-specific PTS							
system EIIAB component	manX	0.0043	-1.76	0.3941	0.18	0.0856	1.04
mannose-specific PTS							
system EIIAB component	manX	0.0084	-1.52	0.4406	-0.51	0.0397	0.68
outer membrane protein F	ompF	0.0009	-4.29	0.3480	0.33	0.1720	1.02
protein Bdm (biofilm-							
dependent modulation							
protein)	bdm	0.0443	-3.36	0.4975	1.44	0.0619	1.16
putative colanic acid							
biosynthesis glycosyl							
transferase	wcaL	0.0025	-1.61	0.3977	0.59	0.1976	2.80
putative lipoprotein	ygdI	0.0029	-2.19	0.1360	0.84	0.0114	1.28
putative T3SS effector							
protein EspO	espO	0.0038	-2.87	0.1631	-0.83	0.4596	0.03
universal stress protein F	uspF	0.0215	-2.64	0.3482	0.21	0.1871	0.54
VgrG family T6SS protein	uspi'	0.0213	-2.04	0.3402	0.41	0.10/1	0.54
Cts1G OR T6SS protein	cts1G,						
Cts1F	cts1G,	0.0203	-1.77	0.2643	0.80	0.2062	2.22

The $\Delta cpxRA$ virulence defect may be due to the strain's inability to adhere adequately to epithelial cells. Our in vitro adherence experiments uncovered a striking decrease in adherence in this strain, similar to what we see in our *in vivo* localization experiments. We detected a slight upregulation in some genes of the classical C. rodentium type 4 pilus operons, kfc and cfc, in multiple strains, including $\Delta cpxRA$ (Table S3) [161, 162]. These operons are largely associated with intestinal colonization and adherence; however, there was no pattern of expression among the strains which could explain the virulence phenotypes. Nevertheless, we detect significant downregulation of a number of genes which could be indirectly contributing to adherence through the alteration of the outer membrane or the capsule of the bacterium. Namely, we detected decreased levels of ompF, which makes up a large component of the outer membrane. While previous work in E. coli uncovered that the Cpx TCS negatively controls expression of ompF, we found that loss of cpxRA lead to the downregulation of ompF [293]. In avian pathogenic E. coli the loss of *ompF* significantly decreases bacterial virulence in both duck and mouse models of infection, as well as decreases adherence in vitro [294, 295]. We also detected a downregulation of the universal stress protein F, uspF, in $\Delta cpxRA$, compared to unchanged expression levels in all other strains. Universal stress proteins compose a family of proteins which respond to different types of cellular stress, including oxidative stress [296]. In E. coli, uspF, a member of the second class of these proteins, promotes fimbria-mediated adhesion of the bacteria [297]. In atypical EPEC, uspF expression was detected at high levels in response to oxidative stress, low pH, high salt concentration, and heat [298]. The decreased expression of uspF in $\Delta cpxRA$ could render the strain unfit to combat cellular stress and/or adhere to the epithelium. Another gene uncovered in our studies is the colanic acid capsular biosynthesis activation protein A, or rcsA, which is part of the Rcs phosphorelay TCS, as well as wcaL, a putative colanic acid biosynthesis glycosyl

transferase [265]. Colanic acid is a capsule protein, which could alter the bacterium's ability to adhere to surfaces. We have previously shown that the deletion of the Rcs TCS leads to moderate attenuation of *C. rodentium*, suggesting that the lack of virulence in the $\Delta cpxRA$ strain could be the result of crosstalk between the Cpx and Rcs TCSs [265]. However, the attenuation of the Rcs TCS mutant was much less pronounced than that of the CpxRA mutant, indicating that decreased expression of *rcs* on its own is unlikely to account for the attenuation of the $\Delta cpxRA$ mutant.

We also detected multiple significantly downregulated transcriptional regulators in the $\Delta cpxRA$ strain, which are either upregulated or unchanged in the other strains (Table 1, Table S3). Specifically, we detected the transcriptional regulators, yiaG, and ttdR, suggesting that the virulence defect could be regulated indirectly by CpxRA (Table 1).

In conclusion, this study characterizes the *Citrobacter rodentium* virulence defect caused by the deletion of the CpxRA TCS to be independent of NlpE and CpxP. The $\Delta nlpE$ and $\Delta cpxP$ deletion strains were fully virulent and able to adhere to cells both *in vitro* and *in vivo*. Furthermore, we studied the regulon of each of these strains, in an effort to uncover the gene(s) responsible for this effect. Future studies will aim to uncover the exact mechanism of attenuation of the Cpx TCS deletion strain, which is likely to involve a multitude of factors, such as T6SS, *ompF*, *uspF* and colanic acid. The delineation of this mechanism could uncover future therapeutic targets for the treatment of enteric pathogens.

ACKNOWLEDGMENTS

This manuscript is dedicated to the memory of our dear colleague Hervé Le Moual. Microscopy was performed at the McGill University Life Sciences Complex Advanced BioImaging Facility (ABIF), and tissues were processed and sectioned at the Goodman Cancer Research Centre Histology Core. Work in SPF laboratory was supported by Discovery Grant 418289–2012 from the National Sciences and Engineering Research Council of Canada (NSERC) and a John R. Evans Leaders Fund – Funding for research infrastructure from the Canadian Foundation for Innovation. This work was also supported by Discovery Grants from the National Sciences and Engineering Research Council of Canada (NSERC) RGPIN-2014-05119 awarded to SG, and RGPIN-2014-04751 awarded to HLM, and by a Fonds de Recherche Quebec Nature et Technologie (FRQNT) Team Grant awarded to HLM and SG. We thank Eugene Kang (McGill University) for his comments on the manuscript.

Author contributions

NG, NM, and LZ participated in the design of the experiments and performed the experiments. HM, SG and SPF designed the experiments and supervised the work. All authors participated in data analysis. The manuscript was written by NG and edited by HM, NM, SG, and SF.

Conflict of interest

The authors declare that the research was conducted in the absence of any commercial or financial relationships that could be construed as a potential conflict of interest.

SUPPLEMENTAL INFORMATION

Table S1: Strains and plasmids used in this study

Strain or plasmid	Description	Reference or source
Citrobacter rodentium		
Wild-type	C. rodentium DBS100	[55]
$\Delta cpxRA$	DBS100 ∆cpxRA	[199]
$\triangle cpxRA::cpxRA$	DBS100 ∆cpxRA::cpxRA	[199]
$\triangle nlpE$	DBS100 <i>∆nlpE</i>	This study
$\triangle cpxP$	DBS100 ∆cpxP	This study
$\Delta nlpE\Delta cpxP$	DBS100 ∆nlpE∆cpxP	This study
Escherichia coli		
χ7213	thr-1 leuB6 fhuA21 lacY1 glnV44 recA1 asdA4 thi-1 RP4-	[263]
	2-Tc::Mu [- pir] Kan ^r	
$\chi 7213(p\Delta nlpE)$	χ 7213 containing p $\Delta nlpE$	This study
χ7213(pΔ <i>cpxP</i>)	χ7213 containing p $ΔcpxP$	This study
Plasmids		
pRE112	Sucrose-sensitive (sacB1)	[264]
	suicide vector; Cm ^r	
p <i>∆nlpE</i>	nlpE deletion construct in pRE112	This study
p <i>∆cpxP</i>	cpxP deletion construct in pRE112	This study

Table S2: Primers used to generate deletion strains

Deletion strain	Primer	Sequence $(5' \rightarrow 3')$	Restriction site
			SILC
$\Delta nlpE$	nlpE_1	GCTCTAGAGGTTGTTAATGTGGCGGATCTCG	XbaI
	nlpE_2	CCGCTCGAGTATCGCGGAGATGAGTGTCTTT	XhoI
	nlpE_3	CCGCTCGAGCCAGGACTGTAACAGTAAATAA	XhoI
	nlpE_4	GGGGTACCTTGTCGAAGGTCGTGCCTAAA	KpnI
$\Delta cpxP$	cpxP_1	GCTCTAGAGGCTATTATCTGGCCGTAGTATAA	XbaI
	cpxP_2	CCGCTCGAGTAGCAACTCACGTTCCCAGTAA	XhoI
	cpxP_3	CCGCTCGAGGCAGCGGTAACTTTGCGCAT	XhoI
	cpxP_4	GGGGTACCGAGTCGAGCTTGGGCAACATCA	KpnI

Table S3: Differentially expressed genes across all strains

Probe ID	p value Δ <i>cpxRA</i> vs WT	Log 2 Δ <i>cpxRA</i> /WT	p value Δ <i>nlpE</i> vs WT	Log 2 ΔnlpE/WT	p value Δ <i>cpxP</i> vs WT	Log2 Δ <i>cpxP</i> /WT	Function	Gene
NZ JXUN01000001.1 cds WP 000850547.1 6	0.0441	1.51	0.1021	2.31	0.0351	1.99	conserved hypothetical protein	
NZ JXUN01000001.1 cds WP 012904982.1 5	0.0250	1.14	0.1006	2.64	0.0734	2.08	lipoyltransferase (lipoate-protein ligase B)	lipB
NZ_JXUN01000004.1_cds_WP_012906987.1_4407	0.0049	1.10	0.0424	1.67	0.1409	1.26	L-fuculose phosphate aldolase	fucA
NZ JXUN01000004.1 cds WP 042622865.1 4404	0.3714	-0.22	0.0099	1.57	0.0679	1.16	putative ABC transporter membrane protein	
NZ_JXUN01000005.1_cds_WP_012905427.1_4548	0.0287	-1.84	0.4551	-0.40	0.0518	2.36	negative regulator of flagellin synthesis (anti-sigma factor)	flgM
NZ_JXUN01000006.1_cds_WP_012905155.1_4704	0.1018	-0.82	0.0986	0.97	0.0425	1.03	putative hydrolase	
NZ_JXUN01000006.1_cds_WP_012905157.1_4706		1.40	0.0071	3.17			putative pyruvate formate-lyase 3-activating enzyme	pflE
NZ_JXUN01000009.1_cds_WP_012907055.1_5204	0.4019	1.60	0.2662	-0.10	0.0410	1.64	fimbrial subunit FimI	fimI
NZ_JXUN01000009.1_cds_WP_012907057.1_5202	0.1918	3.21	0.0228	2.52	0.0181	3.84	fimbrial usher protein FimD	fimD
NZ_JXUN01000009.1_cds_WP_012907059.1_5200	0.1623	1.51	0.1126	1.73	0.0149	2.08	fimbrial minor subunit FimG	fimG
NZ_JXUN01000009.1_cds_WP_012907065.1_5194	0.2046	1.25	0.0331	1.40	0.0282	2.27	putative fimbrial protein	
NZ_JXUN01000009.1_cds_WP_012907069.1_5190	0.4354	0.02	0.0368	1.85	0.0156	2.82	putative lipoprotein	
NZ_JXUN01000009.1_cds_WP_024132834.1_5208	0.1223	5.69	0.3004	1.91	0.0124	4.28	hypothetical protein	
NZ_JXUN01000009.1_cds_WP_024132838.1_5192	0.0367	-1.39	0.3671	0.49	0.3062	-0.08	hypothetical protein	
NZ_JXUN01000009.1_cds_WP_049794260.1_5203	0.1006	2.44	0.2060	0.48	0.0026	4.04	fimbrial chaperone protein FimC	fimC
NZ_JXUN01000010.1_cds_WP_012905524.1_43		-2.70	0.2381	2.11	0.0389	2.70	putative dehydrogenase	
NZ_JXUN01000010.1_cds_WP_012905526.1_41	0.0002	2.34	0.0184	1.98	0.0196	2.00	GntR-family transcriptional regulator	
NZ_JXUN01000010.1_cds_WP_012905527.1_40	0.0500	1.86	0.2765	0.51	0.1879	1.09	SOS mutagenesis and repair protein	umuC
NZ_JXUN01000010.1_cds_WP_012905531.1_37	0.1497	0.67	0.0786	3.06	0.0054	3.32	conserved hypothetical protein	
NZ_JXUN01000010.1_cds_WP_012905546.1_24	0.2844	-0.21	0.0685	1.65	0.0096	2.88	putative serine protein kinase	
NZ_JXUN01000010.1_cds_WP_012905552.1_18	0.0406	-1.24	0.3285	-0.08	0.4225	0.60	conserved hypothetical protein	
NZ_JXUN01000010.1_cds_WP_012905554.1_16		-0.17	0.3621	2.06	0.0158	2.81	putative exported protein	
NZ_JXUN01000010.1_cds_WP_012905555.1_15	0.2913	0.77	0.0457	2.16	0.0012	4.49	putative zinc-binding dehydrogenase	
NZ_JXUN01000010.1_cds_WP_012905556.1_14	0.1984	2.67	0.0547	3.43	0.0059	6.47	major facilitator superfamily protein	
NZ_JXUN01000011.1_cds_WP_000874676.1_385			0.0270	2.74			hypothetical prophage protein	
NZ_JXUN01000011.1_cds_WP_012904645.1_381	0.2828	-0.89	0.4940	-0.40	0.0156	1.31	putative prophage exported protein	
NZ_JXUN01000011.1_cds_WP_012904647.1_383	0.1188	2.72	0.1590	2.67	0.0306	4.64	hypothetical prophage protein	
NZ_JXUN01000011.1_cds_WP_012904648.1_384	0.2210	0.94			0.0071	3.78	hypothetical prophage protein	
NZ_JXUN01000011.1_cds_WP_012904648.1_384	0.2210	0.94			0.0071	3.78	hypothetical prophage protein	
NZ_JXUN01000011.1_cds_WP_024132489.1_377	0.0322	0.98	0.0052	1.24	0.1597	0.72	pseudogene	
NZ_JXUN01000013.1_cds_WP_012904796.1_942	0.3426	0.45	0.0102	4.30	0.0019	3.49	exonuclease SbcC	sbcC
NZ_JXUN01000013.1_cds_WP_012904797.1_941	0.0357	0.88	0.0597	0.67	0.0177	1.41	exonuclease SbcC	sbcC
NZ_JXUN01000013.1_cds_WP_012904798.1_940	0.0694	0.80	0.2603	0.82			phosphate regulon two-component system, response regulator	phoB
NZ_JXUN01000013.1_cds_WP_012904799.1_939	0.2858	0.95	0.3516	-0.14	0.0341	1.61	phosphate regulon two-component system, sensor kinase	phoR

NZ_JXUN01000013.1_cds_WP_012904813.1_925	0.0491	1.87	0.0545	2.25	0.1006	2.78	putative DeoR-family transcriptional regulator	
NZ_JXUN01000013.1_cds_WP_012904818.1_919	0.0378	1.19	0.3270	0.54	0.2843	-0.68	N utilization substance protein B	nusB
NZ_JXUN01000013.1_cds_WP_024132516.1_923	0.4906	0.17	0.0218	1.30	0.0584	1.61	putative lipoprotein	
NZ_JXUN01000014.1_cds_WP_012906680.1_1162	0.0269	0.98	0.0999	0.50	0.0401	1.61	tRNA-specific adenosine deaminase	tadA
NZ_JXUN01000014.1_cds_WP_012906681.1_1163	0.1189	1.10	0.0451	1.90	0.1070	1.75	putative membrane protein	
NZ_JXUN01000014.1_cds_WP_012906685.1_1167	0.0114	1.54	0.0368	1.36	0.0077	3.65	putative ferrodoxin	
NZ_JXUN01000014.1_cds_WP_012906690.1_1172	0.0386	0.59	0.4524	-0.41	0.0219	0.32	Ribonuclease III	rnc
NZ_JXUN01000014.1_cds_WP_012906691.1_1174	0.0425	1.67	0.4078	0.06	0.2834	-0.27	signal peptidase I	lepB
NZ_JXUN01000014.1_cds_WP_012906693.1_1176	0.3656	0.41	0.0062	2.14	0.0035	2.40	conserved hypothetical protein	
NZ_JXUN01000014.1_cds_WP_012906696.1_1179	0.0349	1.45	0.4757	-0.64	0.3721	-1.52	sigma-E factor negative regulator	rseA
NZ_JXUN01000014.1_cds_WP_012906705.1_1189	0.1765	1.10	0.0457	1.97	0.0744	1.57	conserved hypothetical protein	
NZ_JXUN01000014.1_cds_WP_012906706.1_1190	0.3680	-1.40	0.0256	-1.18	0.2913	2.42	putative acyl-CoA synthetase	
NZ JXUN01000014.1 cds WP 024132775.1 1177	0.0281	3.80	0.2929	1.26	0.4433	1.30	sigma-E factor regulatory protein	rseC
NZ JXUN01000014.1 cds WP 043013941.1 1159	0.1605	0.63	0.1093	1.61	0.0271	4.37	two-component system sensor kinase	
NZ JXUN01000015.1 cds WP 012908189.1 1514	0.3288	0.85	0.2475	0.94	0.0494	1.76	cold shock protein	cspA
NZ JXUN01000015.1 cds WP 012908191.1 1516	0.4473	0.84	0.4311	2.14	0.0219	3.57	Major Facilitator Superfamily transporter	
NZ JXUN01000015.1 cds WP 012908193.1 1518	0.4772	-0.07	0.0106	1.28	0.3183	1.31	2-ketogluconate reductase	tkrA
NZ JXUN01000015.1 cds WP 012908197.1 1521	0.0250	1.74			0.0195	3.71	putative acetyltransferase	
NZ JXUN01000015.1 cds WP 012908198.1 1523	0.4682	0.13	0.0110	1.81	0.0090	3.19	putative exported protein	
NZ JXUN01000015.1 cds WP 024133013.1 1515	0.0163	-3.71	0.1442	0.53	0.0466	0.61	putative transcriptional regulator	
NZ JXUN01000015.1 cds WP 042622885.1 1520	0.2745	-0.13	0.2660	-1.10	0.0274	2.11	biotin sulfoxide reductase OR putative outer	bisC
							membrane protein	
NZ_JXUN01000016.1_cds_WP_012907143.1_1767	0.0892	1.11	0.0479	0.82	0.0001	2.98	conserved hypothetical protein	
NZ_JXUN01000016.1_cds_WP_012907148.1_1772	0.2413	0.66	0.1412	1.22	0.0200	4.70	glycerate kinase 2	garK
NZ_JXUN01000016.1_cds_WP_071820599.1_1768	0.0319	2.38	0.0668	1.92	0.0009	3.58	hypothetical protein	
NZ_JXUN01000025.1_cds_WP_012906816.1_3819	0.1689	1.17	0.0317	2.06	0.0209	4.31	glycerophosphoryl diester phosphodiesterase	glpQ
NZ_JXUN01000025.1_cds_WP_012906817.1_3818	0.3879	-0.37	0.1360	0.47	0.0072	1.57	glycerol-3-phosphate transporter	glpT
NZ_JXUN01000025.1_cds_WP_012906819.1_3816					0.0398	5.60	anaerobic glycerol-3-phosphate dehydrogenase	glpB
NZ_JXUN01000025.1_cds_WP_012906820.1_3815		0.56			0.0002	2.66	subunit B anaerobic glycerol-3-phosphate dehydrogenase subunit B or C	glpB, glpC
NZ_JXUN01000025.1_cds_WP_012906830.1_3806	0.0439	1.02	0.0462	0.97	0.0262	1.82	putative aluminum inducible exported protein	ais
NZ_JXUN01000025.1_cds_WP_012906833.1_3803	0.0201	-1.86	0.0741	-1.43	0.4753	0.08	naphthoate synthase	menB
NZ_JXUN01000025.1_cds_WP_012906835.1_3801	0.1055	-1.66	0.0285	1.20	0.0382		menaquinone biosynthesis protein [includes:2- succinyl-6-hydroxy 2,4-cyclohexadiene-1- carboxylate synthase; 2-oxoglutarate decarboxylase]	menD
NZ JXUN01000025.1 cds WP 012906837.1 3799	0.0459	-1.22	0.3767	0.28	0.1215	-0.23	putative membrane protein	
NZ JXUN01000025.1 cds WP 012906839.1 3796	0.0011	-1.65	0.1345	1.07	0.0829	2.63	putative chemotaxis signal transduction protein	
NZ JXUN01000025.1 cds WP 024132801.1 3811		-0.03	0.0408	2.02	0.0110	2.66	putative MR-MLE-family protein	
NZ JXUN01000026.1 cds WP 012907571.1 4109	0.0439	1.14	0.0122	1.69	0.0049	1.31	putative transcriptional regulator	
NZ JXUN01000026.1 cds WP 024132931.1 4114	0.0277	0.92	0.0001	2.21	0.0933	-0.27	conserved hypothetical protein	
NZ JXUN01000027.1 cds WP 012908487.1 4162	0.0223	1.22	0.4663	0.50	0.2547	-1.52	50S ribosomal subunit protein L13	rplM
NZ JXUN01000027.1 cds WP 024133054.1 4154	0.1763	-0.44	0.0180	1.60	0.1581	0.64	putative exported protein	•
NZ_JXUN01000028.1_cds_WP_042622893.1_4179	0.2127	-0.80	0.0459	1.43	0.0276	1.37	bifunctional aspartokinase/homoserine dehydrogenase II]	metL

NZ_JXUN01000030.1_cds_WP_012907268.1_4212	0.0360	-2.35	0.4615	-0.41	0.0283	0.74	PTS system EIIA component OR PTS system EIIB component	
NZ_JXUN01000030.1_cds_WP_012907270.1_4214		0.29	0.0027	1.99			carbohydrate kinase	
NZ_JXUN01000030.1_cds_WP_012907271.1_4215	0.1052	2.36	0.0675	1.77	0.0298	5.78	sugar bisphosphate aldolase	
NZ_JXUN01000030.1_cds_WP_012907275.1_4219	0.2197	-0.55	0.0776	1.24	0.0362	2.26	putative LysR-family transcriptional regulator	
NZ_JXUN01000030.1_cds_WP_012907280.1_4224	0.0622	1.97	0.0382	3.16	0.0335		putative anti-adapter protein IraM	
NZ_JXUN01000030.1_cds_WP_024132871.1_4210	0.0054	-2.34	0.4119	1.15	0.0185	1.13	GntR-family transcriptional regulator	
NZ_JXUN01000030.1_cds_WP_042622895.1_4209	0.3231	-0.66	0.0521	1.73	0.0104	2.36	pseudogene	
NZ_JXUN01000031.1_cds_WP_000104288.1_4248	0.0721	0.79	0.0173	2.18	0.0634	1.52	pseudogene	
NZ_JXUN01000031.1_cds_WP_000599402.1_4245	0.1782	1.17	0.0240	2.74	0.0162	3.42	hypothetical prophage protein	
NZ_JXUN01000031.1_cds_WP_012907697.1_4263	0.0230	1.32	0.4331	-0.46	0.4773	0.88	LexA repressor	lexA
NZ_JXUN01000031.1_cds_WP_012907700.1_4266	0.1757	0.33	0.1289	0.55	0.0172	2.43	4-hydroxybenzoate octaprenyltransferase	ubiA
NZ_JXUN01000031.1_cds_WP_012907701.1_4267	0.1212	0.12	0.1277	0.38	0.0445	0.43	chorismatepyruvate lyase	ubiC
NZ_JXUN01000031.1_cds_WP_012907702.1_4268	0.0042	-4.39	0.0647	-1.17	0.2268	-1.30	maltose operon periplasmic protein	malM
NZ_JXUN01000031.1_cds_WP_012907703.1_4269	0.0164	-5.91	0.1668	-2.38	0.1648	-2.55	maltoporin (maltose-inducible porin)	lamB
NZ_JXUN01000031.1_cds_WP_012907704.1_4270	0.0116	-4.27	0.2263	-1.80	0.2833	1.74	maltose/maltodextrin transport system,ATP-binding	malK
NZ JXUN01000031.1 cds WP 012907706.1 4272	0.0089	-5.80	0.2379	-1.34	0.4134	0.06	protein maltose transport system, permease protein	mslF
NZ JXUN01000031.1 cds WP 012907707.1 4273	0.0068	-5.48	0.2072	-1.30	0.1935	-1.97	maltose transport system, permease protein	malG
NZ JXUN01000031.1 cds WP 012907715.1 4281	0.4077	1.21	0.2072	1.50	0.0378	2.43	putative lipoprotein	marc
NZ JXUN01000031.1 cds WP 012907716.1 4282	,	-2.65	0.1602	1.33	0.0304	3.76	putative exported protein	
NZ_JXUN01000031.1_cds_WP_012907720.1_4286	0.1000	0.80	0.0011	1.31	0.1141	0.67	lysine-sensitive aspartokinase III	lysC
NZ JXUN01000031.1 cds WP 012907723.1 4289	0.4356	0.19	0.0462	1.30	0.0179	2.19	transcriptional regulator	rtcR
NZ_JXUN01000031.1_cds_WP_012907726.1_4292	0.4428	0.17	0.0994	1.44	******		ribosomal large subunit pseudouridine synthase F	rluF
NZ JXUN01000031.1 cds WP 024132954.1 4271	0.0126	-5.88	0.2793	-1.76	0.1719	-1.99	maltose transport system, substrate-binding protein	malE
NZ JXUN01000031.1 cds WP 024132955.1 4276	0.3518	0.56	0.2770		0.0057	2.01	hypothetical protein	
NZ JXUN01000031.1 cds WP 024132956.1 4277	0.3957	-0.01	0.0893	2.93			putative oxidoreductase	
NZ JXUN01000031.1 cds WP 024132957.1 4287	0.3660	-0.56	0.1498	2.32	0.0417	3.97	conserved hypothetical protein	
NZ JXUN01000031.1 cds WP 024132959.1 4295	0.0314	-2.10	0.2802	-0.94	0.4595	0.10	peptidase E	рерЕ
NZ JXUN01000031.1 cds WP 042622896.1 4279	0.2303	0.60	0.0317	1.92	0.0416	1.31	PTS system, cellobiose-specific IIa component	Pep
NZ JXUN01000033.1 cds WP 012904794.1 4331	0.0951	0.67	0.0294	1.36	0.1951	0.23	probable manno(fructo)kinase	mak
NZ_JXUN01000034.1_cds_WP_071820635.1_4348	0.0355	1.42	0.2371	1.17	0.2024	0.00	LifA-like protein OR pseudogene	lifA3
NZ JXUN01000035.1 cds WP 012907858.1 4372	0.1941	-0.03	0.1162	0.72	0.0066	1.31	putative carbohydrate kinase	
NZ JXUN01000035.1 cds WP 012907861.1 4369	0.4752	-1.02	******	***-	0.0017	4.13	putative sugar kinase	
NZ JXUN01000035.1 cds WP 012907862.1 4368	0.4210	-0.48	0.0327	1.54			putative phosphogluconate dehydrogenase	
NZ JXUN01000035.1 cds WP 012907864.1 4366	0.4036	1.25	0.0327	1.5 .	0.0486	2.25	putative N-acylglucosamine 2-epimerase	
NZ JXUN01000036.1 cds WP 012905564.1 4393	0.0464	1.05	0.3842	-0.65	0.3330	-0.40	protease IV	sppA
NZ_JXUN01000040.1_cds_WP_012907886.1_4438	0.2052	-1.17	0.1522	0.85	0.0381	1.88	trk system potassium uptake protein	trkH
NZ JXUN01000040.1 cds WP 012907887.1 4437	0.4758	0.41	0.1322	1.58	0.0209	2.10	conserved hypothetical protein	UKII
NZ JXUN01000040.1 cds WP 012907898.1 4426	0.0063	1.27	0.2027	0.42	0.0209	2.10	probable ubiquinone biosynthesis protein	ubiB
NZ JXUN01000040.1 cds WP 012907899.1 4425	0.0003	1.19	0.3394	-0.26	0.0081	-1.30	conserved hypothetical protein	UUID
NZ JXUN01000040.1 cds WP 012907903.1 4421	0.0179	1.19	0.0168	0.90	0.0061	2.62	putative carboxymethylenebutenolidase	
112_97.01101000040.1_003_W1_012707703.1_4421	0.01/9	1,49	0.0100	0.50	0.0000	2.02	pamare carooxymearyrencoutenonuasc	

NZ_JXUN01000040.1_cds_WP_012907904.1_4420	0.1300	3.24			0.0101	3.33	5-methyltetrahydropteroyltriglutamate- homocysteine methyltransferase	metE
NZ_JXUN01000040.1_cds_WP_012907905.1_4419	0.4401	-0.27	0.0419	2.36	0.0376		trans-activator of metE and metH (LysR-family	metR
NZ JXUN01000040.1 cds WP 012907910.1 4414	0.0922	0.40	0.0291	1.22	0.1417	0.40	transcriptional regulator) threonine efflux protein	rhtC
NZ JXUN01000040.1 cds WP 012907911.1 4413	0.0026	1.23	0.1871	-1.31	0.3431	0.25	ATP-dependent DNA helicase	recQ
NZ_JXUN01000041.1_cds_WP_012904523.1_4456	0.0090	-2.91	0.3646	-0.04	0.1187	2.08	PTS system IIA component	
NZ_JXUN01000041.1_cds_WP_012904529.1_4450	0.0222	1.43	0.2735	1.38	0.4177	0.63	poly(A) polymerase	pcnB
NZ_JXUN01000041.1_cds_WP_012904532.1_4446		0.28	0.0604	1.65	0.0614	1.32	2'-5' RNA ligase	ligT
NZ_JXUN01000045.1_cds_WP_012907660.1_4467	0.3706	0.13			0.0001	3.15	universal stress protein g	uspG
NZ_JXUN01000047.1_cds_WP_001162094.1_4525	0.0683	1.16	0.0406	1.11	0.2844	-1.02	DNA-directed RNA polymerase alpha chain	rpoA
NZ_JXUN01000047.1_cds_WP_001216372.1_4526	0.0178	1.16	0.0129	1.16	0.3913	0.25	50S ribosomal subunit protein L17	rplQ
NZ_JXUN01000047.1_cds_WP_012908423.1_4497	0.1051	-1.83			0.0273	3.65	putative T2SS protein A	gspA
NZ_JXUN01000047.1_cds_WP_012908431.1_4522	0.0625	0.44	0.0148	1.26	0.2948	-0.27	30S ribosomal subunit protein S13	rpsM
NZ_JXUN01000047.1_cds_WP_012908433.1_4527	0.0321	2.83	0.3454	2.30	0.0438	2.53	conserved hypothetical protein	
NZ_JXUN01000047.1_cds_WP_012908434.1_4528	0.1274	1.10	0.0307	0.97	0.0022	1.95	putative Zn(II)-responsive regulator	zntR
NZ_JXUN01000049.1_cds_WP_012905495.1_4543	0.3710	-0.12	0.4851	-0.03	0.0224	1.00	two-component sensor kinase	phoQ
NZ_JXUN01000058.1_cds_WP_012905641.1_4587		-2.35	0.2680	0.26	0.0102	2.78	putative ABC transporter ATP-binding protein	
NZ_JXUN01000058.1_cds_WP_012905642.1_4586	0.0480	3.18			0.1074	2.36	putative ABC transporter ATP-binding protein OR putative ABC transporter membrane protein	
NZ JXUN01000058.1 cds WP 012905648.1 4580	0.4639	-0.47	0.0926	0.65	0.0408	2.27	putative oxidoreductase Fe-S subunit	
NZ_JXUN01000058.1_cds_WP_012905652.1_4575	0.3893	0.10	0.0271	1.15	0.3356	1.20	putative ATP-binding protein of ABC transporter	
NZ_JXUN01000058.1_cds_WP_012905654.1_4573	0.2150	0.68	0.2497	1.08	0.0004	1.62	putative exported protein	
NZ_JXUN01000058.1_cds_WP_024132638.1_4598	0.0437	2.47	0.2874	1.38	0.1565	0.40	conserved hypothetical protein	
NZ_JXUN01000059.1_cds_WP_012904712.1_4608	0.2661	2.07	0.1815	2.42	0.0447	5.25	anaerobic C4-dicarboxylate transporter	dcuA
NZ_JXUN01000059.1_cds_WP_012904714.1_4610	0.0815	0.72	0.0241	1.63	0.0064	2.05	gamma-glutamylputrescine synthetase	puuA
NZ_JXUN01000059.1_cds_WP_012904715.1_4611	0.4939	-0.83	0.2756	-0.27	0.0023	1.61	gamma-glutamyl-gamma-aminobutyrate hydrolase	puuD
NZ_JXUN01000059.1_cds_WP_012904716.1_4612	0.1696	0.66	0.1259	1.19	0.0432	1.37	transcriptional regulator of the polyamine metabolism genes	puuR
NZ_JXUN01000059.1_cds_WP_012904720.1_4616	0.2257	-0.61	0.0689	0.89	0.0234		hypothetical protein	
NZ_JXUN01000059.1_cds_WP_012904721.1_4617	0.1664	-2.56	0.0105	1.15	0.0835	0.15	hypothetical protein	
NZ_JXUN01000059.1_cds_WP_012904724.1_4620	0.1885	1.40	0.0892	1.29	0.0244	2.34	putative fimbrial chaperone protein	
NZ_JXUN01000059.1_cds_WP_012904725.1_4621	0.0362	1.33	0.1124	1.09	0.3664	0.99	putative major fimbrial subunit	
NZ_JXUN01000059.1_cds_WP_012904727.1_4623	0.3278	1.09			0.0315	1.28	putative membrane protein	
NZ_JXUN01000059.1_cds_WP_012904730.1_4626	0.3803	-0.09	0.3371	0.23	0.0383	3.13	putative microcin secretion protein	mchD
NZ_JXUN01000059.1_cds_WP_012904731.1_4627	0.0294	1.46	0.0266	1.55	0.1078	1.04	putative response regulator	
NZ_JXUN01000059.1_cds_WP_012904740.1_4635		-2.07	0.0368	1.72			putative zinc-binding dehydrogenase	
NZ_JXUN01000059.1_cds_WP_012904741.1_4636	0.1420	2.14	0.0106	2.14	0.0621	2.29	hypothetical protein	
NZ_JXUN01000059.1_cds_WP_012904744.1_4639	0.1765	3.04	0.0236	4.53	0.0156	7.09	putative xanthine dehydrogenase, FAD-binding subunit	
NZ_JXUN01000059.1_cds_WP_012904748.1_4643	0.2636	0.36	0.0649	2.23	0.0112	3.51	putative terminal oxidase subunit I	137
NZ_JXUN01000059.1_cds_WP_012904756.1_4652	0.4700	0.44	0.0348	2.04	0.1540	1.70	lactose permease	lacY
NZ_JXUN01000059.1_cds_WP_012904757.1_4653	0.1158	-1.38	0.1364	1.38	0.0055	2.78	beta-galactosidase	lacZ
NZ_JXUN01000059.1_cds_WP_012904759.1_4655	0.1695	0.66	0.0277	1.96	0.0439	2.29	putative AraC-family transcriptional regulator	

NZ_JXUN01000059.1_cds_WP_012904762.1_4658	0.0129	-1.65				1.81	Fe(3+) ions import ATP-binding protein FbpC	fbpC
NZ_JXUN01000059.1_cds_WP_012904764.1_4660	0.2801	0.00	0.2599	1.12			ABC transporter periplasmic iron-binding protein	afuA
NZ_JXUN01000059.1_cds_WP_012904768.1_4664	0.0142	-2.73			0.2835		aurine ABC transporter, substrate-binding protein(sulfate starvation induced protein)	tauA
NZ_JXUN01000059.1_cds_WP_012904769.1_4665		-0.05	0.1508	1.57	0.0395	1.74	taurine ABC transporter, ATP-binding protein	tauB
NZ_JXUN01000059.1_cds_WP_012904775.1_4671	0.2835	0.75	0.0915	1.24	0.0124	3.17	penicillin-binding protein	ampH
NZ_JXUN01000059.1_cds_WP_012904776.1_4672	0.3094	0.15	0.1686	2.22	0.0175	2.92	putative microcin B17 uptake protein	sbmA
NZ_JXUN01000059.1_cds_WP_012904784.1_4680	0.0364	1.11	0.0662	1.58	0.0630	1.91	alkaline phosphatase	phoA
NZ_JXUN01000059.1_cds_WP_012904785.1_4681	0.4110	0.41	0.0234	2.25	0.0934	2.50	phosphate starvation-inducible protein	psiF
NZ_JXUN01000059.1_cds_WP_024132501.1_4622	0.2771	0.80	0.1725	1.19	0.0319	2.66	putative membrane protein	
NZ_JXUN01000059.1_cds_WP_024132503.1_4632	0.4755	0.27	0.0530	1.78	0.0024	3.43	Major Facilitator Superfamily transporter	
NZ_JXUN01000059.1_cds_WP_024132507.1_4654	0.0208	0.95	0.0195	1.22	0.0271	0.84	lactose operon repressor	lacI
NZ_JXUN01000059.1_cds_WP_024132509.1_4675	0.4441	-0.18	0.2667	0.06	0.0399	0.33	putative membrane protein	
NZ_JXUN01000059.1_cds_WP_024132511.1_4677		4.94			0.0023	4.12	putative membrane protein	
NZ_JXUN01000059.1_cds_WP_042622937.1_4645	0.0291	2.13	0.4739	0.57	0.0027	5.50	putative terminal oxidase subunit II	
NZ_JXUN01000059.1_cds_WP_072044760.1_4606	0.3380	0.07	0.4601	-0.14			conserved hypothetical protein	
NZ_JXUN01000060.1_cds_WP_012907149.1_4714	0.0284	0.65	0.0094	1.01	0.0862	1.00	two-component sensor kinase/response regulator	barA
NZ_JXUN01000060.1_cds_WP_012907150.1_4715	0.2377	-0.17	0.0497	1.00	0.2076	0.55	23s rRNA (uracil-5-)-methyltransferase	rumA
NZ_JXUN01000060.1_cds_WP_024132856.1_4722	0.1914	-1.16	0.0217	1.69	0.3217	-0.23	probable hydrolase	
NZ_JXUN01000062.1_cds_WP_012904635.1_4734	0.4475	-0.08	0.2661	-0.43	0.0423	3.01	hypothetical prophage protein	
NZ_JXUN01000062.1_cds_WP_012904636.1_4733	0.0328	-2.60	0.2411	-0.49	0.1271	0.78	putative prophage DNA adenine methylase	dam
NZ_JXUN01000062.1_cds_WP_024132487.1_4726	0.3219	0.30	0.2432	0.54	0.0075	3.28	hypothetical prophage protein	
NZ_JXUN01000063.1_cds_WP_000905061.1_4745	0.2525	0.06	0.0354	1.17	0.0136	1.47	pseudogene	
NZ_JXUN01000063.1_cds_WP_000979945.1_4744	0.4149	-0.18	0.4211	-0.26	0.0194	3.78	pseudogene	
NZ_JXUN01000063.1_cds_WP_012906207.1_4738	0.3618	0.12	0.0287	2.10	0.0264	4.23	pseudogene	
NZ_JXUN01000063.1_cds_WP_012906209.1_4743		-2.63	0.4811	1.39	0.3239	0.15	pseudogene	
NZ_JXUN01000064.1_cds_WP_012907804.1_4771	0.2319	-0.69	0.1364	0.61	0.0415	0.26	Cell division protein zapB	zapB
NZ_JXUN01000064.1_cds_WP_012907805.1_4770	0.0136	-1.14	0.4304	0.25	0.2613	-0.85	glycerol uptake facilitator protein	glpF
NZ_JXUN01000064.1_cds_WP_012907808.1_4767	0.0735	1.40	0.0143	2.33			ferredoxinNADP reductase	fpr
NZ_JXUN01000064.1_cds_WP_012907813.1_4762	0.1980	1.27			0.0301	1.63	putative membrane protein	
NZ_JXUN01000064.1_cds_WP_012907814.1_4761	0.0332	2.74	0.0272	2.55	0.0030	3.35	putative exported protein	
NZ_JXUN01000064.1_cds_WP_012907815.1_4760	0.0632	2.78	0.1393	2.56	0.0135	4.89	putative exported protein	
NZ_JXUN01000064.1_cds_WP_012907821.1_4754	0.0104	-4.36	0.0901	1.25	0.0545	-3.19	periplasmic protein CpxP	cpxP
NZ_JXUN01000064.1_cds_WP_071820663.1_4755	0.1583	1.00	0.0190	1.93	0.0090	2.22	putative exported protein	
NZ_JXUN01000065.1_cds_WP_012904584.1_4778	0.0093	-1.15	0.4739	-0.48	0.1080	-0.05	RcsF, phosphorelay glucose and zinc sensor	rcsF
NZ_JXUN01000066.1_cds_WP_012908943.1_4790	0.1204	-1.28	0.0270	0.67	0.0242	0.72	pCROD1 plasmid	pCROD1
NZ_JXUN01000066.1_cds_WP_042622953.1_4793	0.4538	0.06	0.2147	1.42	0.0253	1.58	pCROD1 plasmid	pCROD1
NZ_JXUN01000067.1_cds_WP_012905017.1_4803	0.4472	0.54	0.0095	2.31	0.0506	2.95	conserved hypothetical protein	
NZ_JXUN01000067.1_cds_WP_012905018.1_4802	0.1877	2.28			0.0069	4.54	lysR-family transcriptional regulator	
NZ_JXUN01000070.1_cds_WP_012906210.1_4813	0.3510	0.68	0.0295	2.11	0.1429	1.26	pseudogene	
NZ_JXUN01000071.1_cds_WP_012906814.1_4817	0.0731	0.59	0.2293	0.30	0.0434	1.17	IS3 family transposase B	
NZ_JXUN01000072.1_cds_WP_012906361.1_4936	0.0834	0.48	0.0435	1.48	0.0159	1.87	histidinol dehydrogenase	hisD

NZ_JXUN01000072.1_cds_WP_012906362.1_4935	0.0581	0.50	0.1053	1.02	0.0234	1.96	histidinol-phosphate aminotransferase	hisC
NZ_JXUN01000072.1_cds_WP_012906363.1_4934	0.0770	0.65	0.1834	0.30	0.0198	1.57	histidinol-phosphate aminotransferase OR histidine biosynthesis bifunctional protein includes histidinol- phosphatase imidazoleglycerol-phosphat dehydratasel	hisC, hisB
NZ_JXUN01000072.1_cds_WP_012906364.1_4933	0.0312	3.90	0.1191	1.57	0.0366	4.73	imidazole glycerol phosphate synthase subunit	hisH
NZ_JXUN01000072.1_cds_WP_012906378.1_4919	0.0241	-2.87	0.3993	0.00	0.0052	-0.92	glucose-1-phosphate thymidylyltransferase	rfbA
NZ_JXUN01000072.1_cds_WP_012906384.1_4913	0.0025	-1.61	0.3977	0.59	0.1976	2.80	putative colanic acid biosynthesis glycosyl transferase	wcaL
NZ_JXUN01000072.1_cds_WP_012906385.1_4912	0.4544	-0.10					putative flippase	wzxC
NZ_JXUN01000072.1_cds_WP_012906386.1_4911	0.3883	0.69	0.0063	3.31	0.1039	4.28	putative colanic biosynthesis UDP-glucose lipid carrier transferase	wcaJ
NZ_JXUN01000072.1_cds_WP_012906388.1_4909		2.49	0.1125	2.10			mannose-1-phosphate guanylyltransferase	manC
NZ_JXUN01000072.1_cds_WP_012906389.1_4908		0.37	0.0453	3.05	0.1200	1.84	putative colanic acid biosynthesis glycosyl transferase	wcaI
NZ_JXUN01000072.1_cds_WP_012906392.1_4905	0.0253	1.68	0.0645	2.02	0.0182	5.54	GDP-mannose 4,6-dehydratase	gmd
NZ_JXUN01000072.1_cds_WP_012906394.1_4903	0.4849	-0.90	0.0543	1.01	0.0195	1.77	putative colanic acid biosynthesis glycosyl transferase	wcaE
NZ_JXUN01000072.1_cds_WP_012906396.1_4901			0.2232	1.49	0.0281	3.69	putative colanic acid biosynthesis glycosyl transferase	wcaE
NZ_JXUN01000072.1_cds_WP_012906401.1_4896	0.0198	-2.23	0.0268	1.42			putative polysaccharide export protein	wza
NZ_JXUN01000072.1_cds_WP_012906404.1_4892	0.0191	1.08	0.4681	-0.11	0.4789	-1.10	deoxycytidine triphosphate deaminase	dcd
NZ_JXUN01000072.1_cds_WP_012906406.1_4890	0.0072	1.66	0.0304	2.32	0.0442	1.82	putative signal transduction protein	
NZ_JXUN01000072.1_cds_WP_012906407.1_4889	0.4819	-0.08			0.0168	3.22	DNA-3-methyladenine glycosidase II	alkA
NZ_JXUN01000072.1_cds_WP_012906408.1_4888		3.72	0.0443	3.90	0.0863		conserved hypothetical protein	
NZ_JXUN01000072.1_cds_WP_012906409.1_4886	0.0935	0.74	0.1771	0.89	0.0093	1.51	multidrug resistance protein	mdtA
NZ_JXUN01000072.1_cds_WP_012906411.1_4884	0.1025	-1.28	0.0344	2.21	0.0188	1.28	multidrug resistance protein	mdtC
NZ_JXUN01000072.1_cds_WP_012906422.1_4873		2.97			0.0076	3.13	ABC transporter, permease protein	
NZ_JXUN01000072.1_cds_WP_012906424.1_4871	0.4501	-0.30			0.0324	1.88	putative mandelate racemase/muconate lactonising enzyme	
NZ_JXUN01000072.1_cds_WP_012906425.1_4870	0.1557	0.73	0.0513	2.13	0.0255	1.90	fructose-bisphosphate aldolase class 1	fbaD
NZ_JXUN01000072.1_cds_WP_012906433.1_4861	0.4483	0.68	0.4067	0.16	0.0400	2.30	putative fimbrial adhesin	
NZ_JXUN01000072.1_cds_WP_012906434.1_4860	0.1455	2.85	0.0219	4.15			fimbrial usher protein	
NZ_JXUN01000072.1_cds_WP_012906435.1_4859		-0.28	0.0380	0.75	0.0041	3.09	fimbrial chaperone protein	
NZ_JXUN01000072.1_cds_WP_012906440.1_4854	0.0504	1.05	0.0268	1.05	0.0066		two-component system response regulator	
NZ_JXUN01000072.1_cds_WP_012906443.1_4851	0.0511	0.52	0.0186	1.31	0.1769	-0.48	putative exported protein	
NZ_JXUN01000072.1_cds_WP_012906444.1_4850	0.4123	0.30	0.0271	1.54	0.0264	1.89	ABC transporter, permease protein	
NZ_JXUN01000072.1_cds_WP_012906445.1_4849	0.0223	0.62	0.1748	1.26	0.0137	0.84	ABC transporter, permease protein	
NZ_JXUN01000072.1_cds_WP_012906446.1_4848	0.4442	-0.46	0.1667	1.11	0.0119	2.52	ABC transporter permease protein	
NZ_JXUN01000072.1_cds_WP_012906448.1_4846	0.3196	-0.81	0.1940	0.40		3.37	Major facilitator superfamily transporter	
NZ_JXUN01000072.1_cds_WP_012906449.1_4845		0.83	0.0477	2.02	0.0479	1.76	Major facilitator superfamily transporter	
NZ_JXUN01000072.1_cds_WP_012906461.1_4831	0.1889	-1.56	0.3862	-0.45	0.0157	2.55	putative short-chain dehydrogenase	
NZ_JXUN01000072.1_cds_WP_012906465.1_4826		-2.43	0.0000	3.19			FAA-hydrolase-family protein	
NZ_JXUN01000072.1_cds_WP_012906466.1_4825	0.3015	0.17	0.2865	-1.17	0.0235	4.18	putative gentisate 1,2-dioxygenase	
NZ_JXUN01000072.1_cds_WP_012906469.1_4822	0.0472	1.56	0.0286	2.45	0.0084	2.81	putative membrane protein	
NZ_JXUN01000072.1_cds_WP_012906472.1_4819	0.0002	1.04	0.2115	0.83	0.0383	0.59	putative exported protein	

NZ_JXUN01000072.1_cds_WP_024132740.1_4907	0.1666	1.28	0.3876	1.04	0.0286	2.26	GDP-mannose mannosyl hydrolase	nudD
NZ_JXUN01000077.1_cds_WP_024132718.1_4962	0.2010	-0.36	0.0537	0.92	0.0109	1.60	pseudogene	
NZ_JXUN01000077.1_cds_WP_042622972.1_4963	0.1940	1.39					hypothetical prophage protein	
NZ_JXUN01000078.1_cds_WP_012905249.1_5030		-2.03	0.0066	2.10	0.0008	2.85	pseudogene	
NZ_JXUN01000078.1_cds_WP_012905253.1_5026	0.0954	2.31	0.0386	1.33	0.0048	3.25	pseudogene	
NZ_JXUN01000078.1_cds_WP_012905260.1_5019	0.0989	1.97			0.0182	4.43	pseudogene	
NZ_JXUN01000078.1_cds_WP_012905261.1_5018	0.1995	0.39	0.0109	1.27			pseudogene	
NZ_JXUN01000078.1_cds_WP_012905267.1_5011	0.3466	0.40			0.0056	3.60	pseudogene	
NZ_JXUN01000078.1_cds_WP_012905268.1_5010	0.3295	-0.75	0.0117	2.15			pseudogene	
NZ_JXUN01000078.1_cds_WP_012905269.1_5009	0.4572	0.52	0.2648	-0.29	0.0392	1.81	pseudogene	
NZ_JXUN01000078.1_cds_WP_012905272.1_5005	0.0270	2.39	0.1167	1.06	0.0474	2.18	LuxR-family transcriptional regulator	
NZ_JXUN01000078.1_cds_WP_012905274.1_5001	0.1684	0.88	0.1632	3.14	0.0045	4.68	leucyl/phenylalanyl-tRNA-protein transferase	aat
NZ_JXUN01000078.1_cds_WP_012905283.1_4990	0.1723	1.12			0.0181	2.21	anaerobic dimethyl sulfoxide reductase chain B	dmsB
NZ_JXUN01000078.1_cds_WP_012905284.1_4989	0.2415	1.02	0.2436	-0.10	0.0343	1.22	anaerobic dimethyl sulfoxide reductase chain C	dmsC
NZ_JXUN01000078.1_cds_WP_012905285.1_4988		0.40	0.0339	2.91	0.0291		putative isochorismatase	
NZ_JXUN01000078.1_cds_WP_012905288.1_4985	0.0205	1.09	0.4843	-0.32		3.07	putative phosphotransferase enzyme II, A componen	
NZ_JXUN01000078.1_cds_WP_012905293.1_4980	0.2415	0.28	0.2385	-0.30	0.0389	1.14	putative DNA binding protein	
NZ_JXUN01000078.1_cds_WP_012905299.1_4974	0.2129	0.22	0.1036	1.08	0.0203		putative membrane protein	
NZ_JXUN01000078.1_cds_WP_012905303.1_4969	0.4135	-0.23	0.4014	0.78	0.0350	-1.83	30S ribosomal protein S1	rpsA
NZ_JXUN01000078.1_cds_WP_024132571.1_5013	0.0762	2.58	0.0360	2.75	0.0148	5.07	pseudogene	
NZ_JXUN01000078.1_cds_WP_024132572.1_5012	0.2473	-1.17	0.0120	1.48	0.0022	2.63	pseudogene	
NZ_JXUN01000078.1_cds_WP_024132575.1_5004	0.1273	2.66	0.0268	1.05	0.0029	2.68	Hypothetical protein	
NZ_JXUN01000078.1_cds_WP_024132576.1_4981	0.0475	-2.30	0.1468	0.88	0.0372	1.06	conserved hypothetical protein	
NZ_JXUN01000078.1_cds_WP_071820571.1_4995	0.0179	0.94	0.0652	1.29	0.1569	-0.36	dna translocase ftsk	ftsK
NZ_JXUN01000080.1_cds_WP_012906959.1_5063	0.2636	0.28	0.2866	-0.38	0.0171	2.98	conserved hypothetical protein	
NZ_JXUN01000080.1_cds_WP_012906961.1_5065	0.0760	1.72	0.1119	0.73			aminopeptidase	ypdE
NZ_JXUN01000080.1_cds_WP_012906964.1_5068	0.1804	-2.05	0.0150	2.61	0.0074	2.17	fructose-like specific PTS system EIIB component 1	fryB
NZ_JXUN01000080.1_cds_WP_012906968.1_5072	0.0581	0.86	0.0298	1.31	0.0885	3.47	putative ion-channel protein	
NZ_JXUN01000080.1_cds_WP_024132823.1_5062	0.3847	-0.87	0.0167	1.22	0.3232	-0.80	conserved hypothetical protein	
NZ_JXUN01000083.1_cds_WP_012905098.1_5082		-1.10	0.0796	2.80	0.0056	2.88	imidazolonepropionase	hutI
NZ_JXUN01000083.1_cds_WP_012905105.1_5089	0.4449	0.46	0.0780	0.86	0.0360	2.04	biotin synthetase	bioB
NZ_JXUN01000083.1_cds_WP_012905106.1_5090	0.4683	0.03	0.0743	1.72	0.0160	4.11	8-amino-7-oxononanoate synthase	bioF
NZ_JXUN01000083.1_cds_WP_012905109.1_5095	0.2048	0.77			0.0389	1.17	UvrABC system protein B (excinuclease ABC	uvrB
NZ JXUN01000083.1 cds WP 012905112.1 5098	0.4521	-0.50	0.3229	1.32	0.0343	2.11	subunit B) molybdenum cofactor biosynthesis protein B	moaB
NZ JXUN01000083.1 cds WP 012905126.1 5112	0.0223	0.94	0.0071	2.15	0.0043	1.99	putative LysR-family transcriptional regulator	
NZ JXUN01000083.1 cds WP 012905127.1 5113	0.4316	-0.20			0.0159	2.89	Major Facilitator Superfamily transporter	
NZ JXUN01000083.1 cds WP 012905128.1 5114	0.0746	2.49	0.0520	1.62	0.0126	3.59	putative exported protein	
NZ_JXUN01000087.1_cds_WP_012904997.1_5122	0.0538	0.76	0.0127	2.24	0.1233		glutamate/aspartate ABC transporter, permease	gltK
						1.00	protein	_
NZ_JXUN01000087.1_cds_WP_012905008.1_5133	0.0111	1.44	0.1319	1.02	0.1929	1.90	putative N-acetylglucosamine metabolism protein	nagD
NZ_JXUN01000087.1_cds_WP_012905010.1_5135	0.1187	-0.63			0.0059	3.22	N-acetylglucosamine-6-phosphate deacetylase	nagA

NZ_JXUN01000088.1_cds_WP_012906542.1_5152	0.4851	0.14	0.2147	0.26	0.0023	1.74	regulatory protein of adaptative response [contains: methylated-DNAprotein-cysteine	ada
NZ JXUN01000088.1 cds WP 012906543.1 5151	0.1173	0.92	0.2793	0.15	0.0067	2.93	methyltransferase] thiamine biosynthesis lipoprotein	apbE
NZ JXUN01000088.1 cds WP 012906544.1 5150	0.0257	3.30	0.0301	1.61	0.0321	1.10	outer membrane protein C	ompC
NZ_JXUN01000088.1_cds_WP_012906551.1_5142	0.0556	1.15	0.1451	1.32	0.0475	3.11	putative ferredoxin	
NZ_JXUN01000088.1_cds_WP_042622990.1_5153	0.3612	1.42	0.3291	-0.69	0.0473	1.59	alpha-ketoglutarate-dependent dioxygenase (alkylated DNA repair protein)	alkB
NZ_JXUN01000089.1_cds_WP_012905069.1_5182	0.2390	0.02	0.2127	0.43	0.0482	1.21	zinc transporter	zitB
NZ_JXUN01000089.1_cds_WP_012905070.1_5181	0.0763	-1.81	0.0086	2.26	0.0501	1.29	putative exported protein	
NZ_JXUN01000089.1_cds_WP_012905078.1_5173	0.4011	0.43			0.0142	5.08	putative Chb operon repressor	chbR
NZ_JXUN01000089.1_cds_WP_012905079.1_5172	0.1674	0.01			0.0408	2.62	6-phospho-beta-glucosidase	chbF
NZ_JXUN01000089.1_cds_WP_012905080.1_5171	0.0326	-2.09	0.0457	1.79	0.0031	4.98	putative chb operon protein ChbG	chbG
NZ_JXUN01000089.1_cds_WP_012905083.1_5168	0.2984	0.28			0.2634	-0.11	galactose-1-phosphate uridylyltransferase	galT
NZ_JXUN01000089.1_cds_WP_012905094.1_5156	0.4190	-0.03	0.4584	0.29	0.0059	4.92	conserved hypothetical protein	
NZ_JXUN01000089.1_cds_WP_071820569.1_5165	0.2966	0.22	0.0065	1.92	0.0111	1.56	putative molybdenum transport ATP-binding protein (photorepair protein PhrA) OR transcriptional regulator	modF, modE
NZ_JXUN01000090.1_cds_WP_000985718.1_5213	0.0712	-1.90	0.0210	0.75	0.0114	1.02	pseudogene	
NZ_JXUN01000091.1_cds_WP_012908668.1_5223	0.0296	2.86	0.0152	2.65	0.0035	3.17	2,4-dienoyl-CoA reductase [NADPH]	fadH
NZ_JXUN01000091.1_cds_WP_012908670.1_5221	0.3930	0.31	0.1644	1.16	0.0012	4.18	aerotaxis receptor protein	air
NZ_JXUN01000091.1_cds_WP_012908672.1_5219	0.4755	-0.35	0.1272	0.56	0.0203	1.45	putative transcriptional Regulator	
NZ_JXUN01000091.1_cds_WP_012908676.1_5216	0.2079	1.93	0.1223	2.14	0.0164	1.77	hypothetical protein	
NZ_JXUN01000091.1_cds_WP_042622996.1_5215	0.2079	-1.11			0.0081	2.53	putative outer membrane efflux protein of T1SS	
NZ_JXUN01000094.1_cds_WP_012908869.1_5232		-0.41	0.0984	2.44	0.0298	4.52	putative PTS system, IIbc component	
NZ_JXUN01000094.1_cds_WP_012908871.1_5234	0.1734	0.40	0.2987	-0.80	0.0055	4.15	putative PTS system, IIa component	
NZ_JXUN01000095.1_cds_WP_012906598.1_5239	0.0131	-1.46	0.4335	0.04	0.3028	-0.30	NADP-dependent malic enzyme	maeB
NZ_JXUN01000095.1_cds_WP_012906600.1_5242					0.0567	1.42	transketolase 2	tktB
NZ_JXUN01000095.1_cds_WP_012906601.1_5243	0.0116	-2.03	0.3489	-1.30	0.0469	0.49	putative exported protein	
NZ_JXUN01000096.1_cds_WP_012907915.1_5304	0.2561	0.82	0.0353	2.09	0.0557	2.43	magnesium transport protein	corA
NZ_JXUN01000096.1_cds_WP_012907921.1_5297	0.1067	0.63	0.0197	0.99	0.4727	-0.10	putative lipoprotein	
NZ_JXUN01000096.1_cds_WP_012907928.1_5290	0.0451	2.10	0.0577	1.34	0.0006	4.45	probable amino acid permease	
NZ_JXUN01000096.1_cds_WP_012907934.1_5284	0.0556	1.61	0.0208	1.70	0.0203	1.11	dTDP-fucosamine acetyltransferase OR dTDP-fucosamine acetyltransferase	rffC, wecD (synonyms)
NZ_JXUN01000096.1_cds_WP_012907936.1_5282	0.0747	0.89	0.0540	1.12	0.0152	2.00	dTDP-glucose 4,6-dehydratase	rffG
NZ_JXUN01000096.1_cds_WP_012907945.1_5272	0.1202	1.76	0.1228	1.60	0.0422	2.21	ATP-dependent DNA helicase	rep
NZ_JXUN01000096.1_cds_WP_012907948.1_5269	0.4786	-0.09	0.1968	0.83	0.0364	2.11	putative glycerate kinase	
NZ_JXUN01000096.1_cds_WP_012907950.1_5266	0.2808	2.75			0.0009	4.48	LysR-family transcriptional regulator	ilvY
NZ_JXUN01000096.1_cds_WP_042623004.1_5259	0.2547	1.62			0.0922	2.47	pseudogene	
NZ_JXUN01000097.1_cds_WP_012906273.1_5312	0.0490	-2.79	0.4766	-0.08	0.2910	-0.40	conserved hypothetical protein	
NZ_JXUN01000097.1_cds_WP_012906275.1_5309	0.1229	-3.08	0.3587	-0.18			LysR-family transcriptional regulator	cbl
NZ_JXUN01000098.1_cds_WP_012904874.1_5321	0.1523	0.81	0.0112	1.98	0.0530	1.48	primosomal replication protein N	priC
NZ_JXUN01000098.1_cds_WP_012904879.1_5327	0.4799	-1.27	0.0172	1.51	0.2718		chaperone (heat shock protein)	htpG
NZ_JXUN01000098.1_cds_WP_012904883.1_5332	0.1409	-1.30	0.3980	-0.54	0.0215	2.34	inosine-guanosine kinase	gsk

NZ_JXUN01000098.1_cds_WP_012904884.1_5333	0.2652	-0.02	0.2323	0.80	0.0089	2.42	putative transport protein	
NZ_JXUN01000098.1_cds_WP_012904885.1_5334	0.1885	-0.34	0.0547	0.74	0.0391	2.55	fosmidomycin resistance protein	fsr
NZ_JXUN01000098.1_cds_WP_012904889.1_5338	0.0297	2.54	0.0068	2.48	0.0034		copper-transporting P-type ATPase	copA
NZ_JXUN01000098.1_cds_WP_012904890.1_5339	0.0271	1.16	0.1866	0.74	0.1598	0.34	copper efflux regulator	cueR
NZ_JXUN01000098.1_cds_WP_012904891.1_5340	0.0560	1.38	0.0657	0.85	0.0343	2.32	putative membrane protein	
NZ_JXUN01000098.1_cds_WP_012904900.1_5349	0.1185	2.47	0.2237	2.46			outer membrane protein	
NZ_JXUN01000098.1_cds_WP_012904910.1_5361	0.0222	1.77	0.4356	-0.47		0.99	putative inner membrane DNA-binding protein	
NZ_JXUN01000098.1_cds_WP_012904920.1_5371		-2.95	0.0488	1.08	0.0569	2.21	conserved hypothetical protein	
NZ_JXUN01000098.1_cds_WP_024132528.1_5346	0.2481	0.07	0.0499	1.22	0.0188	1.69	acyl-coA thioesterase I	tesA
NZ_JXUN01000099.1_cds_WP_012908275.1_5373	0.0064	-4.11	0.1846	-1.22	0.2150	-1.19	putative lipoprotein	
NZ_JXUN01000099.1_cds_WP_012908279.1_5377	0.0728	2.69			0.0063	3.25	putative membrane protein	
NZ_JXUN01000099.1_cds_WP_012908281.1_5379	0.2129	1.07	0.0298	2.31	0.0408	3.61	Hcp family T6SS protein CtsH2	ctsH2
NZ_JXUN01000099.1_cds_WP_012908282.1_5381	0.2672	2.04	0.0696	1.18	0.0275	1.73	2,3-diketo-L-gulonate TRAP transporter, substrate-binding periplasmic protein	yiaO
NZ_JXUN01000099.1_cds_WP_012908283.1_5382			0.0260	3.25	0.0119	4.89	2,3-diketo-L-gulonate TRAP transporter, small permease protein	yiaM
NZ_JXUN01000099.1_cds_WP_012908289.1_5388	0.2551	0.49	0.1824	0.00	0.0079	1.43	conserved hypothetical protein	
NZ_JXUN01000099.1_cds_WP_012908293.1_5392	0.0405	1.64	0.2117	1.35	0.1783	0.94	RNA polymerase sigma-32 factor	rpoH
NZ_JXUN01000099.1_cds_WP_012908300.1_5399	0.0434	1.22	0.1075	1.56	0.1204	1.46	leucine-specific ABC transporter, substrate-binding protein	livK
NZ_JXUN01000099.1_cds_WP_012908305.1_5404	0.0036	2.10	0.0282	1.25	0.0813	0.77	Phage/plasmid maintenance protein	D
NZ_JXUN01000099.1_cds_WP_012908307.1_5406 NZ_JXUN01000099.1_cds_WP_012908309.1_5408	0.2095 0.1889	-0.62 2.23	0.0807	1.61	0.0215 0.0253	2.54 2.08	glycerol-3-phosphate ABC transporter, substrate- binding protein glycerol-3-phosphate ABC transporter, permease	ugpB ugpA
1VZ_JX01V01000079.1_Cds_W1_012900307.1_5400	0.1669	2.23	0.0007	1.01	0.0233	2.00	protein	ugpA
NZ_JXUN01000099.1_cds_WP_012908311.1_5410	0.4988	-0.07			0.0184	2.25	glycerophosphoryl diester phosphodiesterase	ugpQ
NZ_JXUN01000099.1_cds_WP_012908313.1_5412	0.1409	-0.59	0.0380	1.70	0.1522	0.57	gamma-glutamyltranspeptidase	ggt
NZ_JXUN01000099.1_cds_WP_012908317.1_5416	0.0005	2.03	0.3061	0.94	0.2394	-1.61	putative oxidoreductase	
NZ_JXUN01000099.1_cds_WP_012908318.1_5417	0.0109	1.52	0.1164	1.52	0.4500	0.86	conserved hypothetical protein	
NZ_JXUN01000099.1_cds_WP_012908320.1_5419	0.3922	-0.50	0.0447	0.56	0.0644	0.01	thermoresistant gluconokinase	gntK
NZ_JXUN01000099.1_cds_WP_012908326.1_5425		-0.56	0.1010	1.62	0.0203	3.92	glucose-1-phosphate adenylyltransferase	glgC
NZ_JXUN01000099.1_cds_WP_012908327.1_5426	0.3855	0.43	0.3024	0.39	0.0276	1.41	glycogen phosphorylase	glgP
NZ_JXUN01000099.1_cds_WP_012908329.1_5428	0.3280	-1.74	0.3392	0.87	0.0351	2.12	aerobic glycerol-3-phosphate dehydrogenase	glpD
NZ_JXUN01000099.1_cds_WP_012908330.1_5429	0.3058	0.82	0.2561	0.87	0.0305	1.68	thiosulfate sulfurtransferase	glpE
NZ_JXUN01000099.1_cds_WP_012908331.1_5430	0.0167	1.23	0.0481	0.78	0.0107	1.96	putative membrane protein	
NZ_JXUN01000099.1_cds_WP_012908333.1_5432	0.0089	-2.82	0.0107	1.13	0.0483	0.52	regulatory protein	malT
NZ_JXUN01000099.1_cds_WP_012908334.1_5433	0.3009	0.58	0.0222	1.51	0.0002		unknown	
NZ_JXUN01000099.1_cds_WP_012908335.1_5434	0.3861	-0.45	0.0551	1.84	0.0148	2.33	putative membrane protein	
NZ_JXUN01000099.1_cds_WP_012908336.1_5435	0.2917	0.66	0.0277	3.19	0.0708	2.23	Hcp family T6SS protein CtsH4	ctsH4
NZ_JXUN01000099.1_cds_WP_012908337.1_5436	0.0086	-4.75	0.0854	-1.52	0.3346	-1.27	maltodextrin phosphorylase	malP
NZ_JXUN01000099.1_cds_WP_012908340.1_5439	0.0180	2.63	0.0551	2.44	0.1358	0.72	putative competence protein	gntY
NZ_JXUN01000099.1_cds_WP_012908342.1_5441	0.0093	1.11	0.0368	1.97	0.0434		carboxylesterase (biotin synthesis protein BioH)	bioH
NZ_JXUN01000099.1_cds_WP_012908346.1_5445	0.4484	-0.08	0.1073	0.77	0.0185	1.13	ferrous iron transport protein A	feoA
NZ_JXUN01000099.1_cds_WP_012908360.1_5460		0.96	0.0954	2.98	0.1158	3.46	putative fimbrial protein HofO	hofO

NZ_JXUN01000099.1_cds	_WP_012908362.1_5462	0.4103	-0.36	0.1278	0.31	0.0191	2.31	putative fimbrial protein HofQ	hofQ
NZ_JXUN01000099.1_cds	_WP_012908363.1_5464	0.0257	1.01	0.1904	0.69	0.3370	0.61	3-dehydroquinate synthase	aroB
NZ_JXUN01000099.1_cds	_WP_012908372.1_5473	0.0215	-1.04	0.1068	2.34	0.4541	0.54	nitrite reductase (NAD(P)H) small subunit	nirD
NZ_JXUN01000099.1_cds	_WP_012908374.1_5475	0.1563	1.77	0.0147	2.01			major facilitator superfamily protein	tsgA
NZ_JXUN01000099.1_cds	_WP_012908376.1_5477	0.3155	0.91	0.0065	1.80	0.0502	1.19	conserved hypothetical protein	
NZ_JXUN01000099.1_cds	_WP_024133034.1_5387	0.2494	0.48	0.0955	0.93	0.0497	1.17	putative membrane protein	
NZ_JXUN01000099.1_cds	_WP_071820631.1_5423	0.0260	-2.24	0.3410	0.13	0.2877	0.20	1,4-alpha-glucan branching enzyme	glgB
NZ_JXUN01000100.1_cds	_WP_012905356.1_49	0.1350	0.77			0.0306	3.84	hypothetical prophage protein	
NZ_JXUN01000100.1_cds	_WP_012905359.1_52	0.3242	-0.03	0.0813	-2.02			putative phage lysozyme	
NZ_JXUN01000100.1_cds	_WP_012905369.1_63	0.1993	1.53	0.0534	2.77		3.98	putative gluconate dehydrogenase subunit	
NZ_JXUN01000100.1_cds	_WP_012905371.1_65	0.0467	0.55	0.0234	1.42	0.0748	1.25	putative gluconate dehydrogenase subunit	
NZ_JXUN01000100.1_cds	_WP_012905374.1_68	0.4237	0.09	0.1260	1.20	0.0374	4.53	curved DNA-binding protein OR chaperone-	cbpA, cbpM
NZ JXUN01000100.1 cds	WP 012905378 1 72	0.0213	-1.79	0.4617	-0.70	0.1534	-0.30	modulator protein flavoprotein (Trp repressor-binding protein)	wrbA
NZ_JXUN01000100.1_cds		0.1794	1.18	0.0095	3.12	0.0042	3.50	conserved hypothetical protein	
NZ_JXUN01000100.1_cds		0.0890	1.85	0.4473	0.29	0.0159	-3.24	putative exported protein	
NZ JXUN01000100.1 cds		0.0328	2.50	0.4833	0.21	0.1356	-1.34	ferrous iron permease	efeU
NZ JXUN01000100.1 cds		0.0844	1.67	0.4912	0.13	0.0414	0.65	pseudogene	
NZ JXUN01000100.1 cds		0.0909	-1.56	0.1897	1.99	0.0256	3.89	hypothetical prophage protein	
NZ JXUN01000101.1 cds		0.1846	0.59			0.1307	2.65	conserved hypothetical protein	
NZ JXUN01000101.1 cds		0.0055	-5.60	0.3776	0.55	0.1779	-0.14	putative outer membrane autotransporter	
NZ JXUN01000101.1 cds		0.2350	0.92	0.0662	3.56	0.0432	2.21	probable pyruvate-flavodoxin oxidoreductase	
NZ JXUN01000101.1 cds		0.0215	-2.64	0.3482	0.21	0.1871	0.54	universal stress protein F	uspF
NZ_JXUN01000101.1_cds		0.0188	1.28	0.3796	-0.30	0.0048	2.21	hypothetical protein	
NZ_JXUN01000101.1_cds		0.2744	1.02	0.0227	1.43	0.0266	1.49	T3SS effector protein NleC OR universal stress	nleC, uspF
		0.0056	1.22	0.1056	0.67	0.0202		protein F	ī
NZ_JXUN01000102.1_cds		0.0056	1.32	0.1956	0.67	0.0203	4.25	glutamate racemase	murI
NZ_JXUN01000102.1_cds		0.0195	1.69 0.92	0.0183	1.74	0.0335	4.35	putative outer membrane protein	C
NZ_JXUN01000102.1_cds		0.0484		0.0184	1.28	0.1292	1.19	N-acetyl-gamma-glutamyl-phosphate reductase	argC
NZ_JXUN01000103.1_cds		0.0812	1.66			0.0037	2.76	nitrite extrusion protein	narU
NZ_JXUN01000103.1_cds		0.4035	0.20	0.0105	2.74	0.1233	1.89	respiratory nitrate reductase 2 delta chain	narW
NZ_JXUN01000103.1_cds		0.2051	1.35	0.0195	2.74	0.0519	2.72	putative adhesin autotransporter	
NZ_JXUN01000104.1_cds		0.0442	-3.89	0.3614	1.16			hypothetical prophage protein	
NZ_JXUN01000104.1_cds		0.0258	-1.22	0.3954	-0.14	0.1166	1.46	putative phage tail fibre assembly protein	
NZ_JXUN01000104.1_cds		0.2271	2.19	0.1875	2.38			hypothetical prophage protein	
NZ_JXUN01000104.1_cds		0.0101	1.40	0.0199	1.17	0.0107	1.56	LysR-family transcriptional regulator	
NZ_JXUN01000104.1_cds		0.1413	1.87	0.0937	2.01	0.0299	3.31	putative carbon-nitrogen hydrolase	
NZ_JXUN01000104.1_cds		0.3324	-0.66	0.1906	-0.01	0.0204	2.49	acyl-CoA dehydrogenase	fadE
NZ_JXUN01000104.1_cds		0.1877	1.97	0.0834	2.46	0.0154	4.88	lateral flagellar M-ring protein	lfiF
NZ_JXUN01000104.1_cds		0.4560	0.33	0.2136	2.60	0.0245	5.25	hypothetical prophage protein	
NZ_JXUN01000104.1_cds		0.4018	0.95	0.0113	3.05	0.0054	4.59	putative phage tail protein	
NZ_JXUN01000104.1_cds		0.0423	-2.18	0.1188	-0.45	0.4178	1.30	hypothetical prophage protein	
NZ_JXUN01000104.1_cds	_WP_012904633.1_138		4.01	0.0505	4.16	0.0892	3.64	putative phage portal protein	

NZ_JXUN01000104.1_cds_WP_024132480.1_172		0.97	0.2206	0.69	0.0079	3.84	putative exported protein	
NZ_JXUN01000104.1_cds_WP_042623027.1_179	0.0395	0.75	0.3294	-0.31	0.1046	1.83	DNA polymerase III epsilon subunit	dnaQ
NZ_JXUN01000105.1_cds_WP_012908203.1_229	0.4207	0.60	0.0665	1.43	0.0237	2.02	dipeptide ABC transporter, permease protein	dppC
NZ_JXUN01000105.1_cds_WP_012908205.1_227	0.4500	0.84	0.0718	-1.00	0.0289	1.31	dipeptide ABC transporter, ATP-binding protein	dppD, dppF
NZ_JXUN01000105.1_cds_WP_012908215.1_215	0.3721	2.04				0.44	endo-1,4-beta-glucanase (cellulase)	bcsZ
NZ_JXUN01000105.1_cds_WP_012908220.1_209	0.4394	-0.47			0.3313	1.68	2-dehydro-3-deoxygluconokinase	kdgK
NZ_JXUN01000105.1_cds_WP_012908221.1_208	0.1775	1.38			0.0511	2.83	putative signal transduction protein	
NZ_JXUN01000105.1_cds_WP_012908224.1_205	0.0389	1.76	0.0421	2.02	0.0084	3.51	putative membrane protein	
NZ_JXUN01000105.1_cds_WP_012908226.1_201	0.2796	0.12	0.0432	1.57	0.0081	1.92	transcriptional regulator	
NZ_JXUN01000105.1_cds_WP_012908227.1_199	0.4185	1.21	0.0820	2.65	0.0151	4.91	cytoplasmic trehalase	treF
NZ JXUN01000105.1 cds WP 012908233.1 193	0.0839	8.84	0.0890	3.70	0.0343		L-asparginase	
NZ JXUN01000105.1 cds WP 012908236.1 190	0.0611	0.75	0.0516	1.30	0.0287	1.04	oligopeptidase A	prlC
NZ_JXUN01000105.1_cds_WP_024133021.1_207	0.3146	-0.16	0.2506	0.86			putative outer membrane assembly protein	
NZ JXUN01000105.1 cds WP 042623033.1 234	0.0320	2.29	0.0440	1.35	0.0202	2.18	dipeptide ABC transporter, substrate-binding	dppA, eptb
							protein, OR phosphoethanolamine transferase	11 / 1
NZ JXUN01000106.1 cds WP 000169527.1 291	0.3592	-0.02	0.0206	2.13	0.0433	2.54	IS3 transposase A	
NZ_JXUN01000106.1_cds_WP_000269401.1_310	0.2676	0.87	0.3159	1.10	0.0288	1.64	putative P-loop ATPase family protein	
NZ_JXUN01000106.1_cds_WP_001095912.1_284	0.0774	-1.02			0.0013	2.94	putative transcriptional regulator	
NZ_JXUN01000106.1_cds_WP_001360081.1_282		0.25	0.1410	0.71	0.0400	2.60	putative membrane protein	
NZ_JXUN01000106.1_cds_WP_012908787.1_249	0.0498	1.61	0.0436	1.27			isopentenyl-diphosphate delta-isomerase	idi
NZ_JXUN01000106.1_cds_WP_012908798.1_261	0.0289	0.78	0.1782	-0.06	0.0062	2.00	Conserved hypothetical protein	
NZ JXUN01000106.1 cds WP 012908799.1 266	0.1375	0.40	0.2220	0.54	0.0299	1.62	conserved hypothetical protein	
NZ JXUN01000106.1 cds WP 012908802.1 269	0.4794	-0.16	0.0121	3.70	0.0060	2.47	conserved hypothetical protein	
NZ_JXUN01000106.1_cds_WP_012908803.1_270		1.01	0.0152	3.56	0.0415	4.55	conserved hypothetical protein	
NZ_JXUN01000106.1_cds_WP_012908806.1_276	0.0026	1.35	0.0214	2.62	0.0214	4.79	putative adhesin autotransporter	
NZ_JXUN01000106.1_cds_WP_012908819.1_296		1.38	0.0403	1.49	0.0093	3.15	putative haemolysin activator HlyB	hylB
NZ_JXUN01000106.1_cds_WP_012908820.1_297	0.1644	1.56	0.2927	0.45	0.0288	1.52	putative haemolysin activator HlyC	hylC
NZ_JXUN01000106.1_cds_WP_012908828.1_306	0.2173	0.27	0.0615	0.58	0.0342	1.10	hypothetical protein	
NZ_JXUN01000106.1_cds_WP_012908837.1_327	0.2379	1.12	0.1156	0.88	0.0099	2.49	ornithine decarboxylase, constitutive	speC
NZ_JXUN01000106.1_cds_WP_012908838.1_328	0.3984	0.19	0.4649	0.46	0.0248	2.38	nucleoside permease	nupG
NZ_JXUN01000106.1_cds_WP_012908840.1_330	0.0430	-1.30	0.1292	0.54	0.2135	-0.71	probable Fe(2+)-trafficking protein	
NZ_JXUN01000106.1_cds_WP_012908842.1_333	0.1309	0.85	0.1740	0.75	0.0298	2.16	tRNA (guanine-N(7)-)-methyltransferase	trmB
NZ_JXUN01000106.1_cds_WP_021564615.1_283	0.3811	0.91	0.0754	1.24	0.0391	4.70	conserved hypothetical protein	
NZ_JXUN01000106.1_cds_WP_024133105.1_254	0.0623	-2.10	0.0061	-0.73	0.0147	-1.31	putative membrane protein	
NZ_JXUN01000106.1_cds_WP_024133109.1_279	0.0158	-1.62	0.1490	0.88	0.0199	1.91	conserved hypothetical protein	
NZ_JXUN01000106.1_cds_WP_024133111.1_289	0.1131	3.57			0.0422	2.24	Conserved hypothetical protein	
NZ JXUN01000106.1 cds WP 049794266.1 258	0.0872	1.14	0.0866	1.22	0.0315		pseudogene	
NZ JXUN01000106.1 cds WP 064755625.1 322	0.4528	0.67	0.2316	-0.47	0.0106	2.96	IS4 transposase (fragment)	
NZ_JXUN01000106.1_cds_WP_071820646.1_295	0.0126	1.70	0.1305	1.73	0.0052	2.28	conserved hypothetical protein	
NZ_JXUN01000106.1_cds_WP_071820647.1_332	0.0844	1.26	0.1040	1.42	0.0147	2.78	endonuclease I	endA
NZ_JXUN01000107.1_cds_WP_012908617.1_353	0.1922	1.07			0.0068	3.42	pseudogene	
NZ JXUN01000107.1 cds WP 012908622.1 349	0.0431	-1.50	0.2241	1.17	0.1089	1.45	pseudogene, disrupted by prophage CRP49 insertion	gatD
								~

NZ_JXUN01000107.1_cds_WP_012908625.1_345	0.3175	-0.09			0.0415	3.34	component IIB of galactitol-specific phosphotransferase system	gatB
NZ_JXUN01000107.1_cds_WP_012908628.1_342	0.1107	2.14	0.3451	-0.27	0.0448	2.07	tagatose-1,6-bisphosphate aldolase	gatY
NZ_JXUN01000107.1_cds_WP_012908630.1_340	0.2843	0.50	0.1120	1.29			2-dehydro-3-deoxyglucarate aldolase	garL
NZ_JXUN01000107.1_cds_WP_012908631.1_339		-1.80	0.2485	1.77			2-hydroxy-3-oxopropionate reductase	garR
NZ_JXUN01000108.1_cds_WP_012906203.1_365	0.1330	-3.77	0.0285	1.36	0.0281	2.90	cardiolipin synthetase	cls
NZ_JXUN01000108.1_cds_WP_012906204.1_366					0.0613	1.17	flagellar-specific Sigma F (Sigma 28) factor	fliA
NZ_JXUN01000110.1_cds_WP_000361028.1_395	0.3810	1.07	0.3298	0.52	0.0441	2.32	hypothetical prophage protein	
NZ_JXUN01000110.1_cds_WP_012904654.1_393	0.1157	-1.07	0.3695	-0.19	0.0204	2.16	hypothetical prophage protein	
NZ_JXUN01000110.1_cds_WP_012904658.1_396		-1.27			0.2380	0.52	putative phage transposase	
NZ_JXUN01000110.1_cds_WP_012904659.1_397		-2.55			0.0016	3.41	putative phage transposase	
NZ_JXUN01000110.1_cds_WP_012904662.1_402	0.4040	-0.14	0.1365	0.67	0.0065	2.92	glycerol-3-phosphate cytidylyltransferase	tagD
NZ_JXUN01000110.1_cds_WP_024132490.1_389	0.2140	0.24					hypothetical prophage protein	
NZ_JXUN01000111.1_cds_WP_012906864.1_433	0.0439	-2.06	0.4386	-0.75			putative transketolase N-terminal section	
NZ_JXUN01000111.1_cds_WP_012906865.1_432	0.0412	3.61	0.0087	4.18	0.0127	4.93	PTS system EIIC component	
NZ_JXUN01000111.1_cds_WP_012906867.1_430	0.0412	2.18	0.2494	-0.48	0.0587	2.11	PTS system EIIA component	
NZ_JXUN01000111.1_cds_WP_012906872.1_425	0.3772	0.40	0.3839	1.50	0.0445	2.74	putative glutathione S-transferase	
NZ_JXUN01000111.1_cds_WP_012906873.1_424	0.0495	-1.35	0.3053	0.48	0.3755	0.81	D-erythro-7,8-dihydroneopterin triphosphate epimerase	folX
NZ_JXUN01000111.1_cds_WP_012906874.1_423	0.3399	-0.47			0.0096	3.01	conserved hypothetical protein	
NZ_JXUN01000111.1_cds_WP_012906880.1_417	0.1509	0.63	0.0354	1.83	0.0373	2.45	lysine-arginine-ornithine-binding periplasmic protein	argT
NZ_JXUN01000111.1_cds_WP_024132811.1_412	0.2219	4.02	0.1107	1.93	0.0014	5.08	conserved hypothetical protein	
NZ_JXUN01000112.1_cds_WP_012906791.1_461	0.4675	0.23	0.0170	3.38		3.53	putative prophage DNA cytosine methylase	dcm
NZ_JXUN01000112.1_cds_WP_012906793.1_463		-0.73	0.1241	2.23	0.0137	3.82	hypothetical prophage protein	
NZ_JXUN01000112.1_cds_WP_012906796.1_466	0.3235	0.33	0.4623	0.25	0.0377	1.24	putative prophage DNA binding protein	
NZ_JXUN01000112.1_cds_WP_012906803.1_469	0.0053	-2.32	0.3118	1.16	0.3262	-0.04	hypothetical prophage protein	
NZ_JXUN01000112.1_cds_WP_012906804.1_470	0.1360	-2.52	0.1644	1.73	0.0088	2.67	hypothetical prophage protein	
NZ_JXUN01000112.1_cds_WP_012906805.1_471		-1.02			0.0394	1.47	putative prophage exported protein	
NZ_JXUN01000112.1_cds_WP_012906807.1_473		-2.38			0.1247	0.80	putative prophage DNA methylase	
NZ_JXUN01000112.1_cds_WP_012906810.1_476	0.3882	-0.55			0.0103	1.91	hypothetical prophage protein	
NZ_JXUN01000112.1_cds_WP_012906811.1_477	0.4004	-0.36	0.1372	0.30	0.0403	2.15	hypothetical prophage protein	
NZ_JXUN01000112.1_cds_WP_024132791.1_468	0.0254	-3.30	0.4840	0.09	0.1407	1.27	hypothetical prophage protein	
NZ_JXUN01000113.1_cds_WP_012908167.1_482	0.2609	-0.36	0.1265	0.44	0.0125	1.45	selenocysteine-specific elongation factor	selB
NZ_JXUN01000113.1_cds_WP_012908171.1_486	0.1552	1.98			0.0097	2.28	conserved hypothetical protein	
NZ_JXUN01000113.1_cds_WP_012908172.1_487	0.1977	1.01	0.1066	1.83	0.0089	3.77	putative membrane protein	
NZ_JXUN01000113.1_cds_WP_012908173.1_488	0.4217	-0.80	0.2733	0.87	0.0126	1.35	AraC-family transcriptional regulator	
NZ_JXUN01000113.1_cds_WP_012908178.1_492	0.0045	-2.69	0.0797	-0.80	0.2126	-0.98	alpha-amylase	malS
NZ_JXUN01000113.1_cds_WP_012908180.1_495	0.0223	-1.50	0.2083	0.64	0.3861	0.04	xylose operon regulatory protein	xylR
NZ_JXUN01000113.1_cds_WP_012908181.1_496	0.4664	0.25	0.0286	1.60	0.0369	2.70	D-xylose isomerase	xylA
NZ_JXUN01000113.1_cds_WP_012908186.1_502	0.0036	1.41	0.3781	0.20	0.2296	0.72	glycine-tRNA synthetase, beta subunit	glyS
NZ_JXUN01000113.1_cds_WP_024133012.1_490	0.3555	1.51	0.2014	0.40	0.0045	4.22	galactose/methyl galactoside ABC transporter,ATP-binding protein	mglA
NZ_JXUN01000114.1_cds_WP_012906220.1_511	0.4073	-0.99	0.1539	0.26	0.0309	1.50	Flagellar filament cap protein	fliD

NZ_JXUN01000114.1_cds_WP_012906221.1_512	0.0951	-0.46	0.0713	1.40	0.0292	3.14	flagellar protein FliS	fliS
NZ_JXUN01000114.1_cds_WP_012906227.1_518	0.0161	1.39	0.0217	1.07	0.2707	-0.44	protease 7 precursor	ompT
NZ_JXUN01000114.1_cds_WP_012906228.1_519	0.0127	-2.33	0.2143	0.62	0.0141	1.71	putative lipoprotein	
NZ_JXUN01000114.1_cds_WP_012906229.1_520	0.2207	-2.21	0.2249	1.01	0.0298	2.61	flagellar hook-basal body complex protein FliE	fliE
NZ_JXUN01000114.1_cds_WP_012906231.1_522					0.0926	2.91	putative flagellar motor switch protein	fliG
NZ_JXUN01000114.1_cds_WP_012906232.1_523		-0.82	0.0976	0.67	0.0148	2.50	flagellar assembly protein FliH	fliH
NZ_JXUN01000114.1_cds_WP_012906237.1_528	0.0079	-1.57	0.4566	-0.07	0.1301	0.58	flagellar motor switch protein FliM OR flagellar	fliM OR fliN
NZ JXUN01000114.1 cds WP 012906238.1 529		-6.14	0.4395	-1.94	0.0732	0.18	motor switch protein FliN flagellar motor switch protein FliM	fliM
NZ_JXUN01000114.1_cds_WP_012906243.1_534	0.0292	-3.45	0.3549	0.24	0.2449	-0.05	colanic acid capsullar biosynthesis activation protein	rcsA
NZ JXUN01000114.1 cds WP 024132721.1 509	0.0097	-4.21	0.3229	-0.30	0.4916	-1.57	A pseudogene	
NZ JXUN01000115.1 cds WP 012904830.1 550	0.4548	0.20			0.0343	2.29	Major Facilitator Superfamily transporter	
NZ_JXUN01000115.1_cds_WP_012904835.1_555	0.2188	1.29			0.0162	5.02	quinate/shikimate dehydrogenase	
NZ JXUN01000115.1 cds WP 012904856.1 577	0.0006	1.34	0.0180	1.20	0.0021	2.26	putative transcriptional regulator	
NZ JXUN01000115.1 cds WP 012904857.1 578	0.0230	3.53	0.0366	2.14	0.0021	4.21	putative ABC transporter	
NZ JXUN01000115.1 cds WP 012904859.1 580	0.1840	-0.64	0.0500	2.11	0.0021	3.17	nitrogen regulatory protein P-II	glnK
NZ JXUN01000115.1 cds WP 012904863.1 584	0.0790	-0.84	0.4673	0.00	0.0091	1.71	putative exported protein	8
NZ JXUN01000115.1 cds WP 012904864.1 585	0.1934	0.89	0.4073	0.00	0.1248	2.10	putative exported protein	
NZ_JXUN01000115.1_cds_WP_012904865.1_586	0.0400	-1.51	0.2323	0.19	0.1255	0.62	putative signal transduction protein	
NZ JXUN01000116.1 cds WP 012907828.1 593	0.0675	-0.84	0.2323	1.57	0.0192	2.20	L rhamnose-proton symporter	rhaT
NZ JXUN01000116.1 cds WP 012907830.1 595	0.4116	0.30	0.0620	1.85	0.0192	2.81	L-rhamnose operon regulatory protein	rhaS
NZ JXUN01000116.1 cds WP 012907830.1_393	0.4110	6.20	0.0020	4.69	0.0103	4.32	L-rhamnose isomerase	rhaA
NZ_JXUN01000110.1_cds_WF_012907832.1_397	0.2047	0.20	0.0143	1.16	0.0099	3.11	rhamnulose-1-phosphate aldolase	rhaD
	0.2047	-2.93	0.0710	-1.35	0.0113			шар
NZ_JXUN01000116.1_cds_WP_012907834.1_599	0.0260			-1.33 -1.17	0.4016	-0.70	alcohol dehydrogenase	
NZ_JXUN01000116.1_cds_WP_012907835.1_600		-1.53 1.27	0.2563 0.0369			0.50	conserved hypothetical protein	
NZ_JXUN01000116.1_cds_WP_012907836.1_601	0.1705			4.02 0.10	0.0530	3.45	putative porin	
NZ_JXUN01000116.1_cds_WP_012907838.1_603	0.0126	1.25	0.1369		0.0906	1.95	AzlC-like membrane protein	
NZ_JXUN01000116.1_cds_WP_012907840.1_605	0.2245	-0.37 -0.57	0.2450	0.13	0.0381 0.0286	1.19	putative transcription regulator of PTS system	
NZ_JXUN01000116.1_cds_WP_012907841.1_606	0.4301					2.84	Putative PTS system transport protein	
NZ_JXUN01000116.1_cds_WP_012907842.1_607	0.4149	-0.11			0.0321	2.19	putative glucuronyl hydrolase OR Putative PTS system transport protein	
NZ_JXUN01000116.1_cds_WP_012907845.1_610		-0.21			0.0344	3.01	putative PTS system, sorbose-specific IID	
NZ JXUN01000116.1 cds WP 012907846.1 611	0.0371	1.53	0.0148	1.37	0.1046	0.85	component putative exported protein	
NZ_JXUN01000116.1_cds_WP_012907849.1_615	0.2119	1.07	0.0692	1.79	0.0192	3.41	formate dehydrogenase-O, iron-sulfur subunit	fdoH
NZ_JXUN01000116.1_cds_WP_012907850.1_616	0.4698	0.38	0.0143	3.94	0.0253	2.69	formate dehydrogenase, cytochrome b556(fdo)	fdoI
NZ JXUN01000116.1 cds WP 024132531.1 621	0.0604	-1.23	0.0452	1.27	0.0117	2.22	subunit pseudogene	
NZ_JXUN01000116.1_cds_WP_042623058.1_589	0.0895	-1.80	0.3100	0.04	0.0117	3.41	two-component sensor kinase	cpxA
NZ_JXUN01000117.1_cds_WP_012905511.1_623	0.2494	0.78	3.3.00	0.01	0.0173	5.18	putative metal-binding protein	yodA
NZ JXUN01000118.1 cds WP 012906311.1 662	0.0452	-1.49			0.3011	0.94	cobyric acid synthase	cobQ
NZ JXUN01000118.1 cds WP 012906315.1 658	0.0391	-1.41			0.4875	-0.22	cobalamin biosynthesis protein CbiM	cbiM
NZ JXUN01000118.1 cds WP 012906317.1 656	0.3285	0.08	0.2584	-1.12	0.4873	1.61	sirohydrochlorin cobaltochelatase	cbiK
INZ_JAOINO1000110.1_CUS_WF_01270031/.1_030	0.3463	0.08	0.2304	-1.12	0.0434	1.01	Sironyarocinorni cobanociiciatase	COIN

NZ_JXUN01000118.1_cds_WP_012906320.1_653	0.0211	-1.23	0.1584	0.41	0.0070	1.02	cobalamin biosynthesis protein CbiG	cbiG
NZ_JXUN01000118.1_cds_WP_012906328.1_645	0.0584	-0.88	0.1696	0.11	0.0274	1.58	pdu/cob regulatory protein pocR	pocR
NZ_JXUN01000118.1_cds_WP_012906329.1_644	0.3564	-0.66	0.0560	1.22	0.0215	1.42	propanediol diffusion facilitator	pduF
NZ_JXUN01000118.1_cds_WP_012906330.1_643	0.1878	0.71			0.2606	-0.18	propanediol utilisation protein PduA	pduA
NZ_JXUN01000118.1_cds_WP_012906332.1_641		-0.53			0.0088	2.86	glycerol dehydratase large subunit	pduC
NZ JXUN01000118.1 cds WP 012906333.1 640	0.3044	1.31	0.0242	2.53	0.0241	4.15	propanediol utilization dehydratase, medium subunit	pduD
NZ JXUN01000118.1 cds WP 012906334.1 639	0.1089	1.41					propanediol utilization dehydratase, small subunit	pduE
NZ JXUN01000119.1 cds WP 012908241.1 672	0.0101	1.48	0.0710	1.34	0.2465	1.53	putative exported protein	
NZ_JXUN01000119.1_cds_WP_012908242.1_670	0.0387	1.05	0.0062	1.70	0.0018	1.93	putative sigma-54 dependent transcriptional	
						0.4.6	regulator	
NZ_JXUN01000119.1_cds_WP_012908244.1_668					0.2991	0.16	putative transport protein	
NZ_JXUN01000120.1_cds_WP_012908105.1_687	0.0660	1.28	0.0063	3.09	0.0413	3.41	putative carbohydrate transporter	
NZ_JXUN01000120.1_cds_WP_012908106.1_686	0.0148	-2.37					putative glycosyl hydrolase	
NZ_JXUN01000121.1_cds_WP_012907106.1_730	0.4181	0.07	0.0181	1.03	0.3253	0.85	T3SS translocator protein EspD	espD
NZ_JXUN01000121.1_cds_WP_012907107.1_729	0.0685	1.07	0.0086	1.23	0.1337	1.56	T3SS translocator protein EspA	espA
NZ_JXUN01000121.1_cds_WP_012907120.1_712	0.0254	1.18	0.1945	-0.05	0.1977	-0.03	T3SS structural protein EscV	escV
NZ_JXUN01000121.1_cds_WP_012907121.1_711	0.0209	1.74	0.0746	0.32	0.2860	0.30	T3SS regulator Mpc	mpc
NZ_JXUN01000121.1_cds_WP_012907130.1_699	0.0405	1.21	0.2976	0.54	0.1899	-0.71	putative LEE-encoded exported protein	
NZ_JXUN01000121.1_cds_WP_042623068.1_695	0.0305	1.23	0.1155	0.52	0.2832	0.21	T3SS structural protein EscR	escR
NZ_JXUN01000122.1_cds_WP_012907076.1_749	0.4010	-0.44			0.0227	3.85	putative fimbrial chaperone protein	
NZ_JXUN01000122.1_cds_WP_012907077.1_748			0.1358	1.45	0.0012	3.58	putative fimbrial chaperone protein	
NZ_JXUN01000122.1_cds_WP_024132839.1_753	0.0272	2.08	0.2287	0.46	0.1262		putative exported protein	
NZ_JXUN01000123.1_cds_WP_012907160.1_777	0.4262	-0.10	0.0469	1.05			sulfite reductase (NADPH) flavoprotein alpha	cysJ
NZ JXUN01000123.1 cds WP 012907164.1 773	0.1182	1.58	0.0105	2.70	0.0349	1.77	subunit CRISPR-associated protein	
NZ JXUN01000123.1 cds WP 012907174.1 763	0.1182	-2.07	0.0103	1.20	0.0349	1.76	Sulfate adenylyltransferase subunit 2	cysD
NZ JXUN01000123.1 cds WP 012907174.1 763	0.1533	-2.07	0.0216	1.20	0.0490	1.76	Sulfate adenylyltransferase subunit 2 Sulfate adenylyltransferase subunit 2	cysD
NZ_JXUN01000123.1_cds_WP_012907174.1_703 NZ_JXUN01000123.1_cds_WP_012907175.1_762	0.1333	-1.17	0.0210	1.20	0.0490	2.55	Sulfate adenylyltransferase subunit 1	cysN
	0.0211		0.0997	0.95				Cysin
NZ_JXUN01000123.1_cds_WP_012907177.1_760		1.40			0.0018	1.47	putative membrane protein	
NZ_JXUN01000123.1_cds_WP_024132857.1_774	0.0054	-1.95	0.4814	-0.47	0.2569	0.74	CRISPR-associated protein	
NZ_JXUN01000124.1_cds_WP_012908735.1_805	0.4153	0.34	0.0424	0.56	0.1299	-0.24	IS3 family transposase A	3.7
NZ_JXUN01000124.1_cds_WP_012908747.1_790	0.0243	-2.83	0.2320	0.86	0.1291	0.55	osmotically-inducible protein Y	osmY
NZ_JXUN01000124.1_cds_WP_012908749.1_787	0.1462	1.52			0.0066	2.45	putative deoxyribonuclease OR patatin-like phospholipase	
NZ_JXUN01000124.1_cds_WP_012908754.1_782	0.0672	0.61	0.0569	1.20	0.0147	2.57	phosphopentomutase	deoB
NZ_JXUN01000125.1_cds_WP_012907040.1_810	0.1083	1.44	0.0397	2.47	0.0272	4.02	probable membrane protein	
NZ_JXUN01000126.1_cds_WP_012905465.1_825	0.0768	0.92	0.0212	1.20	0.0201	1.82	transcription-repair coupling factor	mfd
NZ_JXUN01000126.1_cds_WP_012905466.1_824	0.1629	-0.93			0.0089	1.64	putative acyltransferase	
NZ_JXUN01000126.1_cds_WP_012905470.1_820	0.0260	2.20	0.2100	0.49	0.0919	2.50	N-acetyl-D-glucosamine kinase	nagK
NZ_JXUN01000126.1_cds_WP_012905471.1_819	0.0361	1.35	0.4806	-0.15	0.3498	0.62	NAD-dependent deacetylase (regulatory protein Sir	npdA
	0.4004		0.456	0.0=			homolog)	-
NZ_JXUN01000126.1_cds_WP_024132618.1_826	0.4301	-0.14	0.4563	0.07	0.0322	1.29	putative peptidoglycan-binding protein	1.0
NZ_JXUN01000127.1_cds_WP_012907527.1_833	0.1825	0.60	0.0572	2.51	0.0090	5.03	D-allose transporter permease protein	alsC
NZ_JXUN01000127.1_cds_WP_012907528.1_834	0.3784	-1.74	0.0188	1.72	0.0122	2.00	D-allose transporter ATP-binding protein AlsA	alsA

NZ_JXUN01000127.1_cds_WP_012907531.1_837	0.3441	0.33	0.0748	1.25	0.0036	4.51	allose 6-phosphate isomerase/ribose-5-phosphate isomerase B	rpiB
NZ_JXUN01000127.1_cds_WP_012907532.1_838	0.4201	1.42	0.0985	2.96	0.0445	4.01	putative exported protein	
NZ_JXUN01000127.1_cds_WP_012907536.1_843		0.87			0.0691	1.96	2-keto-3-deoxygluconate permease	kdgT
NZ_JXUN01000127.1_cds_WP_024132925.1_842	0.3098	0.60	0.2929	1.40	0.0418	1.65	conserved hypothetical protein OR 2-keto-3- deoxygluconate permease	phnA,kdgT
NZ_JXUN01000128.1_cds_WP_012905766.1_847	0.0268	1.41	0.3658	0.47	0.2412	3.07	probable amino acid metabolite efflux	eamA
NZ_JXUN01000128.1_cds_WP_012905767.1_848	0.0397	0.92	0.1244	0.82	0.0603	1.21	multiple antibiotic resistance protein	marB
NZ_JXUN01000128.1_cds_WP_012905775.1_856	0.2514	2.16			0.0236	4.26	putative integral membrane protein	
NZ_JXUN01000128.1_cds_WP_012905777.1_858	0.4452	0.43	0.0412	1.98			putative alcohol dehydrogenase	
NZ_JXUN01000128.1_cds_WP_012905778.1_859	0.1650	1.21			0.0077	2.45	LysR-family transcriptional regulator	
NZ_JXUN01000128.1_cds_WP_012905780.1_861	0.0293	1.80	0.1697	0.97	0.1906	0.95	glutaminase 2	glsA2
NZ_JXUN01000128.1_cds_WP_012905781.1_862	0.1344	0.12	0.2882	-0.34	0.0298	2.66	conserved hypothetical protein	
NZ_JXUN01000128.1_cds_WP_012905783.1_864	0.0930	0.80	0.1490	0.03	0.0038	1.15	altronate oxidoreductase	uxaB
NZ_JXUN01000128.1_cds_WP_012905789.1_870	0.1365	1.07	0.3374	-0.86	0.0379	2.85	putative GntR-family transcriptional regulator	
NZ_JXUN01000128.1_cds_WP_012905791.1_872	0.1764	-0.19	0.0462	1.10	0.4840	0.73	hypothetical protein	
NZ_JXUN01000128.1_cds_WP_012905802.1_883	0.3831	-0.51	0.3355	0.35	0.0047	2.50	putative exported protein	
NZ_JXUN01000128.1_cds_WP_012905804.1_885	0.4587	-0.58	0.3362	0.03	0.0146	2.05	putative hydrolase	
NZ_JXUN01000128.1_cds_WP_012905805.1_886	0.4272	0.47	0.0716	2.55	0.0199	2.01	putative hydrolase	
NZ_JXUN01000128.1_cds_WP_012905812.1_893	0.0806	-0.70	0.3259	0.20	0.0092	2.53	peroxiredoxin (osmotically-inducible protein C)	osmC
NZ_JXUN01000128.1_cds_WP_012905813.1_894	0.0443	-3.36	0.4975	1.44	0.0619	1.16	protein Bdm (biofilm-dependent modulation protein)	bdm
NZ_JXUN01000128.1_cds_WP_012905818.1_899	0.0665	1.07			0.0035	5.99	putative inorganic pyrophosphatase	ppa
NZ_JXUN01000128.1_cds_WP_024132657.1_863	0.1290	1.12	0.0458	1.88	0.2081	0.82	putative signal transduction protein	
NZ_JXUN01000128.1_cds_WP_024132658.1_869	0.2185	0.64	0.0839	1.06	0.0091	1.15	putative membrane protein	
NZ_JXUN01000128.1_cds_WP_024132660.1_878	0.1319	1.16	0.0524	1.15	0.0469	2.99	MerR-family transcriptional regulator	mlrA
NZ_JXUN01000128.1_cds_WP_042623085.1_846	0.1693	1.33	0.0384	1.46	0.0833	1.90	major facilitator superfamily protein	
NZ_JXUN01000128.1_cds_WP_042623086.1_849	0.0646	1.27	0.0015	1.92	0.0740	1.10	multiple antibiotic resistance regulatory protein	marA
NZ_JXUN01000129.1_cds_WP_012905612.1_903	0.0472	3.72	0.0874	2.14	0.0178	4.11	Vitamin B12 ABC transporter, permease protein	btuC
NZ_JXUN01000129.1_cds_WP_012905625.1_915		9.19	0.1718	0.85			putative glycosyl hydrolase, family 3	
NZ_JXUN01000129.1_cds_WP_012905626.1_916	0.4965	-0.18			0.0026	1.91	hypothetical protein	
NZ_JXUN01000130.1_cds_WP_012907511.1_944	0.2511	0.39	0.0355	1.79	0.0388	1.99	putative exported protein	
NZ_JXUN01000130.1_cds_WP_012907514.1_947	0.3727	-0.77			0.1001	1.11	acetyl-coenzyme A synthetase	acs
NZ_JXUN01000130.1_cds_WP_012907515.1_948	0.0111	-1.69	0.4380	0.33	0.1696	3.05	cytochrome c552	nrfA
NZ_JXUN01000130.1_cds_WP_012907516.1_949	0.2151	1.28	0.0953	2.67	0.0106	3.25	cytochrome c-type protein	nrfB
NZ_JXUN01000130.1_cds_WP_012907517.1_950	0.4590	0.23	0.1544	1.19	0.0499	2.20	cytochrome c-type biogenesis protein	nrfC
NZ_JXUN01000130.1_cds_WP_042623091.1_943		2.51				4.12	putative oxidoreductase	
NZ_JXUN01000131.1_cds_WP_012904388.1_1003	0.0632	0.52	0.0666	1.87	0.0029	2.48	threonine synthase	thrC
NZ_JXUN01000131.1_cds_WP_012904390.1_1001	0.1016	0.57	0.0981	0.43	0.0068	1.00	putative transport protein	
NZ_JXUN01000131.1_cds_WP_012904394.1_997	0.0567	0.62	0.0265	1.54	0.0022	2.77	putative membrane protein	
NZ_JXUN01000131.1_cds_WP_012904396.1_995	0.1892	0.58	0.0362	1.29	0.1877	1.37	chaperone protein DnaJ (heat shock protein J)	dnaJ
NZ_JXUN01000131.1_cds_WP_012904399.1_992	0.0855	0.65	0.1674	1.06	0.0201	1.94	conserved hypothetical protein	
NZ_JXUN01000131.1_cds_WP_012904400.1_991		0.81	0.0219	3.21	0.0136	4.74	putative membrane protein	

NZ_JXUN01000131.1_cds_WP_012904401.1_990	0.0369	1.18	0.0611	3.23	0.0480	4.03	putative polysaccharide degrading enzyme	
NZ_JXUN01000131.1_cds_WP_012904402.1_988	0.0151	1.72	0.0556	0.98	0.1603	0.38	Na(+)/H(+) antiporter 1	nhaA
NZ_JXUN01000131.1_cds_WP_012904404.1_986		-1.87	0.0417	2.14	0.0798	2.36	putative glycosyl hydrolase	
NZ_JXUN01000131.1_cds_WP_012904405.1_985	0.1417	0.64			0.3881	1.70	putative transport protein	
NZ_JXUN01000131.1_cds_WP_012904414.1_976	0.1596	0.33			0.4712	1.47	putative PTS system protein	
NZ_JXUN01000131.1_cds_WP_012904416.1_974		0.67				0.25	putative PTS system protein	
NZ_JXUN01000131.1_cds_WP_012904419.1_971	0.3932	-0.90			0.0927	3.33	putative LacI-family transcriptional regulator	
NZ_JXUN01000131.1_cds_WP_012904421.1_969	0.0209	-1.26	0.4502	0.61	0.2437	-0.40	carbamoyl-phosphate synthase small chain	carA
NZ_JXUN01000131.1_cds_WP_012904424.1_966	0.4874	-0.02	0.1011	1.32			carnitinyl-CoA dehydratase	caiD
NZ_JXUN01000131.1_cds_WP_012904426.1_964	0.0086	5.41			0.0351	5.39	crotonobetainyl-CoA:carnitine CoA-transferase	caiB
NZ_JXUN01000131.1_cds_WP_012904427.1_963	0.0446	-0.49	0.1554	0.63	0.0246	2.07	crotonobetainyl-CoA dehydrogenase	caiA
NZ_JXUN01000131.1_cds_WP_012904428.1_962	0.1551	1.13			0.0166	3.59	L-carnitine/gamma-butyrobetaine antiporter	caiT
NZ_JXUN01000131.1_cds_WP_012908891.1_1016	0.0103	1.41	0.4408	-0.79	0.0582	0.02	trp operon repressor	trpR
NZ_JXUN01000131.1_cds_WP_012908893.1_1014	0.0259	1.52	0.4533	-0.39		0.93	phosphoglycerate mutase 2	gpmB
NZ_JXUN01000131.1_cds_WP_012908894.1_1013	0.0094	1.31	0.3452	0.32	0.4199	1.10	right origin-binding protein	rob
NZ_JXUN01000131.1_cds_WP_012908897.1_1010		0.49			0.0215	3.25	two-component system sensor kinase	creC
NZ_JXUN01000131.1_cds_WP_012908898.1_1009	0.0414	1.95	0.0321	2.39	0.0046	3.25	inner membrane protein	creD
NZ_JXUN01000131.1_cds_WP_024133124.1_1027		2.83	0.0265	3.03	0.0066	3.45	carbamate kinase	arcC
NZ_JXUN01000131.1_cds_WP_071820556.1_989	0.1563	0.62	0.3145	1.20	0.0341	1.43	Na(+)/H(+) antiporter 1, or putative polysaccharide	nhaA
NZ IVIN01000122 1 ada WD 012004670 1 1057	0.0440	2.46	0.0743	2.75			degrading enzyme	
NZ_JXUN01000132.1_cds_WP_012904679.1_1057							putative exported protein	1-64
NZ_JXUN01000132.1_cds_WP_012904682.1_1055	0.1142	2.68	0.0772	2.47	0.0454	2.26	Lateral flagellar flaggelin	lafA
NZ_JXUN01000132.1_cds_WP_012904684.1_1053	0.1541	1.55	0.2242	1.33	0.0454	2.26	lateral flagellar chaperone protein	lafC
NZ_JXUN01000132.1_cds_WP_012904686.1_1051	0.1997	2.76	0.1430	3.08	0.0483	2.76	lateral flagellar chaperone protein, OR ateral flagellar hook length control protein	lafD, lafE
NZ_JXUN01000132.1_cds_WP_012904687.1_1050	0.0705	-1.40			0.0202	2.56	lateral flagellar associated protein	lafF
NZ_JXUN01000132.1_cds_WP_012904691.1_1046	0.3924	-0.34	0.2223	-0.83	0.0284	2.95	hypothetical protein	
NZ_JXUN01000132.1_cds_WP_012904700.1_1036	0.0972	0.42	0.0306	1.03	0.4892		T3SS effector protein NleA/EspI	nleA
NZ_JXUN01000133.1_cds_WP_012907097.1_1062	0.0078	3.35			0.0462	5.72	putative ATP-binding protein of T1SS	
NZ_JXUN01000133.1_cds_WP_024132843.1_1064	0.2986	-0.27	0.3814	0.61	0.0363	1.43	large repetitive protein	
NZ_JXUN01000135.1_cds_WP_012907026.1_1099	0.0035	2.89	0.0013	3.25	0.2200	2.32	diaminopimelate decarboxylase	lysA
NZ_JXUN01000135.1_cds_WP_012907027.1_1098	0.2019	-1.89	0.0139	1.79	0.0470		transcriptional activator	lysR
NZ_JXUN01000135.1_cds_WP_012907029.1_1096	0.4892	-0.13	0.0506	0.99	0.0119	2.52	putative pectin degradation protein	kdgF
NZ_JXUN01000135.1_cds_WP_012907031.1_1093	0.0814	3.61	0.1217	1.17	0.0024		putative ABC transporter membrane protein	
NZ_JXUN01000135.1_cds_WP_012907032.1_1092	0.0067	3.38	0.1635	1.24			putative ABC transporter protein	
NZ_JXUN01000135.1_cds_WP_012907033.1_1091	0.2542	-0.65	0.0342	1.35	0.0120	2.29	putative ABC transpoter periplasmic protein	
NZ_JXUN01000135.1_cds_WP_012907037.1_1087	0.0859	4.04			0.0008	4.67	oligogalacturonate lyase	ogl
NZ_JXUN01000135.1_cds_WP_071820590.1_1095	0.0935	3.79	0.0336	2.96		6.86	putative pectin degradation protein OR putative ABC transporter membrane protein	kdgF,
NZ JXUN01000136.1 cds WP 012906579.1 1109	0.0814	1.88	0.0181	1.35	0.1425	1.52	probable N-acetylmuramoyl-L-alanine amidase	amiA
NZ JXUN01000136.1 cds WP 012906581.1 1111	0.1230	-1.09	0.0197	2.63	0.0710	1.60	ethanolamine operon transcriptional regulator	eutR
NZ JXUN01000136.1 cds WP 012906585.1 1115		1.37			0.0229	4.61	ethanolamine ammonia-lyase heavy chain	eutB
		,						***

NZ JXUN01000136.1 cds WP 012906587.1 1117	0.2003	-0.31					ethanolamine utilization protein	eutA
NZ JXUN01000136.1 cds WP 012906588.1 1118	0.2003	2.71	0.0037	2.87	0.0003	3.72	Ethanolamine utilization dehydrogenase	eutG
NZ JXUN01000136.1 cds WP 012906589.1 1119	0.2428	0.84	0.1035	1.79	0.0003	3.72	ethanolamine utilization dehydrogenase	eutG
	0.2428		0.1055	1./9			, ,	
NZ_JXUN01000136.1_cds_WP_012906590.1_1120	0.2140	0.96			0.0205	4.40	ethanolamine utilization aldehyde dehydrogenase	eutE
NZ_JXUN01000136.1_cds_WP_012906592.1_1122	0.2148	1.53			0.0305	4.48	ethanolamine utilization protein	eutM
NZ_JXUN01000136.1_cds_WP_012906595.1_1125	0.2950	0.30	0.0766	1.87	0.0113	3.97	ethanolamine utilization protein	eutQ
NZ_JXUN01000137.1_cds_WP_012907661.1_1148	0.1096	2.27	0.0186	1.16	0.1335	0.05	putative DNA binding protein	
NZ_JXUN01000137.1_cds_WP_012907663.1_1145	0.0344	1.73	0.3262	0.06	0.3826	0.62	UvrABC system protein A (excinuclease ABC subunit A)	uvrA
NZ_JXUN01000137.1_cds_WP_012907666.1_1142	0.2859	0.23	0.2675	0.48	0.0334	1.77	Conserved hypothetical protein	
NZ_JXUN01000137.1_cds_WP_012907667.1_1141	0.0041	1.30	0.0021	1.84	0.0967	1.23	conserved hypothetical protein	
NZ_JXUN01000137.1_cds_WP_012907671.1_1137	0.1111	1.45	0.3108	-0.07	0.0214	2.90	replicative DNA helicase protein DnaB	dnaB
NZ_JXUN01000137.1_cds_WP_012907673.1_1135	0.0229	3.28	0.1518	2.40	0.0648	3.37	putative outer membrane protein	yjbO
NZ_JXUN01000137.1_cds_WP_012907676.1_1132	0.4264	0.31	0.0974	0.79	0.0135	1.27	putative transcriptional regulator	
NZ_JXUN01000138.1_cds_WP_000208241.1_1153	0.0645	1.07	0.0019	1.76	0.0513	0.31	ATP-dependent protease (heat shock protein)	hslV
NZ_JXUN01000140.1_cds_WP_012904435.1_1264	0.1392	1.34	0.0674	2.17	0.0220		major facilitator superfamily protein	
NZ_JXUN01000140.1_cds_WP_012904436.1_1263	0.0491	-1.88	0.2188	1.99	0.0876	1.22	putative lipoprotein	
NZ JXUN01000140.1 cds WP 012904437.1 1262	0.0334	2.19				5.93	putative adhesin autotransporter	
NZ_JXUN01000140.1_cds_WP_012904438.1_1261	0.4898	0.36	0.0099	1.13	0.3323	0.54	glutathione-regulated potassium-efflux system ancillary protein	kefF
NZ JXUN01000140.1 cds WP 012904440.1 1259	0.0899	1.75	0.0589	2.01	0.0466	2.60	hypothetical protein	
NZ JXUN01000140.1 cds WP 012904441.1 1258	0.1139	1.29	0.4816	-0.24	0.0311	1.96	dihydrofolate reductase	folA
NZ JXUN01000140.1 cds WP 012904448.1 1251	0.2557	0.52	0.1271	1.75	0.0398	2.79	DnaJ-like protein	djlA
NZ JXUN01000140.1 cds WP 012904449.1 1250	0.3299	0.75	0.2980	1.49	0.0368	3.54	ribosomal large subunit pseudouridine synthase A	rluA
NZ JXUN01000140.1 cds WP 012904450.1 1249	0.0390	1.41	0.0222	1.09	0.1458	0.91	RNA polymerase-associated protein	rapA
NZ JXUN01000140.1 cds WP 012904454.1 1245		0.31	0.0249	2.58	0.0574	3.40	L-arabinose isomerase	araA
NZ JXUN01000140.1 cds WP 012904456.1 1243	0.1339	1.66			0.0033	3.59	arabinose operon regulatory protein	araC
NZ JXUN01000140.1 cds WP 012904457.1 1242	0.0497	0.71	0.0207	1.10	0.0054	1.39	putative membrane protein	
NZ JXUN01000140.1 cds WP 012904458.1 1241	0.2472	1.31	0.0270	1.67	0.0051	1.57	thiamine ABC transport system, permease protein	thiP, thiQ
NZ_3AUN01000140.1_cds_W1_012704436.1_1241	0.2472	1.31	0.0270	1.07			OR thiamine ABC transport system, ATP-binding protein	um, unq
NZ_JXUN01000140.1_cds_WP_012904461.1_1238	0.3455	-0.13	0.0322	1.25	0.2477		putative substrate-binding protein	
NZ_JXUN01000140.1_cds_WP_012904463.1_1235	0.2333	0.46	0.4935	0.83	0.0016	1.74	3-isopropylmalate dehydratase small subunit	leuD
NZ_JXUN01000140.1_cds_WP_012904468.1_1230	0.2947	1.50	0.0322	1.55	0.0210	1.56	LysR-family transcriptional regulator	leuO
NZ JXUN01000140.1 cds WP 012904484.1 1213	0.3194	0.80	0.4438	-0.56	0.0064	1.76	cell division protein FtsQ	ftsQ
NZ_JXUN01000140.1_cds_WP_012904486.1_1210	0.0445	1.15	0.4846	0.46	0.4998	-1.65	UDP-3-O-[3-hydroxymyristoyl] N-	lpxC
NZ_JXUN01000140.1_cds_WP_012904491.1_1205	0.0363	0.58	0.0310	0.40	0.0490	1.12	acetylglucosamine deacetylase conserved hypothetical protein	
NZ_JXUN01000140.1_cds_WP_012904492.1_1204	0.2160	0.35	0.3112	-0.18	0.0234	2.04	dephospho-CoA kinase	coaE
NZ_JXUN01000140.1_cds_WP_012904499.1_1197	0.4405	0.10	0.2090	0.36	0.0169	1.79	AmpE protein	ampE
NZ_JXUN01000140.1_cds_WP_012904500.1_1196	0.4552	1.00	0.1674	2.34	0.0492	4.13	putative glycosyl hydrolase	
NZ_JXUN01000140.1_cds_WP_012904501.1_1195	0.3053	1.88	0.0694	3.85	0.0494	4.70	putative symporter	
NZ_JXUN01000140.1_cds_WP_024132461.1_1239	0.4103	-0.18	0.2123	0.93	0.0025	2.16	thiamine ABC transport system, substrate-binding	thiB
NZ_JXUN01000140.1_cds_WP_024132463.1_1225	0.0424	1.18	0.2965	-0.18	0.4677	-1.90	protein precursor conserved hypothetical protein	

NZ_JXUN01000140.1_cds_WP_071820557.1_1224	0.0023	1.15	0.1598	0.05	0.4101	0.13	S-adenosyl-L-methionine-dependent methyltransferase	mraW
NZ_JXUN01000141.1_cds_WP_012907285.1_1269	0.2109	-1.69	0.0200	1.10	0.1787	-0.10	hypothetical protein	
NZ_JXUN01000141.1_cds_WP_012907291.1_1280	0.3317	0.05	0.1310	0.61	0.0367	3.44	thiol:disulfide interchange protein	dsbD
NZ_JXUN01000141.1_cds_WP_012907294.1_1283	0.0127	-1.62	0.3017	-0.41	0.0423	0.64	aspartate ammonia-lyase	aspA
NZ_JXUN01000141.1_cds_WP_012907303.1_1296		-2.21	0.0776	1.09	0.0201		transcriptional regulatory protein EntR (Entericidin R)	ecnR
NZ_JXUN01000141.1_cds_WP_012907305.1_1298	0.1612	2.34	0.0826	3.77	0.0062	4.40	outer membrane lipoprotein	blc
NZ_JXUN01000141.1_cds_WP_024132875.1_1273	0.1259	1.87	0.0248	2.93	0.0949	1.96	pseudogene	
NZ_JXUN01000141.1_cds_WP_024132876.1_1281	0.0404	1.46	0.0733	1.61	0.0016	2.23	divalent cation tolerance protein	cutA
NZ_JXUN01000141.1_cds_WP_024132878.1_1289	0.3440	1.12			0.0151	7.87	putative reverse transcriptase	
NZ_JXUN01000141.1_cds_WP_024132881.1_1295	0.0948	-1.36	0.0400	1.31	0.0316		transcriptional regulatory protein EntR (Entericidin R), OR elongation factor P	ecnR, efp
NZ JXUN01000142.1 cds WP 012908072.1 1304	0.0320	2.17	0.0834	0.67	0.4242	0.72	putative fimbrial subunit	kfcH,kfcG
NZ JXUN01000142.1 cds WP 012908073.1 1305	0.0286	1.65	0.0395	0.42	0.0353	1.51	putative fimbrial subunit	kfcF
NZ JXUN01000142.1 cds WP 012908073.1 1305	0.0286	1.65	0.0395	0.42	0.0353	1.51	putative fimbrial subunit	kfcF
NZ JXUN01000142.1 cds WP 012908075.1 1307	0.0344	1.05	0.0009	0.88	0.0118	1.89	putative fimbrial usher protein	kfcD
NZ JXUN01000142.1 cds WP 012908076.1 1308	0.4245	0.22	0.1806	-0.51	0.0060	-1.85	putative fimbrial subunit	
NZ JXUN01000142.1 cds WP 012908078.1 1310	0.3373	0.55	0.4830	0.12	0.0269	-1.89	putative DNA binding protein	
NZ JXUN01000142.1 cds WP 012908088.1 1320	0.1256	1.82	0.1578	0.89	0.0004	3.44	putative tight adherence protein TadZ	tadZ
NZ_JXUN01000142.1_cds_WP_012908091.1_1323	0.0516	0.93	0.2294	0.95	0.0214	2.83	putative tight adherence protein C	tadC
NZ JXUN01000142.1 cds WP 012908092.1 1324	0.1592	7.36	0.0389	4.32	0.1511	5.09	putative tight adherence protein D	tadD
NZ JXUN01000142.1 cds WP 012908093.1 1325	0.4537	-0.15	0.0238	1.43	0.0872	0.14	hypothetical protein	
NZ_JXUN01000142.1_cds_WP_012908097.1_1328	0.1071	1.82	0.0952	0.57	0.0268	1.55	putative ATP binding protein	
NZ_JXUN01000142.1_cds_WP_012908098.1_1329	0.1039	1.07	0.1810	0.96	0.0081	1.83	hypothetical protein	
NZ_JXUN01000142.1_cds_WP_012908102.1_1333	0.1749	1.01	0.2069	0.65			putative tight adherence protein TadE	tadE
NZ JXUN01000142.1 cds WP 012908104.1 1335	0.2428	-0.47	0.2775	0.21	0.0352	3.74	putative exported protein	
NZ_JXUN01000142.1_cds_WP_042623117.1_1321		-1.07			0.0752	1.33	putative tight adherence protein A	tadA
NZ JXUN01000142.1 cds WP 042623118.1 1314	0.0195	1.31	0.1757	0.68	0.0289	1.81	putative LuxR-family transcriptional regulator	
NZ JXUN01000143.1 cds WP 012904946.1 1366	0.0038	-3.01	0.2457	-0.01	0.0281	1.82	putative carboxypeptidase g2	
NZ JXUN01000143.1 cds WP 012904947.1 1365		-2.55	0.2224	-1.46	0.0410	2.18	putative membrane protein	
NZ JXUN01000143.1 cds WP 012904950.1 1362		-3.18	0.4046	0.40	0.0504	0.09	conserved hypothetical protein	
NZ JXUN01000143.1 cds WP 012904961.1 1350	0.1531	-0.79	0.0307	1.37	0.0822	0.10	putative oxidoreductase	
NZ JXUN01000143.1 cds WP 012904963.1 1347	0.4891	0.88	0.2705	1.07	0.0460	1.49	conserved hypothetical protein	
NZ_JXUN01000143.1_cds_WP_012904967.1_1343	0.3118	1.01	0.0060	2.66	0.0154	3.32	apo-citrate lyase phosphoribosyl-dephospho-CoA	citX
NZ_JXUN01000143.1_cds_WP_012904970.1_1340	0.2465	-1.28	0.1593	2.13	0.0485	2.32	transferase citrate lyase acyl carrier protein (citrate lyase gamma chain)	citD
NZ JXUN01000144.1 cds WP 012904987.1 1372	0.0207	1.27	0.1427	1.26	0.1115	0.25	conserved hypothetical protein	
NZ JXUN01000144.1 cds WP 012904993.1 1378	0.0349	1.73	0.0823	1.18	0.0160	2.26	rare lipoprotein B	rlpB
NZ JXUN01000145.1 cds WP 012907386.1 1395	0.0663	-2.23	0.4425	-0.14	0.0042	1.47	putative exported protein	•
NZ JXUN01000145.1 cds WP 042623128.1 1382	0.4600	-0.37	0.2972	1.70	0.0009	3.65	ABC transporter, permease protein	
NZ JXUN01000145.1 cds WP 071820604.1 1391	0.3639	1.16	0.4626	2.15	0.0078	3.15	conserved hypothetical protein	
NZ JXUN01000146.1 cds WP 004853788.1 1435	0.1676	1.25			0.0295	2.83	propanediol utilization protein	pduJ
							1 1 F	1

NZ_JXUN01000146.1_cds_WP_012906336.1_1436	0.4593	-0.05	0.1485	2.62	0.0054	4.84	propanediol utilization: diol dehydratase reactivation	pduH
NZ_JXUN01000146.1_cds_WP_012906337.1_1434	0.3415	1.07	0.1725	1.06	0.0477	2.76	propanediol utilization protein PduK	pduK
NZ_JXUN01000146.1_cds_WP_012906340.1_1431	0.0863	1.11			0.0509	2.50	propanediol utilization: polyhedral bodies	pduN
NZ_JXUN01000146.1_cds_WP_012906342.1_1429	0.2488	1.05	0.0859	2.53	0.0378	1.53	propanediol utilization: CoA-dependent	pduP
NZ JXUN01000146.1 cds WP 012906345.1 1426	0.4048	0.72					propionaldehyde dehydrogenase propanediol utilization protein PduT	pduT
NZ JXUN01000146.1 cds WP 012906354.1 1416	0.0392	-2.46	0.4657	-0.54	0.1238	0.45	conserved hypothetical protein	paul
NZ JXUN01000146.1 cds WP 012907650.1 1401	0.3038	-0.68	0.0231	2.76	0.0010	5.34	urease subunit gamma	ureA
NZ JXUN01000147.1 cds WP 012908851.1 1459	0.3038	-0.32	0.0231	0.06	0.0010	1.83	putative type II secretion system, ATP-	uieA
112_37.01\01000147.1_cds_w1_012700051.1_1457	0.2304	-0.52	0.1304	0.00	0.0403	1.05	binding,protein	
NZ_JXUN01000147.1_cds_WP_012908854.1_1456	0.4392	-0.53	0.0806	1.00			glutathione synthetase	gshB
NZ_JXUN01000147.1_cds_WP_012908856.1_1454	0.1102	1.77			0.0242	1.59	tRNA-processing ribonuclease BN, OR phosphatase	rbn
NZ_JXUN01000147.1_cds_WP_012908859.1_1451	0.2137	0.28	0.0055	1.56	0.0574	2.71	two-component sensor kinase	
NZ_JXUN01000147.1_cds_WP_012908876.1_1440	0.1267	2.63	0.0462	2.45	0.0198	3.08	putative fimbrial chaperone protein	
NZ_JXUN01000147.1_cds_WP_024133119.1_1458	0.0193	1.43	0.1436	0.58	0.3789	0.14	putative holliday junction resolvase	yqgF
NZ_JXUN01000147.1_cds_WP_024133120.1_1450	0.4814	-0.15	0.4005	0.39	0.0009	3.00	transthyretin-like protein	
NZ_JXUN01000147.1_cds_WP_072014921.1_1447	0.2176	-0.62	0.2127	0.73	0.0069	2.58	biosynthetic arginine decarboxylase, OR S-	speA, metK
							adenosylmethionine synthetase	
NZ_JXUN01000148.1_cds_WP_012908450.1_1470	0.2331	0.19	0.0403	1.20	0.0131	1.95	ABC transporter, permease protein	
NZ_JXUN01000148.1_cds_WP_012908453.1_1467	0.3190	-0.74	0.1043	1.36	0.0417	2.56	acriflavin resistance protein F	acrF
NZ_JXUN01000148.1_cds_WP_012908454.1_1466		1.48	0.0066	3.20	0.0076	3.08	acriflavine resistance protein E	acrE
NZ_JXUN01000148.1_cds_WP_024133048.1_1469	0.3258	1.49			0.0236	1.71	Putative ABC transporter, substrate-binding protein	
NZ_JXUN01000149.1_cds_WP_012908698.1_1509	0.3301	0.30	0.0697	2.26	0.0214	2.17	conserved hypothetical protein	
NZ_JXUN01000149.1_cds_WP_012908700.1_1507	0.1074	2.05	0.1637	2.42			conserved hypothetical protein	
NZ_JXUN01000149.1_cds_WP_012908703.1_1504	0.0328	1.53			0.0062	3.41	2-dehydro-3-deoxy-6-phosphogalactonate aldolase	dgoA
NZ_JXUN01000149.1_cds_WP_012908704.1_1503	0.4860	-0.33	0.3585	-0.58	0.0389	1.02	putative transcriptional regulator	
NZ_JXUN01000149.1_cds_WP_012908708.1_1499		2.06	0.0543	2.00	0.0234		putative zinc-binding dehydrogenase	
NZ_JXUN01000149.1_cds_WP_012908712.1_1495	0.0485	1.22	0.0253	1.24	0.3275	2.67	N-acetylgalactosamine-specific PTS system EIIC component 2	agaW
NZ_JXUN01000149.1_cds_WP_012908716.1_1492		0.23	0.0821	1.48	0.0071	3.03	putative sugar isomerase	
NZ_JXUN01000149.1_cds_WP_012908732.1_1476	0.0005	1.30	0.0107	1.71	0.0485	0.99	DNA polymerase III, psi subunit	holD
NZ_JXUN01000149.1_cds_WP_024133090.1_1491	0.1913	-0.92			0.0032	2.60	phosphoglycerol transferase I	mdoB
NZ_JXUN01000150.1_cds_WP_012908043.1_1552	0.0038	-2.87	0.1631	-0.83	0.4596	0.03	putative T3SS effector protein EspO	espO
NZ_JXUN01000150.1_cds_WP_012908056.1_1539	0.1519	2.95	0.3080	0.83	0.0491	1.65	putative ABC transpoter membrane protein	
NZ_JXUN01000150.1_cds_WP_012908062.1_1532		-0.75			0.0199	1.44	putative maltoporin	
NZ_JXUN01000150.1_cds_WP_012908066.1_1528	0.2669	1.33	0.3326	0.85	0.0077	2.21	PTS system, cellobiose-specific IIb component	
NZ_JXUN01000150.1_cds_WP_012908067.1_1527	0.0176	3.29	0.1364	1.85	0.0057	3.42	putative LacI-family transcriptional regulator	
NZ_JXUN01000151.1_cds_WP_012906028.1_1618		2.03	0.1814	1.84		3.53	nitrate transporter permease component	nasE
NZ_JXUN01000151.1_cds_WP_012906029.1_1617		-0.21	0.0371	2.09	0.0427	3.36	nitrate-binding protein	nasF
NZ_JXUN01000151.1_cds_WP_012906044.1_1600	0.0332	1.05	0.2036	0.11	0.0198	3.09	putative sulphate transporter	
NZ_JXUN01000151.1_cds_WP_012906050.1_1594	0.3349	0.08	0.1030	0.59	0.0471	4.18	putative LuxR-family transcriptional regulator	
NZ_JXUN01000151.1_cds_WP_012906053.1_1591		1.07	0.1467	2.44	0.1074	1.05	putative fimbrial usher protein	lpfC
NZ_JXUN01000151.1_cds_WP_012906057.1_1587	0.4627	0.31			0.0492	2.77	conserved hypothetical protein	

NZ_JXUN01000151.1_cds_WP_012906067.1_1577	0.0737	-0.84	0.1453	0.14	0.0324	2.15	Conserved hypothetical protein	
NZ_JXUN01000151.1_cds_WP_012906077.1_1566	0.4925	-0.55	0.4593	0.27	0.0061	1.52	LysR-family transcriptional regulator	
NZ_JXUN01000151.1_cds_WP_042623144.1_1613	0.0114	1.47	0.2744	-0.05	0.0016	2.41	cation transport protein	chaC
NZ_JXUN01000152.1_cds_WP_012905222.1_1623	0.0589	2.03	0.0136	1.68	0.0171	4.25	putative outer membrane efflux protein of T1SS	
NZ_JXUN01000153.1_cds_WP_012904558.1_1630	0.0100	1.50	0.4028	0.48	0.1563	-0.38	undecaprenyl pyrophosphate synthetase	uppS
NZ_JXUN01000153.1_cds_WP_012904559.1_1631	0.0296	1.23	0.1368	1.05	0.0798	0.42	phosphatidate cytidylyltransferase	cdsA
NZ_JXUN01000153.1_cds_WP_012904563.1_1635	0.0119	1.94	0.0680	1.87	0.1773	0.25	UDP-3-O-[3-hydroxymyristoyl] glucosamine N-acyltransferase	lpxD
NZ_JXUN01000153.1_cds_WP_012904564.1_1637	0.0122	1.29	0.3213	0.44	0.3216	-0.07	acyl-[acyl-carrier-protein]UDP-N-acetylglucos amine O-acyltransferase	lpxA
NZ_JXUN01000154.1_cds_WP_012908110.1_1646	0.4377	0.24	0.0763	0.77			ATP-dependent DNA helicase	recG
NZ_JXUN01000154.1_cds_WP_012908113.1_1649	0.0369	1.33	0.4145	0.46	0.3470	-0.30	DNA-directed RNA polymerase omega chain	rpoZ
NZ_JXUN01000154.1_cds_WP_012908121.1_1660	0.2076	-1.47	0.3105	-0.30	0.0145	2.71	DNA repair protein	radC
NZ_JXUN01000155.1_cds_WP_012905843.1_1691	0.2117	-1.39			0.0816	2.30	putative virulence effector protein	
NZ_JXUN01000155.1_cds_WP_012905844.1_1690	0.1968	1.29			0.0356	4.71	putative virulence effector protein	
NZ_JXUN01000155.1_cds_WP_012905850.1_1683	0.2228	-1.66	0.0633	1.42	0.0230	1.78	ABC transporter, ATP-binding protein	
NZ_JXUN01000155.1_cds_WP_012905851.1_1682	0.3159	1.33	0.1426	1.74	0.0184	3.85	ABC transporter, substrate-binding protein	
NZ_JXUN01000155.1_cds_WP_012905852.1_1681					0.0357	4.72	putative GntR-family transciptional regulator	
NZ_JXUN01000155.1_cds_WP_012905858.1_1675	0.1017	1.51	0.0463	1.67	0.1114	0.05	putative AraC-family transcriptional regulator	
NZ_JXUN01000155.1_cds_WP_012905868.1_1665	0.2357	-0.37	0.1733	1.45	0.0079	2.57	Conserved hypothetical protein	
NZ_JXUN01000155.1_cds_WP_012905869.1_1664		0.49			0.0297	4.64	putative protocatechuate 3,4-dioxygenase beta chain	рсаН
NZ_JXUN01000155.1_cds_WP_042623149.1_1688	0.0496	1.02	0.2240	0.03	0.4583	-0.73	putative membrane protein	
NZ JXUN01000156.1 cds WP 012904540.1 1698	0.2288	0.20	0.4515	0.21	0.0030	2.26	H(+)/Cl(-) exchange transporter	clcA
NZ_JXUN01000156.1_cds_WP_012904541.1_1699	0.0045	1.89	0.1602	0.42	0.1726	0.55	conserved hypothetical protein	
NZ JXUN01000156.1 cds WP 012904542.1 1700	0.3571	-0.28	0.0281	0.98	0.0792	2.15	putative membrane protein	
NZ_JXUN01000156.1_cds_WP_012904545.1_1703	0.0303	1.81	0.3856	0.69	0.0614	1.33	deoxyguanosinetriphosphate triphosphohydrolase	dgt
NZ_JXUN01000156.1_cds_WP_012904547.1_1705	0.4551	0.64	0.0212	1.49	0.0072	2.49	carbohydrate diacid regulator	cdaR
NZ JXUN01000156.1 cds WP 024132472.1 1706	0.1460	-0.25	0.3394	-0.06	0.0102	1.26	hypothetical protein	
NZ JXUN01000157.1 cds WP 012904702.1 1715	0.1446	2.28	0.3234	-0.22	0.0419	-1.59	putative membrane-spanning transport protein	aatD
NZ JXUN01000157.1 cds WP 012904706.1 1720	0.1885	1.10	0.2460	-0.32	0.0086	-1.60	AatC, ATP binding protein of ABC transporter	aatC
NZ JXUN01000158.1 cds WP 012908270.1 1734	0.0184	-3.05	0.3004	-0.38	0.1140	0.76	putative acyl carrier protein	
NZ JXUN01000158.1 cds WP 024133030.1 1727	0.0201	-2.43	0.2714	1.14	0.1976	-0.38	putative membrane protein	
NZ JXUN01000159.1 cds WP 012908678.1 1743	0.2488	-0.01			0.0144	4.17	putative ATP-binding protein of T1SS	
NZ_JXUN01000159.1_cds_WP_012908680.1_1745	0.2576	0.54	0.1640	2.32			major facilitator superfamily protein	
NZ JXUN01000159.1 cds WP 012908685.1 1750	0.0038	-3.43	0.3374	0.84	0.3172	0.12	putative membrane protein	
NZ JXUN01000159.1 cds WP 012908686.1 1751	0.2958	0.70			0.2735		putative LysR-family transcriptional regulator	
NZ JXUN01000159.1 cds WP 012908687.1 1752	0.0330	-2.28	0.0693	1.02	0.1859	1.96	putative transport protein	
NZ JXUN01000159.1 cds WP 012908688.1 1753	0.2129	1.68			0.1041	1.86	cystathionine beta-lyase	metC
NZ JXUN01000159.1 cds WP 012908690.1 1755	0.0904	1.14	0.0012	3.22	0.0060	2.84	LysE-family transporter	
NZ JXUN01000159.1 cds WP 012908691.1 1756	0.0832	2.08	0.1539	2.73	0.0000	3.08	putative AraC-family transcriptional regulator	
NZ JXUN01000160.1 cds WP 012904925.1 1784	0.0296	4.72	3.1337	2.73	0.0827	2.01	acetoin reductase	budC
NZ JXUN01000160.1 cds WP 012904926.1 1783	0.4818	-0.10			0.3387	2.24	putative sugar ABC transporter, permease protein	oude
112_37.01101000100.1_cu3_w1_012304320.1_1/83	0.4010	-0.10			0.5507	2.24	patative sugar ABC transporter, permease protein	

NZ_JXUN01000160.1_cds_WP_012904927.1_1782		2.84	0.1699	1.43	0.0274	1.33	putative sugar ABC transporter, ATP-binding protein	
NZ_JXUN01000160.1_cds_WP_012904930.1_1776		1.21					putative N-terminal region of transketolase	
NZ_JXUN01000160.1_cds_WP_012904931.1_1775	0.0877	2.15	0.0888	2.36	0.0280	3.05	putative C-terminal region of transketolase	
NZ_JXUN01000161.1_cds_WP_012908757.1_1809	0.0686	0.53	0.0096	1.09	0.0750	0.89	lipoate-protein ligase A	lplA
NZ_JXUN01000161.1_cds_WP_012908763.1_1803	0.2359	0.36	0.2742	0.14	0.0377	1.11	chromosome intitiation inhibitor	iciA
NZ_JXUN01000162.1_cds_WP_012908135.1_1818	0.1435	-1.59	0.0308	0.90	0.0391	1.30	lipopolysaccharide core biosynthesis protein RfaZ	rfaZ
NZ_JXUN01000162.1_cds_WP_012908136.1_1819	0.1843	-1.92	0.0249	0.62	0.0002	1.10	lipopolysaccharide 1,2-N-	rfaK
NZ JXUN01000162.1 cds WP 012908139.1 1822	0.0343	1.68	0.1086	1.46	0.3527	0.91	acetylglucosaminetransferase ADP-heptose-LPS heptosyltransferase II	rfaF
NZ JXUN01000162.1 cds WP 012908143.1 1826		-2.43	0.0214	1.69	0.0709	1.32	putative glycosyl transferase	
NZ JXUN01000162.1 cds WP 012908155.1 1839	0.0305	1.09	0.0266	1.52	0.0075	2.03	putative RNA-methyltransferase	
NZ JXUN01000162.1 cds WP 012908157.1 1842	0.3421	0.40	0.2033	1.39	0.0130	1.44	L-lactate permease	lctP
NZ JXUN01000162.1 cds WP 012908161.1 1846	0.0853	2.55	0.2012	0.45	0.0417	0.96	mannitol-1-phosphate 5-dehydrogenase	mtlD
NZ JXUN01000162.1 cds WP 012908162.1 1847	0.3104	-0.08	0.0143	1.11	0.0116	0.50	mannitol-specific PTS system EIICBA component	mtlA
NZ_JXUN01000162.1_cds_WP_012908164.1_1849	0.2504	0.02	0.0902	0.96	0.0358		HlyD-family secretion protein	11107.1
NZ_JXUN01000162.1_cds_WP_012908165.1_1850	0.2586	-0.01	0.0424	1.04	0.0243	1.26	putative glutathione S-transferase	
NZ JXUN01000162.1 cds WP 024133008.1 1827	0.1085	0.84	0.3217	0.07	0.0243	2.11	putative grutatione 3-transferase putative polysaccharide deacetylase	
NZ JXUN01000164.1 cds WP 012908455.1 1859	0.1083	3.17	0.0233	3.23	0.0432	4.72	probable acref/enved operon repressor (TetR-family	envR
NZ_JAUN01000104.1_Cus_WF_012700455.1_1657		3.17	0.0233	3.23	0.0231	4.72	transcriptional regulator)	CHVK
NZ_JXUN01000164.1_cds_WP_012908456.1_1860	0.0278	-2.51	0.1254	0.71	0.0115	2.42	predicted membrane protein yhdu	yhdU
NZ_JXUN01000164.1_cds_WP_012908457.1_1861	0.4815	-0.29	0.1220	1.48	0.0106	2.52	putative DNA methylase	
NZ_JXUN01000164.1_cds_WP_012908458.1_1863	0.0038	1.96	0.3264	0.39	0.3207	0.45	tRNA-dihydrouridine synthase B	dusB
NZ_JXUN01000165.1_cds_WP_012905048.1_1872	0.2684	0.28	0.2941	1.15	0.0193	3.51	succinate dehydrogenase cytochrome b-556 subunit,	sdhC, sdhD
							OR succinate dehydrogenase hydrophobic membrane anchor protein	
NZ JXUN01000165.1 cds WP 012905050.1 1874	0.3886	-0.53	0.4936	0.42	0.0137	2.08	succinate dehydrogenase iron-sulfur protein	sdhB
NZ JXUN01000165.1 cds WP 012905051.1 1875	0.0028	-1.79	0.3039	-0.60	0.2108	0.01	2-oxoglutarate dehydrogenase E1 component	sucA
NZ JXUN01000165.1 cds WP 012905058.1 1882	0.0205	2.01	0.2484	1.07	0.3501	2.45	putative exported protein	
NZ JXUN01000165.1 cds WP 012905059.1 1883	0.0163	1.34	0.3338	1.21	0.1495		acyl-CoA thioester hydrolase	
NZ JXUN01000165.1 cds WP 042623167.1 1884	0.0347	1.12	0.3060	0.47	0.4419	1.27	colicin import protein	tolQ
NZ JXUN01000166.1 cds WP 012906629.1 1893	0.0093	-2.29	0.0558	0.89	0.0122	1.66	putative signal transduction protein	1014
NZ_JXUN01000166.1_cds_WP_071820657.1_1909	0.2622	0.12	0.0208	1.43	0.1430	1.33	glycine cleavage system transcriptional repressor	gcvR
NZ_JXUN01000169.1_cds_WP_012906476.1_1922	0.2136	1.55	0.0243	1.81	0.0017	2.26	galactose/methyl galactoside ABC transporter,ATP-	mglA
112_011011011000107.11_000_111_012700170.11_1722	0.2130	1.00	0.02.0	1.01	0.0017	2.20	binding protein	g 1
NZ_JXUN01000170.1_cds_WP_012907799.1_1932	0.0290	1.07	0.2993	0.40	0.3247	0.55	cell division protein	ftsN
NZ_JXUN01000170.1_cds_WP_072044768.1_1933	0.0677	1.01	0.0464	1.15	0.0006	1.49	LacI-family transcriptional repressor	cytR
NZ_JXUN01000171.1_cds_WP_012906132.1_1943	0.3579	0.94	0.0811	2.12	0.0139	4.06	high-affinity zinc uptake system protein	znuA
NZ_JXUN01000171.1_cds_WP_012906135.1_1940	0.0282	0.61	0.0803	0.91	0.0386	1.16	putative exported protein	
NZ_JXUN01000171.1_cds_WP_012906137.1_1938	0.0473	1.03	0.2877	0.15	0.2264	0.29	holliday junction ATP-dependent DNA helicase	ruvA
NZ_JXUN01000173.1_cds_WP_012908922.1_1961	0.2425	0.37	0.1002	2.27	0.0035	3.18	pCROD1 plasmid	pCROD1
NZ_JXUN01000173.1_cds_WP_012908927.1_1964	0.0486	-1.76	0.4324	0.51	0.0742	2.39	pCROD1 plasmid	pCROD1
NZ_JXUN01000173.1_cds_WP_012908929.1_1966	0.1073	-1.04	0.4771	0.02	0.0146	0.94	pCROD1 plasmid	pCROD1
NZ_JXUN01000173.1_cds_WP_024133137.1_1959	0.4009	0.04	0.2987	0.26	0.0348	1.00	pCROD1 plasmid	pCROD1

NZ_JXUN01000173.1_cds_WP_024133138.1_1960	0.4396	1.25	0.0284	0.80	0.0579	0.93	pCROD1 plasmid	pCROD1
NZ_JXUN01000173.1_cds_WP_042623178.1_1956	0.1318	2.98	0.0254	5.49	0.0141	6.40	pCROD1 plasmid	pCROD1
NZ_JXUN01000174.1_cds_WP_012907790.1_1978	0.4896	-0.50	0.0075	1.71	0.0461	1.44	cystathionine gamma-synthase	metB
NZ_JXUN01000174.1_cds_WP_012907793.1_1976	0.1194	1.72	0.0011	2.59	0.0021	2.39	Putative membrane protein	
NZ_JXUN01000174.1_cds_WP_024132967.1_1972	0.3437	-0.18			0.0521	1.77	primosomal protein replication factor	priA
NZ_JXUN01000175.1_cds_WP_012907497.1_1984	0.3343	0.94			0.0393	3.12	dimethyl sulfoxide reductase	
NZ_JXUN01000175.1_cds_WP_012907499.1_1986	0.0331	2.55	0.2663	0.31	0.0668	1.42	putative anaerobic reductase component	
NZ JXUN01000175.1 cds WP 012907504.1 1991	0.0237	-1.68	0.3875	-0.58	0.1572	-1.23	AraC-family transcriptional regulator	soxS
NZ_JXUN01000175.1_cds_WP_012907505.1_1992	0.3515	-0.12	0.3091	0.81	0.0115	2.48	redox-sensitive transcriptional activator	soxR
NZ_JXUN01000175.1_cds_WP_012907506.1_1994	0.1973	0.46	0.0992	0.63	0.0075	3.15	putative glutathione S transferase	
NZ_JXUN01000175.1_cds_WP_024132918.1_1988	0.0298	1.34	0.1395	0.38	0.1681	-0.14	putative membrane protein	
NZ_JXUN01000175.1_cds_WP_042623181.1_1980	0.2409	-2.33	0.2970	-0.49	0.0280	1.65	putative cation-transporting P-type ATPase	
NZ_JXUN01000176.1_cds_WP_012905166.1_2056	0.3516	2.48	0.0519	2.33	0.0219	4.79	ABC transporter, permease protein	
NZ_JXUN01000176.1_cds_WP_012905168.1_2054	0.0041	-2.54	0.2405	0.68	0.0217	1.96	biofilm regulator	bssR
NZ_JXUN01000176.1_cds_WP_012905169.1_2053	0.2165	1.61	0.0422	1.26	0.0187		soluble aldose sugar dehydrogenase	yliT
NZ_JXUN01000176.1_cds_WP_012905176.1_2046	0.0196	0.93			0.0009	2.98	putative phosphatase	
NZ_JXUN01000176.1_cds_WP_012905178.1_2043	0.0243	0.83	0.3473	-0.04	0.1014	1.76	major facilitator superfamily protein	
NZ_JXUN01000176.1_cds_WP_012905179.1_2042	0.0865	2.03	0.0533	2.83	0.0183	3.89	TetR-family transcriptional regulator	
NZ_JXUN01000176.1_cds_WP_012905192.1_2028	0.2201	2.45	0.0285	2.63	0.1689	0.64	23S rRNA (uracil-5-)-methyltransferase	rumB
NZ_JXUN01000176.1_cds_WP_012905196.1_2025		-1.45			0.0362	2.74	putative sulfatase	
NZ_JXUN01000176.1_cds_WP_012905204.1_2017	0.3858	-0.41	0.0306	-1.81	0.2758		putative N-acetylmuramoyl-L-alanine amidase	
NZ_JXUN01000176.1_cds_WP_012905205.1_2016	0.0182	0.91	0.2584	0.11	0.0797	0.80	conserved hypothetical protein	
NZ_JXUN01000176.1_cds_WP_012905208.1_2013	0.4073	0.55	0.0059	2.72	0.0040	1.83	pyruvate oxidase	poxB
NZ_JXUN01000176.1_cds_WP_012905210.1_2011	0.1305	-0.50	0.4192	-0.34			hydroxylamine reductase	hcp
NZ_JXUN01000176.1_cds_WP_012905214.1_2007	0.0515	2.12	0.0853	0.58	0.0311	2.51	conserved hypothetical protein	
NZ_JXUN01000176.1_cds_WP_012905215.1_2006	0.0264	0.45			0.0018	1.63	macrolide-specific efflux protein	macA
NZ_JXUN01000176.1_cds_WP_012905217.1_2004	0.3732	0.33	0.2550	0.61	0.0143	1.00	cold shock-like protein CspD	cspD
NZ_JXUN01000177.1_cds_WP_012906993.1_2090	0.2051	0.87			0.0251	3.68	L-fuculokinase	fucK
NZ_JXUN01000177.1_cds_WP_012906999.1_2084	0.0029	-2.19	0.1360	0.84	0.0114	1.28	putative lipoprotein	ygdI
NZ_JXUN01000177.1_cds_WP_012907001.1_2082	0.0594	0.83	0.0240	1.64	0.0529	1.33	putative Fe-S metabolism associated protein	
NZ_JXUN01000177.1_cds_WP_012907003.1_2080	0.0062	1.07	0.2785	0.30	0.4726	-1.83	membrane-bound lytic murein transglycosylase A	mltA
NZ_JXUN01000177.1_cds_WP_012907004.1_2079	0.1582	0.61	0.2907	-0.13	0.0182		N-acetylmuramoyl-L-alanine amidase	amiC
NZ_JXUN01000177.1_cds_WP_012907005.1_2077	0.2739	0.60	0.1674	0.78	0.0060		amino-acid acetyltransferase (N-acetylglutamate	argA
N/7 IVIINI01000177 1 - J- WD 012007000 1 2072	0.1002	1.50	0.2475	0.12			synthase)	C
NZ_JXUN01000177.1_cds_WP_012907009.1_2073	0.1883	1.56	0.3475	0.13	0.0126	2.00	exodeoxyribonuclease V gamma subunit	recC
NZ_JXUN01000177.1_cds_WP_012907013.1_2069	0.1894	2.27		0.05	0.0136	2.99	prepilin peptidase-dependent protein A	ppdA
NZ_JXUN01000177.1_cds_WP_012907018.1_2064	0.1476	0.06	0.0546	0.86	0.0119	2.15	conserved hypothetical protein	
NZ_JXUN01000177.1_cds_WP_024132829.1_2061	0.0295	-2.14	0.1237	0.66	0.0430	0.84	possible lipoprotein	
NZ_JXUN01000178.1_cds_WP_000087812.1_2112	0.1439	-0.80	0.05		0.0426	2.34	conserved hypothetical protein	
NZ_JXUN01000178.1_cds_WP_000864897.1_2106	0.0296	-2.71	0.3984	0.74	0.2910	0.73	conserved hypothetical protein	
NZ_JXUN01000178.1_cds_WP_012907688.1_2110	0.0329	-2.34	0.4766	-0.33	0.4069	0.84	pseudogene	
NZ_JXUN01000178.1_cds_WP_072044769.1_2094		-1.23	0.0001	2.10			pseudogene	

NZ_JXUN01000179.1_cds_WP_012907432.1_2136	0.0643	1.25			0.0091	1.71	putative conjugative transfer system protein TraL (fragment)	traL
NZ_JXUN01000179.1_cds_WP_012907433.1_2137	0.4026	0.47	0.0423	0.58	0.0422	1.72	putative exported protein	
NZ_JXUN01000179.1_cds_WP_012907443.1_2147	0.1630	8.17					conserved hypothetical protein	
NZ_JXUN01000179.1_cds_WP_012907444.1_2149	0.0347	1.96	0.0237	2.15	0.0523	3.59	pseudogene	
NZ_JXUN01000179.1_cds_WP_012907446.1_2151	0.1400	0.42	0.2503	0.37	0.0057	1.57	putative partitioning protein A	parA
NZ_JXUN01000179.1_cds_WP_024132900.1_2134	0.4067	0.29	0.0286	2.39		1.53	pseudogene	
NZ_JXUN01000179.1_cds_WP_024132903.1_2140	0.0140	2.29			0.0152	2.76	hypothetical protein	
NZ_JXUN01000179.1_cds_WP_042623192.1_2132	0.2621	1.81	0.0399	2.22			pseudogene	
NZ_JXUN01000179.1_cds_WP_042623193.1_2128	0.0006	1.41	0.0263	0.77	0.1234		conserved hypothetical protein	
NZ_JXUN01000180.1_cds_WP_012905313.1_2202	0.4338	0.29	0.3236	0.22	0.0323	2.46	chromosome partition protein	mukF
NZ_JXUN01000180.1_cds_WP_012905321.1_2194	0.0009	-4.29	0.3480	0.33	0.1720	1.02	outer membrane protein F	ompF
NZ_JXUN01000180.1_cds_WP_012905326.1_2189		0.00	0.0394	2.20	0.1236	3.99	putative aliphatic sulfonates ABC transporter, permease protein	ssuC
NZ_JXUN01000180.1_cds_WP_012905336.1_2179	0.3522	0.66	0.0420	1.24	0.0029	1.34	paraquat-inducible protein A	pqiA
NZ_JXUN01000180.1_cds_WP_012905339.1_2175	0.0398	1.18	0.2441	0.69	0.4806	1.07	3-hydroxydecanoyl-[acyl-carrier- protein]dehydratase	fabA
NZ_JXUN01000180.1_cds_WP_012905344.1_2170	0.3600	-0.47	0.0326	0.89	0.0728	1.35	conserved hypothetical protein	
NZ_JXUN01000180.1_cds_WP_012905347.1_2167	0.1699	0.25	0.1163	0.75	0.0412	0.16	helicase IV	helD
NZ_JXUN01000180.1_cds_WP_012905351.1_2163	0.0380	1.19	0.1257	1.51	0.3990	-0.38	conserved hypothetical protein	
NZ_JXUN01000180.1_cds_WP_012905355.1_2159	0.0004	-3.88	0.1680	0.67	0.0490	1.90	putative outer membrane protein	
NZ_JXUN01000180.1_cds_WP_024132580.1_2198	0.0229	2.06	0.1330	0.99	0.1254	3.32	putative exported protein	
NZ_JXUN01000180.1_cds_WP_024132585.1_2168	0.0454	1.79	0.0850	1.24	0.4698	-0.85	putative membrane protein	
NZ_JXUN01000180.1_cds_WP_024132588.1_2160	0.0364	0.99	0.0007	2.62	0.0015	2.40	sulfurtransferase (tRNA 2-thiouridine synthesizing protein E)	tusE
NZ_JXUN01000181.1_cds_WP_012907388.1_2210	0.4218	0.16	0.0562	0.87	0.0465		conserved hypothetical protein	
NZ_JXUN01000181.1_cds_WP_012907389.1_2211		-0.50			0.4050		conserved hypothetical protein	
NZ_JXUN01000181.1_cds_WP_012907396.1_2218	0.2632	-1.15	0.0250	2.20	0.1069	1.25	trehalose operon repressor	treR
NZ_JXUN01000181.1_cds_WP_012907401.1_2223	0.0486	1.24	0.4935	0.53	0.1933	-0.47	pyrBI operon leader peptide	pyrL
NZ_JXUN01000181.1_cds_WP_012907403.1_2225	0.0133	-1.89	0.2426	0.02	0.1839	0.99	conserved hypothetical protein	_
NZ_JXUN01000181.1_cds_WP_012907404.1_2226	0.0048	1.92	0.0170	1.78	0.0061	1.74	ornithine carbamoyltransferase subunit I	argI
NZ_JXUN01000181.1_cds_WP_012907409.1_2231	0.0137	0.63	0.2756	-0.38	0.0874	-0.27	DNA polymerase III, chi subunit	holC
NZ_JXUN01000181.1_cds_WP_012907413.1_2236	0.0642	0.95	0.0479	2.45	0.0253	0.68	conserved hypothetical protein	
NZ_JXUN01000181.1_cds_WP_024132891.1_2219	0.3604	0.86	0.0280	2.36	0.0160	3.10	Mg(2+) transport ATPase, P-type	mgtA
NZ_JXUN01000182.1_cds_WP_042623202.1_2244	0.0306	0.20	0.3832	0.64	0.2180	-2.95	putative outer membrane protein	
NZ_JXUN01000183.1_cds_WP_012908492.1_2248		0.72	0.3639	1.14	0.0464	1.63	putative sialic acid transporter	nanT
NZ_JXUN01000183.1_cds_WP_012908494.1_2250	0.0097	2.03			0.0550	4.99	putative N-acetylmannosamine kinase	nanK
NZ_JXUN01000183.1_cds_WP_012908501.1_2258	0.4536	-0.57	0.0451	1.07	0.0945	0.49	Major Facilitator Superfamily transporter	
NZ_JXUN01000183.1_cds_WP_012908502.1_2259	0.4806	0.05	0.0297	1.47	0.0312	2.42	putative dehydrogenase	rspB
NZ_JXUN01000183.1_cds_WP_012908503.1_2260	0.3172	0.20	0.0303	1.44	0.0288	2.72	putative mannonate dehydratase	
NZ_JXUN01000183.1_cds_WP_012908507.1_2264	0.0015	3.37	0.0250	1.67	0.1104	1.39	conserved hypothetical protein	
NZ_JXUN01000183.1_cds_WP_071820670.1_2255	0.0280	1.02	0.2890	0.33			glutamate synthase [NADPH] large subunit	gltB
NZ_JXUN01000184.1_cds_WP_012908660.1_2281	0.0213	1.61	0.0120	1.81	0.0484		uronate isomerase	uxaC
NZ_JXUN01000184.1_cds_WP_012908661.1_2280	0.4548	-0.71	0.0118	2.35	0.0171	1.96	altronate hydrolase	uxaA

NZ_JXUN01000184.1_cds_WP_012908664.1_2277	0.4651	0.54	0.0261	0.99	0.1328	0.89	putative pH-induced membrane-bound redox modulator	alx
NZ_JXUN01000184.1_cds_WP_072044770.1_2275	0.0315	2.18	0.1113	1.28	0.0221	5.02	conserved hypothetical protein	
NZ_JXUN01000185.1_cds_WP_012906288.1_2296	0.0498	1.50	0.2211	0.53	0.0847	0.63	putative membrane protein	
NZ_JXUN01000185.1_cds_WP_012906289.1_2297	0.0154	2.80	0.0470	3.34	0.0055	3.54	putative outer membrane autotransporter	
NZ_JXUN01000185.1_cds_WP_012906291.1_2299	0.2046	0.55	0.4542	0.50	0.0077	1.73	putative exported protein	
NZ_JXUN01000185.1_cds_WP_012906293.1_2301	0.2170	-0.09			0.0054	2.38	conserved hypothetical protein	
NZ_JXUN01000185.1_cds_WP_012906294.1_2302			0.1446	1.18	0.0401	2.56	conserved hypothetical protein	
NZ_JXUN01000185.1_cds_WP_012906296.1_2304	0.2075	0.79			0.0131	3.28	conserved hypothetical protein	
NZ_JXUN01000185.1_cds_WP_012906305.1_2313	0.1043	-0.46	0.1365	1.18	0.0117	1.38	putative isoaspartyl dipeptidase	
NZ_JXUN01000185.1_cds_WP_024132734.1_2314		-1.78	0.1481	1.72			C4-dicarboxylate transporter	dcuD
NZ_JXUN01000185.1_cds_WP_042623208.1_2311	0.0109	2.35	0.0142	1.33	0.0119	2.63	putative membrane protein	
NZ_JXUN01000185.1_cds_WP_042623211.1_2303	0.1765	-0.66	0.2570	-0.02	0.0477	1.09	hypothetical protein	
NZ_JXUN01000186.1_cds_WP_012908633.1_2334	0.0284	-1.24	0.3381	0.56	0.2848		cytochrome C-type protein	torY
NZ_JXUN01000186.1_cds_WP_012908635.1_2331	0.2534	0.01	0.0400	2.92	0.0164	3.74	tdc operon transcriptional activator	tdcA
NZ_JXUN01000186.1_cds_WP_012908636.1_2330	0.0390	-1.76			0.0731	3.08	catabolic threonine dehydratase	tdcB
NZ_JXUN01000186.1_cds_WP_012908640.1_2326	0.0215	-2.12	0.4018	-0.50	0.3504	1.59	L-serine dehydratase	tdcG
NZ_JXUN01000186.1_cds_WP_024133074.1_2333	0.2904	-1.49	0.2120	1.09	0.0183	2.01	trimethylamine-N-oxide reductase 2 precursor	torZ
NZ_JXUN01000188.1_cds_WP_012908248.1_2338	0.1828	1.95	0.0166	3.08	0.0071	3.26	Conserved hypothetical protein	
NZ_JXUN01000188.1_cds_WP_012908251.1_2340	0.0081	-1.06	0.4999	-0.23	0.2187	-2.36	nickel ABC transporter, ATP-binding protein	nikE
NZ_JXUN01000188.1_cds_WP_012908258.1_2347	0.4874	-0.61	0.0384	-1.69			putative beta-ketoacyl synthase	
NZ_JXUN01000189.1_cds_WP_012905911.1_2375	0.0587	1.43	0.0838	2.12	0.0150	3.57	putative thiolase	
NZ_JXUN01000189.1_cds_WP_012905914.1_2372	0.1642	3.45	0.0307	3.04			putative Pca regulon regulatory protein	pcaR
NZ_JXUN01000189.1_cds_WP_012905920.1_2366	0.2178	-0.67	0.0675	1.80	0.0500	2.79	periplasmic murein tripeptide binding protein	mppA
NZ_JXUN01000189.1_cds_WP_024132620.1_2356	0.0167	2.30	0.0397	2.23	0.0319	0.88	hypothetical protein	
NZ_JXUN01000190.1_cds_WP_012906538.1_2380	0.4735	-0.51	0.2777	0.72	0.0276	4.15	putative membrane transport protein	
NZ_JXUN01000190.1_cds_WP_012906539.1_2381	0.3663	0.12	0.2569	1.25	0.0233	1.56	magnesium transporter	mgtE
NZ_JXUN01000191.1_cds_WP_000103754.1_2400	0.4584	-0.54	0.0661	1.05	0.0456	0.19	acyl carrier protein	acpP
NZ_JXUN01000191.1_cds_WP_012905438.1_2396	0.0277	1.72	0.3667	-0.41	0.1865	-1.41	fatty acid/phospholipid synthesis protein	plsX
NZ_JXUN01000191.1_cds_WP_012905447.1_2406	0.1955	0.37			0.0019	2.16	putative deoxyribonuclease	
NZ_JXUN01000191.1_cds_WP_042623222.1_2388	0.4148	1.17	0.0915	1.30	0.0172	2.66	putative Major Facilitator Superfamily transporter	
NZ_JXUN01000191.1_cds_WP_071820576.1_2392	0.3423	0.44					ribosomal large subunit pseudouridine synthase C	rluC
NZ_JXUN01000192.1_cds_WP_012907963.1_2436	0.2240	2.14			0.0162	3.64	ribose ABC transporter, permease protein	rbsC
NZ_JXUN01000192.1_cds_WP_012907964.1_2435	0.2093	0.64	0.1457	0.32	0.0150	2.56	ribose ABC transporter, ATP-binding protein	rbsA
NZ_JXUN01000192.1_cds_WP_012907965.1_2434	0.4709	0.24	0.0589	1.19	0.0196	1.56	putative ribose transport/metabolism protein	rbsD
NZ_JXUN01000192.1_cds_WP_012907966.1_2433	0.1162	0.89	0.0751	0.41	0.0118	2.03	low affinity potassium transport system protein	kup
NZ_JXUN01000192.1_cds_WP_012907971.1_2429	0.0038	1.65	0.0242	1.17	0.1436	1.60	regulatory protein	asnC
NZ_JXUN01000192.1_cds_WP_012907982.1_2415	0.0408	-1.29	0.1065	-0.77	0.2144	-2.80	glucosaminefructose-6-phosphate	glmS
NZ JXUN01000192.1 cds WP 042623224.1 2439		-0.70	0.0138	3.03	0.0178	3.43	aminotransferase ribose operon repressor	rbsR
NZ JXUN01000193.1 cds WP 012906570.1 2463		-0.67			0.0040	3.50	sulphate ABC transporter, ATP-binding protein OR	cysA, cysW
		***/				2.50	sulphate ABC transporter, permease protein	-y===y==11
NZ_JXUN01000193.1_cds_WP_012906572.1_2465	0.4534	0.93			0.0072	1.61	sulphate ABC transporter, permease protein	cysU

NZ IVIDI01000102 1 - J- WD 0241227(0 1 24(0	0.0174	1.17	0.2557	2.20	0.2002			
NZ_JXUN01000193.1_cds_WP_024132760.1_2460	0.0174	1.17	0.3557	2.20	0.2093	2.24	putative exported protein	
NZ_JXUN01000194.1_cds_WP_012906253.1_2474	0.2043	-0.07	0.0130	1.45	0.0053	2.24	putative phosphohydrolase	
NZ_JXUN01000194.1_cds_WP_012906255.1_2476	0.0712	-1.28	0.0647	0.37	0.0018	2.07	outer membrane porin protein	
NZ_JXUN01000194.1_cds_WP_012906255.1_2476	0.0712	-1.28	0.0647	0.37	0.0018	2.07	outer membrane porin protein	
NZ_JXUN01000194.1_cds_WP_012906266.1_2488	0.1033	1.15	0.0357	2.71	0.0293	4.02	putative DNA-binding protein	
NZ_JXUN01000194.1_cds_WP_024132723.1_2469	0.1878	0.59	0.0382	1.55	0.1062	2.23	conserved hypothetical protein	
NZ_JXUN01000194.1_cds_WP_024132726.1_2485	0.0930	-2.75	0.0310	1.91	0.0327	0.92	putative membrane protein OR putative lipoprotein	
NZ_JXUN01000194.1_cds_WP_024132727.1_2486	0.1893	-1.34	0.0488	1.33	0.1872	1.84	putative membrane protein	
NZ_JXUN01000195.1_cds_WP_001536811.1_2562		-2.25			0.0372	3.80	pseudogene	
NZ_JXUN01000195.1_cds_WP_001575658.1_2557	0.0212	-1.44	0.4686	0.66	0.1600	0.20	pseudogene	
NZ_JXUN01000195.1_cds_WP_012908519.1_2493	0.0314	1.53	0.1304	-0.51	0.1407	2.53	putative organic solvent tolerance ABC-transporter, ATP-binding component	
NZ_JXUN01000195.1_cds_WP_012908520.1_2494	0.0121	2.43	0.1010	1.00			putative organic solvent tolerance protein	
NZ_JXUN01000195.1_cds_WP_012908523.1_2497	0.0174	1.85	0.1858	0.86	0.0014	3.83	putative anti-sigma factor antagonist	
NZ_JXUN01000195.1_cds_WP_012908526.1_2500	0.3935	0.69	0.0159	1.35	0.0040	1.93	sugar fermentation stimulation protein B	sfsB
NZ_JXUN01000195.1_cds_WP_012908528.1_2504	0.0300	1.29	0.2436	1.04	0.2941	0.23	putative membrane protein	
NZ_JXUN01000195.1_cds_WP_012908538.1_2514	0.2690	-0.86	0.0463	1.53	0.1369	1.60	putative Type IV pilin	cfcA
NZ_JXUN01000195.1_cds_WP_012908539.1_2515	0.1663	1.24	0.3242	-0.56		2.24	putative Type IV pilus biogenesis protein	cfcB
NZ_JXUN01000195.1_cds_WP_012908542.1_2518	0.0038	2.64	0.1208	1.92	0.0074		putative Type IV pilus biogenesis protein	cfcE
NZ_JXUN01000195.1_cds_WP_012908543.1_2519	0.1496	-0.90			0.0049	2.14	putative Type IV pilus biogenesis protein	cfcF
NZ_JXUN01000195.1_cds_WP_012908544.1_2520	0.0078	1.44	0.1282	0.91	0.1290	1.93	putative Type IV pilus biogenesis protein	cfcF, cfcG
NZ JXUN01000195.1 cds WP 012908546.1 2522	0.0591	0.80	0.2013	0.37	0.0119	3.92	putative Type IV pilus biogenesis protein CfcH	cfcH
NZ JXUN01000195.1 cds WP 012908547.1 2523		3.83	0.0122	3.53		4.03	putative Type IV pilus biogenesis protein	cfcJ
NZ_JXUN01000195.1_cds_WP_012908549.1_2525	0.3735	-0.40	0.0114	1.29	0.2991	-0.22	putative prepillin peptidase	cfcV
NZ_JXUN01000195.1_cds_WP_012908552.1_2528	0.0424	1.90	0.1587	1.67			argininosuccinate synthetase	argG
NZ JXUN01000195.1 cds WP 012908561.1 2539	0.1229	1.57	0.0365	3.86	0.1983	1.14	possible monooxygenase	
NZ JXUN01000195.1 cds WP 012908567.1 2545	0.1868	1.12			0.0069	3.97	conserved hypothetical protein	
NZ JXUN01000195.1 cds WP 012908572.1 2550	0.2485	0.47	0.0494	1.39	0.0434	2.03	naA initiator-associating factor for replication	diaA
							initiation (putative phophosugar-binding protein)	
NZ_JXUN01000195.1_cds_WP_012908579.1_2559	0.4809	0.25	0.2604	1.75	0.0389	2.04	pseudogene	
NZ_JXUN01000195.1_cds_WP_012908581.1_2561	0.0674	1.57	0.0053	2.01	0.0017		pseudogene	
NZ_JXUN01000195.1_cds_WP_012908584.1_2565	0.3576	-1.30			0.0133	1.14	pseudogene	
NZ_JXUN01000195.1_cds_WP_012908585.1_2566		1.29	0.1362	1.73	0.0170	5.62	pseudogene	
NZ JXUN01000195.1 cds WP 012908587.1 2568	0.4006	-0.17	0.1495	1.05	0.0247	2.71	pseudogene	
NZ JXUN01000195.1 cds WP 012908588.1 2569	0.4842	0.07	0.0981	1.84	0.0439	3.70	pseudogene	
NZ JXUN01000195.1 cds WP 012908591.1 2571	0.1350	-1.53	0.0650	0.70	0.0290	1.74	pseudogene	
NZ JXUN01000195.1 cds WP 024133057.1 2495	0.0344	1.74	0.2088	0.04	0.0730	0.86	putative organic solvent tolerance protein	
NZ JXUN01000195.1 cds WP 024133061.1 2517	0.0265	1.97	0.0556	0.96	0.0096	3.46	putative Type IV pilus biogenesis protein	cfcD
NZ JXUN01000195.1 cds WP 024133066.1 2538	0.1173	1.94	0.0087	2.39			tryptophan-specific transport protein	mtr
NZ JXUN01000195.1 cds WP 042623231.1 2516	0.0030	1.98	0.0858	1.42			putative Type IV pilus biogenesis protein	cfcC
NZ JXUN01000195.1 cds WP 042623232.1 2563	0.0380	1.86	0.0979	0.76	0.0050		pseudogene	
NZ JXUN01000195.1 cds WP 071820634.1 2540	0.0131	-1.72	0.2583	-0.78	0.3806	1.49	putative peptidase	
	0.0101		3.2003	0.70	3.5000	1.17	r	

NZ_JXUN01000196.1_cds_WP_012907182.1_2584		-0.08			0.0952	2.57	multifunctional stationary-phase survival protein [includes: 5'/3'-nucleotidase; exopolyphosphatase]	surE
NZ_JXUN01000196.1_cds_WP_012907189.1_2577	0.3277	0.78			0.0045	2.85	putative 4-hydroxybenzoate decarboxylase subunit	
NZ_JXUN01000196.1_cds_WP_024132862.1_2576	0.3738	-0.10	0.4884	0.59	0.0043	-1.18	putative exported protein	
NZ_JXUN01000198.1_cds_WP_012907583.1_2605		2.22	0.0202	1.87	0.0417	2.40	hypothetical protein	
NZ_JXUN01000198.1_cds_WP_012907587.1_2611	0.2140	-0.41	0.0263	-1.62	0.2323	0.38	hydrogenase 2 maturation protease	hybD
NZ_JXUN01000198.1_cds_WP_012907589.1_2613	0.2485	0.27	0.1070	1.45	0.0217	2.77	probable Ni/Fe-hydrogenase 2 b-type cytochrome	hybB
NZ JXUN01000198.1 cds WP 012907591.1 2615	0.4481	0.21	0.2041	0.16	0.0360	0.46	subunit hydrogenase-2 small chain	hyb0
NZ JXUN01000198.1 cds WP 012907592.1 2617	0.0230	1.98	0.0376	1.57	0.2882	1.02	putative aldo/keto reductase	,
NZ JXUN01000198.1 cds WP 012907593.1 2618	0.1752	0.37	0.1854	0.67	0.0414	1.46	putative membrane protein	
NZ JXUN01000198.1 cds WP 012907595.1 2620	0.0356	-1.08	0.2299	0.49	0.0898	-0.05	conserved hypothetical protein	
NZ JXUN01000198.1 cds WP 012907596.1 2621	0.4227	0.33	0.4267	0.02	0.0179	1.16	conserved hypothetical protein	
NZ_JXUN01000198.1_cds_WP_012907600.1_2625	0.3721	0.14	0.3419	0.65	0.0075	2.84	cystathionine beta-lyase	metC
NZ JXUN01000198.1 cds WP 012907601.1 2626	0.0349	1.37	0.0586	1.07	0.0682	1.67	putative membrane protein	
NZ JXUN01000198.1 cds WP 012907602.1 2628	0.4878	0.74	0.0203	2.19	0.1736	1.70	putative alcohol dehydrogenase	
NZ JXUN01000198.1 cds WP 012907615.1 2641	0.0242	2.00	0.0249	1.38	0.0064	2.13	putative glycosyl hydrolase	
NZ JXUN01000198.1 cds WP 012907616.1 2643	0.02.2	-1.64	0.0131	2.24	0.0099	2.80	conserved hypothetical protein	
NZ JXUN01000198.1 cds WP 012907625.1 2652	0.0502	-0.88	0.2981	0.24	0.0476	0.63	conserved hypothetical protein	
NZ JXUN01000198.1 cds WP 012907630.1 2658	0.4159	0.74	0.2701	0.21	0.4546	1.89	putative disulfide bond formation protein	
NZ JXUN01000198.1 cds WP 024132941.1 2661	0.4311	0.57	0.1562	1.17	0.0330	1.51	glycogen synthesis protein GlgS	glgS
NZ JXUN01000199.1 cds WP 012907541.1 2671	0.1200	0.77	0.0351	1.02	0.0073	1.59	fumarate hydratase class I, anaerobic	fumB
NZ_JXUN01000199.1_cds_WP_012907543.1_2673	0.0069	0.84	0.4118	-0.25	0.4755	1.68	two-component response regulator	dcuR
NZ_JXUN01000199.1_cds_WP_012907544.1_2674	0.3212	1.00	0.3385	0.23	0.0137	1.45	two-component response regulator	dcuR
NZ JXUN01000199.1 cds WP 012907545.1 2675	0.4037	-0.03	0.0104	1.34	0.0512	1.43	putative outer membrane protein	deare
NZ JXUN01000199.1 cds WP 012907549.1 2680	0.0328	-4.42	0.0104	1.54	0.3817	1.92	conserved hypothetical protein	
NZ_JXUN01000199.1_cds_WP_012907550.1_2681	0.3433	0.31			0.0557	4.03	putative major fimbrial subunit	
NZ JXUN01000199.1 cds WP 012907555.1 2686	0.2036	1.89			0.0181	2.92	putative findpri informatisation in putative findprial adhesin	
			0.2671	0.22			•	
NZ_JXUN01000199.1_cds_WP_012907558.1_2689	0.0183 0.0110	-2.40	0.2671	0.23 0.44	0.1909	-2.63	hypothetical protein	
NZ_JXUN01000199.1_cds_WP_012907569.1_2700	0.0110	1.56 1.73	0.1012	1.28	0.0138	3.11 1.91	hypothetical protein	D
NZ_JXUN01000199.1_cds_WP_024132926.1_2668			0.0374	1.28	0.0468	1.91	two-component sensor kinase	pmrB
NZ_JXUN01000199.1_cds_WP_024132928.1_2697	0.3137	-1.29	0.1200	0.54	0.0401		hypothetical protein	
NZ_JXUN01000199.1_cds_WP_042623243.1_2701	0.2918	-0.24	0.1390	0.54	0.0298	1.33	hypothetical protein	C
NZ_JXUN01000199.1_cds_WP_071820661.1_2695	0.0133	1.92	0.0569	3.58			cation efflux system protein	cusC
NZ_JXUN01000200.1_cds_WP_001216673.1_2743	0.0277	1.35	0.1922	1.80	0.0948	-2.20	30S ribosomal subunit protein S6	rpsF
NZ_JXUN01000200.1_cds_WP_012907321.1_2768	0.0611	0.93	0.1064	0.65	0.0078	1.22	DNA mismatch repair protein	mutL
NZ_JXUN01000200.1_cds_WP_012907334.1_2755	0.4715	0.12	0.0355	1.06	0.0470	4.51	putative lipoprotein	
NZ_JXUN01000200.1_cds_WP_012907339.1_2750	0.0276	1.33	0.0728	1.48			ascorbate-specific PTS system EIIB component	ulaB
NZ_JXUN01000200.1_cds_WP_012907344.1_2745	0.1246	1.73	0.0107	3.17	0.0103	3.79	putative exported protein	
NZ_JXUN01000200.1_cds_WP_012907352.1_2735	0.1531	0.92	0.1348	1.54	0.0026	2.85	regulator of cell morphogenesis and NO signaling	ytfE
NZ_JXUN01000200.1_cds_WP_012907353.1_2734	0.1603	-0.55	0.1828	0.26	0.0048	1.66	methyl-accepting chemotaxis protein	tsr
NZ_JXUN01000200.1_cds_WP_012907355.1_2732	0.2015	1.78			0.3914	2.14	conserved hypothetical protein	

NZ_JXUN01000200.1_cds_WP_012907360.1_2727	0.0391	-1.66	0.3151	0.47	0.0834	0.29	conserved hypothetical protein	
NZ_JXUN01000200.1_cds_WP_012907362.1_2725	0.3504	-1.59			0.0412	3.52	L-ribulose-5-phosphate 3-epimerase (L-ascorbate utilization protein E)	ulaE
NZ_JXUN01000200.1_cds_WP_012907365.1_2721		2.92	0.0590	2.80	0.0522	3.31	putative oxidoreductase	
NZ_JXUN01000200.1_cds_WP_012907368.1_2718	0.0380	1.44	0.4692	0.23	0.0684	0.57	putative outer membrane protein assembly factor	
NZ_JXUN01000200.1_cds_WP_012907374.1_2712	0.1088	-1.12	0.0125	0.95	0.4056	-0.15	ABC transporter, substrate-binding protein	
NZ_JXUN01000200.1_cds_WP_012907375.1_2711	0.2801	1.90	0.0306	3.99	0.0916	3.40	ABC transporter, ATP-binding protein	
NZ_JXUN01000200.1_cds_WP_024132885.1_2756	0.0052	-2.04	0.4088	-0.66	0.0199		putative exported protein	
NZ_JXUN01000200.1_cds_WP_024132886.1_2744	0.0065	0.78	0.0474	1.15	0.2661	0.59	hypothetical protein	
NZ_JXUN01000200.1_cds_WP_071820603.1_2731	0.3724	-1.13	0.0079	1.71	0.0507	1.10	conserved hypothetical protein	
NZ_JXUN01000201.1_cds_WP_000207438.1_2791	0.1219	7.25	0.2216	1.77	0.0196	3.88	pseudogene	
NZ_JXUN01000201.1_cds_WP_000342741.1_2778		-0.33	0.0238	1.66	0.1370	1.20	pseudogene, disrupted by prophage CRP49 insertion	
NZ_JXUN01000201.1_cds_WP_000360581.1_2781	0.2464	1.14	0.0348	1.37	0.0062	2.20	pseudogene, disrupted by prophage CRP49 insertion	
NZ_JXUN01000201.1_cds_WP_001146843.1_2800			0.2964	0.36			pseudogene	
NZ_JXUN01000201.1_cds_WP_001279080.1_2780		0.25			0.0268	5.11	pseudogene	
NZ_JXUN01000201.1_cds_WP_012908594.1_2775	0.2051	1.11	0.1422	1.43	0.0393	2.86	pseudogene, disrupted by prophage CRP49 insertion	
NZ_JXUN01000201.1_cds_WP_012908596.1_2779					0.0045	3.49	pseudogene	
NZ_JXUN01000201.1_cds_WP_012908596.1_2779					0.0045	3.49	pseudogene	
NZ_JXUN01000201.1_cds_WP_012908610.1_2796		-0.12			0.0043	2.33	pseudogene	
NZ_JXUN01000201.1_cds_WP_012908611.1_2797	0.0138	2.19			0.0127	3.19	pseudogene	
NZ_JXUN01000201.1_cds_WP_012908613.1_2799		2.99	0.0650	2.03	0.0162	3.91	pseudogene, disrupted by prophage CRP49 insertion	
NZ_JXUN01000201.1_cds_WP_012908616.1_2804	0.0731	-1.61	0.1595	1.12	0.0149	1.50	pseudogene	
NZ_JXUN01000201.1_cds_WP_024133069.1_2776	0.4579	0.10			0.0423	3.66	pseudogene	
NZ_JXUN01000201.1_cds_WP_024133070.1_2777	0.3536	0.54	0.0501	1.47	0.0443	2.65	pseudogene, disrupted by prophage CRP49 insertion	
NZ_JXUN01000201.1_cds_WP_042623249.1_2788			0.4061	-0.12	0.0178	3.37	pseudogene	
NZ_JXUN01000201.1_cds_WP_072044772.1_2803	0.1489	0.80	0.0677	3.05	0.0015	5.54	pseudogene	
NZ_JXUN01000204.1_cds_WP_012906500.1_2834	0.0022	-1.97			0.3697	1.95	putative sugar-phosphate dehydrogenase	
NZ_JXUN01000204.1_cds_WP_012906502.1_2832	0.0034	1.62	0.0509	1.52	0.1577	1.20	putative membrane protein	
NZ_JXUN01000204.1_cds_WP_012906506.1_2827	0.2546	0.12			0.1608	2.32	ABC transporter, permease protein	
NZ_JXUN01000204.1_cds_WP_012906511.1_2821	0.3353	0.78	0.2063	0.81	0.0144	2.19	ribosomal small subunit pseudouridine synthase A	rsuA
NZ_JXUN01000205.1_cds_WP_000105979.1_2877	0.0041	-2.81	0.0991	-1.21	0.0979	-0.92	pCROD2 plasmid	pCROD2
NZ_JXUN01000205.1_cds_WP_000190053.1_2851	0.0424	-1.51	0.1147	-0.66	0.1988	-0.10	pCROD2 plasmid	pCROD2
NZ_JXUN01000205.1_cds_WP_000520549.1_2868	0.0055	-1.96	0.3606	-0.75	0.0749	0.21	pCROD2 plasmid	pCROD2
NZ_JXUN01000205.1_cds_WP_000539545.1_2872	0.0344	-2.51	0.1278	-0.21	0.2795	0.29	pCROD2 plasmid	pCROD2
NZ_JXUN01000205.1_cds_WP_000681613.1_2869	0.0156	-2.77	0.2327	-0.79	0.0875	0.27	pCROD2 plasmid	pCROD2
NZ_JXUN01000205.1_cds_WP_000781818.1_2871	0.0437	-2.19	0.1066	-0.24	0.1156	-0.11	pCROD2 plasmid	pCROD2
NZ_JXUN01000205.1_cds_WP_000854261.1_2867	0.0001	-1.84	0.1742	-0.85	0.4484	0.26	pCROD2 plasmid	pCROD2
NZ_JXUN01000205.1_cds_WP_001293133.1_2846	0.0462	-3.83	0.3428	-0.24	0.2097	-0.59	pCROD2 plasmid	pCROD2
NZ_JXUN01000205.1_cds_WP_001328550.1_2870	0.0497	-3.58	0.2554	-0.96	0.1500	-0.06	pCROD2 plasmid	pCROD2
NZ_JXUN01000205.1_cds_WP_001328551.1_2876	0.0024	-2.92	0.0471	-1.20	0.0582	-1.29	pCROD2 plasmid	pCROD2
NZ_JXUN01000205.1_cds_WP_001407769.1_2866	0.0061	-2.10	0.1217	-0.74	0.4800	0.10	pCROD2 plasmid	pCROD2
NZ_JXUN01000205.1_cds_WP_004239671.1_2847	0.0454	-3.42	0.1889	-0.56	0.1197	-0.83	pCROD2 plasmid	pCROD2

NZ_JXUN01000205.1_cds_WP_012908953.1_2852	0.0236	-2.37	0.2281	-0.38	0.0415	-1.10	pCROD2 plasmid	pCROD2
NZ_JXUN01000205.1_cds_WP_012908959.1_2875	0.0034	-3.10	0.0070	-1.18	0.0197	-1.61	pCROD2 plasmid	pCROD2
NZ_JXUN01000206.1_cds_WP_012905871.1_2882		-0.23	0.3482	-0.52	0.0277	1.24	LysR-family transcriptional regulator	
NZ_JXUN01000206.1_cds_WP_012905872.1_2883	0.0893	1.60			0.0592	2.25	methyl-accepting chemotaxis protein III (ribose an galactose chemoreceptor protein)	trg
NZ_JXUN01000206.1_cds_WP_012905873.1_2884	0.0028	3.66	0.1581	1.10	0.0101	1.60	alcohol dehydrogenase class-III	adhC
NZ_JXUN01000206.1_cds_WP_012905887.1_2899	0.2448	-0.94	0.3842	-0.40	0.0318	2.19	putative acyltransferase	
NZ_JXUN01000206.1_cds_WP_012905888.1_2900	0.0541	0.62	0.3470	-0.35	0.0381	1.25	putative phosphatidate cytidylyltransferase	
NZ_JXUN01000206.1_cds_WP_012905889.1_2901	0.0619	-0.82	0.3189	-0.04	0.0086	2.24	putative CDP-alcohol phosphatidyltransferase	
NZ_JXUN01000206.1_cds_WP_042623257.1_2895	0.3983	0.59	0.2977	0.14	0.0036	3.60	Conserved hypothetical protein	
NZ_JXUN01000207.1_cds_WP_012907643.1_2912	0.4589	0.18	0.4399	0.64	0.0485	1.38	dihydroneopterin aldolase	
NZ_JXUN01000207.1_cds_WP_012907644.1_2913	0.0068	1.03	0.0049	2.12	0.0789	1.80	putative membrane protein	
NZ_JXUN01000207.1_cds_WP_012907645.1_2914	0.0145	-1.67	0.2140	0.77	0.3299	-1.17	LysR-family transcriptional regulator	ttdR
NZ_JXUN01000209.1_cds_WP_012906891.1_2980	0.3531	1.39	0.1313	1.88	0.0228	1.95	putative membrane protein	
NZ_JXUN01000209.1_cds_WP_012906892.1_2979	0.1237	-1.05	0.1400	-1.10	0.0056	1.46	tRNA pseudouridine synthase A	truA
NZ_JXUN01000209.1_cds_WP_012906893.1_2978	0.3321	1.62	0.1986	2.25	0.0468	5.66	putative semialdehyde dehydrogenase	usg
NZ_JXUN01000209.1_cds_WP_012906907.1_2964	0.0668	-1.75			0.0397	1.66	fatty acid oxidation complex alpha subunit [includes: enoyl-CoA hydratase; 3-hydroxyacyl- CoA dehydrogenase; 3-hydroxybutyryl-CoA epimerase]	fadJ
NZ_JXUN01000209.1_cds_WP_012906908.1_2963		0.13	0.0744	1.70	0.0088	4.26	fatty acid oxidation comple beta subunit (3-ketoacyl-CoA thiolase)	fadI
NZ_JXUN01000209.1_cds_WP_012906915.1_2956	0.4902	-0.10	0.1034	1.67	0.0180	1.16	conserved hypothetical protein	
NZ_JXUN01000209.1_cds_WP_012906925.1_2948	0.1270	1.88	0.0110	3.17	0.0135	5.29	putative outer membrane autotransporter	
NZ_JXUN01000209.1_cds_WP_012906926.1_2947		1.37			0.0141	3.72	T6SS lysozyme-related protein Cts1D	cts1D
NZ_JXUN01000209.1_cds_WP_012906929.1_2943	0.0342	2.83	0.0236	3.02	0.0108	3.74	VgrG family T6SS protein Cts1G	ctslG
NZ_JXUN01000209.1_cds_WP_012906931.1_2940		-0.79	0.3435	-0.57	0.0159		T6SS protein Cts1U	cts1U
NZ_JXUN01000209.1_cds_WP_012906940.1_2931	0.4060	0.36			0.0084	1.09	Putative fimbrial subunit	
NZ_JXUN01000209.1_cds_WP_012906947.1_2924		3.82			0.0249	4.61	T6SS protein Cts1O	cts10
NZ_JXUN01000209.1_cds_WP_012906949.1_2922	0.0231	1.79	0.0839	0.68			putative ATP-binding protein of ABC transporter	
NZ_JXUN01000209.1_cds_WP_024132814.1_2960	0.4410	-0.29	0.0076	0.71	0.0102	1.11	long-chain fatty acid transport protein	fadL
NZ_JXUN01000209.1_cds_WP_024132815.1_2958	0.1851	0.07	0.1005	1.02	0.0024	2.14	putative membrane protein	
NZ_JXUN01000209.1_cds_WP_024132815.1_2958	0.1851	0.07	0.1005	1.02	0.0024	2.14	putative membrane protein	
NZ_JXUN01000209.1_cds_WP_024132817.1_2944	0.0203	-1.77	0.2643	0.80	0.2062	2.22	VgrG family T6SS protein Cts1G OR T6SS protein Cts1F	cts1G, cts1F
NZ_JXUN01000209.1_cds_WP_024132819.1_2933	0.2441	2.18	0.1498	1.29	0.0042	1.59	fimbrial usher protein	
NZ_JXUN01000210.1_cds_WP_012905395.1_2996	0.1047	2.59	0.0067	3.19	0.0047	2.49	putative membrane protein	
NZ_JXUN01000210.1_cds_WP_012905400.1_3001		2.01	0.0015	2.47			minor curlin subunit	csgB
NZ_JXUN01000210.1_cds_WP_012905401.1_3002	0.0719	0.85	0.0777	0.70	0.0129		major curlin subunit	csgA
NZ_JXUN01000210.1_cds_WP_012905402.1_3003	0.2483	1.06	0.1718	1.26	0.0451	2.70	putative curli production protein esge precursor	csgC
NZ_JXUN01000210.1_cds_WP_012905403.1_3004	0.2501	2.50	0.2907	1.20	0.0040	4.01	Putative exported protein	
NZ_JXUN01000210.1_cds_WP_012905405.1_3006		0.15	0.1460	2.01	0.0113	2.22	putative phospholipase	
NZ_JXUN01000210.1_cds_WP_012905410.1_3012	0.0476	-1.11	0.1431	0.54	0.0970	0.93	acidic protein	msyB
NZ_JXUN01000210.1_cds_WP_012905412.1_3014	0.0542	0.54	0.0445	1.08	0.0722	1.05	lipid A biosynthesis lauroyl acyltransferase	htrB

NZ_JXUN01000210.1_cds_WP_012905414.1_3016	0.0617	1.29	0.0200	1.21	0.0853	-0.17	putative exported protein	
NZ_JXUN01000210.1_cds_WP_012905420.1_3021	0.0405	1.35	0.1155	1.07	0.3696	-1.55	damage-inducible protein	dinI
NZ_JXUN01000210.1_cds_WP_024132601.1_2991	0.0066	1.40	0.0702	1.38	0.0172	3.27	conserved hypothetical protein	
NZ_JXUN01000210.1_cds_WP_071820575.1_3029	0.3797	-0.44	0.1561	2.10	0.0053	2.32	putative outer membrane protein	
NZ_JXUN01000211.1_cds_WP_012905577.1_3091	0.4592	-0.32	0.3626	-0.65	0.0164	2.82	putative membrane protein	
NZ_JXUN01000211.1_cds_WP_012905578.1_3090	0.3473	0.18	0.1827	0.44	0.0383	2.55	exodeoxyribonuclease III	xthA
NZ_JXUN01000211.1_cds_WP_012905582.1_3086							N-succinylglutamate 5-semialdehyde	astD
NZ JXUN01000211.1 cds WP 012905588.1 3080	0.0402	-3.37	0.2551	0.79	0.0517		dehydrogenase osmotically inducible lipoprotein E	osmE
NZ JXUN01000211.1 cds WP 012905603.1 3065	0.0402	1.28	0.0556	1.95	0.0266	1.45	Conserved hypothetical protein	OSHIL
NZ JXUN01000211.1 cds WP 012905606.1 3062	0.4169	-0.83	0.00350	1.61	0.0260	0.96	putative exported protein	
NZ JXUN01000211.1 cds WP 012905931.1 3032	0.4109	0.82	0.0043	2.25	0.0301	1.70	hypothetical protein	
NZ JXUN01000211.1 cds WP 012905932.1 3033	0.0923	0.82	0.0096	0.70	0.0217	1.51	putative membrane protein	
NZ JXUN01000211.1 cds WP 012905935.1 3036	0.4704	0.39	0.1193	-0.03	0.0397	2.45	outer membrane protein G precursor	ompG
NZ_JXUN01000211.1_cds_WP_012905936.1_3038	0.4704	0.39	0.2019	-0.03	0.0197	2.43	putative beta-phosphoglucomutase OR putative	yejU
NZ_JX0N01000211.1_cds_W1_012703730.1_3036		0.43			0.0004		glycosyl hydrolase	yejo
NZ_JXUN01000211.1_cds_WP_012905940.1_3042	0.3046	2.23	0.1586	2.74			putative oxidoreductase	
NZ_JXUN01000211.1_cds_WP_012905942.1_3044	0.1213	1.78	0.3609	-0.59	0.0206	3.70	putative ABC transporter membrane protein	
NZ_JXUN01000211.1_cds_WP_012905944.1_3046		-2.22			0.0355	3.13	putative sucrose phosphorylase (ec 2.4.1.7) (sucrose	
NZ JXUN01000211.1 cds WP 012905946.1 3048	0.0022	3.54	0.0544	1.53	0.0684	1.18	glucosyltransferase) phage shock protein C	nenC
NZ JXUN01000211.1 cds WP 012905947.1 3049	0.0022	3.18	0.0344	0.87	0.4324	0.34	phage shock protein B	pspC pspB
NZ_JXUN01000211.1_cds_WP_012905948.1_3049 NZ_JXUN01000211.1_cds_WP_012905948.1_3050	0.0216	4.49	0.3384	1.78	0.4324	1.62	phage shock protein A	
NZ JXUN01000211.1 cds WP 012905949.1 3051	0.0028	1.09	0.0490	0.66	0.1121	1.63	Psp operon transcriptional activator	pspA pspF
NZ JXUN01000211.1 cds WP 024132632.1 3089	0.0430	-0.25	0.1192	0.00	0.1381	5.42	hypothetical protein	pspr
	0.0097	2.50	0.1393	0.70	0.0372	3.42	**	nanD
NZ_JXUN01000211.1_cds_WP_024132684.1_3047					0.0202	4.55	phage shock protein D	pspD
NZ_JXUN01000211.1_cds_WP_042623273.1_3093	0.1548	2.18	0.0036	2.35	0.0202	4.55	putative membrane protein	
NZ_JXUN01000212.1_cds_WP_012906147.1_3113	0.0518	0.65	0.1423	1.22 -0.41	0.0131	1.92	conserved hypothetical protein	
NZ_JXUN01000212.1_cds_WP_012906148.1_3112	0.0754	2.04	0.3141	-0.41	0.0147	2.71	conserved hypothetical protein	
NZ_JXUN01000212.1_cds_WP_012906149.1_3111	0.3061	-0.52	0.1500	0.02	0.1172	3.72	copper homeostasis protein	cutC
NZ_JXUN01000212.1_cds_WP_012906150.1_3110	0.0067	0.69	0.1599	0.93	0.3821	1.13	conserved hypothetical protein	
NZ_JXUN01000212.1_cds_WP_012906152.1_3108	0.0267	1.23			0.1453	2.40	conserved hypothetical protein	au 15
NZ_JXUN01000212.1_cds_WP_012906156.1_3104	0.0611	-0.61	0.3133	0.62	0.0475	2.86	flagellar biosynthesis protein FlhB	flhB
NZ_JXUN01000212.1_cds_WP_024132711.1_3120	0.1352	0.39	0.3571	0.20	0.0442	0.71	putative isochorismatase	
NZ_JXUN01000212.1_cds_WP_042623279.1_3118	0.0256	2.43	0.1357	1.18	0.0069	0.93	putative T3SS effector protein EspV	espV
NZ_JXUN01000213.1_cds_WP_012905841.1_3130	0.1771	1.01	0.1017	2.18	0.0469	2.29	putative outer membrane protein	
NZ_JXUN01000214.1_cds_WP_042623282.1_3131	0.0142	2.40	0.0119	2.65	0.0167	2.31	Conserved hypothetical protein	
NZ_JXUN01000215.1_cds_WP_000051841.1_3144	0.2811	0.41	0.1555	1.64			putative membrane protein	aaeX
NZ_JXUN01000215.1_cds_WP_012908473.1_3145	0.4741	0.09	0.0477	0.74	0.1434		LysR-family transcriptional regulator	aaeR
NZ_JXUN01000215.1_cds_WP_012908477.1_3141	0.0825	1.26	0.0760	1.13	0.0347	3.38	succinate-semialdehyde dehydrogenase [NADP+]	gabD
NZ_JXUN01000215.1_cds_WP_012908477.1_3141	0.0825	1.26	0.0760	1.13	0.0347	3.38	succinate-semialdehyde dehydrogenase [NADP+]	gabD
NZ_JXUN01000215.1_cds_WP_042623285.1_3147	0.4217	-0.05	0.0077	0.96	0.0065	1.68	possible exported protein	
NZ_JXUN01000216.1_cds_WP_012908462.1_3157	0.0232	1.20	0.3240	0.23	0.4335	-0.99	biotin carboxylase (acetyl-CoA carboxylase subunit	accC
							A)	

NZ_JXUN01000216.1_cds_WP_012908463.1_3154	0.2357	1.12	0.1224	0.80	0.0187	2.68	putative membrane protein	
NZ_JXUN01000216.1_cds_WP_012908464.1_3153	0.2780	2.12	0.4353	-0.18	0.0375	1.75	putative oxidoreductase	
NZ_JXUN01000216.1_cds_WP_012908466.1_3151	0.3619	0.67	0.0659	0.65	0.0353	0.68	putative signal transduction protein	
NZ_JXUN01000216.1_cds_WP_024133049.1_3150	0.0642	0.76	0.0312	1.32	0.0300	1.23	rod shape-determining protein OR putative signal transduction protein	mreB
NZ_JXUN01000217.1_cds_WP_012905512.1_3160	0.0042	1.16	0.0167	1.08	0.1479	0.56	SOS mutagenesis and repair protein	umuD
NZ_JXUN01000217.1_cds_WP_012905514.1_3162	0.2684	-1.03			0.0385	2.11	putative sugar aldolase	
NZ_JXUN01000217.1_cds_WP_012905515.1_3163					0.1099	2.06	conserved hypothetical protein	
NZ_JXUN01000217.1_cds_WP_012905517.1_3165	0.1009	2.12	0.1431	1.79	0.0147	3.11	conserved hypothetical protein	
NZ_JXUN01000217.1_cds_WP_012905518.1_3166	0.4954	-0.33	0.1582	1.57	0.0371	2.78	hypothetical protein	
NZ_JXUN01000217.1_cds_WP_042623289.1_3169		-1.89	0.1302	0.64	0.0064	2.76	putative aconitate hydratase	
NZ_JXUN01000218.1_cds_WP_012907311.1_3176	0.0205	3.39			0.0181	3.44	putative permease	
NZ_JXUN01000218.1_cds_WP_012907313.1_3174	0.1700	1.49	0.2706	1.03	0.0106	2.72	phosphatidylserine decarboxylase proenzyme	psd
NZ_JXUN01000218.1_cds_WP_012907317.1_3170	0.4274	0.18	0.0809	0.28	0.0021	2.10	putative 4Fe-4S binding protein	
NZ_JXUN01000219.1_cds_WP_012905492.1_3184	0.4983	-0.29	0.0357	0.94	0.0871	0.97	spermidine/putrescine ABC transporter,ATP- binding protein	potA
NZ_JXUN01000220.1_cds_WP_012905655.1_3199	0.3861	0.33	0.1784	1.99			conserved hypothetical protein	
NZ_JXUN01000220.1_cds_WP_012905658.1_3202		-0.03	0.1021	1.02	0.0001	2.08	putative membrane protein	
NZ_JXUN01000220.1_cds_WP_012905660.1_3204					0.0571	4.20	LysR-family transcriptional regulator	
NZ_JXUN01000221.1_cds_WP_071820584.1_3208	0.2384	1.26	0.0524	1.62			nitrite extrusion protein	narK
NZ_JXUN01000222.1_cds_WP_012907869.1_3218	0.1692	0.26	0.1982	0.58	0.0365	1.43	putative membrane protein	
NZ_JXUN01000222.1_cds_WP_012907872.1_3221	0.4349	-0.26	0.0911	1.71	0.0241	1.90	nitrogen regulation protein NR(II) (two-component system sensor kinase)	glnL
NZ_JXUN01000222.1_cds_WP_012907878.1_3228	0.0328	0.93	0.0268	1.08	0.0212	0.91	putative acyltransferase	
NZ_JXUN01000222.1_cds_WP_024132974.1_3216	0.4351	0.03	0.0666	1.93	0.0438	2.70	putative glycosyl hydrolase	
NZ_JXUN01000223.1_cds_WP_012906090.1_3245	0.0160	-1.50	0.4040	0.31	0.1249	0.72	putative transport protein	
NZ_JXUN01000223.1_cds_WP_012906091.1_3247	0.0084	-1.52	0.4406	-0.51	0.0397	0.68	mannose-specific PTS system EIIAB component	manX
NZ_JXUN01000223.1_cds_WP_012906094.1_3250	0.0012	-3.50	0.2147	-0.76	0.4335	1.32	putative membrane protein	
NZ_JXUN01000223.1_cds_WP_012906095.1_3252	0.2616	1.02			0.1481	3.38	putative outer membrane protein	
NZ_JXUN01000223.1_cds_WP_012906096.1_3253	0.1719	0.25			0.0376	2.32	ribosomal RNA large subunit methyltransferase A	rrmA
NZ_JXUN01000223.1_cds_WP_012906105.1_3263	0.0227	-0.93	0.4470	0.33	0.0437	1.16	probable protease (heat shock protein)	htpX
NZ_JXUN01000223.1_cds_WP_012906111.1_3269	0.0003	0.64	0.0265	2.13	0.1070	3.32	Conserved hypothetical protein	
NZ_JXUN01000223.1_cds_WP_012906112.1_3270	0.0306	-2.58	0.2612	0.32	0.1681	-1.09	Conserved hypothetical protein	
NZ_JXUN01000223.1_cds_WP_012906113.1_3271	0.4102	0.55	0.0795	0.96	0.0463	2.00	Conserved hypothetical protein	
NZ_JXUN01000223.1_cds_WP_012906116.1_3274	0.2255	0.25	0.0301	1.27	0.2239	-1.05	unknown	
NZ_JXUN01000223.1_cds_WP_012906120.1_3278	0.2596	0.13	0.0090	1.36	0.0977	1.19	protease II	ptrB
NZ_JXUN01000223.1_cds_WP_012906121.1_3279	0.1700	-1.92			0.0194	1.90	putative membrane protein	
NZ_JXUN01000223.1_cds_WP_012906126.1_3284	0.1170	0.53	0.0085	1.84	0.0023	2.45	phosphogluconate dehydratase	edd
NZ_JXUN01000223.1_cds_WP_012906128.1_3286	0.3065	-0.56	0.0457	0.94	0.0520	0.52	putative hex-regulon repressor (RpiR-family transcriptional regulator)	hexR
NZ_JXUN01000223.1_cds_WP_024132702.1_3246	0.0043	-1.76	0.3941	0.18	0.0856	1.04	mannose-specific PTS system EIIAB component	manX
NZ_JXUN01000223.1_cds_WP_024132707.1_3276	0.0086	-2.57	0.1750	0.07	0.0558	1.65	putative carbon-nitrogen hydrolase	
NZ_JXUN01000223.1_cds_WP_024132708.1_3281	0.0374	1.26	0.3853	-0.24	0.3151	-1.19	conserved hypothetical protein	
NZ_JXUN01000224.1_cds_WP_024132825.1_3291	0.2794	1.00	0.0409	2.38	0.1934	-0.09	hypothetical protein	

NZ_JXUN01000225.1_cds_WP_042623302.1_3296	0.2076	-1.13	0.1586	0.92	0.0487	3.05	fumarate reductase subunit C	frdC
NZ_JXUN01000226.1_cds_WP_012907452.1_3335			0.0627	1.21	0.0128	2.95	putative iron-sulfur binding protein	
NZ_JXUN01000226.1_cds_WP_012907456.1_3330	0.3502	0.33	0.0372	2.36	0.0164	1.21	putative oxidoreductase	
NZ_JXUN01000226.1_cds_WP_012907459.1_3327		-0.88			0.1390	2.54	pyridine nucleotide-disulfide oxidoreductase	
NZ_JXUN01000226.1_cds_WP_012907462.1_3325	0.2047	0.53	0.3291	-0.90	0.0057		carbamate kinase	arcC
NZ_JXUN01000226.1_cds_WP_012907464.1_3323	0.1481	0.93			0.0059	3.91	putative peptidase	
NZ_JXUN01000226.1_cds_WP_012907468.1_3319	0.4566	0.32	0.1322	0.63	0.0156		putative DNA methyltransferase	
NZ_JXUN01000226.1_cds_WP_012907469.1_3318	0.0737	-1.79	0.2967	0.77	0.0085	3.59	putative DNA methyltransferase	
NZ_JXUN01000226.1_cds_WP_012907471.1_3316	0.4191	-0.63	0.1993	-0.25	0.0220	2.78	conserved hypothetical protein	
NZ_JXUN01000226.1_cds_WP_012907473.1_3314	0.3270	-0.60	0.0393	2.59	0.0257	2.46	conserved hypothetical protein	
NZ_JXUN01000226.1_cds_WP_012907474.1_3313	0.4214	-0.09	0.1208	1.91	0.0172	2.87	T6SS protein Cts2A	cts2A
NZ_JXUN01000226.1_cds_WP_012907478.1_3308	0.1936	1.27	0.1196	2.42	0.0222	2.80	T6SS protein Cts2S	cts2S
NZ_JXUN01000226.1_cds_WP_012907481.1_3305	0.2382	0.50	0.3006	0.23	0.0021	2.55	T6SS protein Cts2D	cts2D
NZ_JXUN01000226.1_cds_WP_012907485.1_3301	0.2735	-0.21	0.0378	0.92	0.4865	-0.31	VgrG family T6SS protein Cts2G	cts2G
NZ_JXUN01000226.1_cds_WP_024132908.1_3332	0.2112	1.99			0.0253	3.67	formate dehydrogenase H (FDH-H)	fdhF
NZ_JXUN01000226.1_cds_WP_042623304.1_3315	0.0162	2.51	0.0740	1.35	0.0377	1.64	putative heat shock protein	
NZ_JXUN01000227.1_cds_WP_012906486.1_3345	0.1677	1.06	0.0567	1.39	0.0019	3.76	putative outer membrane protein	
NZ_JXUN01000227.1_cds_WP_012906489.1_3348	0.1291	1.77	0.0539	2.09	0.0240	2.51	putative pyrimidine kinase	
NZ_JXUN01000228.1_cds_WP_012907732.1_3364	0.0398	-0.50	0.0762	0.67	0.0041	1.84	acetate operon repressor	iclR
NZ_JXUN01000228.1_cds_WP_012907734.1_3362	0.1615	6.19	0.0348	2.19	0.0901	5.46	isocitrate dehydrogenase kinase/phosphatase	aceK
NZ_JXUN01000228.1_cds_WP_012907736.1_3360	0.2273	-1.05	0.1241	1.99	0.0463	1.66	malate synthase A	aceB
NZ_JXUN01000228.1_cds_WP_012907737.1_3359	0.0936	0.96	0.0167	1.29	0.0061	2.07	homoserine O-succinyltransferase	metA
NZ_JXUN01000229.1_cds_WP_012906162.1_3369	0.1743	0.60	0.1291	1.53	0.0247	1.59	methyl-accepting chemotaxis protein II (aspartate chemoreceptor protein)	tar
NZ_JXUN01000229.1_cds_WP_012906167.1_3374	0.4939	-0.31	0.0351	1.68	0.0547	2.36	putative fimbrial subunit	
NZ_JXUN01000229.1_cds_WP_012906169.1_3376	0.1148	1.55	0.0180	1.90	0.0263	2.16	chemotaxis protein	cheW
NZ_JXUN01000229.1_cds_WP_012906172.1_3379	0.2127	7.92	0.0993	1.99	0.0079	2.63	chemotaxis protein MotA (motility protein A)	motA
NZ_JXUN01000229.1_cds_WP_012906179.1_3385	0.0386	2.34	0.1154	1.76	0.0114	3.77	L-arabinose ABC transporter, permease protein	araH
NZ_JXUN01000229.1_cds_WP_012906180.1_3387	0.2309	0.70			0.0001	3.20	L-arabinose ABC transporter, substrate-binding	araF
NZ_JXUN01000229.1_cds_WP_012906181.1_3388	0.4516	0.81			0.0483	3.61	protein conserved hypothetical protein	
NZ_JXUN01000229.1_cds_WP_012906182.1_3389	0.4398	0.10	0.0146	1.47	0.0595	1.47	ferritin-like protein 2	ftnB
NZ_JXUN01000229.1_cds_WP_012906186.1_3393		1.38			0.0277	2.61	putative exported protein	
NZ_JXUN01000229.1_cds_WP_024132715.1_3398	0.3338	-0.91	0.1912	0.87	0.0052	0.78	enhancing lycopene biosynthesis protein 1	elbA
NZ_JXUN01000229.1_cds_WP_042623312.1_3366	0.3430	0.15	0.0232	1.71	0.0095	2.59	chemotaxis protein CheY	cheY
NZ_JXUN01000230.1_cds_WP_012906158.1_3406	0.1407	-2.12	0.1152	-0.76	0.0092	2.95	chemotaxis protein CheZ	cheZ
NZ_JXUN01000231.1_cds_WP_012905984.1_3417	0.2146	2.33	0.0199	1.56	0.1107	0.84	tryptophan biosynthesis protein	trpC
NZ_JXUN01000231.1_cds_WP_012905987.1_3414	0.4907	0.07	0.2501	3.26			hypothetical protein	
NZ_JXUN01000231.1_cds_WP_012905989.1_3412		-1.61	0.0640	1.01	0.0114	1.45	conserved hypothetical protein	
NZ_JXUN01000231.1_cds_WP_012905989.1_3412		-1.61	0.0640	1.01	0.0114	1.45	conserved hypothetical protein	
NZ_JXUN01000231.1_cds_WP_012905991.1_3410	0.2152	-0.65	0.0107	1.39	0.0336		putative catalase	
NZ_JXUN01000231.1_cds_WP_012905992.1_3409	0.4665	-0.15	0.2465	1.66	0.0362	2.07	outer membrane protein W	ompW
NZ_JXUN01000231.1_cds_WP_024132689.1_3413	0.0294	-2.79	0.1687	0.32	0.0954		conserved hypothetical protein	-

NZ_JXUN01000232.1_cds_WP_012905038.1_3423	0.0358	1.56	0.3725	0.87	0.1976	0.63	putative oligopeptide transporter	
NZ_JXUN01000232.1_cds_WP_012905043.1_3428	0.0296	1.64	0.0230	1.58	0.0259	3.61	putative membrane protein	
NZ_JXUN01000232.1_cds_WP_042623317.1_3421	0.0532	0.64			0.0100	2.60	deoxyribodipyrimidine photolyase	phrB
NZ_JXUN01000233.1_cds_WP_012905482.1_3434		2.03	0.0951	1.77	0.0102	5.47	conserved hypothetical protein	
NZ_JXUN01000235.1_cds_WP_072044776.1_3439	0.1813	0.87	0.0717	1.48	0.0374	2.10	acetylornithine deacetylase	argE
NZ_JXUN01000236.1_cds_WP_012906527.1_3456	0.2428	-0.14			0.0007	2.43	heme exporter protein B	ccmB
NZ_JXUN01000236.1_cds_WP_012906536.1_3465	0.0332	-1.43	0.2012	0.72	0.0166	1.42	ecotin (serine protease inhibitor)	eco
NZ_JXUN01000236.1_cds_WP_071820655.1_3448	0.3186	0.84			0.0359	1.18	nitrate/nitrite response regulator protein	narP
NZ_JXUN01000238.1_cds_WP_012907778.1_3481	0.2994	-0.08	0.3120	0.70	0.0069		fructose-like specific PTS system EIIB component 3	frwD
NZ_JXUN01000238.1_cds_WP_012907782.1_3476		-0.48	0.0238	2.42		1.34	fructose-like specific PTS system EIIC component 2	frwC
NZ_JXUN01000238.1_cds_WP_012907783.1_3475	0.4752	0.12			0.0237	3.82	multiphosphoryl transfer protein 2	ptsA
NZ_JXUN01000238.1_cds_WP_071820615.1_3471	0.1249	0.67	0.3910	-0.32	0.0203	1.69	5,10-methylenetetrahydrofolate reductase	metF
NZ_JXUN01000239.1_cds_WP_012905457.1_3490	0.0337	1.67	0.3192	0.04	0.4433	-0.54	NADH dehydrogenase	ndh
NZ_JXUN01000239.1_cds_WP_012905458.1_3489	0.0180	-2.16	0.2236	0.04	0.1527	0.57	putative exported protein	
NZ_JXUN01000239.1_cds_WP_012905460.1_3486	0.0882	0.53	0.0337	1.70	0.0392	0.79	lipoprotein	nlpD
NZ_JXUN01000240.1_cds_WP_001044509.1_3505	0.1880	-0.64	0.0701	0.70	0.0065	1.42	DNA-binding protein HU-alpha	hupA
NZ_JXUN01000240.1_cds_WP_001207203.1_3520	0.0273	1.17	0.1259	1.02	0.3682	-1.40	50S ribosomal subunit protein L10	rplJ
NZ_JXUN01000240.1_cds_WP_003862341.1_3524	0.0111	1.51	0.3440	0.01	0.3693	0.57	transcription antitermination protein	nusG
NZ_JXUN01000240.1_cds_WP_012133812.1_3519	0.0165	1.04	0.0942	1.24	0.2005	-0.67	50S ribosomal subunit protein L7/L12	rplL
NZ_JXUN01000240.1_cds_WP_012907741.1_3501	0.4995	0.04	0.1782	1.60	0.0109	1.74	two-component system response regulator	zraR
NZ_JXUN01000240.1_cds_WP_024132963.1_3503	0.4904	-0.44	0.1480	0.05	0.0445	2.96	zinc resistance-associated protein	zraP
NZ_JXUN01000240.1_cds_WP_024132964.1_3512	0.1785	2.15	0.0180	4.19	0.0063	5.08	thiamine biosynthesis protein	thiC
NZ_JXUN01000241.1_cds_WP_042623329.1_3527	0.0710	0.62	0.0063	1.52	0.0786	0.97	possible exported protein	
NZ_JXUN01000242.1_cds_WP_012906716.1_3605	0.2088	0.29	0.0534	1.44	0.0289	2.91	conserved hypothetical protein	
NZ_JXUN01000242.1_cds_WP_012906724.1_3599	0.3493	0.31	0.0362	3.07	0.0125	4.75	putative dihydrodipicolinate synthetase	
NZ_JXUN01000242.1_cds_WP_012906726.1_3597			0.0463	1.50	0.0100	5.05	putative amino acid permease	frlA
NZ_JXUN01000242.1_cds_WP_012906729.1_3594	0.0028	-2.41	0.0736	1.16	0.1093	1.90	putative exported protein	
NZ_JXUN01000242.1_cds_WP_012906731.1_3592	0.0013	-2.51	0.0675	-1.12	0.3793	0.53	outer membrane lipoprotein	
NZ_JXUN01000242.1_cds_WP_012906732.1_3590	0.0186	0.80	0.4454	-0.21	0.0346	-2.37	tRNA (guanine-N(1)-)-methyltransferase	trmD
NZ_JXUN01000242.1_cds_WP_012906733.1_3589	0.0049	1.15	0.3991	0.42	0.0519	-2.65	16S rRNA processing protein	rimM
NZ_JXUN01000242.1_cds_WP_012906740.1_3582	0.0131	2.15	0.3865	0.77	0.1884	1.12	DNA repair protein	recN
NZ_JXUN01000242.1_cds_WP_012906741.1_3581	0.0354	0.61	0.3940	-0.12	0.0286	3.38	putative outer membrane assembly lipoprotein	smpA
NZ_JXUN01000242.1_cds_WP_012906745.1_3577		2.18	0.1083	2.74	0.0328	5.11	large repetitive protein	
NZ_JXUN01000242.1_cds_WP_012906749.1_3573	0.2606	-0.59	0.0282	0.82	0.0642	0.61	putative prophage damage-inducible protein	
NZ_JXUN01000242.1_cds_WP_012906753.1_3569	0.0044	-2.76	0.4159	-0.03	0.2181	-0.13	putative phage tail fibre assembly protein	tfa
NZ_JXUN01000242.1_cds_WP_012906757.1_3565		-1.37	0.1541	1.84	0.0563	2.60	hypothetical prophage protein	
NZ_JXUN01000242.1_cds_WP_012906759.1_3563	0.3135	-1.22	0.1112	1.47	0.0272	3.30	Hypothetical prophage protein	
NZ_JXUN01000242.1_cds_WP_012906761.1_3561	0.0209	-3.25	0.1790	-1.45	0.3926	-0.22	hypothetical prophage protein	
NZ_JXUN01000242.1_cds_WP_012906763.1_3559	0.0183	-2.57	0.4571	-0.15	0.4416	-0.18	hypothetical prophage protein	
NZ_JXUN01000242.1_cds_WP_012906764.1_3558	0.0102	-2.34	0.4741	0.60	0.2571	0.45	hypothetical prophage protein	
NZ_JXUN01000242.1_cds_WP_012906765.1_3557	0.0161	-3.68	0.2348	-0.36	0.3678	0.36	putative phage tail sheath protein	
NZ_JXUN01000242.1_cds_WP_012906767.1_3555	0.0097	-3.96	0.1988	-0.43	0.4454	-0.81	hypothetical prophage protein	

NZ_JXUN01000242.1_cds_WP_012906768.1_3554	0.0146	-2.13	0.3403	0.56	0.3596	0.20	hypothetical prophage protein	
NZ_JXUN01000242.1_cds_WP_012906770.1_3552	0.0015	-4.11	0.3398	0.25	0.4247	0.64	putative phage capsid protein	
NZ_JXUN01000242.1_cds_WP_012906771.1_3551	0.0081	-3.30	0.2501	-0.30	0.3404	-0.41	hypothetical prophage protein	
NZ_JXUN01000242.1_cds_WP_012906772.1_3550	0.0234	-1.90	0.2765	0.70	0.4703	0.37	putative prophage exported protein	
NZ_JXUN01000242.1_cds_WP_012906773.1_3549	0.0388	-2.84	0.3310	0.95	0.1460	1.02	hypothetical prophage protein	
NZ_JXUN01000242.1_cds_WP_012906774.1_3548	0.2356	2.59	0.3311	0.97	0.0067	4.27	putative phage portal protein	
NZ_JXUN01000242.1_cds_WP_012906775.1_3547		-0.74	0.2738	1.12	0.4528	0.10	putative phage head-to-tail joining protein	
NZ_JXUN01000242.1_cds_WP_012906777.1_3545	0.0169	-2.74	0.3672	-0.04	0.3392	-0.06	putative prophage DNA binding protein	
NZ_JXUN01000242.1_cds_WP_012906778.1_3544	0.0252	-2.00	0.4018	1.48	0.3039	1.26	hypothetical prophage protein	
NZ_JXUN01000242.1_cds_WP_012906779.1_3543	0.0638	-2.17			0.0441	2.23	hypothetical prophage protein	
NZ_JXUN01000242.1_cds_WP_012906781.1_3541		-1.70	0.0625	1.79	0.1650	0.67	hypothetical prophage protein	
NZ_JXUN01000242.1_cds_WP_012906783.1_3539	0.0116	-2.93	0.4370	0.06	0.2157	0.30	putative prophage exported protein	
NZ_JXUN01000242.1_cds_WP_012906784.1_3538	0.0377	-2.20	0.4195	0.39	0.2487	0.64	hypothetical prophage protein	
NZ_JXUN01000242.1_cds_WP_012906785.1_3537	0.0157	-3.41	0.3999	0.20	0.2125	1.05	putative phage holin	
NZ_JXUN01000242.1_cds_WP_012906786.1_3536	0.0011	-3.74	0.3362	0.55	0.2884	-0.36	putative prophage DNA adenine methylase	dam
NZ_JXUN01000242.1_cds_WP_012906787.1_3535	0.0032	-2.81	0.4707	-0.09	0.0834	-0.07	hypothetical prophage protein	
NZ_JXUN01000242.1_cds_WP_012906788.1_3534	0.0904	1.76	0.0541	1.99	0.0078	4.35	putative phage antiterminator protein	
NZ_JXUN01000242.1_cds_WP_012906789.1_3533	0.4311	0.28	0.0583	2.11	0.0446	2.68	hypothetical prophage protein	
NZ_JXUN01000242.1_cds_WP_024132786.1_3542	0.0477	-1.39	0.4796	0.07	0.0575	1.53	hypothetical prophage protein	
NZ_JXUN01000242.1_cds_WP_024132787.1_3540	0.0236	-3.22	0.3481	1.15	0.0887	1.85	hypothetical prophage protein OR putative prophage exported protein	
NZ_JXUN01000242.1_cds_WP_042623332.1_3560	0.0404	-1.56	0.4757	1.29	0.1499	2.17	hypothetical prophage protein	
NZ_JXUN01000242.1_cds_WP_071820658.1_3587	0.0092	1.12	0.0640	1.61	0.0327	1.93	putative magnesium transport protein OR signal recognition particle protein	corE, ffh
NZ_JXUN01000243.1_cds_WP_012908380.1_3645	0.0094	1.59	0.0044	2.44	0.0150	1.34	putative membrane protein	
NZ_JXUN01000243.1_cds_WP_012908382.1_3640	0.0338	1.26	0.0308	1.18	0.0698	1.37	probable phosphoribulokinase	prkB
NZ_JXUN01000243.1_cds_WP_012908385.1_3637	0.3355	1.25	0.0220	3.67	0.0500	3.66	putative malonate decarboxylase acyl carrier protein transferase MdcA	mdcA
NZ_JXUN01000243.1_cds_WP_012908389.1_3633		0.68	0.0358	1.14		2.12	putative malonate decarboxylase gamma subunit MdcE	mdcE
NZ_JXUN01000243.1_cds_WP_012908390.1_3632		0.71			0.0119	4.50	putative malonate transporter MdcF	mdcF
NZ_JXUN01000243.1_cds_WP_012908392.1_3630	0.3051	0.57			0.0318	1.70	putative malonyl-CoA: acyl carier protein-SH transacylase MdcH	mdcH
NZ_JXUN01000243.1_cds_WP_024133044.1_3626	0.2814	0.58	0.0508	2.10	0.0100	2.51	glutathione-regulated potassium-efflux system ancillary protein	kefG, kefD
NZ_JXUN01000244.1_cds_WP_012907200.1_3657	0.2177	-0.98	0.0182	1.03	0.4448	0.51	hydrogenase isoenzymes formation protein	hypC
NZ_JXUN01000244.1_cds_WP_012907201.1_3658	0.2107	-0.85	0.0048	1.29	0.1553	0.60	hydrogenase isoenzymes nickel incorporation protein	hypB
NZ_JXUN01000244.1_cds_WP_012907202.1_3659	0.0510	7.27	0.0280	3.37	0.0219	5.39	accessory protein for nickel incorporation into hydrogenase 3	hypA
NZ_JXUN01000244.1_cds_WP_012907206.1_3663		1.50	0.1200	2.60	0.0385	3.36	formate hydrogenlyase subunit 4	hycD
NZ_JXUN01000244.1_cds_WP_012907212.1_3669	0.3545	-1.15	0.0504	1.83	0.0195	1.56	putative plasmid-related protein	
NZ_JXUN01000244.1_cds_WP_012907213.1_3670	0.0260	0.68	0.0724	1.21	0.0017		putative plasmid-related protein	
NZ_JXUN01000244.1_cds_WP_012907220.1_3677	0.3855	1.16			0.0247	4.09	nitric oxide reductase FlRd-NAD(+) reductase	norW
NZ_JXUN01000244.1_cds_WP_012907221.1_3678	0.0765	1.24	0.0065	2.83			nitric oxide reductase FlRd-NAD(+) reductase	norW
NZ_JXUN01000244.1_cds_WP_012907222.1_3679	0.1700	1.28	0.0196	2.90	0.0002	4.08	anaerobic nitric oxide reductase transcription regulator	norR

NZ_JXUN01000244.1_cds_WP_012907223.1_3680	0.1924	-0.90			0.0075	2.07	D-arabinose 5-phosphate isomerase	srlQ
NZ_JXUN01000244.1_cds_WP_012907226.1_3683		-2.52			0.1610	0.47	sorbitol-6-phosphate 2-dehydrogenase (glucitol-6-phosphate dehydrogenase)	srlD
NZ_JXUN01000244.1_cds_WP_012907228.1_3685	0.4275	0.12			0.3185	0.50	glucitol/sorbitol-specific PTS system EIIB component	srlE
NZ_JXUN01000244.1_cds_WP_012907233.1_3690	0.0601	0.79	0.0492	1.81	0.1743	1.76	regulatory protein	recX
NZ_JXUN01000244.1_cds_WP_012907236.1_3696	0.0125	1.32	0.0130	1.17			putative outer membrane protein	
NZ_JXUN01000244.1_cds_WP_012907251.1_3712	0.0131	-2.77	0.2094	0.13	0.2840	2.17	Conserved hypothetical protein	
NZ_JXUN01000244.1_cds_WP_012907252.1_3713	0.3166	-0.36	0.0014	2.13	0.0610	1.20	putative membrane protein	
NZ_JXUN01000244.1_cds_WP_012907256.1_3717	0.1455	-1.76	0.3704	0.05	0.0371	2.31	putative membrane protein	
NZ_JXUN01000244.1_cds_WP_012907259.1_3720	0.2794	1.23	0.0337	2.36	0.0309	1.47	putative membrane protein	
NZ_JXUN01000244.1_cds_WP_012907264.1_3725	0.0363	-2.28	0.4470	0.55	0.2259	-0.41	Putative exported protein	
NZ_JXUN01000245.1_cds_WP_024132686.1_3734	0.4280	0.04	0.0064	1.16	0.1387	-0.41	hypothetical protein	
NZ_JXUN01000245.1_cds_WP_042623339.1_3744	0.2483	-0.40	0.0198	1.49	0.0336	0.94	phage DNA invertase	inv
NZ_JXUN01000246.1_cds_WP_012905223.1_3757	0.1948	0.95	0.0377	1.55	0.0011	2.91	phage DNA invertase	inv
NZ_JXUN01000246.1_cds_WP_042623340.1_3756					0.0487	1.34	pseudogene	
NZ_JXUN01000247.1_cds_WP_012905135.1_3763	0.0470	-1.41	0.4683	0.70	0.3364	0.27	putative exported protein	
NZ_JXUN01000247.1_cds_WP_012905138.1_3766	0.4155	-0.07	0.4324	-1.41	0.0377	3.13	putative exported protein	
NZ_JXUN01000247.1_cds_WP_024132551.1_3764	0.0563	0.84	0.0793	0.70	0.0388	2.07	putative zinc ion binding protein	
NZ_JXUN01000248.1_cds_WP_012905027.1_3779	0.3594	0.61	0.1260	0.89	0.0327		ornithine decarboxylase isozyme, inducible	speF
NZ_JXUN01000248.1_cds_WP_012905030.1_3776	0.4224	-0.02	0.0281	1.46	0.0065		potassium-transporting ATPase C chain	kdpC
NZ_JXUN01000249.1_cds_WP_012905905.1_3787	0.2042	0.37			0.0208	1.03	ATP-independent RNA helicase	dbpA
NZ_JXUN01000249.1_cds_WP_012905907.1_3784	0.0228	-1.22	0.2329	1.03	0.0196	1.46	putative signaling protein	
NZ_JXUN01000249.1_cds_WP_024132680.1_3790	0.0381	-1.33	0.0741	-0.96	0.2934	4.50	pseudogene	
NZ_JXUN01000249.1_cds_WP_024132681.1_3786	0.2667	0.59	0.0522	1.66	0.0478	1.57	ATP-independent RNA helicase OR zinc transport protein	dbpA, zntB
NZ_JXUN01000251.1_cds_WP_001307474.1_3868	0.0836	0.49	0.2484	-0.21	0.0414	-1.13	protein C5 component of RNase P, inner membrane protein	rnpA, oxaA
NZ_JXUN01000251.1_cds_WP_001532742.1_3851	0.0085	2.17	0.0110	1.66	0.0937	0.62	small heat shock protein A	hslT
NZ_JXUN01000251.1_cds_WP_012907984.1_3879	0.1863	2.43	0.4471	1.97	0.0356	4.33	phosphate ABC transporter, permease protein	pstA, pstC
NZ_JXUN01000251.1_cds_WP_012907987.1_3876	0.2480	1.15	0.0286	2.73	0.0216	2.27	phosphate transport system regulatory protein	phoU
NZ_JXUN01000251.1_cds_WP_012907998.1_3862	0.0320	1.58	0.0690	2.14	0.1924	0.52	DNA replication and repair protein	recF
NZ_JXUN01000251.1_cds_WP_012908003.1_3857	0.1490	-1.09	0.0208	1.53	0.1194	1.09	2-dehydro-3-deoxygalactonokinase	dgoK
NZ_JXUN01000251.1_cds_WP_012908006.1_3854			0.1765	0.71	0.0248	2.25	conserved hypothetical protein	
NZ_JXUN01000251.1_cds_WP_012908007.1_3853	0.0437	2.00	0.0149	2.26	0.0031	2.83	Conserved hypothetical protein	
NZ_JXUN01000251.1_cds_WP_012908010.1_3850	0.0153	2.69	0.1486	1.72	0.1719	0.26	small heat shock protein B	hslS
NZ_JXUN01000251.1_cds_WP_012908013.1_3847	0.1519	2.57			0.2130	1.61	putative transcriptional regulator	
NZ_JXUN01000251.1_cds_WP_012908020.1_3840	0.1128	1.86	0.0460	1.49	0.0972	2.85	putative membrane protein	
NZ_JXUN01000251.1_cds_WP_012908024.1_3836	0.0259	2.71	0.0048	2.93	0.0006	2.90	DsdX permease	dsdX
NZ_JXUN01000251.1_cds_WP_012908026.1_3834	0.1005	0.43	0.0052	1.38	0.2172	1.21	multidrug resistance protein D	emrD
NZ_JXUN01000251.1_cds_WP_012908027.1_3833	0.3571	0.41	0.1041	1.08	0.0112	1.51	putative membrane protein	
NZ_JXUN01000251.1_cds_WP_012908033.1_3828	0.0988	1.15			0.0083	2.97	two-component system response regulator	uhpA
NZ_JXUN01000251.1_cds_WP_012908034.1_3827	0.0302	2.27	0.0048	2.92	0.1250	1.42	two-component system response regulator	uhpA

NZ_JXUN01000251.1_cds_WP_012908035.1_3826		2.68	0.0161	4.23	0.0228	6.67	major facilitator superfamily protein	uhpC
NZ_JXUN01000251.1_cds_WP_024132990.1_3872	0.1876	-0.11	0.4569	0.19	0.0245	1.91	conserved hypothetical protein	
NZ_JXUN01000251.1_cds_WP_024132993.1_3844	0.3691	0.08	0.2297	1.82	0.0122	3.20	AraC-family transcriptional regulator	
NZ_JXUN01000252.1_cds_WP_012904510.1_3886	0.3829	0.13			0.0201	2.26	2-keto-3-deoxygluconate permease	
NZ_JXUN01000252.1_cds_WP_042623356.1_3888	0.1681	1.87	0.0540	1.70	0.0124	3.05	4-hydroxythreonine-4-phosphate dehydrogenase	
NZ_JXUN01000253.1_cds_WP_012908901.1_3903	0.0607	2.00	0.0238	2.58	0.0006	2.82	pCROD1 plasmid	pCROD1
NZ_JXUN01000253.1_cds_WP_012908902.1_3904	0.2081	-1.05	0.1378	1.33	0.0177	1.32	pCROD1 plasmid	pCROD1
NZ_JXUN01000253.1_cds_WP_012908903.1_3907	0.1581	0.76	0.0113	1.48	0.0037	2.18	pCROD1 plasmid	pCROD1
NZ_JXUN01000253.1_cds_WP_012908907.1_3909		0.81			0.0119	4.30	pCROD1 plasmid	pCROD1
NZ_JXUN01000253.1_cds_WP_012908946.1_3897	0.2848	-0.57	0.0343	3.09	0.0002	2.88	pCROD1 plasmid	pCROD1
NZ_JXUN01000253.1_cds_WP_012908947.1_3898	0.2432	-0.07	0.0874	2.39	0.0052	3.09	pCROD1 plasmid	pCROD1
NZ_JXUN01000253.1_cds_WP_024133127.1_3902	0.0131	1.69	0.1137	0.37	0.0332	0.91	pCROD1 plasmid	pCROD1
NZ_JXUN01000253.1_cds_WP_024133131.1_3912	0.1802	1.27	0.0092	3.09	0.0048	3.94	pCROD1 plasmid	pCROD1
NZ_JXUN01000253.1_cds_WP_024133143.1_3896	0.0117	2.05	0.0542	3.12	0.0044	3.19	pCROD1 plasmid	pCROD1
NZ_JXUN01000253.1_cds_WP_042623357.1_3895	0.0422	0.74	0.2106	0.37	0.0129	0.99	LEE pathogenicity island	
NZ_JXUN01000253.1_cds_WP_042623358.1_3910	0.4431	-0.76	0.0152	1.01	0.0004	2.55	pCROD1 plasmid	pCROD1
NZ_JXUN01000254.1_cds_WP_002892050.1_3921	0.1314	-1.81	0.1202	1.12	0.0266	1.26	haemolysin expression regulatory protein	
NZ_JXUN01000254.1_cds_WP_012904867.1_3922	0.3240	-1.10	0.4091	0.79	0.0252	0.67	maltose O-acetyltransferase	maa
NZ_JXUN01000254.1_cds_WP_024132525.1_3916	0.3361	-0.16	0.1055	0.58	0.0256	3.64	acrAB operon repressor OR potassium efflux	acrR, kefA
NZ IVIN01000255 1 ada WD 012005664 1 2027	0.0187	2.92			0.2812	0.83	protein	
NZ_JXUN01000255.1_cds_WP_012905664.1_3927			0.2066	0.25			conserved hypothetical protein	1417
NZ_JXUN01000255.1_cds_WP_012905667.1_3930	0.0345	1.47	0.3966	-0.35	0.1955	0.51	multidrug resistance protein	mdtK
NZ_JXUN01000255.1_cds_WP_012905671.1_3934	0.2570	-4.78	0.0478	1.59	0.0265	0.82	LysR-family transcriptional regulator	ID
NZ_JXUN01000255.1_cds_WP_012905675.1_3938	0.2578	-0.32	0.1651	1.02	0.0265	1.19	superoxide dismutase [Fe]	sodB
NZ_JXUN01000255.1_cds_WP_012905676.1_3939	0.0985	0.66	0.0617	1.82	0.0106	1.27	putative exported protein	
NZ_JXUN01000255.1_cds_WP_012905678.1_3941	0.0155	1.29	0.2134	1.65	0.0632	1.39	ribonuclease T	rnt
NZ_JXUN01000255.1_cds_WP_012905683.1_3947	0.4831	1.28	0.0412	1.96	0.0162	2.67	superoxide dismutase [Cu-Zn]	sodC
NZ_JXUN01000255.1_cds_WP_012905684.1_3948	0.4699	-0.19	0.0949	1.26	0.0224	2.67	putative efflux pump protein	
NZ_JXUN01000255.1_cds_WP_012905685.1_3949	0.0592	0.67	0.4407	0.66	0.0247	1.01	HlyD-family secretion protein	
NZ_JXUN01000255.1_cds_WP_012905689.1_3954	0.0488	-1.79	0.4389	1.58	0.2637	1.00	putative lipoprotein	
NZ_JXUN01000255.1_cds_WP_012905694.1_3959	0.1599	1.39	0.3123	0.02	0.0106	2.16	tripeptide permease	tppB
NZ_JXUN01000255.1_cds_WP_012905698.1_3963	0.0857	2.22	0.1286	1.10	0.0060	1.83	electron transport complex protein	rnfD
NZ_JXUN01000255.1_cds_WP_012905699.1_3964	0.2087	1.39	0.1164	0.80	0.0260	2.62	electron transport complex protein	rnfC
NZ_JXUN01000255.1_cds_WP_012905701.1_3966	0.0156	1.42	0.4170	0.34	0.4155	0.00	electron transport complex protein	rnfA
NZ_JXUN01000255.1_cds_WP_012905702.1_3967	0.0018	1.27	0.3587	0.76	0.4924	0.09	putative outer membrane protein	
NZ_JXUN01000255.1_cds_WP_012905703.1_3968	0.1535	0.25	0.0152	1.11	0.0312	0.57	H-NS-and StpA-binding protein	
NZ_JXUN01000255.1_cds_WP_012905708.1_3972	0.4660	-0.72	0.1636	-0.22	0.0268	2.16	protein MalY	malY
NZ_JXUN01000255.1_cds_WP_012905725.1_3989	0.0017	-1.49	0.3656	0.16	0.1575	1.31	AI-2 transport protein TqsA	tqsA
NZ_JXUN01000255.1_cds_WP_012905727.1_3991	0.0442	-2.20	0.4995	0.68	0.0130	1.10	multidrug efflux system protein MdtJ	mdtJ
NZ_JXUN01000255.1_cds_WP_012905730.1_3994	0.3920	0.21	0.4607	-0.31	0.0081	1.60	acid shock protein	asr
NZ_JXUN01000255.1_cds_WP_012905731.1_3995	0.3260	1.31	0.0150	2.22	0.0512	2.55	major facilitator superfamily protein	
NZ_JXUN01000255.1_cds_WP_012905735.1_3999	0.2200	0.19	0.2005	1.36	0.0081	2.84	putative ABC transporter ATP-binding protein	

NZ_JXUN01000255.1_cds_WP_012905736.1_4000	0.1379	1.72	0.0695	2.17	0.0375	1.88	putative ABC transporter membrane protein	
NZ_JXUN01000255.1_cds_WP_012905737.1_4001		2.57	0.1178	1.63	0.0340	4.53	putative ABC transporter periplasmic binding	
NZ_JXUN01000255.1_cds_WP_012905739.1_4003	0.2026	-0.97	0.0694	1.70	0.0016	2.90	protein anaerobic dimethyl sulfoxide reductase maturation protein (twin-arginine leader-binding protein)	dmsD
NZ_JXUN01000255.1_cds_WP_012905744.1_4009	0.3197	-0.11			0.0130	4.64	uronate isomerase	uxaC
NZ_JXUN01000255.1_cds_WP_012905745.1_4010	0.0868	2.29	0.1218	2.09	0.0409	2.52	Major Facilitator Superfamily transporter	
NZ_JXUN01000255.1_cds_WP_012905755.1_4021		-0.79			0.0451		putative membrane protein	
NZ_JXUN01000255.1_cds_WP_024132645.1_3944	0.0625	3.10	0.1962	2.28	0.0339	3.66	TetR-family transcriptional regulator	
NZ_JXUN01000255.1_cds_WP_024132649.1_3969	0.3474	0.19	0.0098	1.29	0.0047	1.66	beta-lactam resistance protein	blr
NZ_JXUN01000255.1_cds_WP_024132653.1_4012	0.0673	-2.81	0.3159	-1.89	0.0292	2.23	Conserved hypothetical protein	
NZ_JXUN01000255.1_cds_WP_042623361.1_3924		2.52	0.0496	0.71	0.0164	2.19	conserved hypothetical protein	
NZ_JXUN01000256.1_cds_WP_012908911.1_4041	0.1534	-2.28	0.3092	1.76	0.0288	3.03	pCROD1 plasmid	pCROD1
NZ_JXUN01000256.1_cds_WP_012908912.1_4040	0.2460	-0.04	0.0742	2.18	0.0013	2.38	pCROD1 plasmid	pCROD1
NZ_JXUN01000256.1_cds_WP_012908914.1_4038	0.0175	-1.17	0.0367	0.93	0.0324	0.47	pCROD1 plasmid	pCROD1
NZ_JXUN01000256.1_cds_WP_012908915.1_4037	0.0834	0.63	0.0032	1.50	0.0269	2.69	pCROD1 plasmid	pCROD1
NZ_JXUN01000256.1_cds_WP_042623365.1_4039	0.0800	1.29			0.0063	2.93	pCROD1 plasmid	pCROD1
NZ_JXUN01000257.1_cds_WP_012904670.1_4052		3.20			0.0089	4.24	lateral flagellar rod protein	lfgD
NZ_JXUN01000257.1_cds_WP_012904671.1_4051	0.1388	1.13	0.0064	3.61			lateral flagellar hook protein	lfgE
NZ_JXUN01000257.1_cds_WP_012904678.1_4043	0.1744	-2.23	0.1640	-0.66	0.0306	1.53	ateral flagellar putative hook associated protein	lafW
NZ_JXUN01000257.1_cds_WP_042623368.1_4056		0.61			0.0087	3.28	lateral flagellar anti-sigma factor 28 protein	lfgM
NZ_JXUN01000258.1_cds_WP_012904933.1_4060	0.3663	-0.98	0.1277	-0.90	0.0211	-3.79	ferrienterobactin TonB-dependent receptor (enterobactin outer-membrane receptor)	fepA
NZ JXUN01000259.1 cds WP 012906634.1 4062	0.2380	-0.42	0.2749	0.63	0.0161	2.21	extracellular metalloprotease	prt1
NZ_JXUN01000259.1_cds_WP_012906636.1_4064	0.3373	1.62	0.0024	1.76	0.0152	2.39	conserved hypothetical protein	
NZ_JXUN01000259.1_cds_WP_012906637.1_4065	0.0200	0.68	0.0728	0.83	0.1069	1.45	GTP-binding protein	engA
NZ_JXUN01000259.1_cds_WP_012906638.1_4066	0.0379	1.61	0.3009	0.78	0.4721	0.59	putative dehydrogenase	
NZ_JXUN01000259.1_cds_WP_012906650.1_4079	0.4527	0.24	0.2589	0.65	0.0497	1.42	2Fe-2S ferredoxin	fdx
NZ_JXUN01000259.1_cds_WP_012906663.1_4094	0.0575	2.30	0.0075	4.55			putative 4Fe-4S binding protein	
NZ_JXUN01000259.1_cds_WP_012906665.1_4096	0.1108	1.39			0.0479	2.39	stationary phase inducible protein	csiE
NZ_JXUN01000259.1_cds_WP_012906666.1_4097	0.0793	0.67	0.1270	1.71	0.0042	3.17	putative 3-phenylpropionate permease	hcaT
NZ_JXUN01000259.1_cds_WP_024132767.1_4098	0.1740	1.15	0.1171	1.79	0.0409	2.40	putative aldose 1-epimerase	
NZ_JXUN01000260.1_cds_WP_001328552.1_4123	0.0563	-2.39	0.1342	-0.91	0.0375	-1.06	pCROD2 plasmid	pCROD2
NZ_JXUN01000261.1_cds_WP_000801440.1_4136	0.0031	-1.41	0.2024	-1.11	0.4797	0.34	pCROD2 plasmid	pCROD2
NZ_JXUN01000261.1_cds_WP_001025397.1_4139	0.0086	-1.72	0.2115	-0.34	0.2007	1.07	pCROD2 plasmid	pCROD2
NZ_JXUN01000261.1_cds_WP_001230707.1_4137	0.0025	-1.75	0.2324	-1.09	0.3980	0.09	pCROD2 plasmid	pCROD2
NZ_JXUN01000261.1_cds_WP_012908950.1_4138	0.0163	-4.22	0.0788	-1.04	0.1501	-0.60	pCROD2 plasmid	pCROD2
NZ_JXUN01000263.1_cds_WP_072044779.1_4143	0.4708	0.01	0.0091	-1.14	0.0011	-1.36	unknown	
NZ_JXUN01000264.1_cds_WP_072044780.1_4144	0.4322	-0.19	0.0038	-1.40	0.0003	-1.76	unknown	
NZ_JXUN01000267.1_cds_WP_012904570.1_4148	0.3584	0.20	0.2035	0.61	0.0241	1.62	pseudogene	
NZ_JXUN01000268.1_cds_WP_042623379.1_4150	0.4445	-0.17	0.0112	-1.31	0.0016	-1.81	unknown	
NZ_JXUN01000269.1_cds_WP_039267547.1_4151	0.4893	-0.12	0.0041	-1.17	0.0004	-1.56	unknown	

NZ_JXUN01000270.1_cds_WP_042623380.1_4166	0.4215	-0.06	0.0091	-1.16	0.0006	-1.54	unknown	
NZ_JXUN01000271.1_cds_WP_000534558.1_4167	0.3703	-0.34	0.0580	-1.06	0.0174	-1.54	unknown	
NZ_JXUN01000275.1_cds_WP_042623384.1_4172	0.1621	0.86	0.3758	0.04	0.0397	1.39	pseudogene OR pCROD1 plasmid	pCROD1
NZ_JXUN01000278.1_cds_WP_012904569.1_4176	0.0278	0.81	0.1898	0.74	0.0845	0.33	pseudogene OR pCROD1 plasmid	pCROD1
NZ_JXUN01000292.1_cds_WP_042623392.1_4195	0.4070	-0.07	0.0142	-1.16	0.0007	-1.28	unknown	
NZ_JXUN01000299.1_cds_WP_012904570.1_4204	0.3893	0.07	0.3818	-0.02	0.0408	1.05	pCROD1 plasmid	pCROD1
NZ_JXUN01000300.1_cds_WP_000534558.1_4233	0.3502	-0.51	0.0655	-1.07	0.0227	-1.63	unknown	
NZ_JXUN01000306.1_cds_WP_042623403.1_4240	0.3168	-0.22	0.2015	-0.70	0.0431	-0.99	unknown	
NZ_JXUN01000314.1_cds_WP_072044785.1_4303	0.3416	-0.08	0.1194	-1.11	0.0351	-1.06	unknown	
NZ_JXUN01000317.1_cds_WP_072044786.1_4306	0.3558	-0.02	0.1872	-0.62	0.0489	-1.03	unknown	
NZ_JXUN01000360.1_cds_WP_042623430.1_4398	0.3618	-0.39	0.0442	-0.97	0.0173	-1.03	unknown	

APPENDIX 1

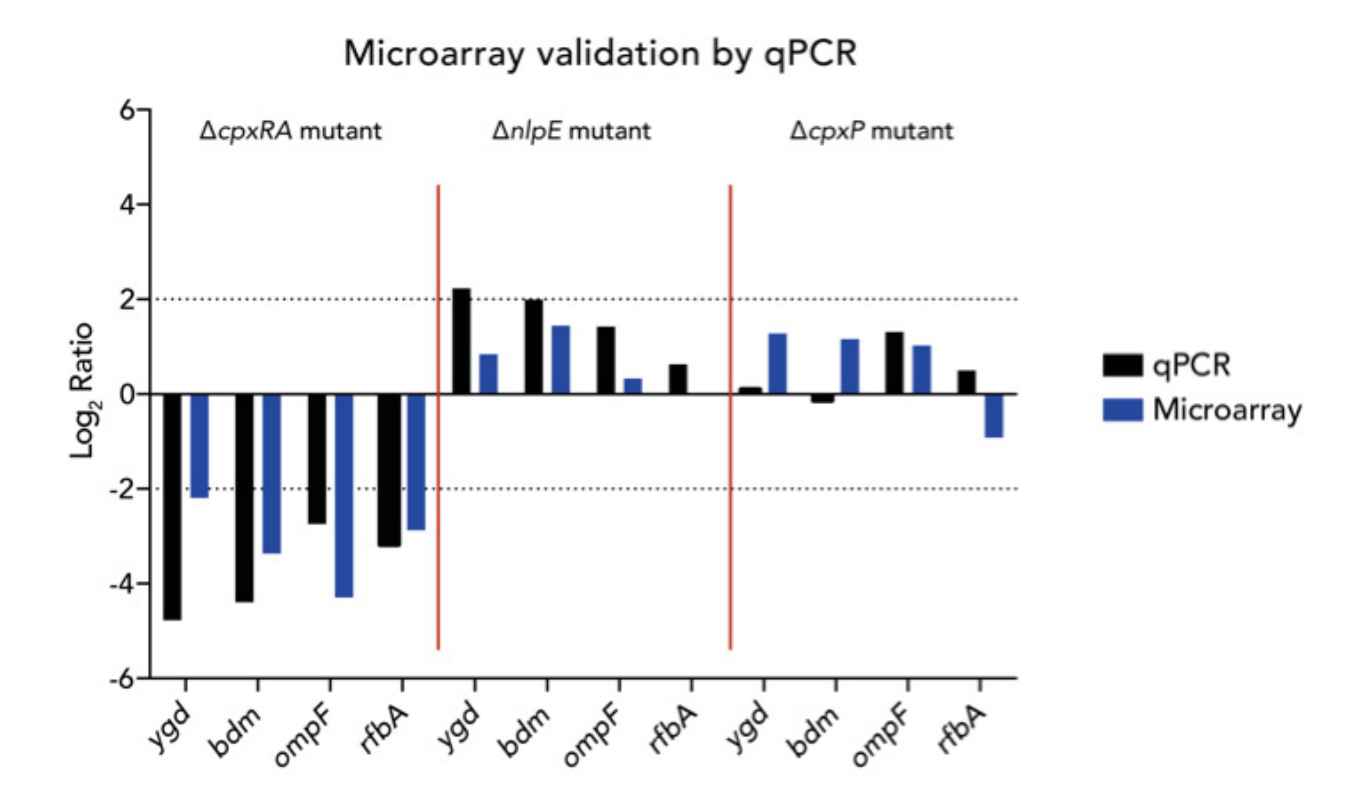


Figure A1: Validation of microarray dataset by qRT-PCR

qRT-PCR was used to evaluate the expression of four genes. *C. rodentium* strains were grown in DMEM to an OD₆₀₀ of 0.5-0.6, and RNA was extracted as described previously for the microarray experiments. 1µg of RNA was reverse transcribed to cDNA using Protoscript II (NEB). qPCR was performed using iTaq Universal SYBR Green (Biorad), and the primers in Table A1. Log2 ratio of $\Delta cpxRA/WT$ depicted in black for the qPCR experiments, and in blue for the microarray analysis.

Table A1 - qPCR primers used for microarray validation

Target	Forward Primer	Reverse Primer
ompF	CCTTCAACCAGACCGAAGAAG	AGAATTTGGCGGCGATACC
rfbA	CCCGCTTTCTTTGTTAACGG	CTGTGCATTAGTGCTTGGTG
16S	TGTCTACTTGGAGGTTGTGCCCTT	TGCAGTCTTCCGTGGATGTCAAGA
bdm	TGTTACCGCAACCTAAGGGG	CCACGCTGGATTTATCGCCT
ygd	CGCAGCAACTGTATTCACCG	CGTCGTCCACCTGTGGTTTA

PREFACE TO CHAPTER 4

In Chapters 2 and 3 of this thesis we explored TCSs as virulence factors of A/E pathogens. While TCSs can act as virulence factors by transcriptional regulation of specific genes, A/E pathogens also encode a pathogenicity island, the Locus of Enterocyte Effacement (LEE), which encodes a multitude of virulence factors. The LEE encodes the ability to form attaching and effacing lesions, as well as a Type 3 Secretion System (T3SS). The T3SS is a molecular apparatus which forms a continuous channel from the bacterial cytoplasm to the host cell cytoplasm, and secreted many effectors into the host cell, for many different functions. Initially, most effectors of the T3SS were also reported to be encoded within the LEE. In 2004, the first non-LEE-encoded effector, non-LEE-encoded effector A, or NleA, was discovered. NleA is required for virulence, and since its discovery it has been implicated with inhibiting COPII vesicle cargo packaging and/or budding, as well as being important for disruption of tight junctions.

In Chapter 4, we detected an apparent mobility shift of NleA on SDS-PAGE gels, when comparing bacterially secreted NleA, to that in host cell translocated NleA. This suggested that NleA is post-translationally modified upon translocation into the host cell. We determined that the apparent mobility shift is not due to phosphorylation, ubiquitination, or N-glycosylation. Using mass spectrometry and a conditionally glycosylation deficient CHO cell line, we have gathered evidence consistent with the possibility that NleA is O-glycosylated upon translocation into the host cell. This modification is conserved *in vivo*.

CHAPTER 4: The Virulence Factor NleA is O-glycosylated Upon Host Cell Translocation.

ABSTRACT

Enteropathogenic and Enterohaemorrhagic Escherichia coli (EPEC and EHEC) are two diarrheal pathogens responsible for morbidity and mortality in developing and developed countries, respectively. Along with the murine model Citrobacter rodentium, they are members of a group known for their characteristic attaching and effacing lesion colonization. These pathogens attach to the enterocyte, efface the microvillar architecture, and form actin rich pedestals beneath the adherent bacteria. Essential to this process is the type 3 secretion system, which they use to translocate effector proteins into the host cell. These proteins modulate host cell pathways to favour bacterial replication and survival. We detected a size shift of one T3SS effector, NleA, following translocation into host cells, leading us to hypothesize that it might be modified by the host. We have determined that NleA is not phosphorylated, ubiquitinated, or N-glycosylated. Using mass spectrometry, bioinformatic analyses, and a conditionally glycosylation-deficient cell line, CHO LDLD, we determined that host cells modify NleA by O-glycosylation. Further, the modification of NleA is conserved *in vivo* during infection of C3H/HeJ mice with *C. rodentium*. This is the first demonstration of this type of modification on a bacterially translocated protein. Further characterization of this host-mediated post-translational modification on NleA is needed in order to understand its role during infection. These findings will increase our understanding of host/pathogen interactions during EPEC, EHEC, and *C. rodentium* infections.

INTRODUCTION

Enteropathogenic and Enterohemorrhagic Escherichia coli (EPEC and EHEC) are Gram negative enteric bacterial pathogens responsible for diarrheal disease in both the developing and developed world [58]. In the case of EHEC, disease can progress to hemorrhagic colitis due to the phage-encoded Shiga toxin, which is lacking in EPEC [58]. The related murine pathogen *Citrobacter rodentium* was first isolated in Japan and the USA in the 1960s, as the etiologic agent for colitis [50, 52]. *C. rodentium* is routinely used to model EPEC and EHEC infection in mice, due to the difficulties in infecting mice with EPEC and EHEC [52, 55]. Despite their slightly differing disease manifestation, all three bacteria are members of a group known as attaching and effacing pathogens (A/E), due to their ability to form characteristic attaching and effacing lesions on the host epithelium [299]. The bacterium will attach to the intestinal epithelium, efface the microvillar architecture, and form actin-rich pedestals beneath the adherent bacteria [3, 58].

A/E pathogens also share the Type 3 Secretion System (T3SS), a multi-subunit system spanning both the inner and outer bacterial membranes, and forming a continuous channel from the bacterium into the host cell in order to deliver effector proteins (reviewed in [17]). Each T3SS-containing pathogen has a unique repertoire of effectors, which alter cellular pathways in order to enhance bacterial survival and replication. EHEC, EPEC, and *C. rodentium* share the Locus of Enterocyte Effacement (LEE)-encoded T3SS and an estimated 22 translocated effector proteins [56].

Multiple effectors translocated by the T3SS have been characterized, many of which are encoded within the LEE. One of the most studied effectors of the T3SS of EHEC, EPEC, and *C. rodentium* is the translocated intimin receptor, or Tir, which plays a major role in the formation of A/E lesions as it initiates actin polymerization, leading to the actin pedestals beneath the bacteria

[103]. Secreted effector Map stimulates filopodia formation, and along with EspF, promotes mitochondrial dysfunction [115, 118]. Further, EspG interacts with tubulin to modulate the host cytoskeleton [148]. Finally, NleH inhibits the cleavage of procaspase-3, leading to decreased apoptosis [300].

The first characterized translocated effector not encoded within the LEE was the non-LEE-encoded effector A, or NleA [132]. NleA is not required for the translocation of other effectors into the host cell, but it is required for virulence [132]. NleA is necessary but not sufficient for disruption of tight junctions between host intestinal epithelial cells [158]. The mechanisms underlying the virulence effects of NleA are not well defined.

Recent work in our lab identified an apparent mobility shift of NleA on SDS-PAGE gels – from the bacterially-secreted size of 50-55kDa to the host-translocated size of approximately 65kDa. This is reminiscent of what has been previously reported in Tir, where upon translocation into the host, it is tyrosine and serine/threonine phosphorylated leading to a 12kDa mobility shift [98, 99]. Further characterization of this host-mediated post-translational modification on NleA is needed in order to understand its role during infection.

MATERIALS AND METHODS

Bacterial strains

Bacteria were routinely cultured at 37°C, 220 rpm in Luria-Bertani (LB) broth (1% [wt/vol] tryptone, 0.5% [wt/vol] yeast extract, 1% [wt/vol] NaCl). For secreted protein assays, bacteria were cultured in M9⁺ media (5X M9: 6.4% [wt/vol] Na₂HPO₄•7H₂O, 1.5% [wt/vol] KH₂PO₄, 0.25% [wt/vol] NaCl, 0.5% [wt/vol] NH₄Cl; M9⁺: 1X M9, 0.8mM MgSO₄, 0.1% casamino acids, 0.004% [wt/vol] glucose, 0.0037% [wt/vol] NaHCO₃).

Secreted proteins

Secreted protein assays were performed as previously described. Briefly, 5 ml overnight cultures were subcultured in M9⁺ media in a 6-well plate (50 μl overnight culture, 2 ml M9⁺), and incubated for 6 hrs at 37°C, 5% CO₂. The samples were transferred to Eppendorf tubes and centrifuged at maximum speed for 1 min. The supernatant was transferred into a clean tube and centrifuged at maximum speed for 2 mins. Next, 900μl of the supernatant was then transferred to a glass tube, and incubated on ice for 1 hr with the addition of 100μl of trichloroacetic acid for protein precipitation. Following precipitation, the samples were transferred to an Eppendorf tube and centrifuged at max speed, at 4°C, for 30 mins. The supernatant was removed, and 1ml of ice-cold acetone was added to each Eppendorf tube. The samples were stored at -80°C overnight. The next day, the samples were centrifuged at maximum speed, at 4°C, for 30 mins. The supernatant was removed, and the pellets were air dried. Finally, the pellets were resuspended in 5X Laemmli buffer (50% glycerol, 0.3M Tris pH 6.8, 5% [wt/vol] SDS, 10% β-mercaptoethanol, bromophenol blue).

Cell culture

HeLa, Caco2/TC7 [301] and CMT-93 cells were routinely cultured in DMEM (Wisent) media, with 10% heat-inactivated FBS. CHO LDLD and K1 cells [302, 303] were routinely cultured in Ham's F-12 media, with 5% heat-inactivated FBS and 1% L-glutamine, and 24hrs prior to infection, they were cultured in Ham's F-12 media, with 1% heat-inactivated FBS and 1% L-glutamine [302]. For glycosylation experiments, the media was supplemented with 20μM galactose (Sigma) and/or 200μM N-acetyl galactosamine (Sigma), in order to induce glycosylation in the mutant cell line.

λ phosphatase treatment

The λ phosphatase treatment was performed as per manufacturer's instructions (NEB, P0753S). Briefly, HeLa cells were infected with UMD207, a strain of EPEC lacking host cells adhesins (intimin, bundle forming pilus) [270]. Cells were harvested and lysed in B150 buffer without phosphatase inhibitors (20mM Tris-HCl pH 8.0, 150mM KCl, 5mM MgCl₂, 10% glycerol, 0.1% NP40, protease inhibitors). Lysates were incubated with or without enzyme for 2 hrs at 30°C. The samples were run on n SDS-PAGE gel, transferred onto a PVDF membrane, and immunoblotted with an anti-NleA antibody [132]. Tir was immunoblotted as a positive control, with a mouse anti-Tir monoclonal antibody 2A8 [304].

Purification and NHS-activated Sepharose coupling to anti-NleA Antibody

Purified EHEC NIeA was run on an SDS-PAGE gel and transferred to a PVDF membrane (Biorad) [157]. The membrane was stained with Ponceau (0.1% [wt/vol] Ponceau S (BioShop), 5% acetic acid), and target section was excised. Anti-NIeA rat serum was incubated with the excised section of western blot PVDF membrane overnight at 4°C. The antibody was eluted from the PVDF membrane with 1ml 2.2M glycine for 3mins with gentle vortexing. The solution was immediately neutralized with 130µl sodium bicarbonate. Dialysis was performed as per manufacturer's instructions (Thermo Scientific). The eluent was placed in dialysis cassette overnight (regenerated cellulose membrane, 10 000MW pore size; Thermo Scientific), with 800ml of coupling buffer (0.2M NaHCO₃, 0.5M NaCl), at 4°C. Next, 3ml of NHS-activated Sepharose 4 Fast Flow (GE Healthcare Life Sciences) slurry were washed with cold 1mM HCl, and combined with purified antibody. Beads were coupled to antibody on labquake overnight, at 4°C. Samples were blocked by standing in 0.1M Tris-buffer for 2.5 hrs. After coupling, the media was washed,

alternating between high and low pH buffers, Tris buffer pH 8.5 and acetate buffer pH 5 (0.1M Sodium acetate, 0.5M NaCl) - 3 x 1 medium volume Tris buffer followed by 3 x 1 medium volume acetate buffer. This process was repeated 3-6 times. Coupled affinity medium was stored in 20% ethanol.

Immunoprecipitation and anti-ubiquitin blotting

Caco2/TC7 cells were seeded in 10cm dishes, and once at confluence, infected with 100µl of overnight culture of UMD207. Approximately 5.5hrs after infection, the cells were washed 6 times with cold PBS^{+/+} (Wisent), and harvested with 1ml cold PBS^{+/+}. The cells were centrifuged at 1500 x g at 4°C for 5 mins in a clinical centrifuge to pellet the cells. The cell pellets were lysed with 5ml of lysis buffer (20mM Tris-HCl pH 7.5, 50mM NaCl, 1% NP40, 3 mM MgCl₂, 1 mM CaCl₂, 1 mM Na₃VO₄, 10mM NaF, 50mM Na₄P₂O₇, protease inhibitors), on a labquake for 30 mins at 4°C. The samples were sonicated three times for 15s at 60% amplitude in a bath sonicator. The lysed cells were centrifuged at maximum speed for 15 mins, at 4°C in a microfuge. The supernatant was transferred to a clean microfuge tube, containing 40 µl of protein G Plus (Santa Cruz; prewashed in lysis buffer) per sample, and incubated 1 hr on the labquake at 4°C. Following incubation, the samples were centrifuged at 1500 x g at 4°C for 5 mins. 75µL of the supernatant was stored, as the pre-IP lysate, 15µl of 5X Laemmli sample buffer was added, and the sample was boiled for 5 mins. To the remaining supernatant, 40μL of the NHS-activated sephanose beads that have been coupled to rat anti-NleA affinity purified antibody were added, and incubated for 2 hrs on the labquake at 4°C. Following incubation, the samples were centrifuged at 1500 x g, at 4°C, and 75µl of supernatant were stored as the post-IP lysate. Upon addition of 15µL of Laemmli sample buffer, the post-IP lysates were boiled for 5 mins. The beads were washed 4 times with lysis buffer: each

wash is composed of ≥ 10 mins on labquake at 4°C, centrifugation at 1500 x g at 4°C for 5 mins. Following the washes, the beads were resuspended in $100\mu\text{L}$ of Laemmli sample buffer to elute the protein, and boiled for 5 mins. All samples were then run on an SDS-PAGE gel, transferred to a PVDF membrane, and immunoblotted for total ubiquitin (Ub (P4D1), sc-8017, Santa Cruz).

Membrane prep for deglycosylation assay

HeLa cells were infected with $100\mu l$ of a 17.5hr overnight culture of EPEC WT per 10cm plate, until a lawn of bacteria appeared in the plate (4-5hrs). The cells were harvested in PBS^{+/+}. Cells were centrifuged at 1000 x g for 5 mins at 4°C. The supernatant was aspirated, and the pellets were resuspended in 1.5ml homogenization buffer (250mM sucrose, 3mM pH 7.4 imidazole, 0.5mM EDTA, 1mM VO₄, 1mM NaF). Samples were centrifuged at 3000 x g for 10 mins at 4° C. The supernatant was aspirated and the samples were resuspended in $300\mu l$ of homogenization buffer. The samples were mechanically lysed by passing through a 22-gauge needle, and centrifuged at 3000 x g for 15 mins at 4° C. The supernatant was transferred to an ultracentrifuge tube, and centrifuged at 41 000 x g in a TL100 Beckman centrifuge in TLS55 rotor for 20 mins at 4° C. The supernatant was aspirated, and the pellet (membrane fraction), was resuspended in $125\mu l$ of dH_2O .

Deglycosylation enzyme

The deglycosylation assay was performed as per manufacturer's instructions (NEB, P6039). Briefly, 2µl of 10X Glycoprotein Denaturing Buffer was added to 18µl of each sample, and they were denatured at 100°C for 10 mins. The samples were let to cool on ice, and centrifuged at maximum speed for 10s. Following centrifugation, 5µl of 10X GlycoBuffer 2 was added to each sample, followed by 5µl of Deglycosylation Enzyme Cocktail or dH₂O as a control. The contents

were mixed gently, and incubated at 37°C for 4 hrs. Following incubation, samples were run on a western blot, and immunoblotted with an anti-NleA antibody. For the positive control, Fetuin (provided by the manufacturer) was processed in a similar manner. Samples were run on an SDS-PAGE, and stained by Coomassie.

Mouse infection and preparation of colon extracts

This study was carried out in accordance with the recommendations of the Canadian Council on Animal Care. The protocol was approved by the McGill University Animal Care Committee. Female C3H/HeJ mice were purchased from Jackson Laboratories and maintained in a specific pathogen free facility. Wild-type *C. rodentium* DBS100 was grown overnight in 3ml LB broth, 220rpm, at 37°C, and mice were orally gavaged with 100µl of overnight culture, containing 2-3 x 10⁸ CFU. The infectious dose was verified by plating of serial dilutions of the inoculum on LB agar. The mice were euthanized at day 9 post infection, and colon samples were harvested, and flash frozen in liquid nitrogen. Samples were placed in 500µl of B150 buffer (20mM Tris-HCl pH 8.0, 150mM KCl, 10% glycerol, 5mM MgCl₂, 0.1% NP-40, 5mM NaF, 1mM NaVO₄, protease inhibitor). The samples were homogenized with a Polytron, and incubated on ice for 10 mins. The homogenates were sonicated three times at 60% amplitude for 15s, in 5s intervals, and incubated on ice for 10 mins. The samples were centrifuged at 13,000 rpm for 15 mins at 4°C. The supernatant was transferred to clean Eppendorfs tubes, and the stored at -80°C until use.

Mass Spectrometry

Excised gel cubes, containing the protein band of interest, were reduced, alkylated and digested with proteomics-grade Trypsin (Promega) at a concentration of 12 ng/µl [305].

Digested peptides were extracted with 100 μl of 100% Acetonitrile, transferred to a clean Eppendorf tube and dried in a Speed Vac for 1 hour. The dried peptides were then reconstituted in 40 μl of water supplemented with 0.1% formic acid (FA) and transferred to a 200 μl sample vial. The peptide samples were subjected to LC reverse phase nanoflow chromatography using a Proxeon Easy nLC (Thermo Scientific). The peptides were trapped onto a 2 cm C18 trapping column (Acclaim PepMap 100, Thermo Scientific) and were separated at a flow rate of 350 nl/minute on a 15 cm C18 analytical nanocolumn (Acclaim PepMap RSLC, Thermo Scientific) with a water/Acetonitrile gradient covering 3%-38% Acetonitrile over 100 minutes.

The eluting peptides were analyzed by an Orbitrap Q-Exactive HF (Thermo Scientific) operating with a duty cycle of 10 MSMS fragment spectra per precursor scan. The resolution was set at 120,000 (scan speed 2 spectra per second) for precursor scans, over mass range of 375-1400 m/z, and 30,000 (scan speed 25 spectra per second) for fragment spectra. The mass spectrometer was operated with a dynamic exclusion set at 8 seconds and maximum trap fill.

Bioinformatic analysis:

The acquired spectra were converted into Mascot Generic Files (mgf) using Mascot Distiller (Matrix Sciences) and searched against a mini-database, consisting of just the gene of interest. Serches were performed using the Mascot proteomics search engine (Matrix Sciences), setting mass tolerance of 5 ppm for precursor ions and 50 mDa for MSMS ions and allowing for oxidized Methionine as a variable modification. The searches were performed with a specified number of variable modifications at a time (phosphorylations on Serine and Threonines, various glycoform modifications). The Mascot data output was transferred to Scaffold (Proteome Software) for data validation. Redundant spectral counts were used as quantitative measure and spectra were accepted for peptides/proteins.

RESULTS

NleA undergoes an apparent molecular weight shift upon translocation into the host cell.

We have identified a significant change in mobility of the T3SS-translocated effector protein NleA between bacterially-secreted proteins and the NleA found in infected intestinal epithelial cells. We detected a larger than expected apparent size of host-translocated NleA on SDS-PAGE gels (\sim 55 to \sim 65 kDa) (Figure 1).

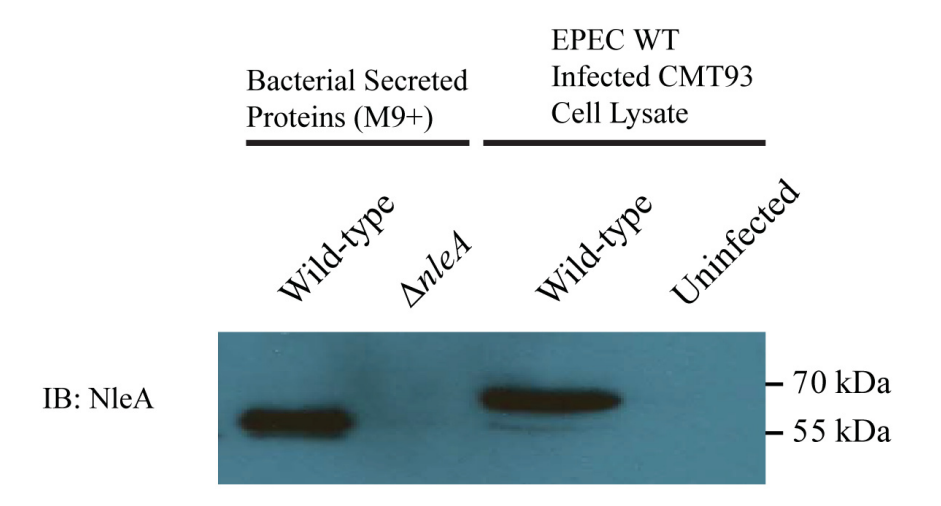


Figure 1: NleA is modified upon host translocation.

Western blot analysis of wild-type (lane 1) and $\Delta nleA$ EPEC (lane 2) secreted proteins prepared from M9+ media, and EPEC-infected CMT93 cells (lane 3) or uninfected CMT93 cells (lane 4), immunoblotted for NleA.

NleA is not phosphorylated, ubiquitinated, or N-glycosylated by the host.

To gain insight into the possible modification of NleA, we performed bioinformatics analyses to investigate whether the NleA protein sequence would be predicted to be modified by common mammalian post-translational modifications. We assessed phosphorylation of NleA by infecting HeLa cells with wild-type EPEC and incubating the lysates with λ phosphatase enzyme, which cleaves phosphates from serine, threonine and serine residues (Figure 2). After evaluating these samples on a western blot, and immunoblotting for NleA, we detected no change in size shift after treatment with λ phosphatase (Figure 2A). In contrast, Tir, which has been previously reported to be phosphorylated upon host translocation, was used as a positive control and showed a striking decrease in apparent size after treatment (Figure 2B) [99]. To assess the possibility of ubiquitination, we infected Caco2/TC7 cells with wild-type EPEC, and immunoprecipitated NleA from the cell lysates. We evaluated the samples on a western blot, by immunoblotting for NleA and total ubiquitin. We detected a striking enrichment of NleA in the IP lysate, however we detected no ubiquitin in that lysate (Figure 3). As such, NleA is not ubiquitinated upon translocation into the host cell.

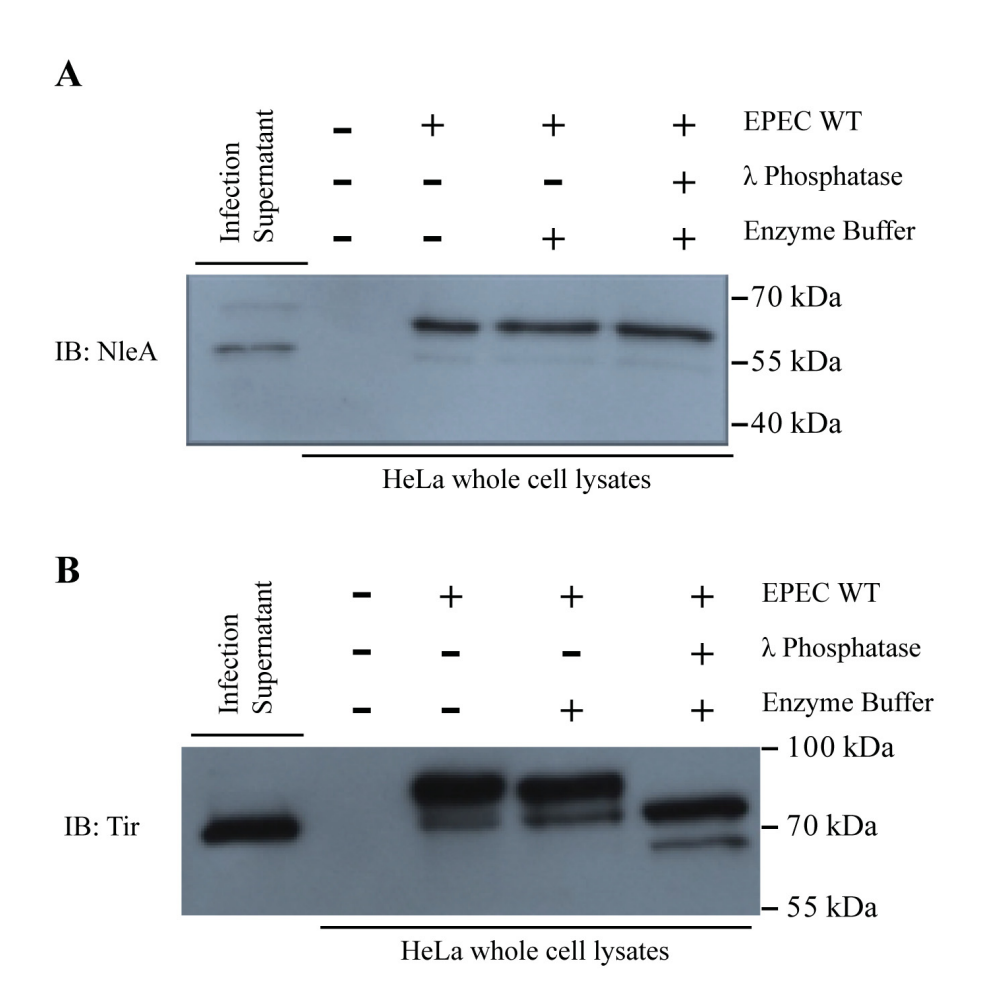


Figure 2: Phosphorylation is not responsible for the apparent size shift of NleA.

Western blot of HeLa whole cell lysates, infected with UMD207 and treated with λ phosphatase. Samples were immunoblotted for NleA (A) and Tir (B). In lane 1, the infection supernatant denotes the bacterially secreted protein. Lane 2 shows uninfected HeLa cell lysates. Lanes 3-5 depict infected HeLa cell lysates, in the absence (lanes 3, 4) or presence of λ phosphatase (lane 5).

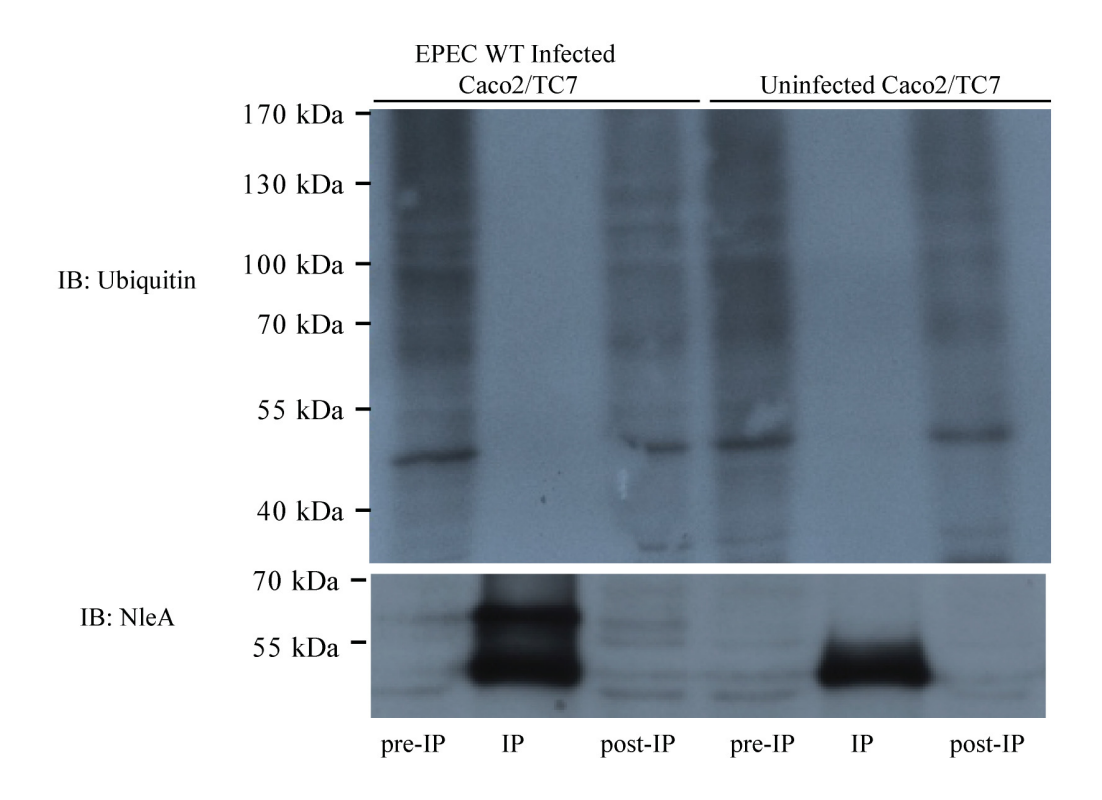


Figure 3: NleA is not ubiquitinated upon translocation into the host cell.

Western blot analysis of wild-type EPEC infected and uninfected Caco2/TC7 cells, after immunoprecipitation with NHS-sepharose coupled to anti-NleA antibody. Western was immunoblotted for total ubiquitin and NleA. Lanes 1 and 4 depict the pre-immunoprecipitation (pre-IP) lysates of infected and uninfected Caco2/TC7 cells. Lanes 2 and 5 depict the immunoprecipitated (IP) samples of infected and uninfected Caco2/TC7 cells. Lanes 3 and 6 depict the post-immunoprecipitation (post-IP) lysates of infected and uninfected Caco2/TC7 cells.

To assess glycosylation, we infected HeLa cells with wild-type EPEC, and isolated the membranes of the cells. We treated the samples with a deglycosylation enzyme mix comprised of PNGase F, O-glycosidase, neuraminidase, and β -N-acetylglucosaminidase which target N-linked oligosaccharides, core 1 and core 3 O-linked disaccharides, terminal, non-reducing α 2,3, α 2,6, and α 2,8 linked N-acetylneuraminic acid residues, terminal, non-reducing β 1-4 linked D-galactopyranosyl residues, and β -N-Acetylglucosamine residues, respectively. After evaluating the samples on a western blot and immunoblotting for NleA, we detected no change in size shift between treated and untreated samples (Figure 4). Through these experiments, we have determined that the apparent size shift of NleA is not likely to be attributed to phosphorylation, ubiquitination, or N-glycosylation.

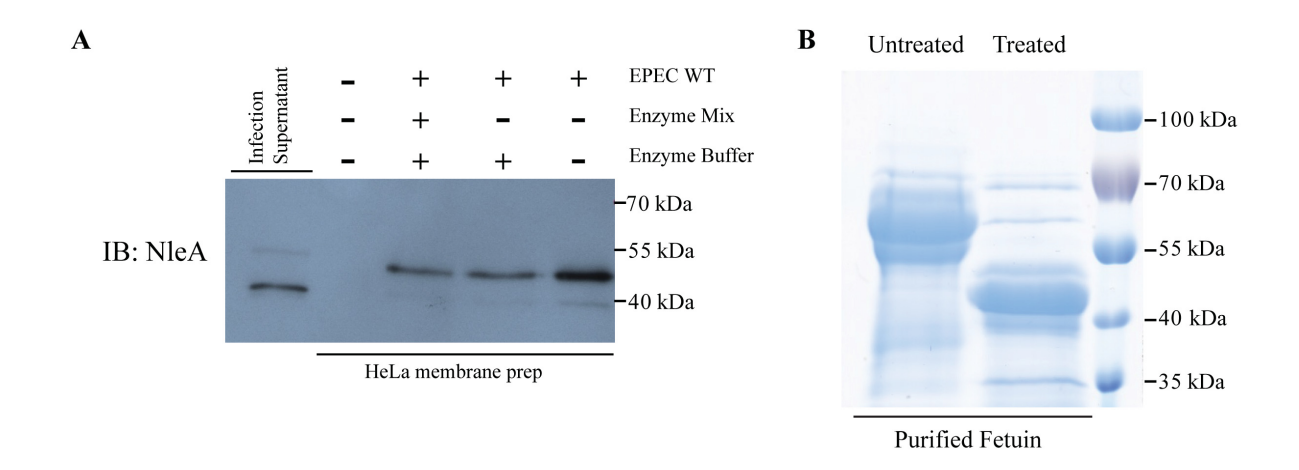


Figure 4: The apparent size shift of NleA is not due to enzyme-cleavable forms of glycosylation.

HeLa cell membranes were isolated and treated with deglycosylation enzymes. (A) Samples were probed for NleA. In lane 1, infection supernatant depicts bacterially secreted NleA. Lane 2 depicts uninfected HeLa cells. Lanes 3-5 depict infected HeLa cell membranes, in the absence (lanes 4, 5) or presence of deglycosylation enzymes (lane 3). (B) Coomassie-stained SDS-PAGE of glycosylated (untreated) and deglycosylated (treated) fetuin positive control.

The conditionally glycosylation-deficient CHO cell line LDLD suggests NleA is O-glycosylated.

Next, we immunoprecipitated NleA similarly to the ubiquitination experiments, and we performed mass spectrometry analysis, to attempt to further determine the post translational modification of NleA. Although mass spectrometry analysis was not conclusive, it revealed a region of NleA that differed between host-modified NleA and bacterially-secreted NleA. The detected peptide was only detectable in the bacterially-secreted version of NleA (Figure 5A), and not in the host-translocated NleA (Figure 5B). Bioinformatic analysis of this serine/threonine-rich region by NetOGly4.0 predicted this to be the site of mucin-type O-glycosylation (Figure 5C) [306].

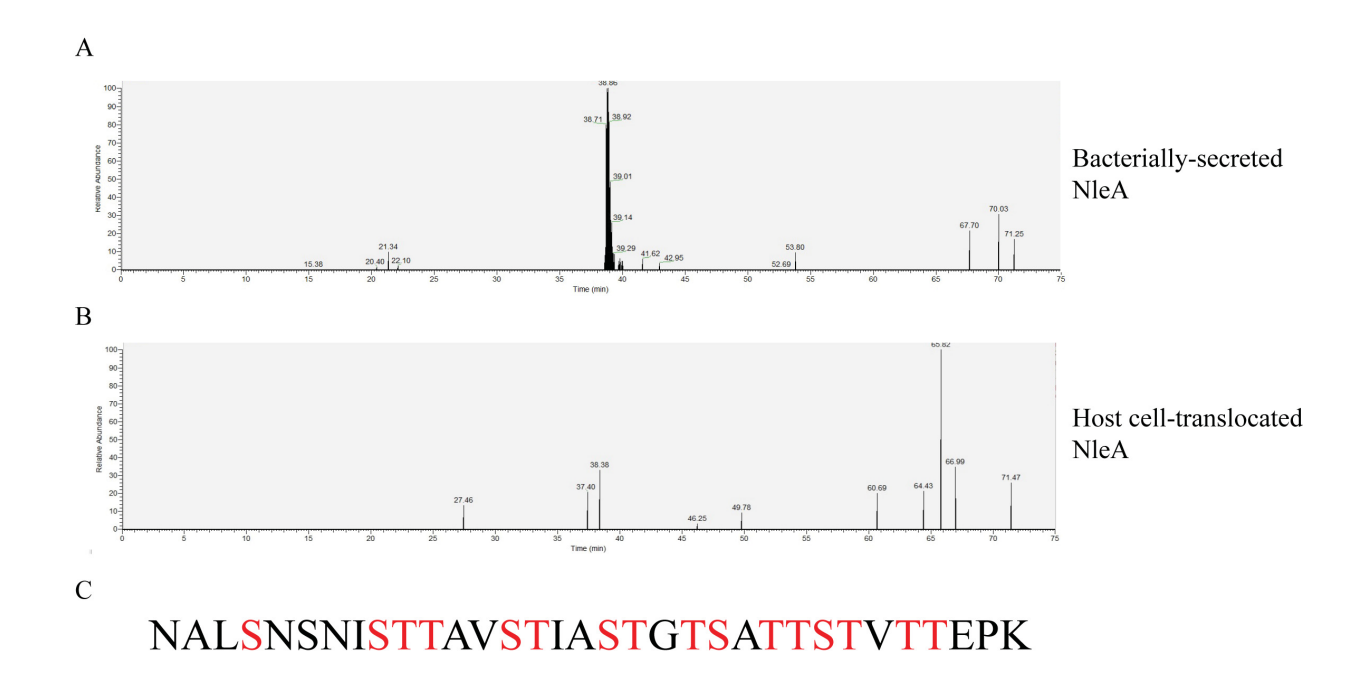
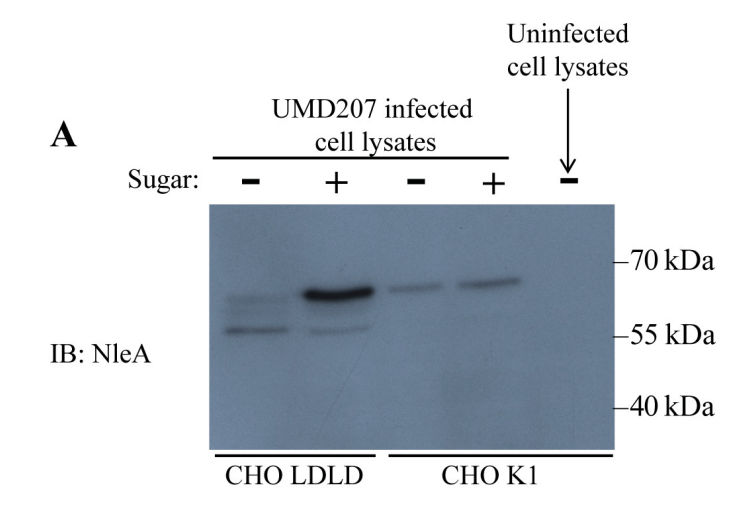


Figure 5: Mass spectrometry analysis reveals differences in bacterially secreted and host-translocated NleA profiles.

Part of the mass spectrometry analysis of bacterially-secreted (A) and host-translocated NleA (B). Amino acid peptide sequence which not detected in the host-translocated NleA sample (C), with serine and threonine residues highlighted in red.

To further investigate the possibility of O-glycosylation, we used a modified CHO cell line with a conditional deficiency in glycosylation (LDLD) which can be complemented by the addition of galactose and N-acetyl galactosamine to the cell culture media. We have obtained strong evidence that NleA is O-glycosylated (Figure 6). The post-translational modification of NleA is lost when the cells are cultured in regular Ham's F12 media, and restored upon supplementation with sugars (Figure 6A). Further, we supplemented the media of the cells with either galactose or N-acetyl galactosamine, and only in the presence of N-acetyl galactosamine was the modification restored (Figure 6B). The addition of galactose alone was not sufficient to restore the modification. In the parent cell line, CHO K1, which is wild-type for glycosylation under all conditions, sugar supplementation did not affect NleA size, which was comparable to the host-translocated size in all media.



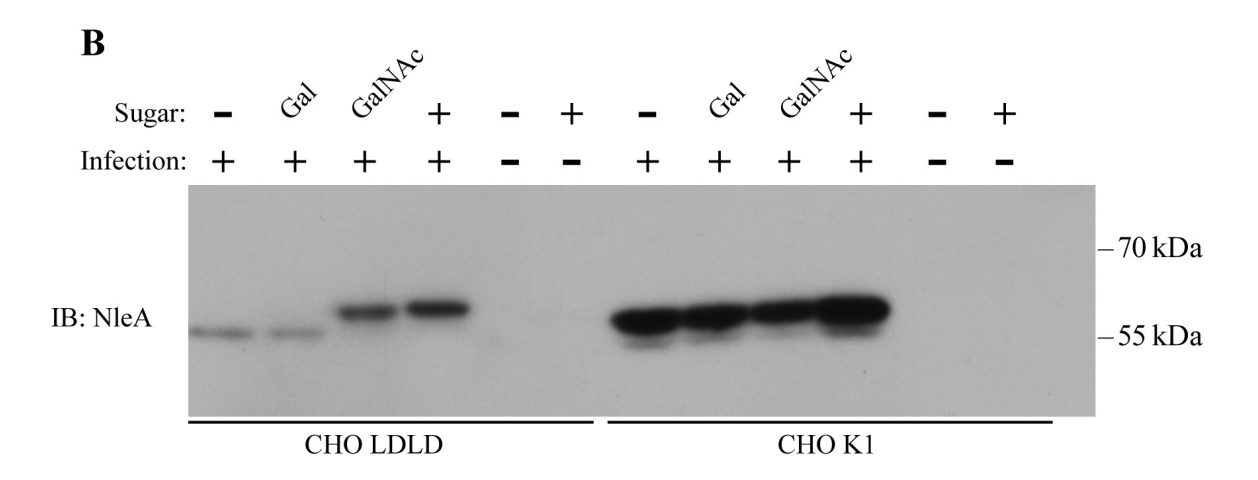


Figure 6: The apparent molecular weight shift of NleA is abrogated in conditionally glycosylation-deficient cells and restored with addition of sugars.

CHO K1 and LDLD cell lines were infected with UMD207 or not, and the media was supplemented with galactose (Gal) and/or N-acetylgalactosamine (GalNAc), both sugars (+), or neither (-). Samples were immunoblotted for NleA. (A) Cells were cultured in 5% heat-inactivated fetal bovine serum, and (B) in 1% heat-inactivated fetal bovine serum.

The post translational modification of NleA is conserved in vivo.

Finally, we aimed to determine whether this post translational modification is conserved *in vivo*, using a susceptible mouse model. To this end, we infected C3H/HeJ mice with wild-type *C. rodentium*, and extracted protein from the colon of day 9 infected mice. By western blot, we detected the host-translocated NleA to be larger than the NleA secreted by wild-type *C. rodentium* (Figure 7). In the same SDS-PAGE, as internal controls, we ran samples of the CHO K1 and LDLD cell lines, with and without sugar supplementation, and we detected that the secreted NleA is similar in size to the unmodified LDLD NleA, whereas the tissue NleA is more reminiscent of the modified NleA found after sugar supplementation (Figure 7).

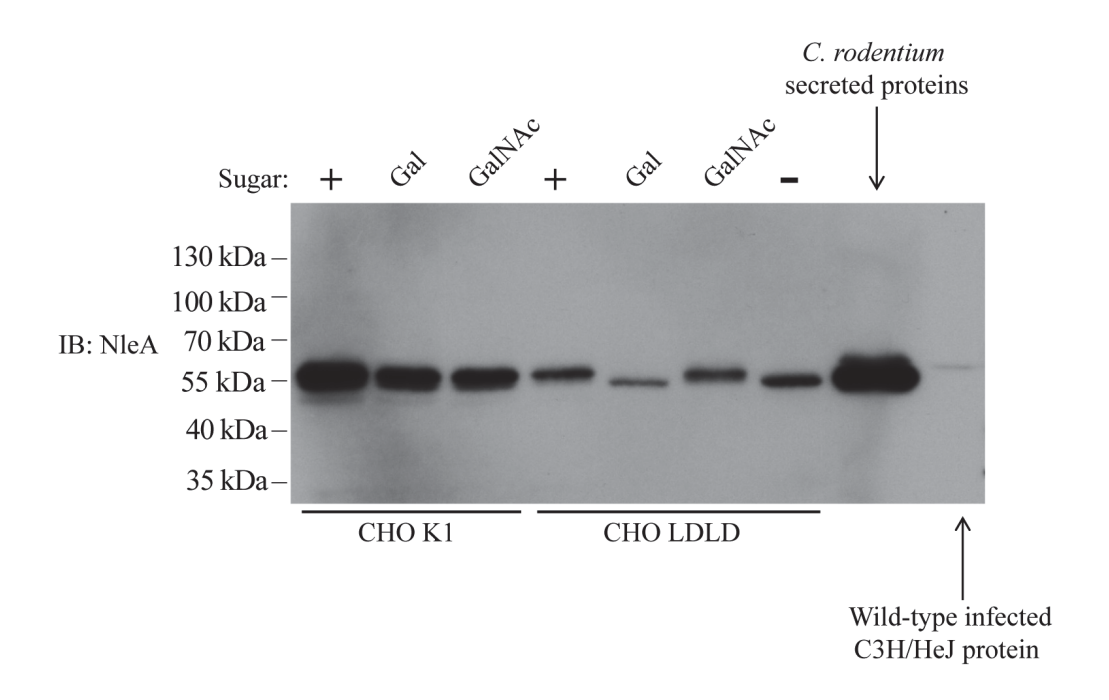


Figure 7: NleA molecular weight shift is conserved in vivo.

Lanes 1-7 depict infected CHO K1 and LDLD cell lysates, supplemented with galactose (Gal), N-acetylgalactosamine (GalNAc), both sugars (+), or neither (-). Lane 8 depicts secreted proteins of wild-type *C. rodentium*, and lane 9 depicts a C3H/HeJ infected mouse tissue protein lysate at day 9 post infection. Samples were immunoblotted for NleA.

DISCUSSION

EPEC and EHEC are foodborne diarrheal pathogens responsible for morbidity and mortality in both the developing and developed world. The T3SS is an essential virulence determinant of these extracellular A/E pathogens. The T3SS translocates protein effectors into the host cell, to carry out specific functions. Of the secreted effectors, NleA is essential for virulence of C. rodentium in mice. We have detected a mobility shift on SDS-PAGE gels of NleA, upon translocation into the host cell. This size shift is not due to phosphorylation, ubiquitination, or N-glycosylation. Through the use of mass spectrometry, we have detected a 33-amino acid NALSNSNISTTAVSTIASTGTSATTSTVTTEPK, rich in serine and threonine residues which disappears during analysis of the host-translocated-NleA. Multiple glycosylation sites on this peptide, as predicted by NetOGLy4.0, suggest that this peptide is unable to be detected through the mass spectrometer – characteristic of heavily O-glycosylated peptides [306]. To further determine whether this was the case, we used a conditionally glycosylation-deficient cell line, CHO LDLD, and the wild-type parent cell line, CHO K1. This result is not conflicting with the results of the deglycosylation experiment (Figure 4) because the deglycosylation mix targeted all types of N-glycosylation and only the most common types of O-glycosylation, not including mucin-type O-glycosylation.

The CHO LDLD cell line is deficient in the 4-epimerase enzyme, required for the conversion of UDP-glucose (UDP-Glc) to UDP-galactose (UDP-Gal) and UDP-N-acetyl glucosamine (UDP-GlcNAc) to UDP-N-acetyl galactosamine (UDP-GalNAc) [307]. UDP-Gal is often a terminal sugar component of both N- and O-glycans [308]. In contrast, UDP-GalNAc is the first sugar added in the construction of an O-glycan [308]. The 4-epimerase deficiency can be bypassed by

the addition of galactose and N-acetyl galactosamine to the cell culture media [302]. Upon introduction of these sugars, salvage pathways will convert galactose to galactose 1-phosphate and UDP-Gal, and N-acetyl galactosamine will be converted to N-acetyl galactosamine 1-phosphate and UDP-GalNAc [309]. We detect that the sole addition of N-acetyl galactosamine in the cell culture media is sufficient to restore the post-translational modification to NleA, thereby further supporting our hypothesis that NleA is O-glycosylated.

As mentioned previously, the translocated intimin receptor, Tir, is essential for the formation of A/E lesions and the T3SS [103]. In EPEC, Tir is phosphorylated at tyrosine 474, serine 434 and serine 463 [98, 99]. The function of the serine phosphorylation remains unclear. *In vitro*, the EPEC tyrosine 474 phosphorylation has been shown to be essential for pedestal formation, but not attachment and effacement [310, 311]. In EHEC, tyrosine 474 is not conserved, and in *C. rodentium* the mutation of this tyrosine to an unphosphorylatable amino acid (phenylalanine) does not affect disease [101, 102]. While the tyrosine phosphorylation of Tir may not be important for virulence of A/E pathogens, it provides a precedent for post-translational modification of virulence factors.

The O-glycosylation of NleA is the first report of such a modification on a bacterially-translocated effector. Further evaluation of the modification is required to determine the exact implication of it in the context of host-pathogen interaction; however, there are multiple possibilities. Upon translocation into the host cell, NleA goes to the Golgi apparatus, where it interacts with COPII vesicles and protein trafficking [155]. COPII vesicles mediate trafficking of selected cargo to the plasma membrane or for secretion, and NleA has been shown to interact with Sec24 – a component

of COPII vesicles, and the protein which determines cargo selection [156]. This interaction leads to the inhibition of COPII vesicle production [155]. Given that the Golgi apparatus is a site in the host cell of mucin-type GalNAc O-glycosylation, it is likely that NleA is modified at this site [312]. In future, we aim to confirm the O-glycosylation of NleA using lectin staining both in vitro and in vivo during mouse infection. Glycosylation is known to increase protein stability, and may be required for the stability of NleA [313]. We aim to examine this possibility in vitro by performing trafficking experiments at both early and late infection timepoints, using gentamicin treatment, followed by detection of NleA. These experiments will allow us to determine protein stability in wild-type cells, but also in the LDLD cells, to further delineate the purpose of the apparent modification. Further, the glycan may act as a label for NleA to be packed into COPII vesicles and trafficked to the membrane or other cellular sites. One possible reason for this could be due to the depletion of mucus in the intestine during infection. Perhaps NleA is glycosylated and by being trafficked to the plasma membrane it can act as a food source for the extracellular bacteria. Delineating the mechanism and the importance of the modification of NleA could provide new insight into the host-pathogen interaction between A/E pathogens and the host.

CHAPTER 5: DISCUSSION

General Overview/Summary

Enteropathogenic and Enterohemorrhagic E. coli are foodborne diarrheal pathogens transmitted through the fecal oral route, responsible for diarrheal disease in the developing and developed world. The murine model of these two pathogens is Citrobacter rodentium, manifesting as self-limiting colitis in resistant mice, and fatal diarrhea in susceptible mice. These pathogens are members of a group of bacteria which form characteristic attaching and effacing (A/E) lesions on enterocytes, whereby they efface the microvillar architecture and form actin rich pedestals beneath the adherent bacteria. During an infection, the bacteria must be able to sense the host gut environment and adapt gene expression accordingly, and to do this they can use two-component signal transduction systems (TCS). Further, in order to cause disease, they must be able to activate their virulence system, which, in the case of A/E pathogens, is the Locus of Enterocyte Effacement (LEE). The LEE encodes the ability to form A/E lesions, but also a type 3 secretion system (T3SS) and many effectors, which are responsible for a multitude of functions within the host cell. During our early work, we uncovered that the Non-LEE-encoded-effector A (NleA) undergoes an apparent mobility shift upon translocation into the host cell. This thesis aimed to determine the role of TCSs and post-translational modification on T3SS effectors in A/E pathogen fitness and virulence. In this thesis, we show that the manipulation of multiple TCSs (CpxRA, RcsBC, ArcAB, RstAB, ZraRS, UhpAB, BarA/UvrY) can lead to altered virulence of C. rodentium. The deletion of the RcsBC TCS leads to modest attenuation of C. rodentium, which could be due to an altered capsule, although further experiments are required to determine the relationship between virulence and capsule. The deletion of the ArcAB TCS leads to a slight attenuation of C. rodentium, and may be due to a defect in the regulation of the T3SS, an essential component of A/E pathogenesis. Deletion of the CpxRA TCS leads to severe attenuation, with 100% survival of susceptible mice. The attenuation of the $\Delta cpxRA$ strain is independent of auxiliary proteins NlpE and CpxP, and microarray analysis revealed many candidate genes and pathways for further evaluation. Finally, we show that the T3SS effector NleA, which is required for *C. rodentium* virulence appears to be O-glycosylated upon translocation into the host cell.

Two-component systems during infection with *C. rodentium*

In chapter two of this thesis, we performed a global analysis of the *in vivo* expression and virulence effects of all 26 TCS encoded within the *C. rodentium* genome. This work confirmed the strong virulence effect of CpxRA, and showed that CpxRA is the TCS with the most striking role in *C. rodentium* virulence. Moderate virulence effects were seen for the ArcAB and RcsBC TCS mutants, and modest effects on virulence were uncovered for 3 other TCSs (RstAB, ZraRS, UhpAB). Lastly, the UvrY/BarA mutant demonstrated a modest hyper-virulent phenotype. Below, I summarize each of the TCSs implicated in *C. rodentium* virulence and provide some hypotheses as to what mechanisms may be involved in the virulence effects. Notably, the TCSs with the most striking virulence attenuation phenotypes, ArcAB, RcsBC, and CpxRA were also among the most highly expressed *in vivo* and were also reported in a study in commensal *E. coli* MP1, where deletion of these three TCSs lead to colonization defects in the mouse intestine [248]. This suggests that the mechanisms for sensing and adapting to the host intestinal environment may be shared by both pathogenic and commensal bacteria.

ArcAB

The ArcAB TCS is composed of the ArcB membrane kinase, which becomes phosphorylated upon stimulus by reduced quinones in anaerobic conditions, and consequently activates the ArcA response regulator [314-316]. The ArcAB TCS is involved in sensing anaerobic conditions and adjusting energy production [254]. Since the gut is an environment with low oxygen, it is possible that the low oxygen environment of the gut is what leads to ArcAB expression. Conversely, in some pathogens, ArcAB has been linked to the bacterium's ability to withstand reactive oxygen species, which may also be relevant in C. rodentium infection. In Salmonella enterica serovar Typhimurium, ArcAB has been implicated in protection against reactive oxygen species and survival within macrophages, leading to a systemic infection [317, 318]. In Haemophilus influenzae, loss of ArcAB also leads to susceptibility to reactive oxygen species [319]. In both of these pathogens, the mechanism of susceptibility to reactive oxygen species is likely to involve Dps, a previously reported DNA-binding protein with protective roles in E. coli under starvation conditions, whereby it binds to DNA to protect it from oxidative stress [318, 320]. The ferritin-like Dps protein sequesters iron and limits oxyradical formation [318]. In both S. enterica and H. influenzae, deletion of dps rendered the bacteria susceptible to reactive oxygen species, a phenotype which was fully restored upon complementation of dps [318, 319]. In E. coli K12, ArcAB is also important for resistance to reactive oxygen species in aerobic conditions, likely through a mechanism different than that in Salmonella and Haemophilus *influenzae*, as no difference in gene expression of *dps* was detected [321].

In this thesis, we demonstrate that in *C. rodentium*, loss of ArcA leads to the slight attenuation of the pathogen, and it is likely due to a defect in the regulation of the T3SS, as is evident both at the protein and transcript level of expression. Decreased T3SS expression is in

agreement with both the *in vivo* localization and the *in vitro* adherence studies we have performed. Although this is the first example of a link between ArcAB and T3SS regulation, there already exists a link between the induction of ArcAB in micro-aerobic conditions, as well as the induction of T3SS in micro-aerobic conditions [322-324]. Given that the mid-colon of mice is a micro-aerobic environment, it is tempting to speculate that ArcAB is activated for energy generation, and concurrently ArcAB activates the T3SS for the successful colonization of the intestine [325, 326].

RcsBC

The Rcs phosphorelay TCS is composed of the membrane-bound histidine kinase RcsC, which is autophorphorylated, and consequently transfers the phosphate to a second conserved receiver domain within RcsC [171]. The phosphate is then transferred to the phosphorelay protein RcsD, and then to the response regulator RcsB [171]. The Rcs TCS has been implicated in response to envelope stress, such as loss of 4 penicillin-binding proteins [327], mutations in LPS biosynthesis [171], treatment with compounds that target the peptidoglycan, such as lysozyme [328], \(\beta\)-lactams [329], MreB inhibitor A22 [330], and defective lipoprotein sorting, due to mutation of LolA [331]. Rcs is also known as a regulator of capsule synthesis, including the biosynthesis of colanic acid in the capsule of bacteria [171]. In extraintestinal pathogenic E. coli (ExPEC), Rcs plays a role in protecting the bacteria from serum bactericidal activity through regulation of colanic acid [332]. Microarray analysis of Klebsiella pneumoniae revealed that Rcs plays a role in the regulation of a multitude of genes, involved in carbohydrate transport and metabolism, inorganic ion transport, and energy conversion [333]. In E. coli, Rcs has also been shown to be a regulator of ftsA and ftsZ, genes involved in cell division [334, 335]. In this thesis, we demonstrate that in C. rodentium, loss of RcsB leads to moderate attenuation, which is

correlated with the significant downregulation of the *wcaA* gene of the colanic acid biosynthesis operon. We also detected an altered *in vivo* localization, with the vast majority of *C. rodentium* in the lumen of the intestine, as opposed to adhered to the mucosa. The link between colanic acid and intestinal adherence is not clear at present and future experiments are needed to determine that the capsule is indeed altered in the Rcs mutant strain and the exact consequence of an altered capsule, upon infection. Notably, no experiments assessing the role of the capsule in *C. rodentium* infection are reported in the literature.

RstAB

The RstAB TCS is composed of the RstB histidine kinase and the RstA response regulator [336]. Both rstA and rstB are regulated by another TCS, PhoPQ [337]. The PhoPQ TCS responds to low-levels of Mg^{2+} , α -helical antimicrobial peptides, as well as acidic pH of 5.5 [338-342]. While the exact environmental conditions that induce RstAB are unknown, in avian pathogenic E. coli (APEC), loss of RstAB reduced virulence $in\ vivo$ at both early and late timepoints, as well as decreased pathology and reduced survival in chicken macrophages [252]. In E. coli K12, loss of RstA lead to delay in the initiation of DNA replication, thereby increasing doubling time of the mutants [343]. In $Salmonella\ enterica$, the expression of RstA resulted in a decrease in the cellular levels of RpoS and RpoS-inducible proteins [344]. RpoS is a sigma factor critical for bacterial endurance in host adaptation and stationary phase growth [344]. RpoS has also been implicated in regulation of virulence of S. enterica, exhibiting a decreased ability to colonize the Peyer's patches of the intestine [345-347]. In this thesis, we demonstrate that a RstAB mutant of C. rodentium is slightly attenuated. While our systematic analysis of all TCSs did not reveal a virulence defect in the $\Delta phoPO$ strain in the context of C. rodentium infection, the fact that the $\Delta rstAB$ strain showed

a slight attenuation suggests that, while the regulons of the two TCSs may somewhat overlap, they are distinct, and they play different roles in virulence. The RstAB system appears to be activated by another environmental stimulus, which is possibly not under the control of PhoPQ.

UhpAB

The UhpAB TCS is composed of the UhpB histidine kinase, the UhpA response regulator, as well as a second upstream membrane bound sensor, UhpC [348]. In *E. coli*, UhpAB is activated in the presence of glucose-6-phosphate [348]. The exact implication of this TCS in the intestine is yet to be determined, despite the differing levels of glucose-6-phosphatase in the intestine [253]. In mice, glucose-6-phosphatase, the enzyme that catalyzes the removal of glucose from glucose-6-phosphate, is mainly found in high amounts in the kidneys, liver, and the small intestine [253]. Within the small intestine, there is a gradient, with the highest concentrations of glucose-6-phosphatase in the duodenum and the jejenum [253]. It is tempting to speculate that the concentration of the substrate itself is present in a similar pattern. While *C. rodentium* colonizes the colon of mice, it must first pass through the small intestine, where the increased levels of glucose-6-phosphate could be enough to activate UhpAB, even in transit. In this thesis, we demonstrate that a UhpAB mutant of *C. rodentium* is slightly attenuated, raising the possibility that the transient activation may be required for full virulence of *C. rodentium*.

ZraRS

The ZraRS TCS is composed of the histidine kinase ZraS, and the response regulator ZraR. There exists a third component to this TCS, ZraP, which is a periplasmic protein that scavenges zinc, the primary activator of this TCS. In *E. coli*, loss of ZraRS signaling renders the bacteria

more susceptible to multiple classes of antibiotics [349]. This TCS has been implicated in envelope stress response to zinc and lead [350]. The majority of zinc is provided by dietary uptake, with zinc absorption occurring throughout the intestine [351]. Zinc has been reported to be a co-factor for multiple processes, ranging from cellular metabolism to virulence factors; however, when present in large quantities, zinc can also be toxic [352]. In this thesis, we demonstrate that a ZraRS mutant of *C. rodentium* is slightly attenuated, which could suggest that loss of ability to respond to zinc may have compromised the ability of the bacteria to carry out specific functions necessary for full virulence.

BarA/UvrY

This TCS is composed of the BarA histidine kinase and the UvrY response regulator. BarA responds to short chain fatty acids, such as formate and acetate [353]. This is especially relevant in the intestine, as the microbiota produce short chain fatty acids as by-products of the metabolism of carbohydrates [213, 354]. Acetate comprises approximately 55% of short chain fatty acids in the colon [355]. Notably, BarA/UvrY controls the expression of noncoding RNAs csrB and csrC, which interact with CsrA to prevent it from binding onto mRNA targets [255, 256]. In uropathogenic *E. coli* (UPEC), loss of BarA/UvrY leads to decreased virulence *in vivo* during mouse infection, and decreased survival during *in vitro* long term growth experiments [227, 356]. In this thesis, we demonstrate that loss of UvrY signaling in *C. rodentium* leads to a slightly hypervirulent strain, where susceptible mice succumb to infection slightly prior to wild-type-infected animals. Due to the unexpected virulence result, it is possible to speculate that the BarA-UvrY system is responsible for the transcription of downstream negative regulators of virulence factors of *C. rodentium*, whose transcription would increase in the absence of *uvrY*. However, it is

unlikely that these virulence factors include the T3SS, as we detected no difference in the total protein secretion profile of the $\Delta uvrY$ strain, relative to wild-type.

QseBC

Recently, the QseBC and QseFE TCSs have been implicated in virulence of *C. rodentium*. These TCSs sense epinephrine and norepinephrine in the gut of the host, and upon loss of these neurotransmitters and/or the TCSs, the bacterium exhibits decreased colonization and decreased virulence *in vivo* [176]. In our hands, mutation of these TCSs did not lead to an attenuated phenotype. While the specific reason for this is unknown, it is notable there is a discrepancy between infectious doses, between this study and the studies of others. We and others in the field routinely infect susceptible mice with 2-3x10⁸ CFU, whereas the recent paper on the QseBC and QseFE TCSs instead used a 10⁵ CFU infectious dose, which is much lower [176]. It is possible that lower infectious doses could reveal other TCSs with more subtle effects on virulence, than we are able to detect in our study.

CpxRA

TCSs have been proposed as potential drug targets, as an anti-virulence strategy, as opposed to classical antibiotics. The idea behind this is that these drugs would inhibit specific functions of bacteria, as opposed to being bactericidal, which may decrease the generation of resistance against these compounds [357, 358]. TCSs are a rather attractive target for treatment of infection due to the fact that they are lacking in mammals, decreasing the chance of off-target effects of any drugs. As such, TCSs are beginning to be evaluated as potential targets. Notably, the small molecule savarin has been designed against the *Staphylococcus aureus* AgrCA TCS,

which is responsible for quorum sensing [359]. Inhibition of ArgA lead to decreased virulence of *S. aureus*, but did not affect *S. epidermidis*, the skin commensal [359]. Another prominent example is LED209, a small molecule which prevents the activation of QseBC by preventing the autophosphorylation of QseC, and shows a modest decrease in virulence of *Francisella tularensis* and *Salmonella typhimurium in vitro* and *in vivo* [360]. In the context of CpxRA, phosphatase inhibitors of CpxA have been evaluated with some success in uropathogenic *E. coli* [361]. The CpxRA TCS is an attractive target for therapeutics, as it plays an important role in virulence of *C. rodentium*, and the manipulation of this TCS could alter the outcome of an infection. However, Gram negative bacteria are known to be rather difficult to target by conventional antibiotics due to their characteristic double membrane. The Cpx TCS is composed of the inner membrane-bound histidine kinase CpxA, the cytoplasmic response regulator CpxR, and targeting a drug to them is no small task. As such, we wanted to evaluate an upstream sensor of CpxRA, and determine whether its manipulation would also alter the outcome of infection. To this end, we targeted NlpE, the reported outer membrane lipoprotein activator of CpxRA.

Along with σ^E , Cpx is one of the key envelope stress responses of Gram negative bacteria. The literature reports the outer membrane-bound lipoprotein NlpE as an activator of the Cpx response. Cpx responds to a multitude of stimuli, some NlpE-dependent, some NlpE-independent, and some uncharacterized. In terms of NlpE-dependent cues, the Cpx response is activated upon binding to abiotic surfaces, such as glass beads, as well as due to artificial mislocalization of NlpE [181, 182, 189]. Alkaline pH, a known inducer of Cpx, is NlpE-independent [179, 184]. Overproduction of Type IV pilus subunits is an inducer where the role of NlpE is unknown [185]. *In vitro*, it has been shown that NlpE contributes to the upregulation of EHEC T3SS, and downregulation of flagellin [269]. Prior to our work, the role of NlpE in *C. rodentium* virulence

was unknown. In this thesis, we show that infection by *C. rodentium*, and the virulence effect of CpxRA in this system, is independent of the auxiliary proteins NlpE and CpxP. CpxP is a periplasmic negative regulator, generally at a stoichiometry ratio of 10:1 CpxP:CpxA; however, upon deletion of *cpxP* we detected no hyper-activation of the Cpx response, which we hypothesized would be mirrored by increased survival of susceptible mice, as it has been shown that constitutive activation of Cpx leads to an attenuated phenotype in other bacteria [191, 362].

The $\Delta cpxRA$ C. rodentium strain presented a striking attenuation with 100% survival of susceptible mice. In contrast, the auxiliary protein mutants $\Delta nlpE$ and $\Delta cpxP$ were comparable to wild-type C. rodentium in virulence, as well as localization in vivo and adherence in vitro. As such, in an attempt to elucidate the mechanism behind the attenuation of the $\Delta cpxRA$ strain, we performed microarrays, using $\Delta nlpE$ and $\Delta cpxP$ as internal comparison controls. We detected a multitude of genes which were downregulated or upregulated relative to wild-type, and some genes were specific to one strain, whereas others were shared between two or all three strains. In order to further analyze the data, we hypothesized that loss of virulence may correlate with loss of gene expression, meaning that genes which were downregulated in the $\Delta cpxRA$ strain should be either unchanged or upregulated in the $\Delta nlpE$ and $\Delta cpxP$ strains.

A previous microarray analysis of the NlpE-dependent effects in *E. coli* used NlpE overexpression as the inducing cue for the CpxRA TCS, and detected many genes in peptidoglycan crosslinking, antibiotic resistance, small RNAs, and membrane integrity [198, 363-365]. In contrast, in our analysis we deleted NlpE from *C. rodentium*, and grew the bacteria in previously determined inducing conditions (DMEM).

In our microarray analysis of the $\Delta cpxRA$ strain, we detected the downregulation of multiple genes involved in maltose metabolism, such as the maltoporin *lamB*, the substrate-binding

protein *malE*, the permease protein *malG*, the maltodextrin phosphorylase *malP*, the periplasmic protein *malM*, the ATP-binding protein *malK*, and the permease protein mslF. In the intestine, *E coli* uses up to seven different sugars for its growth and colonization [281, 366]. Glycogen is known as the primary carbon source for energy storage of enteric bacteria such as *E. coli*, in order to ensure energy availability in times of starvation [367]. Breakdown of glycogen involves maltose as an intermediate, and a recent paper reported that ability to use maltose as a source of energy gives EHEC a competitive advantage to colonize the mouse intestine, when compared to commensal *E. coli* [280]. As such, the downregulation of these genes may play a role in the virulence effect of the cpxRA mutant, due to its inability to use maltose as a carbon source. Further experiments to specifically test the role of maltose metabolism in *C. rodentium* virulence would be needed to further evaluate this hypothesis.

Within our microarray dataset we detected significant downregulation of the genes cts1F and cts1G in the $\Delta cpxRA$ strain, both associated with the T6SS. The type 6 secretion system (T6SS) is a needle-like apparatus which can be required in interbacterial competition, but can also inject effectors into host cells that interfere with the cytoskeleton [275-277]. In *Salmonella enterica* serovar Typhimurium, a functional T6SS, encoded within the SPI-6 pathogenicity island, is absolutely required for successful intestinal colonization [368]. *S. enterica* targets commensal bacteria with the T6SS [368]. The *C. rodentium* genome encodes two T6SS clusters, CTS1 and CTS2 [56, 278]. The CTS1 T6SS has a premature stop codon in the cts1I gene, due to a frameshift mutation, but due to slippage this is overcome, leading once again to a functional T6SS [278, 279]. Two genes of the CTS1 were differentially regulated in our microarray analysis. The gene cts1F encodes a Forkhead-associated protein, whereas cts1G encodes a protein within the VrgG family which act as cell-puncturing devices at the tip of the T6SS and are then secreted into the host cell

for actin crosslinking [56, 276]. Surprisingly, the role of the T6SS in *C. rodentium* virulence has yet to be assessed, as per the literature. We hypothesize that, the downregulation of CTS1 in *C. rodentium* $\Delta cpxRA$ could be disabling it from competing with commensal bacteria for colonization.

In all, we do recognize the limitations of microarrays as opposed to more recent techniques such as RNA sequencing, given the number of steps and manipulations the samples must undergo in order to be labelled and read successfully, leading to loss of information. Despite the limitations of microarrays, we were able to validate our results (Appendix - Figure A1), and detect some interesting candidates for further assessment. Notably, a very recent paper published in December 2018, while this thesis was in preparation, evaluated the regulon of CpxRA using RNA sequencing and SILAC. While the analysis was done in different growth conditions than the ones we used, which could have a direct effect on gene expression, we did note some similarities. Both our study and the paper by Vogt and colleagues detected multiple genes of maltose metabolism, as well as the outer membrane protein F, *ompF*, to be downregulated in the CpxRA mutant [369]. This suggests that both of these targets may be rather robust and likely candidates, and it further validates our microarray analysis.

NleA undergoes an apparent mobility shift upon translocation into the host cell

Bacterial effectors are secreted into the host cells to carry out a myriad of functions, often with a certain amount of redundancy. Bacterial effectors can act in a multitude of ways, by direct binding, functional mimicry, structural mimicry, post-translational modification of host proteins, as well as by exhibiting novel protease function [370]. Post-translational modification of an

effector may be a protective response by the host, or conversely, the pathogen may hijack host cell processes for its own protection. Some common post-translational modifications include phosphorylation, lipidation, SUMOylation, and ubiquitination [371]. Most commonly, these modifications aid to target the effectors to a particular subcompartment of the host cell, or to regulate the function of the effector [371]. The A/E pathogen effector Tir is phosphorylated at tyrosine, serine and threonine residues, leading to a 12kDa increase in apparent mobility [99]. Similarly, the effector CagA of *Helicobacter pylori* is tyrosine phosphorylated by the host, affecting its ability to trigger cell elongation and cytoskeleton rearrangement [372, 373]. Ubiquitination adds a ubiquitin molecule on lysine residues [374]. Ubiquitination of the Salmonella effectors SopE and SptP lead to their targeting by the proteasome for degradation [375]. In contrast, the ubiquitination of SopB leads to activation of effector function and relocalization within the host cell [376, 377]. SUMOylation involves the addition of small ubiquitinlike modifier (SUMO) family of proteins on lysine residues [378]. The addition of these molecules can alter many pathways, such as metabolic pathways, endocytic trafficking of receptors, and resistance to pathogens [379]. In the zoonotic pathogen Anaplasma phagocytophilum, the poly-SUMOylation of effector AmpA enhances its ability to survive within the host [380]. Finally, one possible type of lipidation is S-prenylation, which adds isoprene groups to cysteine residues within 5 amino acids of the C terminus [371]. The isoprene groups are usually farnesyl or geranylgeranyl [371]. The Legionella pneumophila effector AnkB is farnesylated, and this modification is critical for activity, as loss of farnesylation lead to decreased survival *in vivo*, in mouse lungs [381, 382].

In contrast, the apparent mobility shift of NleA is due to neither phosphorylation, nor ubiquitination, as shown by experiments with λ phosphatase, and immunoblotting of total ubiquitin in immunoprecipitated NleA samples, respectively. Further, NleA does not undergo N-

glycosylation or the most common types of O-glycosylation, as suggested by experiments with deglycosylation enzymes PNGase F, O-glycosidase, neuraminidase, β 1-4 Galactosidase, and β -N-acetylglucosaminidase. However, with the use of the conditionally glycosylation-deficient CHO cell line LDLD, we have obtained data consistent with the possibility that NleA is O-glycosylated. It is known that NleA localizes to the Golgi of host cells, which is a common site of mucin-type O-GlcNAc glycosylation. Although this remains to be confirmed, if true it would represent the first report of an O-glycosylated bacterial effector. Further experiments are required to confirm this modification and to denote the role this modification may play during infection.

Conclusion

The A/E pathogens *C. rodentium*, EPEC, and EHEC, form characteristic attaching and effacing lesions in order to colonize the host. In order to sense the environment of the host and respond to stimuli, these pathogens use TCSs. In Chapter 2 of this thesis, we evaluated all 26 TCSs of *C. rodentium* and their effect in virulence of this murine-specific pathogen. We identified and characterized several TCSs with positive roles in the virulence of *C. rodentium*. The $\Delta arcA$ strain possesses a significant decrease in the expression of components of the T3SS, and the $\Delta rcsB$ strain may have a defect in colanic acid synthesis, providing potential explanations for their virulence effects. The $\Delta cpxRA$ strain showed the most striking virulence defect, and it was neither due to T3SS regulation nor colanic acid biosynthesis. In Chapter 3, we evaluated this virulence effect further by deleting the outer membrane lipoprotein NlpE, as well as the periplasmic regulator CpxP in *C. rodentium* and evaluating their effects in virulence. We have determined that the virulence effect of CpxRA is independent of the auxiliary proteins NlpE and CpxP. Using microarrays, we detected 393 genes differentially regulated in the $\Delta cpxRA$ strain, of which 162 genes were

downregulated in the $\Delta cpxRA$ strain while being upregulated or unchanged in the Cpx auxiliary protein deletion strains. This group of genes is composed of genes playing a role in a multitude of pathways, such as T6SS, colanic acid synthesis, and maltose metabolism. Finally, in Chapter 4 of this thesis, we detected a host-mediated post-translational modification of the T3SS secreted effector NleA. We determined that the apparent mobility shift of NleA on SDS-PAGE gels is not due to phosphorylation, ubiquitination, or N-glycosylation. Using a conditionally glycosylation deficient cell line, we have gathered evidence that NleA may be O-glycosylated by the host. To our knowledge, this is the first report of an O-glycosylated bacterial effector, and the implication in virulence of *C. rodentium* remains to be determined.

REFERENCES

- 1. Croxen, M.A., et al., *Recent advances in understanding enteric pathogenic Escherichia coli*. Clin Microbiol Rev, 2013. **26**(4): p. 822-80.
- 2. Goosney, D.L., S. Gruenheid, and B.B. Finlay, *Gut feelings: enteropathogenic E. coli* (EPEC) interactions with the host. Annu Rev Cell Dev Biol, 2000. **16**: p. 173-89.
- 3. Moon, H.W., et al., *Attaching and effacing activities of rabbit and human enteropathogenic Escherichia coli in pig and rabbit intestines*. Infect Immun, 1983. **41**(3): p. 1340-51.
- 4. Elliott, S.J., et al., *The complete sequence of the locus of enterocyte effacement (LEE) from enteropathogenic Escherichia coli E2348/69*. Molecular Microbiology, 1998. **28**(1): p. 1-4
- 5. McDaniel, T.K., et al., A genetic locus of enterocyte effacement conserved among diverse enterobacterial pathogens. Proc Natl Acad Sci U S A, 1995. **92**(5): p. 1664-8.
- 6. Deng, W., et al., *Dissecting virulence: systematic and functional analyses of a pathogenicity island.* Proc Natl Acad Sci U S A, 2004. **101**(10): p. 3597-602.
- 7. Deng, W., et al., Locus of Enterocyte Effacement from Citrobacter rodentium: Sequence Analysis and Evidence for Horizontal Transfer among Attaching and Effacing Pathogens. Infection and Immunity, 2001. **69**(10): p. 6323.
- 8. Nguyen, Y. and V. Sperandio, *Enterohemorrhagic E. coli (EHEC) pathogenesis*. Front Cell Infect Microbiol, 2012. **2**: p. 90.
- 9. Kenny, B., et al., Enteropathogenic E. coli (EPEC) transfers its receptor for intimate adherence into mammalian cells. Cell, 1997. **91**(4): p. 511-20.
- 10. Kalman, D., et al., Enteropathogenic E. coli acts through WASP and Arp2/3 complex to form actin pedestals. Nat Cell Biol, 1999. 1(6): p. 389-91.
- 11. Nataro, J.P. and J.B. Kaper, *Diarrheagenic Escherichia coli*. Clin Microbiol Rev, 1998. **11**(1): p. 142-201.
- 12. Tacket, C.O., et al., *Role of EspB in experimental human enteropathogenic Escherichia coli infection.* Infect Immun, 2000. **68**(6): p. 3689-95.
- 13. Trabulsi, L.R., R. Keller, and T.A. Tardelli Gomes, *Typical and atypical enteropathogenic Escherichia coli*. Emerg Infect Dis, 2002. **8**(5): p. 508-13.
- 14. Chen, H.D. and G. Frankel, *Enteropathogenic Escherichia coli: unravelling pathogenesis*. FEMS Microbiol Rev, 2005. **29**(1): p. 83-98.
- 15. Vallance, B.A. and B.B. Finlay, *Exploitation of host cells by enteropathogenic Escherichia coli*. Proc Natl Acad Sci U S A, 2000. **97**(16): p. 8799-806.
- 16. Ochoa, T.J. and C.A. Contreras, *Enteropathogenic escherichia coli infection in children*. Curr Opin Infect Dis, 2011. **24**(5): p. 478-83.
- 17. Kaper, J.B., J.P. Nataro, and H.L. Mobley, *Pathogenic Escherichia coli*. Nat Rev Microbiol, 2004. **2**(2): p. 123-40.
- 18. Riley, L.W., et al., *Hemorrhagic colitis associated with a rare Escherichia coli serotype*. N Engl J Med, 1983. **308**(12): p. 681-5.
- 19. Wells, J.G., et al., *Laboratory investigation of hemorrhagic colitis outbreaks associated with a rare Escherichia coli serotype*. J Clin Microbiol, 1983. **18**(3): p. 512-20.
- 20. Burnens, A.P., et al., *Prevalence and clinical significance of vero-cytotoxin-producing Escherichia coli (VTEC) isolated from cattle in herds with and without calf diarrhoea.* Zentralbl Veterinarmed B, 1995. **42**(5): p. 311-8.

- 21. Griffin, P.M. and R.V. Tauxe, *The epidemiology of infections caused by Escherichia coli O157:H7*, other enterohemorrhagic E. coli, and the associated hemolytic uremic syndrome. Epidemiol Rev, 1991. **13**: p. 60-98.
- 22. Hancock, D.D., et al., *The prevalence of Escherichia coli O157.H7 in dairy and beef cattle in Washington State.* Epidemiol Infect, 1994. **113**(2): p. 199-207.
- Wells, J.G., et al., *Isolation of Escherichia coli serotype O157:H7 and other Shiga-like-toxin-producing E. coli from dairy cattle.* J Clin Microbiol, 1991. **29**(5): p. 985-9.
- 24. Pruimboom-Brees, I.M., et al., *Cattle lack vascular receptors for Escherichia coli O157:H7 Shiga toxins*. Proc Natl Acad Sci U S A, 2000. **97**(19): p. 10325-9.
- 25. Le Saux, N., et al., *Ground beef consumption in noncommercial settings is a risk factor for sporadic Escherichia coli O157:H7 infection in Canada*. J Infect Dis, 1993. **167**(2): p. 500-2.
- 26. Mead, P.S., et al., *Risk factors for sporadic infection with Escherichia coli O157:H7*. Arch Intern Med, 1997. **157**(2): p. 204-8.
- 27. Morgan, G.M., et al., *First recognized community outbreak of haemorrhagic colitis due to verotoxin-producing Escherichia coli O 157.H7 in the UK*. Epidemiol Infect, 1988. **101**(1): p. 83-91.
- 28. Besser, R.E., et al., An outbreak of diarrhea and hemolytic uremic syndrome from Escherichia coli O157:H7 in fresh-pressed apple cider. Jama, 1993. **269**(17): p. 2217-20.
- 29. Swinbanks, D., *Japan shuns radishes after 'possible link' to E. coli.* Nature, 1996. **382**(6592): p. 567.
- 30. From the Centers for Disease Control and Prevention. Outbreaks of Escherichia coli O157:H7 infection associated with eating alfalfa sprouts--Michigan and Virginia, June-July 1997. Jama, 1997. 278(10): p. 809-10.
- 31. Keene, W.E., et al., *A swimming-associated outbreak of hemorrhagic colitis caused by Escherichia coli O157:H7 and Shigella sonnei*. N Engl J Med, 1994. **331**(9): p. 579-84.
- 32. Swerdlow, D.L., et al., *A waterborne outbreak in Missouri of Escherichia coli 0157:H7 associated with bloody diarrhea and death.* Ann Intern Med, 1992. **117**(10): p. 812-9.
- 33. Yang, B., et al., Enterohemorrhagic Escherichia coli senses low biotin status in the large intestine for colonization and infection. Nature Communications, 2015. **6**: p. 6592.
- 34. Beckett, D., Biotin sensing at the molecular level. J Nutr, 2009. 139(1): p. 167-70.
- 35. Said, H.M., *Cell and molecular aspects of human intestinal biotin absorption*. J Nutr, 2009. **139**(1): p. 158-62.
- 36. Karmali, M.A., et al., Sporadic cases of haemolytic-uraemic syndrome associated with faecal cytotoxin and cytotoxin-producing Escherichia coli in stools. Lancet, 1983. 1(8325): p. 619-20.
- 37. Tarr, P.I., C.A. Gordon, and W.L. Chandler, *Shiga-toxin-producing Escherichia coli and haemolytic uraemic syndrome*. The Lancet, 2005. **365**(9464): p. 1073-1086.
- Wong, C.S., et al., *Risk factors for the hemolytic uremic syndrome in children infected with Escherichia coli O157:H7: a multivariable analysis.* Clin Infect Dis, 2012. **55**(1): p. 33-41.
- 39. Rangel, J.M., et al., *Epidemiology of Escherichia coli O157:H7 outbreaks, United States, 1982-2002.* Emerg Infect Dis, 2005. **11**(4): p. 603-9.
- 40. Mayer, C.L., et al., *Shiga toxins and the pathophysiology of hemolytic uremic syndrome in humans and animals.* Toxins (Basel), 2012. **4**(11): p. 1261-87.

- 41. Scheutz, F., et al., *Multicenter evaluation of a sequence-based protocol for subtyping Shiga toxins and standardizing Stx nomenclature.* J Clin Microbiol, 2012. **50**(9): p. 2951-63.
- 42. Boerlin, P., et al., Associations between virulence factors of Shiga toxin-producing Escherichia coli and disease in humans. J Clin Microbiol, 1999. **37**(3): p. 497-503.
- 43. O'Brien, A.D. and R.K. Holmes, *Shiga and Shiga-like toxins*. Microbiol Rev, 1987. **51**(2): p. 206-20.
- 44. Strockbine, N.A., et al., Two toxin-converting phages from Escherichia coli O157:H7 strain 933 encode antigenically distinct toxins with similar biologic activities. Infect Immun, 1986. 53(1): p. 135-40.
- 45. Schuller, S., *Shiga toxin interaction with human intestinal epithelium*. Toxins (Basel), 2011. **3**(6): p. 626-39.
- 46. Obrig, T.G., *Escherichia coli Shiga Toxin Mechanisms of Action in Renal Disease*. Toxins (Basel), 2010. **2**(12): p. 2769-2794.
- 47. Bauwens, A., et al., Facing glycosphingolipid-Shiga toxin interaction: dire straits for endothelial cells of the human vasculature. Cell Mol Life Sci, 2013. **70**(3): p. 425-57.
- 48. Tesh, V.L., *Activation of cell stress response pathways by Shiga toxins*. Cell Microbiol, 2012. **14**(1): p. 1-9.
- 49. Croxen, M.A. and B.B. Finlay, *Molecular mechanisms of Escherichia coli pathogenicity*. Nat Rev Microbiol, 2010. **8**(1): p. 26-38.
- 50. Muto, T., et al., *Infectious megaenteron of mice. I. Manifestation and pathological observation.* Jpn J Med Sci Biol, 1969. **22**(6): p. 363-74.
- 51. Brennan, P.C., et al., *Citrobacter freundii associated with diarrhea in laboratory mice* Lab Anim Care, 1965. **15**: p. 266-75.
- 52. Barthold, S.W., et al., *The etiology of transmissible murine colonic hyperplasia*. Lab Anim Sci, 1976. **26**(6 Pt 1): p. 889-94.
- 53. Lenz, A., J. Tomkins, and A.J. Fabich, *Draft Genome Sequence of Citrobacter rodentium DBS100 (ATCC 51459), a Primary Model of Enterohemorrhagic Escherichia coli Virulence.* Genome Announc, 2015. **3**(3).
- 54. Schauer, D.B., et al., *Genetic and biochemical characterization of Citrobacter rodentium sp. nov.* J Clin Microbiol, 1995. **33**(8): p. 2064-8.
- 55. Schauer, D.B. and S. Falkow, *The eae gene of Citrobacter freundii biotype 4280 is necessary for colonization in transmissible murine colonic hyperplasia.* Infect Immun, 1993. **61**(11): p. 4654-61.
- 56. Petty, N.K., et al., *The Citrobacter rodentium Genome Sequence Reveals Convergent Evolution with Human Pathogenic Escherichia coli.* J Bacteriol, 2010. **192**(2): p. 525-38.
- Wiles, S., et al., Organ specificity, colonization and clearance dynamics in vivo following oral challenges with the murine pathogen Citrobacter rodentium. Cell Microbiol, 2004. **6**(10): p. 963-72.
- 58. Mundy, R., et al., *Citrobacter rodentium of mice and man*. Cell Microbiol, 2005. **7**(12): p. 1697-706.
- 59. Borenshtein, D., et al., *Development of fatal colitis in FVB mice infected with Citrobacter rodentium.* Infect Immun, 2007. **75**(7): p. 3271-81.
- 60. Diez, E., et al., *Identification and characterization of Cri1, a locus controlling mortality during Citrobacter rodentium infection in mice.* Genes Immun, 2011. **12**(4): p. 280-90.
- 61. van der Flier, L.G. and H. Clevers, *Stem cells, self-renewal, and differentiation in the intestinal epithelium.* Annu Rev Physiol, 2009. **71**: p. 241-60.

- 62. Papapietro, O., et al., *R-spondin 2 signalling mediates susceptibility to fatal infectious diarrhoea*. Nat Commun, 2013. **4**: p. 1898.
- 63. Kim, Y.S. and S.B. Ho, *Intestinal goblet cells and mucins in health and disease: recent insights and progress.* Curr Gastroenterol Rep, 2010. **12**(5): p. 319-30.
- 64. Atuma, C., et al., *The adherent gastrointestinal mucus gel layer: thickness and physical state in vivo*. Am J Physiol Gastrointest Liver Physiol, 2001. **280**(5): p. G922-9.
- 65. Johansson, M.E., J.M. Larsson, and G.C. Hansson, *The two mucus layers of colon are organized by the MUC2 mucin, whereas the outer layer is a legislator of host-microbial interactions.* Proc Natl Acad Sci U S A, 2011. **108 Suppl 1**(Suppl 1): p. 4659-65.
- 66. Johansson, M.E., K.A. Thomsson, and G.C. Hansson, *Proteomic analyses of the two mucus layers of the colon barrier reveal that their main component, the Muc2 mucin, is strongly bound to the Fcgbp protein.* J Proteome Res, 2009. **8**(7): p. 3549-57.
- 67. Kang, E., et al., Loss of disease tolerance during Citrobacter rodentium infection is associated with impaired epithelial differentiation and hyperactivation of T cell responses. Sci Rep, 2018. **8**(1): p. 847.
- 68. Gibson, D.L., et al., *Toll-like receptor 2 plays a critical role in maintaining mucosal integrity during Citrobacter rodentium-induced colitis.* Cell Microbiol, 2008. **10**(2): p. 388-403.
- 69. Gibson, D.L., et al., *Interleukin-11 reduces TLR4-induced colitis in TLR2-deficient mice and restores intestinal STAT3 signaling*. Gastroenterology, 2010. **139**(4): p. 1277-88.
- 70. Khan, M.A., et al., *Toll-Like Receptor 4 Contributes to Colitis Development but Not to Host Defense during Citrobacter rodentium Infection in Mice.* Infection and Immunity, 2006. 74(5): p. 2522-2536.
- 71. Collins, J.W., et al., *Citrobacter rodentium: infection, inflammation and the microbiota.* Nature Reviews Microbiology, 2014. **12**: p. 612.
- 72. Gibson, D.L., et al., MyD88 signalling plays a critical role in host defence by controlling pathogen burden and promoting epithelial cell homeostasis during Citrobacter rodentium-induced colitis. Cell Microbiol, 2008. **10**(3): p. 618-31.
- 73. Rathinam, V.A., et al., *TRIF licenses caspase-11-dependent NLRP3 inflammasome activation by gram-negative bacteria.* Cell, 2012. **150**(3): p. 606-19.
- 74. Kayagaki, N., et al., *Non-canonical inflammasome activation targets caspase-11*. Nature, 2011. **479**(7371): p. 117-21.
- 75. Liu, Z., et al., Role of Inflammasomes in Host Defense against Citrobacter rodentium Infection. J Biol Chem, 2012. **287**(20): p. 16955-64.
- 76. Vallance, B.A., et al., *Mice Lacking T and B Lymphocytes Develop Transient Colitis and Crypt Hyperplasia yet Suffer Impaired Bacterial Clearance during Citrobacter rodentium Infection. Infection and Immunity, 2002. 70(4): p. 2070-2081.*
- 77. Simmons, C.P., et al., Central Role for B Lymphocytes and CD4⁺ T Cells in Immunity to Infection by the Attaching and Effacing Pathogen Citrobacter rodentium. Infection and Immunity, 2003. 71(9): p. 5077-5086.
- 78. O'Quinn, D.B., et al., *Emergence of the Th17 pathway and its role in host defense*. Adv Immunol, 2008. **99**: p. 115-63.
- 79. Monteleone, I., F. Pallone, and G. Monteleone, *Th17-related cytokines: new players in the control of chronic intestinal inflammation.* BMC Med, 2011. **9**: p. 122.

- 80. Ota, N., et al., *IL-22 bridges the lymphotoxin pathway with the maintenance of colonic lymphoid structures during infection with Citrobacter rodentium.* Nature Immunology, 2011. **12**: p. 941.
- 81. Willing, B.P., et al., *Altering Host Resistance to Infections through Microbial Transplantation*. PLOS ONE, 2011. **6**(10): p. e26988.
- 82. Ghosh, S., et al., Colonic microbiota alters host susceptibility to infectious colitis by modulating inflammation, redox status, and ion transporter gene expression. Am J Physiol Gastrointest Liver Physiol, 2011. **301**(1): p. G39-49.
- 83. Ivanov, II, et al., *Induction of intestinal Th17 cells by segmented filamentous bacteria*. Cell, 2009. **139**(3): p. 485-98.
- 84. Kamada, N., et al., Regulated Virulence Controls the Ability of a Pathogen to Compete with the Gut Microbiota. Science, 2012. **336**(6086): p. 1325-1329.
- 85. Coburn, B., I. Sekirov, and B.B. Finlay, *Type III secretion systems and disease*. Clin Microbiol Rev, 2007. **20**(4): p. 535-49.
- 86. Garmendia, J., G. Frankel, and V.F. Crepin, *Enteropathogenic and enterohemorrhagic Escherichia coli infections: translocation, translocation, translocation.* Infect Immun, 2005. **73**(5): p. 2573-85.
- 87. Cornelis, G.R., *The type III secretion injectisome*. Nat Rev Microbiol, 2006. **4**(11): p. 811-25.
- 88. McDaniel, T.K. and J.B. Kaper, A cloned pathogenicity island from enteropathogenic Escherichia coli confers the attaching and effacing phenotype on E. coli K-12. Mol Microbiol, 1997. **23**(2): p. 399-407.
- 89. Knutton, S., et al., A novel EspA-associated surface organelle of enteropathogenic Escherichia coli involved in protein translocation into epithelial cells. Embo j, 1998. 17(8): p. 2166-76.
- 90. Sekiya, K., et al., Supermolecular structure of the enteropathogenic Escherichia coli type III secretion system and its direct interaction with the EspA-sheath-like structure. Proc Natl Acad Sci U S A, 2001. **98**(20): p. 11638-43.
- 91. Ide, T., et al., Characterization of translocation pores inserted into plasma membranes by type III-secreted Esp proteins of enteropathogenic Escherichia coli. Cell Microbiol, 2001. **3**(10): p. 669-79.
- 92. Zarivach, R., et al., *Structural analysis of a prototypical ATPase from the type III secretion system.* Nat Struct Mol Biol, 2007. **14**(2): p. 131-7.
- 93. Jarvis, K.G. and J.B. Kaper, Secretion of extracellular proteins by enterohemorrhagic Escherichia coli via a putative type III secretion system. Infect Immun, 1996. **64**(11): p. 4826-9.
- 94. Deng, W., et al., Regulation of type III secretion hierarchy of translocators and effectors in attaching and effacing bacterial pathogens. Infect Immun, 2005. **73**(4): p. 2135-46.
- 95. Wang, D., et al., *Hierarchal type III secretion of translocators and effectors from Escherichia coli O157:H7 requires the carboxy terminus of SepL that binds to Tir.* Mol Microbiol, 2008. **69**(6): p. 1499-512.
- 96. Dean, P. and B. Kenny, *The effector repertoire of enteropathogenic E. coli: ganging up on the host cell.* Curr Opin Microbiol, 2009. **12**(1): p. 101-9.
- 97. Dean, P., M. Maresca, and B. Kenny, *EPEC's weapons of mass subversion*. Current Opinion in Microbiology, 2005. **8**(1): p. 28-34.

- 98. Backert, S., et al., *PKA-mediated phosphorylation of EPEC-Tir at serine residues 434 and 463: A novel pathway in regulating Rac1 GTPase function.* Gut Microbes, 2010. **1**(2): p. 94-9.
- 99. Kenny, B., *Phosphorylation of tyrosine 474 of the enteropathogenic Escherichia coli* (EPEC) Tir receptor molecule is essential for actin nucleating activity and is preceded by additional host modifications. Mol Microbiol, 1999. **31**(4): p. 1229-41.
- 100. Schuller, S., et al., *Tir phosphorylation and Nck/N-WASP recruitment by enteropathogenic and enterohaemorrhagic Escherichia coli during ex vivo colonization of human intestinal mucosa is different to cell culture models.* Cell Microbiol, 2007. **9**(5): p. 1352-64.
- 101. Allen-Vercoe, E., et al., Amino Acid Residues within Enterohemorrhagic Escherichia coli 0157:H7 Tir Involved in Phosphorylation, α-Actinin Recruitment, and Nck-Independent Pedestal Formation. Infect Immun, 2006. 74(11): p. 6196-205.
- 102. Deng, W., et al., Citrobacter rodentium translocated intimin receptor (Tir) is an essential virulence factor needed for actin condensation, intestinal colonization and colonic hyperplasia in mice. Mol Microbiol, 2003. **48**(1): p. 95-115.
- 103. Campellone, K.G. and J.M. Leong, *Tails of two Tirs: actin pedestal formation by enteropathogenic E. coli and enterohemorrhagic E. coli O157:H7*. Curr Opin Microbiol, 2003. **6**(1): p. 82-90.
- 104. Campellone, K.G., D. Robbins, and J.M. Leong, *EspFU is a translocated EHEC effector that interacts with Tir and N-WASP and promotes Nck-independent actin assembly.* Dev Cell, 2004. **7**(2): p. 217-28.
- 105. Garmendia, J., et al., *TccP is an enterohaemorrhagic Escherichia coli O157:H7 type III effector protein that couples Tir to the actin-cytoskeleton.* Cell Microbiol, 2004. **6**(12): p. 1167-83.
- 106. Frankel, G. and A.D. Phillips, *Attaching effacing Escherichia coli and paradigms of Tirtriggered actin polymerization: getting off the pedestal.* Cellular Microbiology, 2008. **10**(3): p. 549-556.
- 107. Cantarelli, V.V., et al., Tyrosine phosphorylation controls cortactin binding to two enterohaemorrhagic Escherichia coli effectors: Tir and EspFu/TccP. Cell Microbiol, 2007. 9(7): p. 1782-95.
- 108. Weiss, S.M., et al., *IRSp53 links the enterohemorrhagic E. coli effectors Tir and EspFU for actin pedestal formation*. Cell Host Microbe, 2009. **5**(3): p. 244-58.
- 109. Kenny, B. and M. Jepson, *Targeting of an enteropathogenic Escherichia coli (EPEC)* effector protein to host mitochondria. Cell Microbiol, 2000. **2**(6): p. 579-90.
- 110. Kenny, B., et al., Co-ordinate regulation of distinct host cell signalling pathways by multifunctional enteropathogenic Escherichia coli effector molecules. Mol Microbiol, 2002. 44(4): p. 1095-1107.
- 111. Alto, N.M., et al., *Identification of a bacterial type III effector family with G protein mimicry functions*. Cell, 2006. **124**(1): p. 133-45.
- Huang, Z., et al., Structural insights into host GTPase isoform selection by a family of bacterial GEF mimics. Nat Struct Mol Biol, 2009. **16**(8): p. 853-60.
- 113. Jepson, M.A., et al., Synergistic roles for the Map and Tir effector molecules in mediating uptake of enteropathogenic Escherichia coli (EPEC) into non-phagocytic cells. Cell Microbiol, 2003. 5(11): p. 773-83.

- 114. Dean, P. and B. Kenny, *Intestinal barrier dysfunction by enteropathogenic Escherichia coli is mediated by two effector molecules and a bacterial surface protein.* Mol Microbiol, 2004. **54**(3): p. 665-75.
- 115. Ma, C., et al., Citrobacter rodentium infection causes both mitochondrial dysfunction and intestinal epithelial barrier disruption in vivo: role of mitochondrial associated protein (Map). Cell Microbiol, 2006. **8**(10): p. 1669-86.
- 116. A., G.J., et al., *Attaching and effacing pathogen-induced tight junction disruption in vivo*. Cellular Microbiology, 2006. **8**(4): p. 634-645.
- 117. Mundy, R., et al., *Identification of a novel Citrobacter rodentium type III secreted protein, EspI, and roles of this and other secreted proteins in infection.* Infect Immun, 2004. **72**(4): p. 2288-302.
- 118. Nougayrede, J.P. and M.S. Donnenberg, *Enteropathogenic Escherichia coli EspF is targeted to mitochondria and is required to initiate the mitochondrial death pathway*. Cell Microbiol, 2004. **6**(11): p. 1097-111.
- 119. Dean, P., et al., The enteropathogenic E. coli effector EspF targets and disrupts the nucleolus by a process regulated by mitochondrial dysfunction. PLoS Pathog, 2010. **6**(6): p. e1000961.
- 120. Nagai, T., A. Abe, and C. Sasakawa, *Targeting of enteropathogenic Escherichia coli EspF* to host mitochondria is essential for bacterial pathogenesis: critical role of the 16th leucine residue in EspF. J Biol Chem, 2005. **280**(4): p. 2998-3011.
- 121. Marchès, O., et al., *EspF of Enteropathogenic Escherichia coli Binds Sorting Nexin 9*. Journal of Bacteriology, 2006. **188**(8): p. 3110-3115.
- 122. Nougayrede, J.P., G.H. Foster, and M.S. Donnenberg, *Enteropathogenic Escherichia coli effector EspF interacts with host protein Abcf2*. Cell Microbiol, 2007. **9**(3): p. 680-93.
- 123. Thanabalasuriar, A., et al., *The bacterial virulence factor NleA is required for the disruption of intestinal tight junctions by enteropathogenic Escherichia coli.* Cell Microbiol, 2010. **12**(1): p. 31-41.
- 124. Dean, P., et al., *The bacterial effectors EspG and EspG2 induce a destructive calpain activity that is kept in check by the co-delivered Tir effector*. Cell Microbiol, 2010. **12**(9): p. 1308-21.
- 125. Tomson, F.L., et al., Enteropathogenic Escherichia coli EspG disrupts microtubules and in conjunction with Orf3 enhances perturbation of the tight junction barrier. Mol Microbiol, 2005. **56**(2): p. 447-64.
- 126. Holmes, A., et al., *The EspF Effector, a Bacterial Pathogen's Swiss Army Knife*. Infection and Immunity, 2010. **78**(11): p. 4445-4453.
- 127. Hodges, K., et al., *The enteropathogenic Escherichia coli effector protein EspF decreases sodium hydrogen exchanger 3 activity.* Cell Microbiol, 2008. **10**(8): p. 1735-45.
- 128. Guttman, J.A., et al., *Aquaporins contribute to diarrhoea caused by attaching and effacing bacterial pathogens*. Cell Microbiol, 2007. **9**(1): p. 131-41.
- Dean, P., et al., *Potent diarrheagenic mechanism mediated by the cooperative action of three enteropathogenic Escherichia coli-injected effector proteins. Proceedings of the National Academy of Sciences of the United States of America, 2006. 103(6): p. 1876-1881.*
- 130. Weflen, A.W., et al., *E. coli secreted protein F promotes EPEC invasion of intestinal epithelial cells via an SNX9-dependent mechanism.* Cell Microbiol, 2010. **12**(7): p. 919-29.

- 131. Marchès, O., et al., Enteropathogenic and enterohaemorrhagic Escherichia coli deliver a novel effector called Cif, which blocks cell cycle G2/M transition. Molecular Microbiology, 2003. **50**(5): p. 1553-1567.
- 132. Gruenheid, S., et al., *Identification and characterization of NleA, a non-LEE-encoded type III translocated virulence factor of enterohaemorrhagic Escherichia coli O157:H7*. Mol Microbiol, 2004. **51**(5): p. 1233-49.
- 133. Loukiadis, E., et al., *Distribution, functional expression, and genetic organization of Cif, a phage-encoded type III-secreted effector from enteropathogenic and enterohemorrhagic Escherichia coli.* J Bacteriol, 2008. **190**(1): p. 275-85.
- 134. García-Angulo, V.A., et al., Regulation of Expression and Secretion of NleH, a New Non-Locus of Enterocyte Effacement-Encoded Effector in Citrobacter rodentium. J Bacteriol, 2008. 190(7): p. 2388-99.
- 135. Pham, T.H., et al., Escherichia coli virulence protein NleH1 interaction with the v-Crk sarcoma virus CT10 oncogene-like protein (CRKL) governs NleH1 inhibition of the ribosomal protein S3 (RPS3)/nuclear factor κB (NF-κB) pathway. J Biol Chem, 2013. 288(48): p. 34567-74.
- 136. Dahan, S., et al., EspJ is a prophage-carried type III effector protein of attaching and effacing pathogens that modulates infection dynamics. Infect Immun, 2005. **73**(2): p. 679-86.
- 137. Blasche, S., et al., *The EHEC-host interactome reveals novel targets for the translocated intimin receptor.* Sci Rep, 2014. **4**: p. 7531.
- 138. Young, J.C., et al., *The Escherichia coli effector EspJ blocks Src kinase activity via amidation and ADP ribosylation*. Nat Commun, 2014. **5**: p. 5887.
- 139. Kelly, M., et al., Essential Role of the Type III Secretion System Effector NleB in Colonization of Mice by Citrobacter rodentium. Infection and Immunity, 2006. 74(4): p. 2328-2337.
- 140. El Qaidi, S., et al., *NleB/SseK effectors from Citrobacter rodentium, Escherichia coli, and Salmonella enterica display distinct differences in host substrate specificity.* J Biol Chem, 2017. **292**(27): p. 11423-11430.
- 141. Baruch, K., et al., *Metalloprotease type III effectors that specifically cleave JNK and NF-kappaB*. Embo j, 2011. **30**(1): p. 221-31.
- 142. Shames, S.R., et al., *The pathogenic Escherichia coli type III secreted protease NleC degrades the host acetyltransferase p300.* Cell Microbiol, 2011. **13**(10): p. 1542-57.
- 143. Yen, H., et al., *NleC*, a type III secretion protease, compromises NF-kappaB activation by targeting p65/RelA. PLoS Pathog, 2010. **6**(12): p. e1001231.
- Wu, B., et al., NleG Type 3 effectors from enterohaemorrhagic Escherichia coli are U-Box E3 ubiquitin ligases. PLoS Pathog, 2010. **6**(6): p. e1000960.
- 145. Gao, X., et al., *Bacterial effector binding to ribosomal protein s3 subverts NF-kappaB function.* PLoS Pathog, 2009. **5**(12): p. e1000708.
- 146. Echtenkamp, F., et al., *Characterization of the NleF effector protein from attaching and effacing bacterial pathogens.* FEMS Microbiol Lett, 2008. **281**(1): p. 98-107.
- 147. Blasche, S., et al., *The E. coli effector protein NleF is a caspase inhibitor*. PLoS One, 2013. **8**(3): p. e58937.
- 148. Hardwidge, P.R., et al., Modulation of host cytoskeleton function by the enteropathogenic Escherichia coli and Citrobacter rodentium effector protein EspG. Infect Immun, 2005. 73(5): p. 2586-94.

- 149. Gao, X., et al., *NleB*, a bacterial effector with glycosyltransferase activity, targets GAPDH function to inhibit NF-kappaB activation. Cell Host Microbe, 2013. **13**(1): p. 87-99.
- 150. Pearson, J.S., et al., *A type III effector antagonizes death receptor signalling during bacterial gut infection.* Nature, 2013. **501**(7466): p. 247-51.
- 151. Li, S., et al., *Pathogen blocks host death receptor signalling by arginine GlcNAcylation of death domains.* Nature, 2013. **501**(7466): p. 242-6.
- 152. Pearson, J.S., et al., *EspL is a bacterial cysteine protease effector that cleaves RHIM proteins to block necroptosis and inflammation.* Nature Microbiology, 2017. **2**: p. 16258.
- 153. Miyahara, A., et al., Enterohemorrhagic Escherichia coli effector EspL2 induces actin microfilament aggregation through annexin 2 activation. Cell Microbiol, 2009. 11(2): p. 337-50.
- 154. Coombes, B.K., et al., *Molecular analysis as an aid to assess the public health risk of non-O157 Shiga toxin-producing Escherichia coli strains*. Appl Environ Microbiol, 2008. **74**(7): p. 2153-60.
- 155. Kim, J., et al., *The bacterial virulence factor NleA inhibits cellular protein secretion by disrupting mammalian COPII function.* Cell Host Microbe, 2007. **2**(3): p. 160-71.
- 156. Lee, M.C., et al., *Bi-directional protein transport between the ER and Golgi*. Annu Rev Cell Dev Biol, 2004. **20**: p. 87-123.
- 157. Thanabalasuriar, A., et al., Sec24 interaction is essential for localization and virulence-associated function of the bacterial effector protein NleA. Cell Microbiol, 2012. **14**(8): p. 1206-18.
- 158. Thanabalasuriar, A., J. Kim, and S. Gruenheid, *The inhibition of COPII trafficking is important for intestinal epithelial tight junction disruption during enteropathogenic Escherichia coli and Citrobacter rodentium infection.* Microbes Infect, 2013. **15**(10-11): p. 738-44.
- 159. Yen, H., N. Sugimoto, and T. Tobe, *Enteropathogenic Escherichia coli Uses NleA to Inhibit NLRP3 Inflammasome Activation*. PLoS Pathog, 2015. **11**(9): p. e1005121.
- 160. Levine, M.M., et al., The diarrheal response of humans to some classic serotypes of enteropathogenic Escherichia coli is dependent on a plasmid encoding an enteroadhesiveness factor. J Infect Dis, 1985. **152**(3): p. 550-9.
- 161. Hart, E., et al., RegA, an AraC-like protein, is a global transcriptional regulator that controls virulence gene expression in Citrobacter rodentium. Infect Immun, 2008. **76**(11): p. 5247-56.
- 162. Mundy, R., et al., *Identification of a novel type IV pilus gene cluster required for gastrointestinal colonization of Citrobacter rodentium.* Molecular Microbiology, 2003. **48**(3): p. 795-809.
- 163. Keepers, T.R., et al., *A murine model of HUS: Shiga toxin with lipopolysaccharide mimics the renal damage and physiologic response of human disease.* J Am Soc Nephrol, 2006. **17**(12): p. 3404-14.
- 164. Psotka, M.A., et al., *Shiga toxin 2 targets the murine renal collecting duct epithelium*. Infect Immun, 2009. 77(3): p. 959-69.
- 165. Mallick, E.M., et al., *A novel murine infection model for Shiga toxin-producing Escherichia coli.* J Clin Invest, 2012. **122**(11): p. 4012-24.
- 166. Mascher, T., J.D. Helmann, and G. Unden, *Stimulus perception in bacterial signal-transducing histidine kinases*. Microbiol Mol Biol Rev, 2006. **70**(4): p. 910-38.

- 167. Willett, J.W. and S. Crosson, *Atypical modes of bacterial histidine kinase signaling*. Mol Microbiol, 2017. **103**(2): p. 197-202.
- 168. Galperin, M.Y., Structural classification of bacterial response regulators: diversity of output domains and domain combinations. J Bacteriol, 2006. **188**(12): p. 4169-82.
- 169. Laub, M.T. and M. Goulian, *Specificity in two-component signal transduction pathways*. Annu Rev Genet, 2007. **41**: p. 121-45.
- 170. Wanner, B.L., Is cross regulation by phosphorylation of two-component response regulator proteins important in bacteria? J Bacteriol, 1992. 174(7): p. 2053-8.
- 171. Majdalani, N. and S. Gottesman, *The Rcs phosphorelay: a complex signal transduction system*. Annu Rev Microbiol, 2005. **59**: p. 379-405.
- 172. Laloux, G. and J.F. Collet, *Major Tom to Ground Control: How Lipoproteins Communicate Extracytoplasmic Stress to the Decision Center of the Cell.* J Bacteriol, 2017. **199**(21).
- 173. Takeda, S., et al., A novel feature of the multistep phosphorelay in Escherichia coli: a revised model of the RcsC --> YojN --> RcsB signalling pathway implicated in capsular synthesis and swarming behaviour. Mol Microbiol, 2001. **40**(2): p. 440-50.
- 174. Purves, D., et al., *Neuroscience*. 2nd ed. Scholarpedia. Vol. 4. 2001, Sunderland, MA: Sinauer Associates, Inc.
- 175. Furness, J.B., *Types of neurons in the enteric nervous system.* J Auton Nerv Syst, 2000. **81**(1-3): p. 87-96.
- 176. Moreira, C.G., et al., Bacterial Adrenergic Sensors Regulate Virulence of Enteric Pathogens in the Gut. MBio, 2016. 7(3).
- 177. Carlson-Banning, K.M. and V. Sperandio, *Enterohemorrhagic Escherichia coli outwits hosts through sensing small molecules*. Current Opinion in Microbiology, 2018. **41**: p. 83-88.
- 178. Cosma, C.L., et al., *Mutational activation of the Cpx signal transduction pathway of Escherichia coli suppresses the toxicity conferred by certain envelope-associated stresses.* Mol Microbiol, 1995. **18**(3): p. 491-505.
- 179. Danese, P.N., et al., *The Cpx two-component signal transduction pathway of Escherichia coli regulates transcription of the gene specifying the stress-inducible periplasmic protease*, *DegP*. Genes Dev, 1995. **9**(4): p. 387-98.
- 180. Pogliano, J., et al., Regulation of Escherichia coli cell envelope proteins involved in protein folding and degradation by the Cpx two-component system. Genes Dev, 1997. 11(9): p. 1169-82.
- 181. Snyder, W.B., et al., Overproduction of NlpE, a new outer membrane lipoprotein, suppresses the toxicity of periplasmic LacZ by activation of the Cpx signal transduction pathway. J Bacteriol, 1995. 177(15): p. 4216-23.
- 182. Delhaye, A., J.F. Collet, and G. Laloux, *Fine-Tuning of the Cpx Envelope Stress Response Is Required for Cell Wall Homeostasis in Escherichia coli*. MBio, 2016. **7**(1): p. e00047-16.
- 183. Miyadai, H., et al., Effects of lipoprotein overproduction on the induction of DegP (HtrA) involved in quality control in the Escherichia coli periplasm. J Biol Chem, 2004. **279**(38): p. 39807-13.
- 184. DiGiuseppe, P.A. and T.J. Silhavy, *Signal detection and target gene induction by the CpxRA two-component system.* J Bacteriol, 2003. **185**(8): p. 2432-40.

- 185. Nevesinjac, A.Z. and T.L. Raivio, *The Cpx envelope stress response affects expression of the type IV bundle-forming pili of enteropathogenic Escherichia coli*. J Bacteriol, 2005. **187**(2): p. 672-86.
- 186. Danese, P.N. and T.J. Silhavy, *CpxP*, a stress-combative member of the *Cpx regulon*. J Bacteriol, 1998. **180**(4): p. 831-9.
- 187. Prigent-Combaret, C., et al., Complex regulatory network controls initial adhesion and biofilm formation in Escherichia coli via regulation of the csgD gene. J Bacteriol, 2001. **183**(24): p. 7213-23.
- 188. Bury-Mone, S., et al., *Global analysis of extracytoplasmic stress signaling in Escherichia coli.* PLoS Genet, 2009. **5**(9): p. e1000651.
- 189. Otto, K. and T.J. Silhavy, *Surface sensing and adhesion of Escherichia coli controlled by the Cpx-signaling pathway*. Proc Natl Acad Sci U S A, 2002. **99**(4): p. 2287-92.
- 190. Mileykovskaya, E. and W. Dowhan, *The Cpx two-component signal transduction pathway is activated in Escherichia coli mutant strains lacking phosphatidylethanolamine*. J Bacteriol, 1997. **179**(4): p. 1029-34.
- 191. Raivio, T.L. and T.J. Silhavy, *Transduction of envelope stress in Escherichia coli by the Cpx two-component system.* J Bacteriol, 1997. **179**(24): p. 7724-33.
- 192. Raivio, T.L., et al., *Tethering of CpxP to the inner membrane prevents spheroplast induction of the cpx envelope stress response.* Mol Microbiol, 2000. **37**(5): p. 1186-97.
- 193. Raivio, T.L., D.L. Popkin, and T.J. Silhavy, *The Cpx envelope stress response is controlled by amplification and feedback inhibition.* J Bacteriol, 1999. **181**(17): p. 5263-72.
- 194. Buelow, D.R. and T.L. Raivio, *Cpx signal transduction is influenced by a conserved N-terminal domain in the novel inhibitor CpxP and the periplasmic protease DegP*. J Bacteriol, 2005. **187**(19): p. 6622-30.
- 195. Macritchie, D.M., et al., Activation of the Cpx envelope stress response down-regulates expression of several locus of enterocyte effacement-encoded genes in enteropathogenic Escherichia coli. Infect Immun, 2008. **76**(4): p. 1465-75.
- 196. MacRitchie, D.M., N. Acosta, and T.L. Raivio, *DegP is involved in Cpx-mediated posttranscriptional regulation of the type III secretion apparatus in enteropathogenic Escherichia coli*. Infect Immun, 2012. **80**(5): p. 1766-72.
- 197. Guest, R.L., et al., A Bacterial Stress Response Regulates Respiratory Protein Complexes To Control Envelope Stress Adaptation. J Bacteriol, 2017. 199(20).
- 198. Raivio, T.L., S.K. Leblanc, and N.L. Price, *The Escherichia coli Cpx envelope stress response regulates genes of diverse function that impact antibiotic resistance and membrane integrity.* J Bacteriol, 2013. **195**(12): p. 2755-67.
- 199. Thomassin, J.L., et al., *The CpxRA Two-Component System Is Essential for Citrobacter rodentium Virulence*. Infect Immun, 2015. **83**(5): p. 1919-28.
- 200. Tanner, J.R., et al., *The CpxRA two-component system contributes to Legionella pneumophila virulence*. Mol Microbiol, 2016. **100**(6): p. 1017-38.
- 201. Gal-Mor, O. and G. Segal, *Identification of CpxR as a positive regulator of icm and dot virulence genes of Legionella pneumophila*. J Bacteriol, 2003. **185**(16): p. 4908-19.
- 202. Mitobe, J., E. Arakawa, and H. Watanabe, *A sensor of the two-component system CpxA affects expression of the type III secretion system through posttranscriptional processing of InvE*. J Bacteriol, 2005. **187**(1): p. 107-13.
- 203. Nakayama, S. and H. Watanabe, *Identification of cpxR as a positive regulator essential for expression of the Shigella sonnei virF gene.* J Bacteriol, 1998. **180**(14): p. 3522-8.

- 204. Humphreys, S., et al., *Role of the two-component regulator CpxAR in the virulence of Salmonella enterica serotype Typhimurium*. Infect Immun, 2004. **72**(8): p. 4654-61.
- 205. Acosta, N., S. Pukatzki, and T.L. Raivio, *The Vibrio cholerae Cpx envelope stress response senses and mediates adaptation to low iron.* J Bacteriol, 2015. **197**(2): p. 262-76.
- 206. Acosta, N., S. Pukatzki, and T.L. Raivio, *The Cpx system regulates virulence gene expression in Vibrio cholerae*. Infect Immun, 2015. **83**(6): p. 2396-408.
- 207. Leuko, S. and T.L. Raivio, *Mutations that impact the enteropathogenic Escherichia coli Cpx envelope stress response attenuate virulence in Galleria mellonella*. Infect Immun, 2012. **80**(9): p. 3077-85.
- 208. Spinola, S.M., et al., *Activation of the CpxRA system by deletion of cpxA impairs the ability of Haemophilus ducreyi to infect humans.* Infect Immun, 2010. **78**(9): p. 3898-904.
- 209. Labandeira-Rey, M., et al., *A Haemophilus ducreyi CpxR deletion mutant is virulent in human volunteers*. J Infect Dis, 2011. **203**(12): p. 1859-65.
- 210. De la Cruz, M.A., et al., The Two-Component System CpxRA Negatively Regulates the Locus of Enterocyte Effacement of Enterohemorrhagic Escherichia coli Involving $\sigma(32)$ and Lon protease. Front Cell Infect Microbiol, 2016. **6**.
- 211. Barthold, S.W., et al., *Transmissible murine colonic hyperplasia*. Vet Pathol, 1978. **15**(2): p. 223-36.
- 212. Law, R.J., et al., *In vitro and in vivo model systems for studying enteropathogenic Escherichia coli infections*. Cold Spring Harb Perspect Med, 2013. **3**(3): p. a009977.
- 213. Collins, J.W., et al., *Citrobacter rodentium: infection, inflammation and the microbiota.* Nat Rev Microbiol, 2014. **12**(9): p. 612-23.
- Vallance, B.A., et al., *Host Susceptibility to the Attaching and Effacing Bacterial Pathogen Citrobacter rodentium.* Infect Immun, 2003. **71**(6): p. 3443-53.
- 215. Parkinson, J.S. and E.C. Kofoid, *Communication modules in bacterial signaling proteins*. Annu Rev Genet, 1992. **26**: p. 71-112.
- 216. Stock, A.M., V.L. Robinson, and P.N. Goudreau, *Two-component signal transduction*. Annu Rev Biochem, 2000. **69**: p. 183-215.
- 217. Oshima, T., et al., *Transcriptome analysis of all two-component regulatory system mutants of Escherichia coli K-12*. Mol Microbiol, 2002. **46**(1): p. 281-91.
- 218. Zhou, L., et al., *Phenotype microarray analysis of Escherichia coli K-12 mutants with deletions of all two-component systems.* J Bacteriol, 2003. **185**(16): p. 4956-72.
- 219. Beier, D. and R. Gross, *Regulation of bacterial virulence by two-component systems*. Curr Opin Microbiol, 2006. **9**(2): p. 143-52.
- 220. Dalebroux, Z.D. and S.I. Miller, *Salmonellae PhoPQ regulation of the outer membrane to resist innate immunity*. Curr Opin Microbiol, 2014. **17**: p. 106-13.
- 221. Beier, D. and R. Gross, *The BvgS/BvgA phosphorelay system of pathogenic Bordetellae: structure, function and evolution.* Adv Exp Med Biol, 2008. **631**: p. 149-60.
- 222. Mizuno, T., Compilation of all genes encoding two-component phosphotransfer signal transducers in the genome of Escherichia coli. DNA Res, 1997. **4**(2): p. 161-8.
- 223. Bergholz, T.M., et al., *Global transcriptional response of Escherichia coli O157:H7 to growth transitions in glucose minimal medium.* BMC Microbiol, 2007. 7: p. 97.
- 224. Partridge, J.D., et al., *Transition of Escherichia coli from aerobic to micro-aerobic conditions involves fast and slow reacting regulatory components.* J Biol Chem, 2007. **282**(15): p. 11230-7.

- 225. Partridge, J.D., et al., *Escherichia coli transcriptome dynamics during the transition from anaerobic to aerobic conditions*. J Biol Chem, 2006. **281**(38): p. 27806-15.
- 226. Landstorfer, R., et al., Comparison of strand-specific transcriptomes of enterohemorrhagic Escherichia coli O157:H7 EDL933 (EHEC) under eleven different environmental conditions including radish sprouts and cattle feces. BMC Genomics, 2014. **15**: p. 353.
- 227. Palaniyandi, S., et al., *BarA-UvrY two-component system regulates virulence of uropathogenic E. coli CFT073*. PLoS One, 2012. **7**(2): p. e31348.
- 228. Debnath, I., et al., *The Cpx stress response system potentiates the fitness and virulence of uropathogenic Escherichia coli*. Infect Immun, 2013. **81**(5): p. 1450-9.
- 229. Nagamatsu, K., et al., *Dysregulation of Escherichia coli alpha-hemolysin expression alters the course of acute and persistent urinary tract infection.* Proc Natl Acad Sci U S A, 2015. **112**(8): p. E871-80.
- 230. Cai, W., et al., A novel two-component signaling system facilitates uropathogenic Escherichia coli's ability to exploit abundant host metabolites. PLoS Pathog, 2013. **9**(6): p. e1003428.
- 231. Schwan, W.R., Survival of uropathogenic Escherichia coli in the murine urinary tract is dependent on OmpR. Microbiology, 2009. **155**(Pt 6): p. 1832-9.
- 232. Pacheco, A.R., et al., *Fucose sensing regulates bacterial intestinal colonization*. Nature, 2012. **492**(7427): p. 113-7.
- 233. Chekabab, S.M., et al., *PhoB activates Escherichia coli O157:H7 virulence factors in response to inorganic phosphate limitation.* PLoS One, 2014. **9**(4): p. e94285.
- 234. Njoroge, J. and V. Sperandio, *Enterohemorrhagic Escherichia coli virulence regulation by two bacterial adrenergic kinases, QseC and QseE*. Infect Immun, 2012. **80**(2): p. 688-703.
- 235. Reading, N.C., et al., A novel two-component signaling system that activates transcription of an enterohemorrhagic Escherichia coli effector involved in remodeling of host actin. J Bacteriol, 2007. **189**(6): p. 2468-76.
- 236. Moreira, C.G., et al., *Bacterial adrenergic sensors regulate virulence of enteric pathogens in the gut.* MBio, 2016. **7**(3): p. e00826-16.
- 237. Ye, J., et al., *Primer-BLAST: a tool to design target-specific primers for polymerase chain reaction.* BMC Bioinformatics, 2012. **13**: p. 134.
- 238. Livak, K.J. and T.D. Schmittgen, *Analysis of relative gene expression data using real-time quantitative PCR and the* $2^{-\Delta ACT}$ *method.* Methods, 2001. **25**(4): p. 402-8.
- 239. Jishage, M. and A. Ishihama, *Regulation of RNA polymerase sigma subunit synthesis in Escherichia coli: intracellular levels of sigma 70 and sigma 38.* J Bacteriol, 1995. **177**(23): p. 6832-5.
- 240. Sambrook, J., E.F. Fritsch, and T. Maniatis, *Molecular Cloning: A Laboratory Manual*, ed. C.S. Harbor. 1989, NY: Cold Spring Harbor Laboratory Press.
- 241. Schauer, D.B. and S. Falkow, *The eae gene of Citrobacter freundii biotype 4280 is necessary for colonization in transmissible murine colonic hyperplasia*. Infect. Immun., 1993. **61**(11): p. 4654-61.
- 242. Sit, B., et al., Active Transport of Phosphorylated Carbohydrates Promotes Intestinal Colonization and Transmission of a Bacterial Pathogen. PLoS Pathog, 2015. 11(8): p. e1005107.
- 243. Thomassin, J.-L., et al., *The CpxRA two-component system is essential for Citrobacter rodentium virulence*. Infect Immun, 2015. **83**(5): p. 1919-1928.

- 244. Hammar, M., Z. Bian, and S. Normark, *Nucleator-dependent intercellular assembly of adhesive curli organelles in Escherichia coli*. Proc Natl Acad Sci U S A, 1996. **93**(13): p. 6562-6.
- 245. Chen, C.Y., et al., *Multiple mechanisms responsible for strong Congo-red-binding variants of Escherichia coli O157:H7 strains.* Pathog Dis, 2016. **74**(2): p. ftv123.
- 246. Stevenson, G., et al., *Organization of the Escherichia coli K-12 gene cluster responsible for production of the extracellular polysaccharide colanic acid.* J Bacteriol, 1996. **178**(16): p. 4885-93.
- 247. Cameron, E.A. and V. Sperandio, *Frenemies: Signaling and Nutritional Integration in Pathogen-Microbiota-Host Interactions*. Cell Host Microbe, 2015. **18**(3): p. 275-84.
- 248. Lasaro, M., et al., Escherichia coli isolate for studying colonization of the mouse intestine and its application to two-component signaling knockouts. J Bacteriol, 2014. **196**(9): p. 1723-32.
- 249. Reboul, A., et al., Yersinia pestis requires the 2-component regulatory system OmpR-EnvZ to resist innate immunity during the early and late stages of plague. J Infect Dis, 2014. **210**(9): p. 1367-75.
- 250. Oyston, P.C., et al., The response regulator PhoP is important for survival under conditions of macrophage-induced stress and virulence in Yersinia pestis. Infect Immun, 2000. **68**(6): p. 3419-25.
- 251. Petit-Hartlein, I., et al., *Biophysical and physiological characterization of ZraP from Escherichia coli, the periplasmic accessory protein of the atypical ZraSR two-component system.* Biochem J, 2015. **472**: p. 205-216.
- 252. Gao, Q., et al., *RstA* is required for the virulence of an avian pathogenic Escherichia coli *O2 strain E058*. Infect Genet Evol, 2015. **29**: p. 180-8.
- Watanabe, M., et al., *Distribution of glucose-6-phosphatase activity in mice studied by in vitro whole-body autoradiography.* J Histochem Cytochem, 1983. **31**(12): p. 1426-9.
- 254. Alvarez, A.F., C. Rodriguez, and D. Georgellis, *Ubiquinone and menaquinone electron carriers represent the yin and yang in the redox regulation of the ArcB sensor kinase.* J Bacteriol, 2013. **195**(13): p. 3054-61.
- 255. Liu, M.Y., et al., *The RNA molecule CsrB binds to the global regulatory protein CsrA and antagonizes its activity in Escherichia coli.* J Biol Chem, 1997. **272**(28): p. 17502-10.
- 256. Liu, M.Y. and T. Romeo, *The global regulator CsrA of Escherichia coli is a specific mRNA-binding protein.* J Bacteriol, 1997. **179**(14): p. 4639-42.
- 257. Vakulskas, C.A., et al., *Regulation of bacterial virulence by Csr (Rsm) systems*. Microbiol Mol Biol Rev, 2015. **79**(2): p. 193-224.
- 258. Heath, A., et al., A two-component regulatory system, CsrR-CsrS, represses expression of three Streptococcus pyogenes virulence factors, hyaluronic acid capsule, streptolysin S, and pyrogenic exotoxin B. Infect Immun, 1999. 67(10): p. 5298-305.
- 259. Bem, A.E., et al., *Bacterial histidine kinases as novel antibacterial drug targets*. ACS Chem Biol, 2015. **10**(1): p. 213-24.
- 260. Stephenson, K. and J.A. Hoch, *Two-component and phosphorelay signal-transduction systems as therapeutic targets.* Curr Opin Pharmacol, 2002. **2**(5): p. 507-12.
- 261. Le Sage, V., et al., An outer membrane protease of the omptin family prevents activation of the Citrobacter rodentium PhoPQ two-component system by antimicrobial peptides. Mol Microbiol, 2009. **74**(1): p. 98-111.

- 262. Viau, C., et al., Absence of PmrAB-mediated phosphoethanolamine modifications of Citrobacter rodentium lipopolysaccharide affects outer membrane integrity. J Bacteriol, 2011. **193**(9): p. 2168-76.
- 263. Roland, K., R. Curtiss, 3rd, and D. Sizemore, Construction and evaluation of a delta cya delta crp Salmonella typhimurium strain expressing avian pathogenic Escherichia coli 078 LPS as a vaccine to prevent airsacculitis in chickens. Avian Dis, 1999. 43(3): p. 429-41.
- 264. Edwards, R.A., L.H. Keller, and D.M. Schifferli, *Improved allelic exchange vectors and their use to analyze 987P fimbria gene expression*. Gene, 1998. **207**(2): p. 149-57.
- 265. Thomassin, J.L., et al., Systematic Analysis of Two-Component Systems in Citrobacter rodentium Reveals Positive and Negative Roles in Virulence. Infect Immun, 2017. **85**(2).
- 266. Snyder, W.B. and T.J. Silhavy, *Beta-galactosidase is inactivated by intermolecular disulfide bonds and is toxic when secreted to the periplasm of Escherichia coli*. J Bacteriol, 1995. **177**(4): p. 953-63.
- 267. Jubelin, G., et al., *CpxR/OmpR interplay regulates curli gene expression in response to osmolarity in Escherichia coli.* J Bacteriol, 2005. **187**(6): p. 2038-49.
- 268. Vogt, S.L., et al., *The Cpx envelope stress response both facilitates and inhibits elaboration of the enteropathogenic Escherichia coli bundle-forming pilus.* Mol Microbiol, 2010. **76**(5): p. 1095-110.
- 269. Shimizu, T., K. Ichimura, and M. Noda, *The Surface Sensor NlpE of Enterohemorrhagic Escherichia coli Contributes to Regulation of the Type III Secretion System and Flagella by the Cpx Response to Adhesion.* Infect Immun, 2016. **84**(2): p. 537-49.
- 270. Donnenberg, M.S. and J.B. Kaper, Construction of an eae deletion mutant of enteropathogenic Escherichia coli by using a positive-selection suicide vector. Infect Immun, 1991. **59**(12): p. 4310-7.
- 271. Hanahan, D., J. Jessee, and F.R. Bloom, *Plasmid transformation of Escherichia coli and other bacteria*. Methods Enzymol, 1991. **204**: p. 63-113.
- 272. Ullman-Cullere, M.H. and C.J. Foltz, *Body condition scoring: a rapid and accurate method for assessing health status in mice*. Lab Anim Sci, 1999. **49**(3): p. 319-23.
- 273. Schindelin, J., et al., *Fiji: an open-source platform for biological-image analysis.* Nat Methods, 2012. **9**(7): p. 676-82.
- 274. Faucher, S.P. and H.A. Shuman, *Methods to study legionella transcriptome in vitro and in vivo*, in *Methods Mol Biol*. 2013. p. 567-82.
- 275. Zoued, A., et al., *Architecture and assembly of the Type VI secretion system.* Biochimica et Biophysica Acta (BBA) Molecular Cell Research, 2014. **1843**(8): p. 1664-1673.
- 276. Pukatzki, S., et al., *Type VI secretion system translocates a phage tail spike-like protein into target cells where it cross-links actin.* Proceedings of the National Academy of Sciences, 2007. **104**(39): p. 15508.
- 277. Russell, A.B., et al., *Type VI secretion delivers bacteriolytic effectors to target cells*. Nature, 2011. **475**(7356): p. 343-7.
- 278. Gueguen, E. and E. Cascales, *Promoter swapping unveils the role of the Citrobacter rodentium CTS1 type VI secretion system in interbacterial competition.* Appl Environ Microbiol, 2013. **79**(1): p. 32-8.
- 279. Gueguen, E., et al., *Transcriptional Frameshifting Rescues Citrobacter rodentium Type VI Secretion by the Production of Two Length Variants from the Prematurely Interrupted tssM Gene.* PLoS Genet, 2014. **10**(12).

- 280. Jones, S.A., et al., *Glycogen and maltose utilization by Escherichia coli O157:H7 in the mouse intestine*. Infect Immun, 2008. **76**(6): p. 2531-40.
- 281. Chang, D.E., et al., *Carbon nutrition of Escherichia coli in the mouse intestine*. Proc Natl Acad Sci U S A, 2004. **101**(19): p. 7427-32.
- 282. Marchler-Bauer, A., et al., *CDD/SPARCLE: functional classification of proteins via subfamily domain architectures.* Nucleic Acids Res, 2017. **45**(Database issue): p. D200-3.
- 283. Krogh, A., et al., *Predicting transmembrane protein topology with a hidden Markov model: application to complete genomes.* J Mol Biol, 2001. **305**(3): p. 567-80.
- 284. Petersen, T.N., et al., SignalP 4.0: discriminating signal peptides from transmembrane regions. Nat Methods, 2011. **8**(10): p. 785-6.
- 285. Dong, T. and H.E. Schellhorn, *Global effect of RpoS on gene expression in pathogenic Escherichia coli 0157:H7 strain EDL933*. BMC Genomics, 2009. **10**: p. 349.
- 286. Saint-Ruf, C., et al., *Massive diversification in aging colonies of Escherichia coli.* J Bacteriol, 2014. **196**(17): p. 3059-73.
- 287. Sim, S.H., et al., Escherichia coli ribonuclease III activity is downregulated by osmotic stress: consequences for the degradation of bdm mRNA in biofilm formation. Mol Microbiol, 2010. **75**(2): p. 413-25.
- 288. Prigent-Combaret, C., et al., *Abiotic surface sensing and biofilm-dependent regulation of gene expression in Escherichia coli.* J Bacteriol, 1999. **181**(19): p. 5993-6002.
- 289. Francez-Charlot, A., et al., Osmotic regulation of the Escherichia coli bdm (biofilm-dependent modulation) gene by the RcsCDB His-Asp phosphorelay. J Bacteriol, 2005. **187**(11): p. 3873-7.
- 290. Selinger, D.W., et al., *RNA expression analysis using a 30 base pair resolution Escherichia coli genome array.* Nat Biotechnol, 2000. **18**(12): p. 1262-8.
- 291. Domka, J., J. Lee, and T.K. Wood, *YliH (BssR) and YceP (BssS) regulate Escherichia coli K-12 biofilm formation by influencing cell signaling*. Appl Environ Microbiol, 2006. **72**(4): p. 2449-59.
- 292. Cotter, P.A. and S. Stibitz, *c-di-GMP-mediated regulation of virulence and biofilm formation*. Curr Opin Microbiol, 2007. **10**(1): p. 17-23.
- 293. Batchelor, E., et al., *The Escherichia coli CpxA-CpxR envelope stress response system regulates expression of the porins ompF and ompC*. J Bacteriol, 2005. **187**(16): p. 5723-31.
- 294. Rolhion, N., A.F. Carvalho, and A. Darfeuille-Michaud, *OmpC* and the σE regulatory pathway are involved in adhesion and invasion of the Crohn's disease-associated Escherichia coli strain LF82. Molecular Microbiology, 2007. **63**(6): p. 1684-1700.
- 295. Hejair, H.M.A., et al., Functional role of ompF and ompC porins in pathogenesis of avian pathogenic Escherichia coli. Microbial Pathogenesis, 2017. **107**: p. 29-37.
- 296. Kvint, K., et al., *The bacterial universal stress protein: function and regulation.* Current Opinion in Microbiology, 2003. **6**(2): p. 140-145.
- 297. Nachin, L., U. Nannmark, and T. Nystrom, *Differential roles of the universal stress proteins of Escherichia coli in oxidative stress resistance, adhesion, and motility.* J Bacteriol, 2005. **187**(18): p. 6265-72.
- 298. de Souza, C.S., et al., Characterization of the universal stress protein F from atypical enteropathogenic Escherichia coli and its prevalence in Enterobacteriaceae. Protein Sci, 2016. **25**(12): p. 2142-51.

- 299. Knutton, S., D.R. Lloyd, and A.S. McNeish, *Adhesion of enteropathogenic Escherichia coli to human intestinal enterocytes and cultured human intestinal mucosa*. Infect Immun, 1987. **55**(1): p. 69-77.
- 300. Hemrajani, C., et al., *NleH effectors interact with Bax inhibitor-1 to block apoptosis during enteropathogenic Escherichia coli infection.* Proc Natl Acad Sci U S A, 2010. **107**(7): p. 3129-34.
- 301. Chantret, I., et al., *Differential expression of sucrase-isomaltase in clones isolated from early and late passages of the cell line Caco-2: evidence for glucose-dependent negative regulation.* J Cell Sci, 1994. **107 (Pt 1)**: p. 213-25.
- 302. Kingsley, D.M., et al., Reversible defects in O-linked glycosylation and LDL receptor expression in a UDP-Gal/UDP-GalNAc 4-epimerase deficient mutant. Cell, 1986. 44(5): p. 749-59.
- 303. Kozarsky, K., D. Kingsley, and M. Krieger, *Use of a mutant cell line to study the kinetics and function of O-linked glycosylation of low density lipoprotein receptors.* Proc Natl Acad Sci U S A, 1988. **85**(12): p. 4335-9.
- 304. de Grado, M., et al., *Identification of the intimin-binding domain of Tir of enteropathogenic Escherichia coli*. Cell Microbiol, 1999. **1**(1): p. 7-17.
- 305. Shevchenko, A., et al., *Mass Spectrometric Sequencing of Proteins from Silver-Stained Polyacrylamide Gels.* Analytical Chemistry, 1996. **68**(5): p. 850-858.
- 306. Steentoft, C., et al., *Precision mapping of the human O-GalNAc glycoproteome through SimpleCell technology*. Embo j, 2013. **32**(10): p. 1478-88.
- 307. Krieger, M., et al., Chapter 3 Analysis of the Synthesis, Intracellular Sorting, and Function of Glycoproteins Using a Mammalian Cell Mutant with Reversible Glycosylation Defects, in Methods in Cell Biology, A.M. Tartakoff, Editor. 1989, Academic Press. p. 57-84.
- 308. Varki A, C.R., Esko JD, et al., *Structures Common to Different Glycans*, in *Essentials of Glycobiology*. 2009, Cold Spring Harbor (NY).
- 309. Wertz, G.W., M. Krieger, and L.A. Ball, Structure and cell surface maturation of the attachment glycoprotein of human respiratory syncytial virus in a cell line deficient in O glycosylation. J Virol, 1989. **63**(11): p. 4767-76.
- 310. Kenny, B., *The enterohaemorrhagic Escherichia coli (serotype O157:H7) Tir molecule is not functionally interchangeable for its enteropathogenic E. coli (serotype O127:H6) homologue.* Cell Microbiol, 2001. **3**(8): p. 499-510.
- 311. DeVinney, R., et al., Enterohaemorrhagic and enteropathogenic Escherichia coli use a different Tir-based mechanism for pedestal formation. Mol Microbiol, 2001. **41**(6): p. 1445-58.
- 312. Brockhausen, I. and P. Stanley, *O-GalNAc Glycans*. Essentials of Glycobiology ed. C.R. Varki A, Esko JD, et al. 2017, Cold Spring Harbor (NY): Cold Spring Harbor Laboratory Press.
- 313. SolÁ, R.J. and K. Griebenow, *Effects of Glycosylation on the Stability of Protein Pharmaceuticals*. J Pharm Sci, 2009. **98**(4): p. 1223-45.
- 314. Georgellis, D., A.S. Lynch, and E.C. Lin, *In vitro phosphorylation study of the arc two-component signal transduction system of Escherichia coli*. J Bacteriol, 1997. **179**(17): p. 5429-35.
- 315. Georgellis, D., O. Kwon, and E.C. Lin, *Quinones as the redox signal for the arc two-component system of bacteria*. Science, 2001. **292**(5525): p. 2314-6.

- 316. Kwon, O., D. Georgellis, and E.C. Lin, *Phosphorelay as the sole physiological route of signal transmission by the arc two-component system of Escherichia coli*. J Bacteriol, 2000. **182**(13): p. 3858-62.
- 317. Pardo-Este, C., et al., *The ArcAB two-component regulatory system promotes resistance to reactive oxygen species and systemic infection by Salmonella Typhimurium.* PLoS One, 2018. **13**(9): p. e0203497.
- 318. Halsey, T.A., et al., *The ferritin-like Dps protein is required for Salmonella enterica serovar Typhimurium oxidative stress resistance and virulence*. Infect Immun, 2004. **72**(2): p. 1155-8.
- 319. Wong, S.M., et al., *The ArcA regulon and oxidative stress resistance in Haemophilus influenzae*. Mol Microbiol, 2007. **64**(5): p. 1375-90.
- 320. Almiron, M., et al., *A novel DNA-binding protein with regulatory and protective roles in starved Escherichia coli*. Genes Dev, 1992. **6**(12b): p. 2646-54.
- 321. Loui, C., A.C. Chang, and S. Lu, *Role of the ArcAB two-component system in the resistance of Escherichia coli to reactive oxygen stress.* BMC Microbiol, 2009. **9**: p. 183.
- 322. Alexeeva, S., K.J. Hellingwerf, and M.J. Teixeira de Mattos, *Requirement of ArcA for redox regulation in Escherichia coli under microaerobic but not anaerobic or aerobic conditions.* J Bacteriol, 2003. **185**(1): p. 204-9.
- 323. Gunsalus, R.P. and S.J. Park, *Aerobic-anaerobic gene regulation in Escherichia coli:* control by the ArcAB and Fnr regulons. Research in Microbiology, 1994. **145**(5): p. 437-450.
- 324. Schuller, S. and A.D. Phillips, *Microaerobic conditions enhance type III secretion and adherence of enterohaemorrhagic Escherichia coli to polarized human intestinal epithelial cells*. Environ Microbiol, 2010. **12**(9): p. 2426-35.
- 325. He, G., et al., Noninvasive measurement of anatomic structure and intraluminal oxygenation in the gastrointestinal tract of living mice with spatial and spectral EPR imaging. Proc Natl Acad Sci U S A, 1999. **96**(8): p. 4586-91.
- 326. Jones, S.A., et al., *Respiration of Escherichia coli in the mouse intestine*. Infect Immun, 2007. **75**(10): p. 4891-9.
- 327. Evans, K.L., et al., *Eliminating a set of four penicillin binding proteins triggers the Rcs phosphorelay and Cpx stress responses in Escherichia coli.* J Bacteriol, 2013. **195**(19): p. 4415-24.
- 328. Callewaert, L., et al., *The Rcs two-component system regulates expression of lysozyme inhibitors and is induced by exposure to lysozyme*. J Bacteriol, 2009. **191**(6): p. 1979-81.
- 329. Laubacher, M.E. and S.E. Ades, *The Rcs phosphorelay is a cell envelope stress response activated by peptidoglycan stress and contributes to intrinsic antibiotic resistance.* J Bacteriol, 2008. **190**(6): p. 2065-74.
- 330. Cho, S.H., et al., *Detecting envelope stress by monitoring beta-barrel assembly*. Cell, 2014. **159**(7): p. 1652-64.
- 331. Tao, K., S. Narita, and H. Tokuda, *Defective lipoprotein sorting induces lolA expression through the Rcs stress response phosphorelay system.* J Bacteriol, 2012. **194**(14): p. 3643-50.
- 332. Miajlovic, H., et al., Response of extraintestinal pathogenic Escherichia coli to human serum reveals a protective role for Rcs-regulated exopolysaccharide colanic acid. Infect Immun, 2014. **82**(1): p. 298-305.

- 333. Su, K., et al., Genome-wide identification of genes regulated by RcsA, RcsB, and RcsAB phosphorelay regulators in Klebsiella pneumoniae NTUH-K2044. Microb Pathog, 2018. **123**: p. 36-41.
- 334. Gervais, F.G., P. Phoenix, and G.R. Drapeau, *The rcsB gene, a positive regulator of colanic acid biosynthesis in Escherichia coli, is also an activator of ftsZ expression.* J Bacteriol, 1992. **174**(12): p. 3964-71.
- 335. Carballès, F., et al., *Regulation of Escherichia coli cell division genes ftsA and ftsZ by the two-component system rcsC-rcsB*. Molecular Microbiology, 1999. **34**(3): p. 442-450.
- 336. Yamamoto, K., et al., Functional Characterization in Vitro of All Two-component Signal Transduction Systems from Escherichia coli. Journal of Biological Chemistry, 2005. **280**(2): p. 1448-1456.
- 337. Eguchi, Y., et al., Signal Transduction Cascade between EvgA/EvgS and PhoP/PhoQ Two-Component Systems of Escherichia coli. Journal of Bacteriology, 2004. **186**(10): p. 3006-3014.
- 338. Groisman, E.A., *The Pleiotropic Two-Component Regulatory System PhoP-PhoQ*. Journal of Bacteriology, 2001. **183**(6): p. 1835-1842.
- 339. Castelli, M.E., E. Garcia Vescovi, and F.C. Soncini, *The phosphatase activity is the target for Mg2+ regulation of the sensor protein PhoQ in Salmonella*. J Biol Chem, 2000. **275**(30): p. 22948-54.
- 340. Prost, L.R., et al., *Activation of the Bacterial Sensor Kinase PhoQ by Acidic pH*. Molecular Cell, 2007. **26**(2): p. 165-174.
- 341. Bader, M.W., et al., *Recognition of Antimicrobial Peptides by a Bacterial Sensor Kinase*. Cell, 2005. **122**(3): p. 461-472.
- 342. Véscovi, E.G., F.C. Soncini, and E.A. Groisman, Mg2+ as an Extracellular Signal: Environmental Regulation of Salmonella Virulence. Cell, 1996. **84**(1): p. 165-174.
- 343. Yao, Y., et al., Absence of RstA results in delayed initiation of DNA replication in Escherichia coli. PLoS One, 2018. **13**(7): p. e0200688.
- 344. Cabeza, M.L., et al., *Induction of RpoS degradation by the two-component system regulator RstA in Salmonella enterica*. J Bacteriol, 2007. **189**(20): p. 7335-42.
- 345. Nickerson, C.A. and R. Curtiss, 3rd, *Role of sigma factor RpoS in initial stages of Salmonella typhimurium infection.* Infect Immun, 1997. **65**(5): p. 1814-23.
- 346. Fang, F.C., et al., *The alternative sigma factor katF (rpoS) regulates Salmonella virulence*. Proc Natl Acad Sci U S A, 1992. **89**(24): p. 11978-82.
- 347. Coynault, C., V. Robbe-Saule, and F. Norel, *Virulence and vaccine potential of Salmonella typhimurium mutants deficient in the expression of the RpoS (sigma S) regulon.* Mol Microbiol, 1996. **22**(1): p. 149-60.
- 348. Verhamme, D.T., et al., *Glucose-6-phosphate-dependent phosphoryl flow through the Uhp two-component regulatory system.* Microbiology, 2001. **147**(12): p. 3345-3352.
- 349. Rome, K., et al., *The Two-Component System ZraPSR Is a Novel ESR that Contributes to Intrinsic Antibiotic Tolerance in Escherichia coli.* Journal of Molecular Biology, 2018.
- 350. Petit-Hartlein, I., et al., *Biophysical and physiological characterization of ZraP from Escherichia coli, the periplasmic accessory protein of the atypical ZraSR two-component system.* Biochem J, 2015. **472**(2): p. 205-16.
- 351. Gopalsamy, G.L., et al., *The relevance of the colon to zinc nutrition*. Nutrients, 2015. **7**(1): p. 572-83.

- 352. Porcheron, G., et al., *Iron, copper, zinc, and manganese transport and regulation in pathogenic Enterobacteria: correlations between strains, site of infection and the relative importance of the different metal transport systems for virulence.* Front Cell Infect Microbiol, 2013. **3**: p. 90.
- 353. Chavez, R.G., et al., *The physiological stimulus for the BarA sensor kinase*. J Bacteriol, 2010. **192**(7): p. 2009-12.
- 354. Morrison, D.J. and T. Preston, *Formation of short chain fatty acids by the gut microbiota and their impact on human metabolism.* Gut Microbes, 2016. **7**(3): p. 189-200.
- 355. Lawhon, S.D., et al., *Intestinal short-chain fatty acids alter Salmonella typhimurium invasion gene expression and virulence through BarA/SirA*. Molecular Microbiology, 2002. **46**(5): p. 1451-1464.
- 356. Pernestig, A.K., et al., *The Escherichia coli BarA-UvrY two-component system is needed for efficient switching between glycolytic and gluconeogenic carbon sources.* J Bacteriol, 2003. **185**(3): p. 843-53.
- 357. Mühlen, S. and P. Dersch, *Anti-virulence Strategies to Target Bacterial Infections*, in *How to Overcome the Antibiotic Crisis : Facts, Challenges, Technologies and Future Perspectives*, M. Stadler and P. Dersch, Editors. 2016, Springer International Publishing: Cham. p. 147-183.
- 358. Rasko, D.A. and V. Sperandio, *Anti-virulence strategies to combat bacteria-mediated disease*. Nature Reviews Drug Discovery, 2010. **9**: p. 117.
- 359. Sully, E.K., et al., Selective chemical inhibition of agr quorum sensing in Staphylococcus aureus promotes host defense with minimal impact on resistance. PLoS Pathog, 2014. **10**(6): p. e1004174.
- 360. Rasko, D.A., et al., *Targeting QseC signaling and virulence for antibiotic development*. Science, 2008. **321**(5892): p. 1078-80.
- 361. Dbeibo, L., et al., Evaluation of CpxRA as a Therapeutic Target for Uropathogenic Escherichia coli Infections. Infect Immun, 2018. **86**(3).
- 362. Surmann, K., et al., Molecular and proteome analyses highlight the importance of the Cpx envelope stress system for acid stress and cell wall stability in Escherichia coli. Microbiologyopen, 2016. **5**(4): p. 582-96.
- 363. Bernal-Cabas, M., J.A. Ayala, and T.L. Raivio, *The Cpx envelope stress response modifies peptidoglycan cross-linking via the L,D-transpeptidase LdtD and the novel protein YgaU*. J Bacteriol, 2015. **197**(3): p. 603-14.
- 364. Guest, R.L. and T.L. Raivio, *Role of the Gram-Negative Envelope Stress Response in the Presence of Antimicrobial Agents.* Trends in Microbiology, 2016. **24**(5): p. 377-390.
- 365. Vogt, S.L., et al., *The Cpx envelope stress response regulates and is regulated by small noncoding RNAs.* J Bacteriol, 2014. **196**(24): p. 4229-38.
- 366. Fabich, A.J., et al., Comparison of carbon nutrition for pathogenic and commensal Escherichia coli strains in the mouse intestine. Infect Immun, 2008. **76**(3): p. 1143-52.
- 367. Boos, W. and H. Shuman, *Maltose/maltodextrin system of Escherichia coli: transport, metabolism, and regulation.* Microbiol Mol Biol Rev, 1998. **62**(1): p. 204-29.
- 368. Sana, T.G., et al., Salmonella Typhimurium utilizes a T6SS-mediated antibacterial weapon to establish in the host gut. Proc Natl Acad Sci U S A, 2016. **113**(34): p. E5044-51.
- 369. Vogt, S.L., et al., *Characterization of the Citrobacter rodentium Cpx regulon and its role in host infection.* Molecular Microbiology. **0**(ja).

- 370. Scott, N.E. and E.L. Hartland, *Post-translational Mechanisms of Host Subversion by Bacterial Effectors*. Trends in Molecular Medicine, 2017. **23**(12): p. 1088-1102.
- 371. Popa, C.M., M. Tabuchi, and M. Valls, *Modification of Bacterial Effector Proteins Inside Eukaryotic Host Cells*. Front Cell Infect Microbiol, 2016. **6**: p. 73.
- 372. Backert, S., N. Tegtmeyer, and M. Selbach, *The versatility of Helicobacter pylori CagA effector protein functions: The master key hypothesis.* Helicobacter, 2010. **15**(3): p. 163-76
- 373. Mueller, D., et al., *c-Src and c-Abl kinases control hierarchic phosphorylation and function of the CagA effector protein in Western and East Asian Helicobacter pylori strains.* J Clin Invest, 2012. **122**(4): p. 1553-66.
- 374. Behrends, C. and J.W. Harper, *Constructing and decoding unconventional ubiquitin chains*. Nat Struct Mol Biol, 2011. **18**(5): p. 520-8.
- 375. Kubori, T. and J.E. Galan, *Temporal regulation of salmonella virulence effector function by proteasome-dependent protein degradation*. Cell, 2003. **115**(3): p. 333-42.
- 376. Thomas, M. and D.W. Holden, *Ubiquitination a bacterial effector's ticket to ride*. Cell Host Microbe, 2009. **5**(4): p. 309-11.
- 377. Narayanan, L.A. and M.J. Edelmann, *Ubiquitination as an efficient molecular strategy employed in salmonella infection*. Front Immunol, 2014. **5**: p. 558.
- 378. Guo, C. and J.M. Henley, Wrestling with stress: roles of protein SUMOylation and deSUMOylation in cell stress response. IUBMB Life, 2014. **66**(2): p. 71-7.
- 379. Wilson, V.G., *Sumoylation at the host-pathogen interface*. Biomolecules, 2012. **2**(2): p. 203-27.
- 380. Beyer, A.R., et al., *The Anaplasma phagocytophilum effector AmpA hijacks host cell SUMOylation*. Cell Microbiol, 2015. **17**(4): p. 504-19.
- 381. Price, C.T., et al., *Host-mediated post-translational prenylation of novel dot/icm-translocated effectors of legionella pneumophila.* Front Microbiol, 2010. 1: p. 131.
- 382. Price, C.T., et al., *Exploitation of conserved eukaryotic host cell farnesylation machinery by an F-box effector of Legionella pneumophila*. J Exp Med, 2010. **207**(8): p. 1713-26.

Appendix

Subject: RE: Co-author Consent for use of published work

Date: Monday, November 19, 2018 at 7:02:52 PM GMT-05:00

From: Jean-Mathieu Leclerc

To: Natalie Giannakopoulou

Hi Natalia,

No problem, I grant you permission to use this manuscript in your thesis.

Regards,

Jean-Mathieu

De: Natalie Giannakopoulou <natalia.giannakopoulou@mail.mcgill.ca>

Envoyé: 19 novembre 2018 12:16 À: jean-mathieu.leclerc@hotmail.com

Objet: Co-author Consent for use of published work

Hi Jean-Mathieu Leclerc,

I am in the process of submitting my Ph.D. Thesis and was hoping that you would grant me permission to use the following manuscript in my thesis:

Thomassin JL, Leclerc JM, Giannakopoulou N, Zhu L, Salmon K, Portt A, Daigle F, Le Moual H & Gruenheid S (2017) Systematic Analysis of Two-Component Systems in Citrobacter rodentium Reveals Positive and Negative Roles in Virulence. *Infection and immunity* **85**.

Thank you, Natalia Giannakopoulou Subject: Re: Manuscript Permission for PhD Thesis

Date: Monday, November 19, 2018 at 12:30:43 PM GMT-05:00

From: Jenny-Lee Thomassin, Ms **To:** Natalie Giannakopoulou

Hi Natalie,

With pleasure! Good luck with the defense!

Jenny

From: Natalie Giannakopoulou

Sent: November 19, 2018 11:53:55 AM

To: Jenny-Lee Thomassin, Ms

Subject: Manuscript Permission for PhD Thesis

Hi Jenny-Lee Thomassin,

I am in the process of submitting my Ph.D. Thesis and was hoping that you would grant me permission to use the following manuscript in my thesis:

Thomassin JL, Leclerc JM, Giannakopoulou N, Zhu L, Salmon K, Portt A, Daigle F, Le Moual H & Gruenheid S (2017) Systematic Analysis of Two-Component Systems in Citrobacter rodentium Reveals Positive and Negative Roles in Virulence. *Infection and immunity* **85**.

Thank you, Natalia Giannakopoulou